



UNIVERSITY OF
BIRMINGHAM

**STRUCTURE AND FUNCTION OF THE NEURAMINIDASE
PRODUCED BY *MANNHEIMIA HAEMOLYTICA***

by

RICARDO CORONA TORRES

A thesis submitted to the University of Birmingham for the degree of
DOCTOR OF PHILOSOPHY

Institute of Microbiology and Infection
College of Medical and Dental Sciences
University of Birmingham
October, 2016

UNIVERSITY OF
BIRMINGHAM

University of Birmingham Research Archive

e-theses repository

This unpublished thesis/dissertation is copyright of the author and/or third parties. The intellectual property rights of the author or third parties in respect of this work are as defined by The Copyright Designs and Patents Act 1988 or as modified by any successor legislation.

Any use made of information contained in this thesis/dissertation must be in accordance with that legislation and must be properly acknowledged. Further distribution or reproduction in any format is prohibited without the permission of the copyright holder.

Abstract

The Gram negative bacillus *Mannheimia haemolytica* is a natural inhabitant of the upper respiratory tract in ruminants and the most common secondary agent of the bovine respiratory disease complex. It is known to produce the extracellular neuraminidase NanH, which has a yet unknown biological role but is suspected to be important for bacterial adhesion to host cells, colonisation, capsule synthesis and biofilm formation. The structure of NanH is not known therefore, the functional domains of NanH, the tertiary structure and the residues involved in catalysis were predicted by sequence homology to the coordinates of other neuraminidases solved by crystallography. The catalytic domain was delimited from residues 23 to 435 and purified. The predicted catalytic residues were substituted in the recombinant NanH for confirmation of their role in hydrolysis of sialic acid. The function of the additional domains is unknown but analysis of NanH sequence and other associated genes found in the chromosome of *M. haemolytica*, suggest the presence of an autotransporter domain. The role of NanH in colonisation and infection is not known however, molecular characterisation is presented in this work. These data provide the basic knowledge required for future studies on using Nanh as a therapeutic and prophylactic target.

Acknowledgements

This project was funded by a CONACyT scholarship.

My supervisor Prof Tim Mitchell for giving me the opportunity of working with his group for a summer placement in Glasgow and now a PhD project in Birmingham.

Dr Andrea Mitchell for helping me directly with laboratory techniques and giving me valuable advice in every lab meeting.

My mum Angélica, my dad Federico and my brother Miguel for giving me their support through all my academic life.

All current and former members of the pneumococcal research group for having direct or indirect participation in my project. An additional acknowledgement to Dr J.Herbert, Dr C.Krone, Dr C.Dalziel and Dr K.Mughal for being directly involved in laboratory techniques teaching.

Dr V.Bavro for the big participation he had in the structural biology and for making one of the models.

My co-supervisor Prof Ian Henderson for the discussion about autotransporter proteins.

Members of the Institute of Microbiology and Infection (IMI), for participating at some point during my studies. An additional acknowledgement to R.Chandler, X.Wang and C.Domínguez for all your support and advice.

L.Gómez for all your support, especially during the writing period and for drawing the disease mechanism diagram.

Table of contents

| | |
|--|-----------|
| 1 Introduction | 1 |
| 1.1 <i>Bovine respiratory disease</i> | 1 |
| 1.1.1 <i>Aetiology</i> | 2 |
| 1.1.2 <i>Pathology</i> | 5 |
| 1.1.3 <i>Prevention and treatment</i> | 6 |
| 1.1.3.1 <i>Vaccination</i> | 6 |
| 1.2 <i>Mannheimia haemolytica</i> | 7 |
| 1.2.1 <i>Virulence factors</i> | 8 |
| 1.2.1.1 <i>Capsule</i> | 8 |
| 1.2.1.2 <i>Outer membrane proteins</i> | 8 |
| 1.2.1.3 <i>Endotoxin: Lipopolysaccharide (LPS)</i> | 9 |
| 1.2.1.4 <i>Leukotoxin</i> | 9 |
| 1.2.1.5 <i>Iron regulated proteins (IRP)</i> | 11 |
| 1.2.1.6 <i>Neuraminidase</i> | 11 |
| 1.2.2 <i>Immune response to <i>M. haemolytica</i> infection</i> | 11 |
| 1.3 <i>Neuraminidases</i> | 12 |
| 1.3.1 <i>Sialic acids</i> | 12 |
| 1.3.2 <i>Neuraminidases as virulence factors</i> | 15 |
| 1.3.3 <i>Structure of neuraminidases</i> | 15 |
| 1.3.4 <i>Bacterial neuraminidases</i> | 16 |
| 1.3.5 <i>Neuraminidase reaction</i> | 17 |

1.3.6 Neuraminidases produced by Pasteurellaceae 18

1.3.6.1 Neuraminidases in *P. multocida* 19

1.3.7 Neuraminidase produced by *M. haemolytica* 20

1.3.7.1 The role of neuraminidase in the metabolism of sialic acids in *M. haemolytica* 21

1.3.8 Neuraminidases of *Streptococcus pneumoniae*, a respiratory disease comparative model 22

1.3.8.1 Role of desialylation in pneumococcal infection 23

1.3.8.2 Desialylation-independent interaction of neuraminidases in pneumococcal infection 25

1.3.9 Inhibitors of neuraminidases 25

1.4 Type V secretion system 26

1.5 Conclusion 28

1.6 Aims of the project 29

2 Materials and methods 30

2.1 Bacterial strains 30

2.2 Genomic DNA isolation 30

2.3 Whole genome sequencing 31

2.4 Sanger sequencing 32

2.5 Sequence alignments 34

2.6 Prediction of functional domains (BLAST) 34

2.7 Predictions of tertiary structure (Phyre2) 34

2.8 *M. haemolytica* cell lysates 35

| | |
|--|-----------|
| 2.8.1 Concentration of culture supernatants | 36 |
| 2.9 Cloning and purification of <i>M. haemolytica</i> NanH catalytic domain | 36 |
| 2.9.1 Plasmid construction | 36 |
| 2.9.1.1 PCR amplification | 37 |
| 2.9.1.2 DNA digestion and T4 ligation | 38 |
| 2.9.1.3 Chemical transformation into <i>E. coli</i> KRX competent cells | 39 |
| 2.9.1.4 Identification of recombinant colonies by PCR | 40 |
| 2.9.1.5 Plasmid isolation and analysis by sequencing | 41 |
| 2.9.2 Protein expression | 42 |
| 2.9.3 Protein purification by HaloTag system | 43 |
| 2.9.4 Anion exchange chromatography (AEC) | 45 |
| 2.0.5 SDS-PAGE and western blot | 45 |
| Coomassie blue staining | 46 |
| Western blot | 47 |
| Horseradish peroxidase (HRP) detection with 4-chloro-1-naphthol solution | 47 |
| Detection by enhanced chemiluminescence (ECL) | 48 |
| 2.9.6 Mass spectrometry | 48 |
| 2.9.7 Neuraminidase activity assay | 49 |
| 2.9.7.1 Standard curve | 49 |
| 2.9.7.2 Sample dilutions | 50 |
| 2.9.7.3 Substrate | 50 |

2.9.7.4 Neuraminidase specific activity 50

2.9.8 Production of an anti-NanH antibody 53

2.10 *M. haemolytica* NanH catalytic domain 53

2.10.1 Site directed mutagenesis 53

3 Sequence analysis 59

3.1 Identification of sialic acid metabolism enzymes 60

3.2 Autotransporters 64

3.3 Autotransporter chaperones 64

3.4 NanH sequence conservation 65

3.5 Conclusions 72

4 Prediction of NanH tertiary structure 73

4.1 NanH architecture (BLAST) 73

4.2 Prediction of tertiary structure 75

4.3 Homology to TrSA 78

4.4 Predicted catalytic mechanism 81

4.5 Homology to Hbp and completion of β -barrel model 84

4.6 Conclusions 86

5 Delineation of the catalytic domain of NanH 87

5.1 Identification of neuraminidase activity in *M. haemolytica* 87

5.2 Expression and purification of NanH 88

5.2.1 Cloning and expression of NanH23 (Signal peptide absent) 88

5.3 Cloning and expression of different nanH truncations 93

5.4 Purification of the catalytic domain 98

5.5 Conclusions 104

6 Evaluation of NanH catalytic residues by amino acid substitution 105

6.1 Cloning and expression of mutants in NanH23 and NanHcat. 105

6.2 Disruption of arginine triad 108

6.3 Disruption on stabilisation of intermediate state 110

6.4 Proton donor residue 113

6.5 Hydrophobic pocket 115

6.6 Mutation of residues possibly involved indirectly 117

6.7 Comparison of enzyme activity after mutation. 120

6.8 Conclusions 122

7 Discussion 123

8 Final conclusions 132

9 References 134

List of figures

Figure 1. Pathogenesis of BRD 4

Figure 2. Structure of Neu5Ac derivatives 14

Figure 3. Tertiary structure of influenza, trypanosomal and pneumococcal neuraminidases 16

Figure 4. Diagram of proposed sialic acid metabolism 22

Figure 5. Standard curve made with known concentrations of *C. perfringens* neuraminidase 52

Figure 6. Alignment of *nmA* among *M. haemolytica* serotypes A1 and A6 62

Figure 7. Alignment of *nmA* among *M. haemolytica* serotypes A1, A2 and A6 63

Figure 8. Multiple sequence alignment of *nanH* from publicly available sequences of *M. haemolytica* 67

Figure 9. Multiple sequence alignment of translated *nanH* sequences showing AUNK01000017 variation 67

Figure 10. Multiple sequence alignment of translated *nanH* sequences showing LFYB01000017 variation 68

Figure 11. Multiple sequence alignment of NanH sequences from strains PHL213, ATCC 33396, MexA1 and MexA2 68

Figure 12. Multiple sequence alignment of neuraminidases with *Pasteurellaceae* origin 71

Figure 13. Diagram of NanH domains according to predictions made by sequence homology 74

Figure 14. Alignment of NanH to consensus sequence of conserved domains Cd15482 and Pfam03797 75

Figure 15. Multidomain 3D model of NanH 76

Figure 16. Alignment of NanH predicted 3D model and TrSA 3D structure 78

Figure 17. Sequence alignment and predicted secondary structure of NanH catalytic domain compared to TrSA 79

Figure 18. 3D model showing predicted catalytic residues of NanH by homology to TrSA 80

Figure 19. Predicted mechanism of NanH catalysis 82

Figure 20. 3D model showing predicted catalytic residues of NanH by homology to NanB 83

Figure 21. Predicted 3D model of NanH β -barrel domain 84

Figure 22. Sequence alignment and predicted secondary structure of NanH β -barrel domain compared to Hbp 85

Figure 23. Specific neuraminidase activity of *M. haemolytica* culture fractions 87

Figure 24. Map of NanH23 in pFN18K 89

Figure 25. Coomassie blue stained gel showing expression of NanH23 90

Figure 26. Coomassie blue stained gel showing NanH23 purification fractions 91

Figure 27. Coomassie blue stained gel showing NanH23 after protein concentration 92

Figure 28. Neuraminidase activity of NanH truncations expressed in *E. coli* 95

Figure 29. Coomassie blue stained gels showing expression of the different truncations of NanH 96

Figure 30. Western blot showing expression of the different truncations of NanH with an anti-HaloTag antibody 97

Figure 31. Coomassie blue stained gel showing NanHcat purification fractions 99

Figure 32. Coomassie blue stained gel showing AEC purification fractions 100

Figure 33. Neuraminidase activity of NanHcat purification fractions 101

Figure 34. Western blot showing expression of the different truncations of NanH with an anti-NanHcat antibody 103

Figure 35. Western blot showing expression of mutants in NanH23 with anti-HaloTag antibody 106

Figure 36. Western blot showing expression of mutants in NanHcat with anti-HaloTag antibody 107

Figure 37. Diagram showing putative arginine arginine triad in NanH 108

Figure 38. Neuraminidase activity of R356A mutants 109

Figure 39. Diagram showing putative amino acids that stabilise intermediate state 110

Figure 40. Neuraminidase activity of E277A and Y390D mutants 112

Figure 41. Diagram showing putative proton donor 113

Figure 42. Neuraminidase activity of D100A mutation 114

Figure 43. Diagram showing putative hydrophobic pocket 115

Figure 44. Neuraminidase activity of W164A mutant 116

Figure 45. Diagram showing putative interactions with OH-4 117

Figure 46. Diagram showing alternative docking model in which Ser330 coordinates Glu277 and Arg356 118

Figure 47. Neuraminidase activity of D138A and S330A 119

Figure 48. Coomassie blue stained gel and western blot using anti-NanHcat antibody showing purified mutant proteins 120

Figure 49. Neuraminidase activity of purified proteins 121

List of tables

Table 1. Concentration of components required for PCR using MyTaq mix. 32

Table 2. Temperature conditions required for PCR using MyTaq mix, *M. haemolytica* genomic DNA as template and primers required for amplification of *nanH*. 32

Table 3. Required concentration of DNA sample submitted for Sanger sequencing. 33

Table 4. Primers used for NanH sequencing 33

Table 5. Concentration of components required for PCR using Velocity DNA taq polymerase. 37

Table 6. Temperature conditions required for PCR using Velocity DNA taq polymerase, *M. haemolytica* genomic DNA as template and primers required for amplification of *nanH*. 37

Table 7. Components required for digestion of PCR product and plasmid vector using enzyme blend (Sgfl and PmeI). 38

Table 8. Components of DNA ligation using T4 DNA ligase (HC) to insert PCR product into plasmid vector pFN18K digested by enzymes Sgfl and PmeI. 39

Table 9. Concentration of components required for PCR using MyTaq mix for colony PCR. 40

Table 10. Temperature conditions required for PCR using MyTaq mix, *E. coli* transformed colonies as template and primers required for amplification of the cloning region of pFN18K (i.e. 7F and 7G). 41

Table 11. Primers used for cloning procedure 42

Table 12. Ingredients for preparing polyacrylamide gel 46

Table 13. Origin and clonality of antibodies used for western blot. 48

- Table 14.** Sample layout of neuraminidase activity assay 50
- Table 15.** List of primers used for site directed mutagenesis 55
- Table 16.** Concentration of components required for PCR using QuikChange II XL Site-Directed Mutagenesis Kit (Agilent, UK). 56
- Table 17.** Temperature conditions required for PCR using QuikChange II XL Site-Directed Mutagenesis Kit (Agilent, UK), pFN18KNanH23 plasmid as template and primers required for amplification of the plasmid with the desired mutation. 56
- Table 18.** Information about the sequences retrieved for comparison of genes of interest for this study 59
- Table 19.** Loci of genes that codify for enzymes involved in sialic acid metabolism 61
- Table 20.** Accession number of putative autotransporters of *M. haemolytica* 64
- Table 21.** Accession number of identified chaperones in *P. multocida* and homologues in *M. haemolytica* 65
- Table 22.** Summary of data used by Phyre² to predict a 3D model 77
- Table 23.** Diagrams depicting truncations made in NanH 93
- Table 24.** List of proteins matched to peptides identified by mass spectrometry. Peptide sequences aligned against *E. coli* database 102
- Table 25.** List of proteins matched to peptides identified by mass spectrometry. Peptide sequences aligned against *M. haemolytica* database 102

List of abbreviations

AEC: Anion exchange chromatography

BHI: Brain heart infusion

BHV-1: Bovine herpes virus-1

BPI-3: Bovine parainfluenza virus-3

BRD: Bovine respiratory disease

BRSV: Bovine respiratory syncytial virus

BSM: Bovine submaxillary mucin

BVDV: Bovine viral diarrhoea virus

CBM: Carbohydrate binding module

CPB: Citrate-phosphates buffer

CPS: Capsule

CRP: cAMP receptor protein

E1: Elute 1

E2: Elute 2

ECL: Enhanced chemiluminescence

FBS: Foetal bovine serum

Fru: Fructose

FT: Flowthrough

GlcNAc: N-acetyl-D-glucosamine

HN: hemagglutinin-neuraminidase

IL: Interleukin

Ins: Insoluble debris

IRP: Iron regulated protein

IT: Intramolecular *trans*-sialidases

KDN: Deaminated neuraminic acid

LC MS/MS: Liquid chromatography tandem mass spectrometry

LKT: Leukotoxin

LPS: Lipopolysaccharide

ManNAc: N-acetylmannosamine

ManNAcA: N-acetylmannosaminuroic acid

MUAN: 2'-(4-Methylumbelliferyl)- α -D-N-acetylneuraminic acid

Neu: de-N-acylated neuraminic acid

Neu5Ac: N-acetylneuraminic acid

Neu5Ac2en / DANA: 2,3-Dehydro-2-deoxy-N-acetylneuraminic acid

Neu5Gc: N-glycolylneuraminic acid

NeuC-like: UDP-N-acetylglucosamine-2-epimerase (Similar to NeuC of *E. coli*)

NmaA: UDP-N-acetylglucosamine-2-epimerase

NmaB: UDP-N-acetylmannosamine dehydrogenase

OMP: Outer membrane protein

PBMC: Peripheral blood mononuclear cells

PEP: Phosphoenol pyruvate

PMN: Polymorphonuclear neutrophils

PST: Polysialyl transferase

S-TEV: TEV cleaved soluble fraction

SDS-PAGE: Sodium dodecyl sulfate - Polyacrylamide gel electrophoresis

Sol: Soluble lysate

SSA-1: specific serotype 1 antigen

Sup: Culture supernatant

TNF- α : Tumour necrosis factor α

TVSS: Type V secretion system

1 Introduction

1.1 Bovine respiratory disease

Pneumonia in ruminants has always represented one of farmers' major concerns due to the high economic losses caused by surges in calf mortality figures and decreased growth rates. The incidence of the disease has been reported to be as high as 64% in beef cattle in The United States (Schneider et al., 2009), causing a decrease of nearly 6% in the average daily growth (Wittum et al., 1996).

In addition to the losses caused by a decrease in the general quality of the meat and the yield obtained after slaughter, treatment and prevention have been reported to represent 7% of total production costs in the bovine industry (Snowder et al., 2007). A different study in the USA estimated annual losses for beef cattle producers of \$500 million (Miles, 2009).

The bovine respiratory disease (BRD) is caused by the interaction of three components: adverse environmental factors that provide a suitable environment for respiratory disease, a primary agent which is usually a respiratory viral pathogen and a secondary agent which are bacteria from the family *Pasteurellaceae* that naturally inhabit the upper respiratory tract but reach the lower respiratory tract as opportunistic pathogens (Aitken, 2007, Maxie and Jubb, 2007, Panciera and Confer, 2010). Bovines are not exclusively affected by BRD, it is a problem that extends to all ruminants such as ovines, caprines and small camelids either domestic or wild.

BRD is also known as shipping fever due to the occurrence of pneumonia after transportation even though shipping is just one of the possible external factors that can cause the disease. Some authors also refer to BRD as ovine or bovine

pasteurellosis because the secondary agents are the responsible for causing the pneumonic lesions (Saadati et al., 1997, Aitken, 2007).

1.1.1 Aetiology

As previously mentioned, BRD is a complex formed by environmental factors, primary agents and secondary agents (Figure 1). The environmental factors represent external disturbances that create stressful conditions for the animals and affect the respiratory tract directly or indirectly. High variations in temperature and humidity in a short time can greatly disturb the respiratory tract. Therefore the region and the season of the year can have a big influence if the animals have inadequate housing. Other stressful situations are related to inadequate husbandry and farming practices such as a reduced food and water intake, high population density and poor hygienic conditions. However, some routine veterinary procedures such as transportation and weaning can predispose to BRD. Calves who fail to receive colostrum in the first 12 hours after birth, are at high risk of developing BRD (Edwards, 2010, Hodgson et al., 2012) .

The most common primary agents are bovine herpes virus-1 (BHV-1) (Yates et al., 1983), bovine parainfluenza virus-3 (BPI-3) (Jericho et al., 1982), bovine respiratory syncytial virus (BRSV) (Trigo et al., 1984, Sharma and Woldehiwet, 1990), bovine viral diarrhoea virus (BVDV) (Fulton et al., 2000) and *Mycoplasma* sp. (Dassanayake et al., 2010, Besser et al., 2014). Even though primary agents can cause respiratory disease in ruminants on their own, most of them only cause death when they are associated with a secondary bacterial infection hence, their importance relies more on the various mechanisms they use to facilitate infection of bacterial opportunists (Pancieria and Confer, 2010). For instance, infection with BHV-1 can increase bacterial colonisation by lysis of respiratory epithelial cells

during multiplication therefore, debilitating the host tissue. BRSV is known to multiply in ciliated respiratory cells and type II pneumocytes which can decrease bacterial clearance (Valarcher and Taylor, 2007, Sacco et al., 2014). The immune response is also known to be affected by BHV-1 by induction of apoptosis of CD4⁺ T cells, peripheral blood mononuclear cells (PBMC), polymorphonuclear neutrophils (PMN) and inhibition of CD8⁺ T cell activation (Jones and Chowdhury, 2007, Muylkens et al., 2007).

Mannheimia haemolytica, previously known as *Pasteurella haemolytica*, is the main secondary agent responsible for causing pneumonia in ruminants (Aitken, 2007, Zecchinon et al., 2005). The former species *Pasteurella haemolytica* was divided into two biotypes depending on the biochemical property to either ferment arabinose or trehalose as biotype A and T respectively. They were subsequently classified in thirteen A serotypes (A1, A2, A5, A6, A7, A8, A9, A12, A13, A14, A16 and A17) and four T serotypes (T3, T4, T10 and T15) (Zecchinon et al., 2005, Gyles, 2004). In 1990, all members of biotype T were reclassified as a different species called *Pasteurella trehalosi* which was again reclassified in a new genus as *Bibersteinia trehalosi* following 16S rRNA gene sequencing classification (Quinn, 2011, Blackall et al., 2007). In 1999, serotypes of *P. haemolytica* biotype A were reclassified into *Mannheimia haemolytica* except for serotype A11 which was included in the same genus but classified as *Mannheimia glucosida* (Gyles, 2004, Angen et al., 1999). The most common serotypes of *M. haemolytica* that can cause disease are A1 and A2 being A1 prevalence higher in cattle (Singh et al., 2011, Jaramillo-Meza et al., 2007) while A2 is more common in small ruminants (Davies and Donachie, 1996).

Pasteurella multocida can also cause BRD as a secondary agent but with a lower frequency than *M. haemolytica*. (Dabo et al., 2007). *P. multocida* is classified in 5

serogroups (A, B, C, D, E and F) and 16 serotypes. Serotype A3 is the most common isolate in BRD caused by *P. multocida* but strains from serogroup D have also been found, particularly in small ruminants (Ewers *et al.*, 2006, Arumugam *et al.*, 2011).

Histophilus somni is another Pasteurellaceae member that can produce BRD less commonly than *M. haemolytica* or *P. multocida*. *H. somni* does not have a capsule, it produces a lipo-oligosaccharide (LOS) that promotes platelet activation causing characteristic thrombotic lesions in the pulmonary vessels (Corbeil, 2007, Czuprynski, 2009).

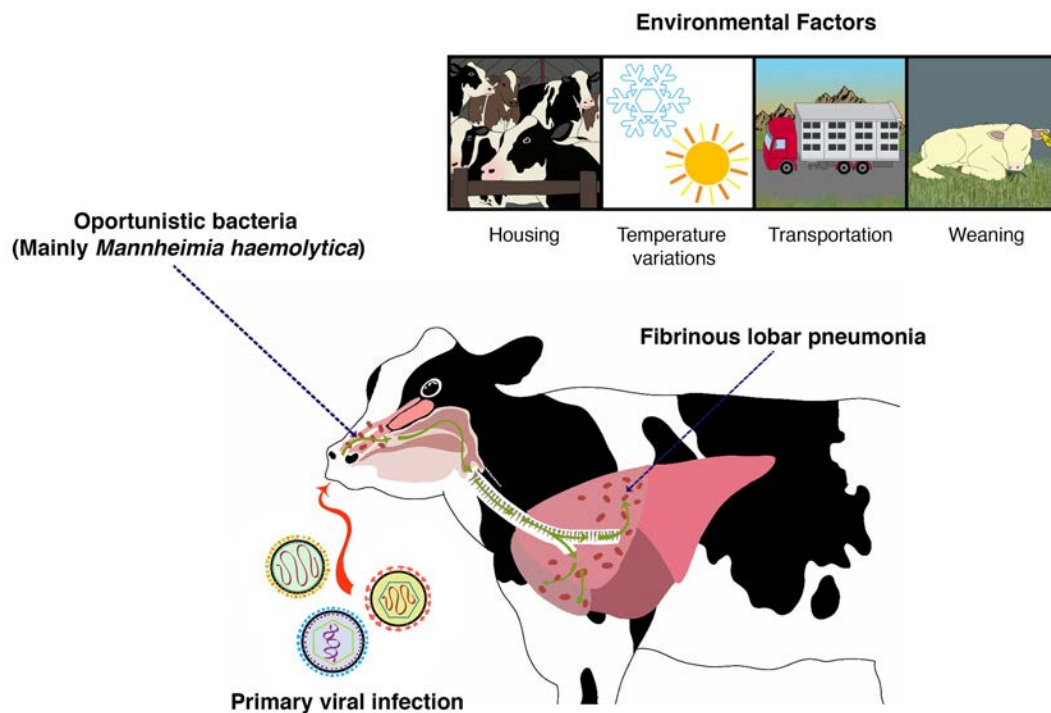


Figure 1. Pathogenesis of BRD. In the presence of adverse environmental factors in addition to infection with primary viral agents, bacterial commensals of the upper respiratory tract (mainly *M. haemolytica*) reach the lower respiratory tract. Lung consolidation is caused by the accumulation of neutrophils and ROS release due to leukotoxin driven lysis.

1.1.2 Pathology

The characteristic lesions found in necropsy, when BRD is caused by *M. haemolytica*, are areas of consolidation within lobes or that extend to complete lobes. Most commonly, the cranial lobes of the lung are affected with a fibrinous bronchopneumonia characterised by the presence of coagulated fibrin, augmented thickness of the interlobular septa, oedema and well defined foci of coagulative necrosis. As *M. haemolytica* multiplies, it can extend from the initially infected bronchi to the adjacent lobules, cover the whole lobe and infect the pleura resulting in an acute fibrinous pleuropneumonia that can cause a rapid death (Pancieria and Confer, 2010, Rehmtulla and Thomson, 1981). In contrast, when BRD is caused by *P. multocida*, lesions are usually suppurative and abscesses may be formed (Dabo et al., 2007).

The pneumonic lesions of BRD are caused by the indirect effect of the leukotoxin (LKT), the main virulence factor of *M. haemolytica*. In the presence of *M. haemolytica* in the lung, chemoattractant factors such as IL-8 and leukotriene B4 are produced by the alveolar macrophages that attract neutrophils to the infection site. However, LKT produces lysis of the neutrophils by small pore formation that is specific to ruminant leukocytes. Neutrophil lysis translates into the release of more chemoattractants that causes an exaggerated infiltration of neutrophils and macrophages, obstructing the alveoli and damaging the tissue due to released ROS (Maxie and Jubb, 2007).

The microscopic appearance of affected tissue is characterised by foci of coagulative necrosis in which the alveolar space is blocked by the presence of coagulated fibrin, neutrophils and macrophages in addition to necrotic leukocytes marking the limits of the foci (Maxie and Jubb, 2007).

1.1.3 Prevention and treatment

Treatment with antibiotics is generally effective to control the disease and limit the extension of the lesions in the lung. A study by Schneider et al. showed that carcass quality can be maintained at a good level despite infection when animals received treatment (Schneider et al., 2009). A review on methods to control BRD published by Edwards T.A., emphasises the importance of eliminating the external factors that predispose BRD by primarily improving animal housing and farming practices (Edwards, 2010). They also describe a procedure known as metaphylaxis, in which animals at high risk of developing BRD (Such as animals to be shipped or just received) are mass medicated to prevent an outbreak. Typical antimicrobials used include cephalosporines, florfenicol, tetracyclines, macrolides and tulathromycin (Edwards, 2010). However, there are various studies that independently have isolated field strains of *M. haemolytica* and *P. multocida* which are resistant to most of the previously mentioned antimicrobials (Sarangi et al., 2015, Rainbolt et al., 2016, Klima et al., 2014). Therefore antimicrobial usage should be reduced and prevention of the disease must be prioritised.

1.1.3.1 Vaccination

Most vaccines that are commercially available worldwide, are based on the chemical inactivation of *M. haemolytica*, *P. multocida* and *Histophilus somni*. These mixtures mainly contain killed *M. haemolytica* cultures made with the most common serotypes that cause disease in cattle and domestic small ruminants such as A1, A2 and A6. Additionally, in order to provide an immune response against LKT, cultures are grown at conditions that increase expression of the toxin (Jaramillo-Meza et al., 2007). The use of bacterin-toxoid mixtures can reduce

morbidity and mortality however, the response is specific not only to the capsular serotype but also to the different alleles of LKT (Lacasta et al., 2015).

In order to produce an immunogen that can protect in a less specific way, various studies have been performed. Gilmour et al (Gilmour et al., 1991) developed a vaccine, which is currently available in Europe as Bovipast®. It is based on the immune response against the iron regulated proteins (IRP) produced by *M. haemolytica*. Their vaccine contains IRP from serotypes A1, A2, A6 and A7, providing increased cross protection against other serotypes compared to other vaccines (Gilmour et al., 1991, Lacasta et al., 2015).

A live vaccine was developed by making a truncation in the *lktA* gene to genetically inactivate and attenuate a serotype A1 strain. Vaccination with this mutant provided protection against serotype A1 and A6 after challenge (Crouch et al., 2012). Live attenuated vaccines are currently licensed and available in the USA as Once PMH®.

Finally, there are studies focused on outer membrane antigens with promising results. Confer and Ayalew studied the protein PlpE which is highly conserved among the different serotypes of *M. haemolytica* (Ayalew et al., 2006), they identified the neutralising epitopes and made a fusion protein with the neutralising epitope of LKT that induced the production in mice of antibodies that neutralised LKT activity *in vitro* (Ayalew et al., 2008). Additionally, intra-nasal vaccination in calves provided antibody protection against challenge with *M. haemolytica* serotypes A1 and A6 (Ayalew et al., 2009).

1.2 *Mannheimia haemolytica*

M. haemolytica is a Gram negative bacterium with a rod or cocobacillus shape, it is a facultative anaerobe that normally inhabits the upper respiratory tract of

ruminants as a commensal. It is non-motile, it produces β -haemolysis and it is surrounded by a capsular polysaccharide which is the basis for serotyping (Lo et al., 2001, Quinn, 2011, Gyles, 2004).

1.2.1 Virulence factors

1.2.1.1 Capsule

The capsular polysaccharide of *M. haemolytica* is known to be a protective factor against the immune system by reducing neutrophil and alveolar macrophage phagocytosis, conferring protection against complement mediated lysis and reducing exposure of protein antigens (Chae et al., 1990, Czuprynski et al., 1991, Lindhout et al., 2013). The capsule also promotes adhesion to the respiratory epithelium which aids colonisation (Singh et al., 2011, Gyles, 2004, Quinn, 2011).

The difference between capsules of serotypes A1 and A2 is that the polysaccharide of A1 is formed by N-acetylmannosaminuroic acid (ManNAcA) and N-acetylmannosamine (ManNAc) (Lo et al., 2001, McKerral and Lo, 2002, Adlam et al., 1984) while serotype A2 has a polysialic acid capsule (Solana et al., 2001, Lindhout et al., 2013).

1.2.1.2 Outer membrane proteins

Several outer membrane proteins (OMP) of *M. haemolytica* have been identified as immunogens exhibited on the surface that are important for bacterial adherence and colonisation of the respiratory tract (Pandher et al., 1999). For instance, OmpA is an OMP that has been proven to be important for adherence of *M. haemolytica* to the respiratory epithelium (Kisiela and Czuprynski, 2009) by binding to the cell-surface fibronectin (Confer and Ayalew, 2013). Animals that recover from BRD and vaccinated animals, usually have high titers of anti-OmpA

antibodies (*Mahasreshiti et al., 1997*). Additional data has shown allelic variations in OmpA isolated from bovine and ovine strains of *M. haemolytica*, suggesting a role of OmpA in species specificity (*Davies and Lee, 2004, Hounsome et al., 2011*). Finally, a recent study showed that bovine apolactoferrin has a bactericidal effect on *M. haemolytica* by binding to OmpA (*Samaniego-Barron et al., 2016*).

Adhesion to the respiratory epithelium is also aided by the adhesin MhA which recognises N-acetyl-D-glucosamine residues (*Jaramillo et al., 2000*). Additionally, MhA can bind to a GlcNAc rich receptor expressed by neutrophils that stimulates oxidative burst (*De la Mora et al., 2006, De la Mora et al., 2007*).

The lipoprotein PlpE, is another important OMP that has been studied as a vaccine candidate due to its conservation and high immunogenicity via complement activation (*Ayalew et al., 2006, Pandher et al., 1998, Ayalew et al., 2009, Confer et al., 2009, Batra et al., 2016*).

1.2.1.3 Endotoxin: Lipopolysaccharide (LPS)

Similar to other Gram negative bacteria, the LPS of *M. haemolytica* is formed by a polysaccharide side chain or O antigen, a lipid A and inner and outer cores of oligosaccharides (*Singh et al., 2011*). The LPS plays an important role in the pathogenicity of *M. haemolytica* by activating the coagulation cascade, promoting platelet activation, activating macrophages and inducing the production of tumour necrosis factor α (TNF- α) which translate into thrombus formation, oedema and acute inflammation (*Gyles, 2004, Songer and Post, 2005*).

1.2.1.4 Leukotoxin

The leukotoxin is a small pore-forming toxin, member of the RTX family of toxins that contain characteristic repeats of the motif GGXGDXUX (X=Any amino acid,

U=Large hydrophobic amino acids, i.e. L/V/I/F/Y). RTX toxins are codified in an operon formed by four genes: CABD (Linhartova et al., 2010, Chenal et al., 2015). The gene *lktA* codifies the leukotoxin structural protein LktA, which contains the RTX motifs, also known as calcium binding motifs. Calcium ions are known to be required for the cytotoxic activity of RTX toxins and for appropriate folding of the motifs (Chenal et al., 2009).

RTX toxins are synthesised as protoxins that are activated by a post-translational acylation of internal lysine residues. It is thought that acylation is required to increase the hydrophobicity of the protein and form the small pores (Zecchinon et al., 2005). Even though LktA goes through the acylation step thanks to the acyltransferase LktC, recent experiments have shown that inhibition of acylation diminished LktA cytotoxicity but does not abolish it completely (Batra et al., 2015).

Secretion of RTX toxins is performed via the type I secretion system (TISS) in which 3 main components are involved: an ATP-binding cassette exporter (ABC transporter) that forms a complex with a membrane fusion protein (MFP) and an outer membrane protein codified in the bacterial chromosome. The ABC transporter of Lkt is encoded by *lktB* and the MFP is encoded by *lktD* (Delepelaire, 2004, Tseng et al., 2009).

The leukotoxin of *M. haemolytica* has specific cytotoxicity on ruminant leukocytes by specific attachment to β_2 integrins of ruminant origin on the CD18 fraction. β_2 integrins are formed by the β subunit CD18 and a variable α subunit that can be CD11a (CD11a/CD18 or LFA-1), CD11b (CD11b/CD18 or Mac-1), CD11c (CD11c/CD18 or CR4) or CD11d (Dileepan et al., 2005a, Dileepan et al., 2005b, Dassanayake et al., 2007a, Dassanayake et al., 2007b). Primary infection with BHV-1 has been reported to enhance the effects of LKT by enhancing expression of BoLFA-1 in infected PMN and PBMCs (Leite et al., 2002, Leite et al., 2005).

Even though the leukotoxin of *M. haemolytica* is an important component of the vaccines used against BRD, the sequence of the leukotoxin proteins is highly variable. Davies et al identified the variable regions in the sequence and classified the different alleles into 8 allelic groups of *lktA* (Davies et al., 2001, Davies et al., 2002).

1.2.1.5 Iron regulated proteins (IRP)

Donachie et al (Donachie and Gilmour, 1988) described that when *M. haemolytica* is grown in media with limited concentrations of iron, two immunogenic proteins are expressed and now are the basis for the commercial vaccine Bovipast®. A 35kDa IRP was characterised as FbpA, which is known to be part of the iron uptake system FbpABC (Lainson et al., 1991, Kirby et al., 1998)

1.2.1.6 Neuraminidase

M. haemolytica is known to produce an extra-cellular neuraminidase *in vitro* and during active pneumonic infection in cattle and small ruminants (Straus and Purdy, 1994, Straus et al., 1998). The biological role of the neuraminidase produced by *M. haemolytica* has not been confirmed but it is possible that it aids colonisation of the respiratory epithelium, similarly to other respiratory pathogens such as *Streptococcus pneumoniae* in humans (Singh et al., 2011).

1.2.2 Immune response to *M. haemolytica* infection

The alveolar macrophages secrete IL-8, IL- β , TNF- α , GRO α , ENA, platelet-activating factor and leukotriene B4 in response to LPS and LKT (Yoo et al., 1995a, Yoo et al., 1995b). Neutrophil recruitment is then mediated by IL-8, a

neutrophil chemoattractant and activator that stimulates oxydative burst and phagocytosis (Caswell et al., 1999, Meade et al., 2012).

Recent reports showed that Th17 and $\gamma\delta$ T cells respond to *M. haemolytica* and BRSV co-infection by the augmented expression of IL-17, IL-21 and IL-22 which increase the secretion of IL-8 and therefore, increase neutrophil recruitment (McGill et al., 2016).

1.3 Neuraminidases

Neuraminidases, also known as sialidases, are a family of enzymes found in eukaryotic cells, bacteria, protozoa and viruses that cleave terminal sialic acids from oligosaccharides, glycoproteins or glycolipids present on the surface of mammalian cells (Taylor, 1996).

1.3.1 Sialic acids

Sialic acids are a family of 9 carbon acidic terminal monosaccharides bound on C-2 by an α -ketosidical link to C-3 or C-6 of a sugar residue (α 2-3-, α 2-6- linkages) (Figure 2). In some molecules, more than one sialic residue can be bound to a glycan by an α 2-8- linkage to form an oligosialic acid or a polysialic acid (Varki, 1992, Varki and Schauer, 2009).

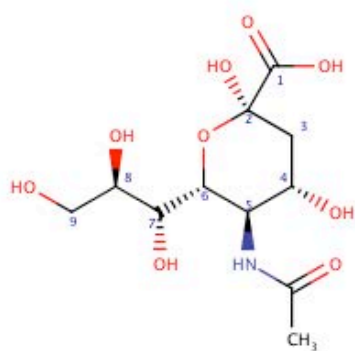
Depending on the group bound to C-5, sialic acids can be divided into four types: N-acetylneuraminic acid (Neu5Ac), N-glycolylneuraminic acid (Neu5Gc), deaminated neuraminic acid (KDN) and de-N-acylated neuraminic acid (Neu) (Varki, 1992, Varki and Schauer, 2009).

Neu5Ac is the most common sialic acid, it is present on all mammalian cell surfaces and it is also produced by invertebrates, bacteria and fungi. It contains a

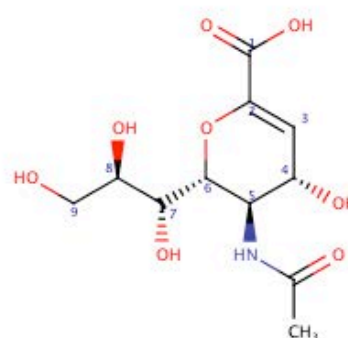
CH₃-COHN- group bound to C-5 and a hydroxyl group bound to C-2 in the free form (Angata and Varki, 2002).

Biologically important molecules present in mammals that contain sialic acid residues include mucins, immunoglobulin A, lactoferrin and sialo-oligosaccharides found in milk.

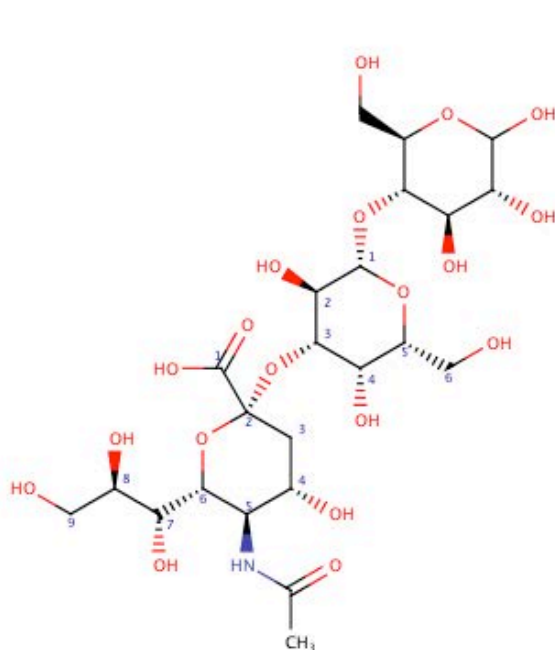
Mucins are highly sialylated glycoproteins produced by goblet cells on mucosal surfaces to lubricate and form a barrier that traps external particles (Lewis and Lewis, 2012). The glycocalix of endothelial cells of pulmonary arteries and microvascular vessels also contains abundant sialylated glycoproteins that keep the integrity of the endothelium (Cioffi et al., 2012). For that reason, colonisation by various respiratory pathogens might be influenced by the expression of neuraminidases.



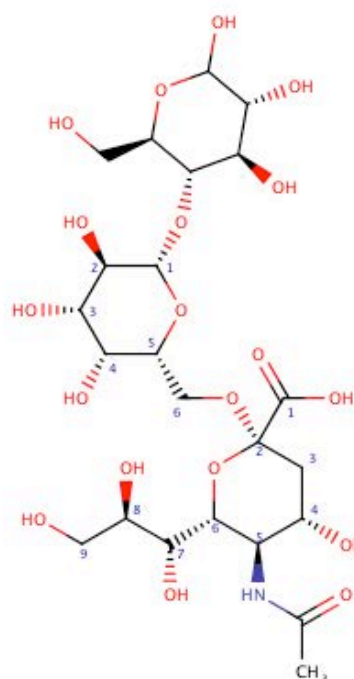
N-Acetylneuraminic acid(Neu5Ac)



2,3-Dehydro-2-deoxy-N-acetylneuraminic acid(Neu5Ac2en / DANA)



$\alpha(2,3)$ -Sialyllactose



$\alpha(2,6)$ -Sialyllactose

Figure 2. Structure of Neu5Ac derivatives obtained from Pubchem. Free Neu5Ac (CID: 444885) is bound to a hydroxyl group on C-2 while the inhibitor DANA (CID: 65309) is unsaturated. The α -ketosidical linkages 2,3 and 2,6 are depicted by $\alpha(2,3)$ -Sialyllactose (CID: 9963744) and $\alpha(2,6)$ -Sialyllactose (CID: 9963743) respectively.

1.3.2 Neuraminidases as virulence factors

Cleaving terminal sialic acids has proved to be a determinant factor in the onset of respiratory disease. The influenza virus type A and B exhibit different types of neuraminidases in a tetrameric haemagglutinin-neuraminidase (HN) complex. Sialidase activity is important for preventing aggregation of newly formed viral particles and for cleaving Neu5Ac from mucin of mucosal surfaces to reach their target cells (Shtyrya et al., 2009). In BRD, BPI-3 virus is also known to exhibit HN (Ellis, 2010). Bacterial species can produce sialidases for using sialic glycans as carbon source, to reveal glycoproteins and glycolipids that are targeted by toxins or to remove mucin and facilitate colonisation (Taylor, 1996, Kim et al., 2011).

1.3.3 Structure of neuraminidases

The sequence of neuraminidases can be highly variable but they all share the catalytic domain structure. For instance, the neuraminidase of influenza virus type A and B only share 30% of identity but their secondary and tertiary structure are identical (Shtyrya et al., 2009).

The typical tertiary structure of all neuraminidases consists of a propeller-like structure, known as β -propeller, formed by 6 antiparallel β -sheets with 4 strands each that surround the site where the substrate is cleaved (Taylor, 1996) (Figure 3). Neuraminidases can exist as monomeric molecules, such as the pneumococcal neuraminidases (Gut et al., 2011), or as multimeric molecules like the influenza neuraminidase which forms a tetramer (Shtyrya et al., 2009).

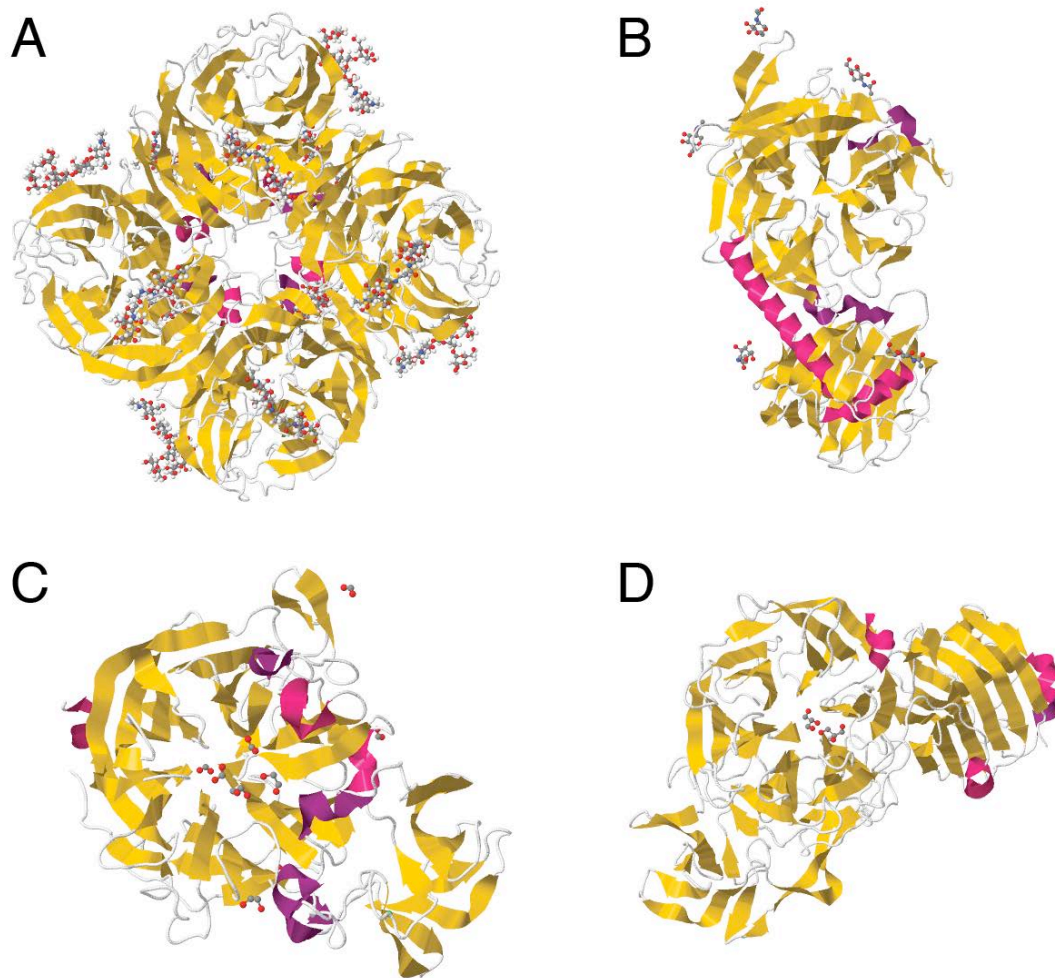


Figure 3. Tertiary structure of (A) neuraminidase of influenza virus A (PDB: 1NN2) (Varghese and Colman, 1991), (B) *T.rangeli* TrSA (PDB:1MZ5) (Buschiazzo et al., 2000), (C) *S.pneumoniae* NanA (PDB:2YA4) (Gut et al., 2011) and (D) NanB (PDB: 2VW0) (Xu et al., 2008).

1.3.4 Bacterial neuraminidases

The sequence of bacterial neuraminidases has been reported to show 30% identity between species, particularly due to the variability on their adjacent domains. However, they all share two types of motifs that can be considered the bacterial sialidases molecular signatures (Taylor, 1996). The first one is the RIP/ RLP motif which contains one arginine that directly interacts with the substrate. The second one is the Asp-box motif or bacterial neuraminidase repeats (BNR) (Xu et al., 2008) formed by Ser/Thr-X-Asp-[X]-Gly-X-Thr-Trp/Phe (X=any amino

acid), they are found between 1 to 5 times in the sequence of bacterial neuraminidases and although they are known to represent the fold between third and fourth strand of the β -sheets of the propeller, additional functions remain unknown (Roggentin et al., 1989, Gaskell et al., 1995).

1.3.5 Neuraminidase reaction

Neuraminidases can be classified into three groups according to the type of catalytic reaction they perform to cleave sialic residues: Hydrolytic sialidases, *trans*-sialidases and intramolecular *trans*-sialidases. Interestingly, TrSA is a hydrolytic neuraminidase produced by *Trypanosoma rangeli* while TcTS is a *trans*-sialidase produced by *Trypanosoma cruzi* (Amaya et al., 2003, Amaya et al., 2004). These neuraminidases are closely related as they are both produced by trypanosomal species and they show 70% amino acid identity but the substitution of just five key residues is sufficient to alter the mechanism of TrSA from hydrolysis to *trans*-glycosylation (Paris et al., 2005, Jers et al., 2014).

Hydrolysis is the most common type of reaction and it is performed by important neuraminidases such as the influenza neuraminidases, the pneumococcal neuraminidase NanA and the *P. multocida* neuraminidases NanH and NanB. The catalytic amino acids involved in the reaction and the mechanism are highly conserved among hydrolytic sialidases. Based on residue numbering of the neuraminidase TrSA, the reaction initiates when a sialylated glycan (Neu5Ac-OR) reaches the active site and the carboxylate group formed by C-1 binds to an arginine triad formed by Arg36, Arg246 and Arg315. The strong ionic interaction between these positively charged residues and the carboxylic group of the sialic residue, results in a change of conformation of Neu5Ac that allows hydroxylation by Asp60 of the O-2 bound to the glycan (HOR). A carbocation is formed on C-2

and stabilised by a covalent bond to Tyr343 aided by Glu231, which is believed to act as the proton acceptor. Finally, the unstable oxocarbenium is hydroxylated by a water molecule resulting in the release of Neu5Ac. Additional interactions include positioning of the C-5 bound N-acetyl chain into a hydrophobic pocket formed by Met96, Phe114, Trp121 and Val177. (Taylor and von Itzstein, 1994, Shtyrya et al., 2009, Buschiazzi et al., 2000).

The second group of neuraminidases is known as *trans*-sialidases. In this reaction, Neu5Ac is transferred to a different sugar by a *trans*-glycosylase reaction in which the oxocarbenium is hydroxylated by an acceptor sugar. The products are a hydroxylated donor glycan (HOR) and a sialylated acceptor sugar (Neu5Ac-OR'). Typically, *trans*-sialidases are specific to α 2-3- bonds (Amaya et al., 2003, Amaya et al., 2004).

Sialidases from the third group are known as intramolecular *trans*-sialidases (IT), also have specific cleavage to α 2-3- linked sialic acid and react by *trans*-glycosylation. In this reaction, the oxocarbenium is attacked by the hydroxyl group bound to C-7, resulting in a covalent bond between C-2 and O-7 therefore, 2,7-anhydro-NeuAc is released as a product from this reaction instead of Neu5Ac (Gut et al., 2011, Xu et al., 2011).

1.3.6 Neuraminidases produced by *Pasteurellaceae*

In addition to *M. haemolytica*, neuraminidase activity has been demonstrated in other members of the family *Pasteurellaceae* that include *P. multocida* (Scharmann et al., 1970), *Avibacterium gallinarum*, *A. volantium* (Hinz and Muller, 1977, Muller and Mannheim, 1995) and *Haemophilus parasuis* (Lichtensteiger and Vimr, 1997).

Regarding secondary agents that produce BRD, neuraminidase activity of *M. haemolytica* was reported and an exo-sialidase has been purified from culture supernatants (Straus et al., 1993a). Neuraminidase activity was also reported in *P. multocida* and an exo-sialidase was also purified from culture supernatants (White et al., 1995). Later, Mizan et al reported that *P. multocida* produces two neuraminidases: NanH and NanB (Mizan et al., 2000). Lichtensteiger and Vimr evaluated the possible sialidase activity of various members of the *Pasteurellaceae* family including *H. somni* however, they reported no activity from the clinical isolate that they tested (Lichtensteiger and Vimr, 1997).

1.3.6.1 Neuraminidases in *P. multocida*

The first report of the purification of a neuraminidase from *P. multocida* was obtained from culture supernatants by White et al however, when Mizan et al performed their experiments to isolate NanH and NanB, they were only able to see neuraminidase activity in cell lysates (White et al., 1995). The sequence analysis of NanB shows the typical structure of a protein secreted via type V secretion system (TVSS) due to the presence of a putative signal sequence on the N-terminus and a β -barrel domain on the C-terminus suggesting that it might be possible to find NanB in culture supernatants. Even though, the sequence of NanH did not show homology to known autotransporters, the predicted secondary structure showed the typical arrangement of 14 β -sheets that can form a β -barrel, a molecular signature and a signal peptide on the N-terminus (Mizan et al., 2000). Both neuraminidases of *P. multocida* were able to cleave α 2-3- and α 2-6- linked Neu5Ac by hydrolysis with preferential activity on α 2-3- linkages. However, NanB had a higher enzymatic speed on α 2-6- linkages than NanH. None of them have shown activity on α 2-8- bound Neu5Ac (Mizan et al., 2000).

1.3.7 Neuraminidase produced by *M. haemolytica*

Early reports of the neuraminidase produced by *M. haemolytica*, mention the production *in vitro* being mainly observed in bacterial lysates and, to a lesser extent, in culture supernatants (Scharmann et al., 1970, Frank and Tabatabai, 1981). However, extracellular production was confirmed by Straus et al (Straus et al., 1993b) when they concentrated the culture supernatant of a serotype A1 isolate of *M. haemolytica* and purified a sialidase with a molecular weight between 150 - 200kDa. In addition, they showed the presence of neutralising antibodies obtained from sera of experimentally infected goats (Straus and Purdy, 1994) and naturally infected cattle (Straus et al., 1998).

Neuraminidase activity was thought to be serotype related (Frank and Tabatabai, 1981). However, the only serotype without activity was A11, which was later reclassified as *Mannheimia glucosida* (Straus et al., 1993a). Therefore, we can conclude that all serotypes of *M. haemolytica* show neuraminidase activity (Singh et al., 2011).

When Straus et al isolated the neuraminidase secreted by *M. haemolytica*, they evaluated different substrates that included N-Acetylneuramin lactose, fetuin and bovine submaxillary mucin (BSM) concluding that hydrolysis rate decreased in the latter. These data suggest that the neuraminidase of *M. haemolytica* can cleave various α -ketosidical linkages such as the α 2-6- linkages found in N-Acetylneuramin lactose, the α 2-3- linkages found in fetuin and, in a lower degree, terminal sialic acid in BSM which is also α 2-3- linked (Straus et al., 1993a).

Finally, the whole genome sequence project published by Gioia et al reported an incomplete gene with the molecular signatures typical of neuraminidases that contain a C-terminal β -barrel domain (Gioia et al., 2006). In addition, Fernández et

al submitted the sequence of a neuraminidase of *M. haemolytica* with a 53% identity and 69% similarity to NanH of *P. multocida* and complete identity to the neuraminidase reported by Gioia et al (GenBank accession: EF215852.1) (Fernández Martínez, 2007).

1.3.7.1 The role of neuraminidase in the metabolism of sialic acids in *M. haemolytica*

Sialic acid is known to be required for the synthesis of the capsular polysaccharide of *M. haemolytica* by the formation of α 2,8-linked polysialic acid of serotype A2 capsules (Solana et al., 2001) or can be used to form ManNAc required by serotype A1 strains (Lo et al., 2001).

In *P. multocida*, free Neu5Ac is necessary for the production of CMP-Neu5Ac that is used for the sialylation of oligosaccharides such as the polysaccharide component of LPS (Thon et al., 2012). *P. multocida* is thought to obtain Neu5Ac by the effect of other bacteria occupying the same niche or by desialylation of Neu5Ac bound glycans of the host aided by the production of NanB and NanH following the sialic acid metabolism pathway known as scavenging (Steenbergen et al., 2005).

In contrast, *M. haemolytica* is believed to be able to synthesise Neu5Ac from ManNAc by a *de novo* pathway (Vimr et al., 2004, Barrallo et al., 1999). Additionally, *M. haemolytica* is also able to uptake free Neu5Ac cleaved from the host by its own neuraminidase therefore, it might be able to use both mechanisms to obtain Neu5Ac (Solana et al., 2001) (Figure 4).

Finally, ManNAc can also be catalysed into fructose-6-phosphate which can be used as an energy source through glycolysis (Severi et al., 2007, Ferrero and Aparicio, 2010, Li and Chen, 2012).

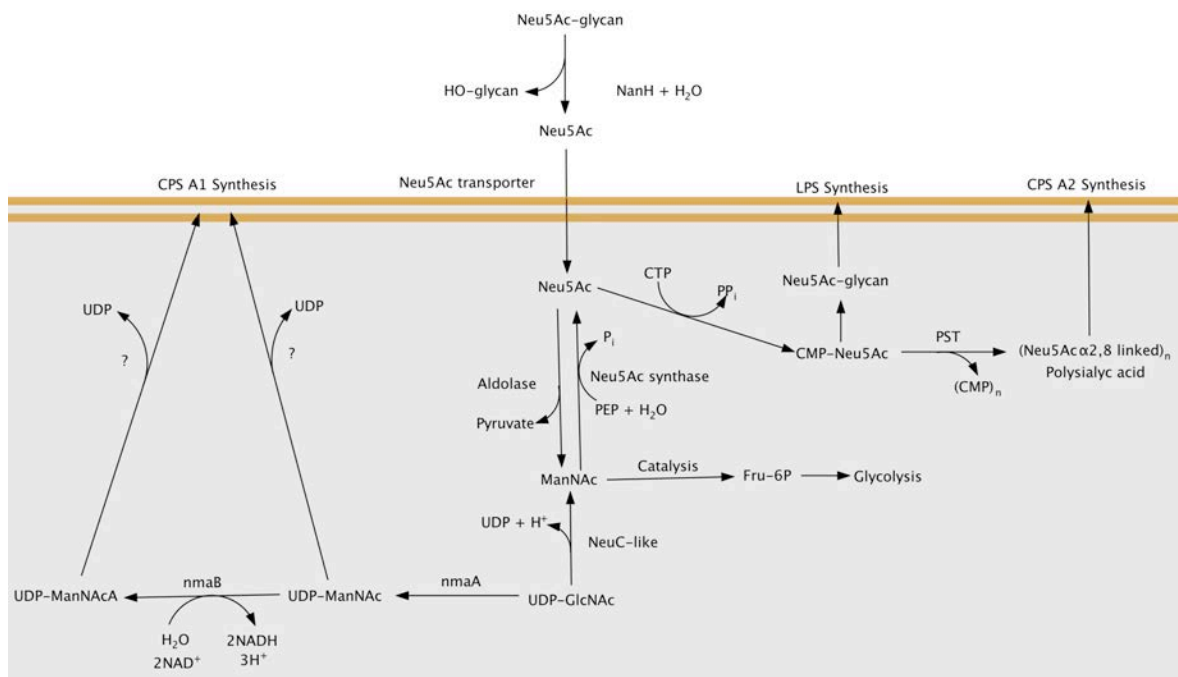


Figure 4. Diagram of proposed sialic acid metabolism based on metabolic pathways of *E. coli* (Severi et al., 2007, Ferrero and Aparicio, 2010, Li and Chen, 2012) and experimental data on *M. haemolytica* published by Lo et al (Lo et al., 2001), McKerral (McKerral and Lo, 2002) et al and Barrallo et al (Barrallo et al., 1999). Neu5Ac = N-Acetylneuraminic acid, ManNAc = N-Acetylmannosamine, ManNAcA = N-Acetylmannosaminourate, GlcNAc = N-Acetylglucosamine, Fru = Fructose, PEP = Phosphoenol piruvate, CPS = Capsule, PST = Polysialyl transferase, NeuC-like = UDP-N-acetylglucosamine-2-epimerase (Similar to NeuC of *E. coli*), NmaA = UDP-N-acetylglucosamine-2-epimerase, NmaB = UDP-N-acetylmannosamine dehydrogenase.

1.3.8 Neuraminidases of *Streptococcus pneumoniae*, a respiratory disease comparative model

S.pneumoniae produces 3 neuraminidases: NanA, NanB and NanC. All pneumococcal strains have a *nanA* gene, *nanB* is present in ~96% and *nanC* is only present in ~50% of strains (Pettigrew et al., 2006).

They share a similar structure which consists of a signal peptide at the beginning of the sequence, a lectin-like binding domain or carbohydrate binding module (CBM) which increases activity by recognising sialic acid (Xu et al., 2008), a catalytic domain which contains 4 Asp-box repeats and a third domain inserted into the catalytic domain. Additionally, NanA has a fourth domain which contains a

motif formed by Leu-Pro-Glu-Thr-Gly that attaches the enzyme to the bacterial membrane known as LPXTG anchor motif (*Xu et al., 2008, Camara et al., 1994, Hsiao et al., 2009*).

NanA catalyses sialic acid by hydrolysis cleaving either α 2-8-, α 2-3- or α 2-6-linked sialic acid into Neu5Ac while NanB is an IT so it reacts by *trans*-glycosilation strictly on α 2-3- bonds producing 2,7-anhydro-NeuAc (*Xu et al., 2008, Gut et al., 2008*). NanC has been reported to cleave α 2-3- linkages and catalyse into 2-deoxy-2,3-dehydro-N-acetylneuraminic acid (Nau5Ac2en or DANA) which is a sialidase inhibitor but after the accumulation of this product, NanC is able to then hydrate it into Neu5Ac. The molecular weight of NanA, NanB and NanC is 115kDa, 78kDa and 82kDa respectively (*Xu et al., 2011, Hayre et al., 2012*).

1.3.8.1 Role of desialylation in pneumococcal infection

Bacterial neuraminidases have been related to colonisation depending on the agent that produces them and the site of the disease. In cases like *Vibrio cholerae* infection, neuraminidase is crucial in the pathogenesis of disease since desialylation of host glycoconjugates reveals a toxin receptor (Corfield, 1992, Taylor, 1996).

Pneumococcal neuraminidases have different roles in colonisation and onset of infection depending on the site of *S.pneumoniae* interaction with the host. Desialylation of glycoconjugates in host cells and competing bacteria has been proposed as an important mechanism of adherence since *S.pneumoniae* produces other 2 surface exoglycosidases that may act consecutively after neuraminidases to effectively reveal adherence factors by deglycosylation (King et al., 2006, Kadioglu et al., 2008). Previous work has demonstrated that the presence of NanA and NanB increases colonisation and onset of infection in lower and upper

respiratory tract (Manco et al., 2006, Brittan et al., 2012) with an additional interaction being proposed which is the usage of sialic acid as a carbon source for bacterial growth (Burnaugh et al., 2008, Marion et al., 2011).

The role of desialylation by pneumococcal neuraminidases has not only been studied in the respiratory tract but in other models of pneumococcal infection with particular attention to its ability to reveal receptors. In the blood stream, platelets expose glycoconjugates susceptible to desialylation that are recognised by the Ashwell-Morell receptor in hepatocytes for elimination which results in moderation of the severity of disseminated intravascular coagulation (Grewal et al., 2008, Grewal et al., 2013).

Neuraminidase activity on PBMC causes augmented TLR exposure provoking exacerbated injury caused by their ligands such as increased recruitment of PMNs, induction of TNF- α , IL-1 β and chemokines caused by LPS association with TLR4 (Feng et al., 2012, Feng et al., 2013).

In pneumococcal haemolytic uraemic syndrome, NanA removes terminal sialic acid from glycoproteins in red blood cells revealing an antigen called Thomsen-Friedenreich antigen or T-antigen that is recognised by IgM antibodies causing erythrocyte agglutination and lysis (Loirat et al., 2012, Mele et al., 2014, Coats et al., 2011, Smith et al., 2013) .

Neuraminidases have been associated with pneumococcal biofilm formation. Parker et al showed that the inhibition of neuraminidase activity *in vitro* reduces biofilm formation (Parker et al., 2009). Upregulation of *nanA* and *nanB* has also been reported in biofilm models *in vitro*, particularly in the presence of sialic acid in the media (Trappetti et al., 2009, Oggioni et al., 2006).

Although research on neuraminidase has not primarily focused on its use as a vaccine, studies have shown that immunisation of chinchillas with NanA prevents

colonisation of the upper respiratory tract and middle ear therefore, by investigating colonisation increase in the otitis media model, more evidence was provided to support colonisation hypotheses (Long et al., 2004, Tong et al., 2005).

1.3.8.2 Desialylation-independent interaction of neuraminidases in pneumococcal infection

Studies on pneumococcal meningitis have shown that neuraminidases play an important role in blood-brain barrier adherence increasing colonisation due to a possible interaction of the lectin-like domain rather than desialylation (Uchiyama et al., 2009), as a result, NanA induces chemokine production and neutrophil recruitment (Banerjee et al., 2010).

1.3.9 Inhibitors of neuraminidases

Current inhibitors of sialidases that were developed as a treatment for influenza virus infection are based on the natural inhibitor DANA, an analogue of the transition state of Neu5Ac formed during hydrolysis. As shown in figure 2, C-2 of DANA is unsaturated therefore, it can form strong bonds to the catalytic site of neuraminidases without cleavage. Even though DANA is unable to block sialidase activity *in vivo*, it was used as a molecule backbone for designing the worldwide licensed antivirals zanamivir and oseltamivir. A problem that has to be tackled in the field of influenza research, is the quick mutation rate of the virus that has led to resistance to both antivirals in most of the seasonal strains. Newer neuraminidase inhibitors have been recently developed such as peramivir and lanamivir. Peramivir is currently licensed in the USA, Japan and Korea while lanamivir is only licensed in Japan (Yen, 2016, Air, 2012).

The viral neuraminidase inhibitors have been tested against pneumococcal neuraminidases in the hope of providing an added benefit to antivirals on a secondary infection with *S.pneumoniae*. Zanamivir and oseltamivir can partially inhibit activity of NanA compared to inhibition of the influenza neuraminidases (Gut et al., 2011). Treatment with oseltamivir resulted in augmented survival of experimentally infected mice (McCullers, 2004). Recently, Xu et al associated the high variability of NanA sequence to activity inhibition, showing that variations in the inserted domain and the lectin-like binding domain influence the susceptibility of NanA to neuraminidase inhibitors (Xu et al., 2016).

1.4 Type V secretion system

The sequences of the neuraminidases produced by *P. multocida* and *M. haemolytica* suggest secretion via type V secretion system (TVSS) (May et al., 2001, Gioia et al., 2006). Therefore, it is important to understand how this system works. The general structure of a protein secreted via TVSS contains an N-terminal signal sequence followed by a passenger domain, a linker sequence and a C-terminal β -barrel domain. There are five proposed subclasses of autotransporter mechanisms known as type Va, Vb, Vc, Vd and Ve. The general secretion mechanisms start by expression of the unfolded protein in the cytoplasm and transport to the periplasmic space via Sec system. Once in the periplasm, the signal peptide is cleaved off (Henderson et al., 2004, Leo et al., 2012).

The following steps vary depending on the type of autotransporter. The classical mechanism or type Va is typical of proteins such as the IgA protease of *Neisseria meningitidis*, EspP produced by *E. coli*, pertactin and BrkA, both produced by *Bordetella pertussis* (Leo et al., 2012). In this type of autotransporter, the chaperones Skp, FkpA, SurA and DegP prevent folding of the protein. The BAM

complex then recognises a conserved C-terminal motif (Robert et al., 2006) and the β -barrel inserts into the outer membrane. Two models of translocation have been proposed. In the hairpin model, the unfolded passenger domain is thought to be translocated into the extracellular space through the β -barrel while the second model suggests translocation through the BamA β -barrel. Both models propose that folding takes place after secretion although misfolded proteins may be present in the periplasmic space but they get degraded by DegP (Leyton et al., 2012). The passenger protein can remain attached to the β -barrel as a membrane associated protein or may be cleaved by asparagine cyclisation due to the interaction of an aspartate in the β -barrel that binds to an asparagine in the linker domain (Dautin et al., 2007, Barnard et al., 2007, Barnard et al., 2012).

Secretion system type Vb, also known as the two-partner secretion pathway, is transported through the outer membrane via a β -barrel however, the passenger domain (TpsA) and the β -barrel (TpsB) are expressed as independent proteins that recognise each other by a TPS domain in TpsA that interacts with a POTRA domain in TpsB (Henderson et al., 2004, Leo et al., 2012). In type Vc secretion, the β -barrel is thought to be a trimeric structure formed by the C-terminus domain of three molecules forming a single channel (Henderson et al., 2004). Type Vd is a recently described mechanism that resembles a combination between type Va and Vb as a single protein contains a passenger and a β -barrel domain but a POTRA domain is present between them. Type Ve is a suggested mechanism that acts in the same way as type Va however, the position of the domains is inverted therefore, the β -barrel is formed by the N-terminal domain and the passenger domain is on the C-terminus (Leo et al., 2012).

The functionality of TVSS in *M. haemolytica* has not been confirmed however, genome sequence analysis shows that *M. haemolytica* might produce two IgA

peptidases that contain a pertactin-like type Va autotransporter domain and two genes codifying for two YadA-like autotransporters that possibly form a trimeric pore typical of type Vc autotransporter (Gioia et al., 2006). Additionally, Daigneault and Lo showed the formation of Ahs trimmers, a protein suspected to form YadA-like β -barrel structures (Daigneault and Lo, 2009). The specific serotype 1 antigen (SSA-1) is an outer membrane protein that has been studied as a vaccine candidate (Lo et al., 1991, Ayalew et al., 2011) and it is also believed to be exported by TVSS due to its similarity to the group of the subtilase autotransporters (Henderson et al., 2004). The genome sequence of *P. multocida* also shows YadA and pertactin like autotransporters that have not been confirmed to be functional either (May et al., 2001).

Neuraminidases produced by both *P. multocida* and *M. haemolytica* are believed to be exported via TVSS due to the presence of all the autotransporter components in their sequence (Gioia et al., 2006, Mizan et al., 2000) however, the functionality of their autotransporter domain has not been confirmed.

1.5 Conclusion

Despite current efforts to eliminate BRD by treatment and prophylaxis, the disease still causes important economic losses for bovine, ovine and caprine producers due to mortality and reduction of carcass quality.

Neuraminidase has been poorly studied in *M. haemolytica* however, it might play an important role in colonisation, infection and metabolism. Therefore, by identifying the major structural moieties of the *M. haemolytica* neuraminidase we can propose this protein as a target for either treatment or prevention of BRD.

1.6 Aims of the project

Identify genes involved with the *M. haemolytica* neuraminidase that can provide information about the biological role of the enzyme. Clone and purify recombinant *M. haemolytica* NanH. Characterise the catalytic site of NanH to identify potential inhibition targets that can be studied in depth for future treatment and prophylactic strategies.

2 Materials and methods

2.1 Bacterial strains

Two of the strains of *Mannheimia haemolytica* used in this study were obtained from ATCC via LGC standards, UK in a lyophilised form. A sample was streaked from the pellets into 5% sheep blood agar and incubated at 37°C for overnight. One colony of each strain was transferred to 10ml of brain heart infusion (BHI) and incubated at 37°C with shaking for overnight. Cultures were centrifuged at 3000 x g for 10 minutes, the supernatant was discarded and the pellet was resuspended in BHI + 15% glycerol for storage at -80°C.

The first strain obtained from ATCC was strain PHL213 also known as SH789 or ATCC BAA-410. It is a serotype A1 strain originally isolated from the lung of a bovine with pneumonia (Fedorova and Highlander, 1997, Highlander et al., 2000) and it was first genome sequenced (Accession no. AASA00000000.1) by Gioia et al (Gioia et al., 2006).

The second strain is the type strain NCTC 9380 or ATCC 33396, originally isolated in the UK in 1956. It is a serotype 2 strain that was used by Angen et al for the reclassification of *Pasteurella haemolytica* into *Mannheimia haemolytica* by 16S rRNA sequencing (Angen et al., 1999).

2.2 Genomic DNA isolation

Strain 33396 was grown from the previously made glycerol stock in 5% sheep blood agar at 37°C for overnight. A colony was transferred into 10ml of BHI and incubated at 37°C with shaking for overnight. The culture was centrifuged at 3000 x g for 10 minutes, the supernatant was discarded and genomic DNA was isolated using the Wizard Genomic DNA Purification Kit (Promega, UK) from the cell pellet.

Concentration of isolated genomic DNA was measured using the Quant-iT dsDNA Assay Kit, broad range (Thermo Fisher Scientific, UK). Fluorescence was measured using the Qubit fluorometer (Thermo Fisher Scientific, UK).

Additionally, genomic DNA from two strains isolated in Mexico was kindly provided by Dr José Francisco Morales Álvarez. The strains, identified as MexA1 and MexA2, had been serotyped as A1 and A2 respectively. They are currently used as a source of leukotoxin for producing a toxoid used in immunisation of bovine, ovine and caprine calves, manufactured by INIFAP (Instituto Nacional de Investigaciones Forestales Agrícolas y Pecuarias) in Mexico.

2.3 Whole genome sequencing

A sample of genomic DNA from strains ATCC 33396, MexA1 and MexA2 was submitted to Microbes-NG for whole genome sequencing by the Illumina MiSeq platform. Sequencing of strains MexA1 and MexA2 was still under process at the time this work was submitted but the sequence of ATCC 33396 was obtained.

The Microbes-NG facility now has a standard analysis pipeline as follows: to identify the closest available reference genome using Kraken, and map the reads to this using BWA mem. Variants relative to the reference will be detected using [freebayes](#). Concurrently a de novo assembly of the reads is generated using [SPAdes](#), and the reads mapped back to the resultant contigs, again using BWA mem. The contigs are reordered and reoriented relative to the reference genome based on a [MUMmer](#) whole-genome alignment, and an automated annotation is performed using [Prokka](#) (<https://microbesng.uk/microbesng-faq/>).

However, whilst the facility developed this pipeline WGS data was analysed within the research group by Dr A. Mitchell. The raw data was downloaded as fastq files and both reference and de novo assemblies were performed on each data set

using the assembly functions of the CLC Genomics Workbench software package v9 (Qiagen - <https://www.qiagenbioinformatics.com/products/clc-genomics-workbench/>). Automated annotation was performed by submitting draft assemblies for Rapid Annotation using Subsystem Technology at <http://rast.nmpdr.org/> (Overbeek et al., 2014).

2.4 Sanger sequencing

The sequence of *nanH* of strains PHL213, MexA1 and MexA2 were amplified by PCR using MyTaq PCR mix (Bioline, UK) by preparing the following mix and optimising to the following thermo cycling conditions:

| Component | Concentration |
|--------------------------|-------------------------|
| 2x MyTaq mix | 25µl x (n+1) |
| Primers (10pmol/µl each) | 0.5µl x (n+1) (Each) |
| Water (Molecular grade) | Made up to 50µl x (n+1) |

n = Number of samples + 1 positive control + 1 negative control.

Table 1 . Concentration of components required for PCR using MyTaq mix.

| Step | Temperature | Time | Cycles |
|------------------|-------------|------------|--------|
| Initial denature | 95°C | 1min | 1 |
| Denature | 95°C | 30s | |
| Annealing | 55°C | 30s | 35 |
| Extension | 72°C | 1min | |
| Final extension | 72°C | 10min | 1 |
| Final hold | 4°C | Indefinite | |

Table 2. Temperature conditions required for PCR using MyTaq mix, *M. haemolytica* genomic DNA as template and primers required for amplification of *nanH*.

A 5µl sample of each PCR product was diluted in FastDigest green buffer 10x (Thermo Fisher Scientific, UK) and loaded on a 1% agarose gel + SYBR Safe Stain (Thermo Fisher Scientific, UK) made in TAE buffer. Gel electrophoresis was performed at 100V for 25min.

After confirmation of the presence of a ~2.4kbp band, the amplified reaction was cleaned using the Wizard SV Gel and PCR Clean-Up System (Promega, UK).

Sanger sequencing service was provided by The Functional genomics Laboratory in the School of Biosciences at the University of Birmingham (<http://www.birmingham.ac.uk/facilities/genomics/about/sequencing.aspx>).

The genomic DNA template was diluted with the appropriate sequencing primer as shown:

| Component | Concentration |
|-------------------------|-----------------|
| DNA template | ~100ng |
| Primer | 3.2pmol |
| Water (Molecular grade) | Make up to 10µl |

Table 3. Required concentration of DNA sample submitted for Sanger sequencing.

Sequencing results were trimmed depending on peak quality and aligned against the sequence of NanH (EF215852) using software CLC Main Workbench 7 (Qiagen).

| Primer name | Sequence |
|-------------|-----------------------------|
| EcoRI-NanH | CGCGCGGAATTCAATGAGAAAAATCAA |
| XhoI-NanH-R | CGCGCTCGAGTTACCAGTTATAACTTA |
| NanH-int-R2 | CTTTAATAGTGGCAGCTGG |
| NanH-int-F2 | TCCAGGTTTCAGGTAATGCC |
| NanH-int-F3 | GATGTGCGGTTTGAATTG |
| NanHfl1 | CGGAAAAAGGGACAATGGATAACC |
| NanHfl2 | GGGTTATGGGATTGATTATGC |

Table 4. Primers used for NanH sequencing.

2.5 Sequence alignments

Multiple sequence alignments were performed using the tool CLUSTALO (Sievers et al., 2011), incorporated as a plugin of the software CLC Main Workbench 7 (Qiagen).

Results were highlighted for conservation using ESPript 3.0 (Robert and Gouet, 2014).

2.6 Prediction of functional domains (BLAST)

All protein alignments performed with BLAST were done through the NCBI online tool by comparing sequences to non-redundant protein sequences (nr) (databases: GenBank CDS translations, PDB, SwissProt, PIR, PRF) using the blastp (protein-protein BLAST) algorithm (Marchler-Bauer and Bryant, 2004, Marchler-Bauer et al., 2009, Marchler-Bauer et al., 2011, Marchler-Bauer et al., 2015).

2.7 Predictions of tertiary structure (Phyre²)

Protein tertiary structure was modelled by sequence homology to the coordinates of similar proteins with a known tertiary structure that had been previously solved by crystallography methods using the server Phyre² (Kelley and Sternberg, 2009, Kelley et al., 2015).

The sequence alignment was retrieved from the table of results provided by Phyre² and results were highlighted for the conservation of primary and secondary structure using ESPript 3.0 (Robert and Gouet, 2014).

Tertiary structure models were analysed with MacPymol (Schrödinger). This software was used for tertiary structure alignments, identification of active site, prediction of enzyme-substrate interactions and for sketching final figures.

2.8 *M. haemolytica* cell lysates

M. haemolytica strains 33396 and PHL213 stored at -80°C were resuscitated by transferring a sample from glycerol stock into 5% sheep blood agar using a sterile plastic loop and incubating at 37°C for overnight. One colony of each strain was then transferred into 10ml of RPMI 1640 (Sigma, UK) + 3% Foetal bovine serum (FBS) (Sigma, UK) and incubated at 37°C with shaking for overnight. One millilitre of each overnight culture was transferred into 50ml of RPMI 1640 + 3% FBS and incubated at 37°C with shaking until OD₆₀₀ reached ~0.6. The cultures were centrifuged at 3000 x g for 5 minutes, the pellets were resuspended in 200ml of RPMI 1640 + 3% FBS pre-warmed at 37°C and incubated for an additional 4 hours.

Bacterial cultures were centrifuged at 3000 x g for 15 minutes, the supernatant was filter sterilised with a 500ml Vacuum filter/storage bottle system, 0.22µm pore (Corning, UK) and stored at 4°C identified as “Supernatant” or “Sup”. The cell pellet was resuspended in 10ml PBS and centrifuged again under the same conditions. The pellet was washed in the same way 3 times and resuspended in 10ml PBS afterwards. Washed pellets were supplemented with 50µl of 25x cComplete EDTA free protein inhibitor cocktail (Roche, UK), 1mM benzamidine (Sigma, UK) and 1µg/ml DNase I (Sigma, UK).

The cell pellet was disrupted in a constant systems cell disrupter at 12KPsi and centrifuged at 12000 x g for 25 minutes. The supernatant was filter sterilised with a 0.2µm pore syringe filter (Millipore, UK) and stored at -20°C labelled as “Soluble lysate” or “Sol”. The pellet was washed in PBS 3 times, resuspended in 10ml of PBS afterwards and 1ml was stored at -20°C labelled as “Insoluble cell debris” or “Ins”.

2.8.1 Concentration of culture supernatants

After filter sterilising the culture supernatants, 100ml from each strain were concentrated using an Amicon Ultra-15 Centrifugal filter unit (Millipore, UK) with a cut-off point of 100kDa. The flow-through was subsequently concentrated with a 50kDa cut-off point centrifugal filter unit. Concentrate solutes were resuspended in 500µl and stored at -20°C. A sample of each fraction was stored at -20°C in order to analyse supernatant fractions smaller than 50kDa, between 50kDa and 100kDa and larger than 100kDa.

2.9 Cloning and purification of *M. haemolytica* NanH catalytic domain

2.9.1 Plasmid construction

Plasmid constructs were initially designed in vector pET33b for 6x His-tag purification however, when the constructs were made and cloned into *E. coli* strain α-select (Bioline, UK), the random mutation rate was very high. Additionally, when a construct with no mutations was obtained and cloned into BL21 (DE3) (NEB, UK) for protein expression, no soluble protein was expressed.

In order to solve both problems, the HaloTag System engineered by Promega was used instead. Briefly, protein purification is performed by fusing the protein of interest to a HaloTag for increased solubility. The HaloTag forms a covalent bond with the HaloTag resin and it is subsequently cleaved off using a TEV protease. The TEV protease is fused to a 6x His-tag so it can be removed by nickel affinity. The resulting preparation contains a purified protein without a peptide Tag.

Plasmid constructs were made according to instructions of the manufacturer of vector pFN18K (Promega, UK) which is part of the HaloTag System.

2.9.1.1 PCR amplification

Inserts were amplified by PCR using velocity DNA taq polymerase (Bioline, UK), a high fidelity polymerase used to decrease the mutation rate. Reaction mix and PCR conditions were prepared as follows:

| Component | Concentration |
|-----------------------------|------------------------------------|
| 5x Hi-Fi Reaction Buffer | 10µl |
| 100mM dNTP Mix | 0.5µl |
| DNA template | 50-100ng |
| Primers | 10pmol each |
| Velocity DNA taq polymerase | 0.5U |
| DMSO | 1.5µl (Only when template is gDNA) |
| Water (Molecular grade) | Made up to 50µl per reaction |

Table 5. Concentration of components required for PCR using Velocity DNA taq polymerase.

| Step | Temperature | Time | Cycles |
|------------------|-------------|------------|--------|
| Initial denature | 98°C | 2 min | 1 |
| Denature | 98°C | 30s | |
| Annealing | 55°C | 30s | 30 |
| Extension | 72°C | 15s / kb | |
| Final extension | 72°C | 10min | 1 |
| Final hold | 4°C | Indefinite | |

Table 6. Temperature conditions required for PCR using Velocity DNA taq polymerase, *M. haemolytica* genomic DNA as template and primers required for amplification of *nanH*.

PCR products were diluted in FastDigest green buffer 10x (Thermo Fisher Scientific, UK) and loaded on a 1% agarose gel + SYBR Safe Stain (Thermo Fisher Scientific, UK) made in TAE buffer. Gel electrophoresis was performed at 100V for 25min.

The size of the bands was compared to invitrogen 1Kb Plus DNA Ladder (Thermo Scientific, UK). Bands with the expected size were excised from the gel and cleaned using Wizard SV Gel and PCR Clean-Up System (Promega, UK) however, DNA was eluted in 25µl in the last step to increase the concentration in the samples. The concentration of the PCR product was calculated using Quant-It dsDNA Assay Kit BR and read in Qubit fluorometer.

2.9.1.2 DNA digestion and T4 ligation

Plasmid vector pNF18K and PCR product were digested using the Flexi Enzyme Blend (Sgfl & Pmel) (Promega, UK) in separate reaction mixes as follows:

| Component | PCR product digestion | Vector digestion |
|------------------------------|-----------------------|------------------|
| 5x Flexi Digest Buffer | 4µl | 4µl |
| DNA | ~500ng | 200ng |
| Enzyme blend (Sgfl and Pmel) | 4µl | 2µl |
| Water (Molecular grade) | 12µl | Make up to 20µl |

Table 7. Components required for digestion of PCR product and plasmid vector using enzyme blend (Sgfl and Pmel).

Reactions were incubated at 37°C for 1 hour. Vector digestion mix was incubated at 65°C for 20min for enzyme inactivation and kept on ice until next step. PCR product digestion mix was cleaned using Wizard SV Gel and PCR Clean-Up system. The concentration of the PCR product was calculated using Quant-It dsDNA Assay Kit BR and read in Qubit fluorometer.

Digested PCR product and vector were ligated using T4 DNA Ligase (HC) (Promega, UK) by setting the following mix:

| Component | Concentration |
|-------------------------|-----------------------|
| Digested vector | 10 μ l |
| Digested PCR product | 3 μ l |
| T4 DNA Ligase (HC) | ~150ng |
| Water (Molecular grade) | Make up to 20 μ l |

Table 8. Components of DNA ligation using T4 DNA ligase (HC) to insert PCR product into plasmid vector pFN18K digested by enzymes Sgfl and Pmel.

Ligation reaction was incubated for 1 hour at room temperature and cloned into *E. coli* Single Step (KRX) Competent Cells (Promega, UK) by chemical transformation.

2.9.1.3 Chemical transformation into E. coli KRX competent cells

Cells initially stored at -80°C, were thawed on ice and 50 μ l were transferred into 1.5ml microfuge tubes. 5 μ l of ligation mix were transferred into one of the tubes containing thawed cells, additionally, a positive control transformation reaction was set with 50ng of pET33bPLY (Made by previous members of the group, this plasmid provides kanamycin resistance just as pFN18K) and a negative control transformation with 5 μ l of molecular grade water. Cells with DNA sample were incubated on ice for 30min and heat shocked for 20s at 42°C followed by a 2 minute incubation on ice. Heat shocked cells were resuspended in 500 μ l of SOC media and incubated at 37°C with shaking for 1 hour. A sample of 100 μ l was transferred to an LB agar plate and a second one of 100 μ l into an LB plate containing 50 μ g/ml kanamycin. For the control reactions, only 1 plate of plain LB and 1 plate of LB + antibiotic were prepared while cells transformed with ligation mix were transferred into 1 plain LB plate and 4 plates of LB + antibiotic in order to increase the probability of finding a correct plasmid.

2.9.1.4 Identification of recombinant colonies by PCR

Colonies were analysed by colony PCR using primers 7F and 7G that amplify the sequence within the plasmid pFN18K localised between the T7 promoter and T7 terminator that contains the Sgfl and PmeI cloning site in which the PCR product is expected to be cloned.

The PCR reaction mix was prepared using MyTaq Mix (Bioline, UK) at the following concentrations:

| Component | Concentration |
|--------------------------------|-------------------------------|
| 2x MyTaq Mix | 12.5 μ l x (n+1) |
| Primers (10pmol/ μ l each) | 0.25 μ l x (n+1) (Each) |
| Water (Molecular grade) | Made up to 25 μ l x (n+1) |

n = Number of analysed colonies + 1 positive control + 1 negative control.

Table 9. Concentration of components required for PCR using MyTaq mix for colony PCR.

Reaction mix was prepared as a master mix and divided in 200 μ l microfuge tubes depending on the number of colonies to be analysed in addition to 1 positive and 1 negative control. Using sterile pipette tips, colonies were transferred to each tube and then to a plate containing LB agar + 50 μ g/ml kanamycin with a grid drawn on the outside in order to identify each colony properly. The PCR reaction was set in a thermo cycler under the following conditions:

| Step | Temperature | Time | Cycles |
|------------------|-------------|------------|--------|
| Initial denature | 95°C | 1min | 1 |
| Denature | 95°C | 30s | |
| Annealing | 55°C | 30s | 30 |
| Extension | 72°C | 2min | |
| Final extension | 72°C | 10min | 1 |
| Final hold | 4°C | Indefinite | |

Table 10. Temperature conditions required for PCR using MyTaq mix, *E. coli* transformed colonies as template and primers required for amplification of the cloning region of pFN18K (i.e. 7F and 7G).

The PCR products were analysed by gel electrophoresis on a 1% agarose gel + SYBR Safe Stain as previously described.

Colonies in which it was possible to identify a band with the size of the insert plus HaloTag gene, T7 promoter and T7 terminator, were transferred into 10ml of LB + 50µg/ml Kanamycin by duplicate and incubated at 37°C with shaking for overnight. Obtained cultures were centrifuged at 3000 x g for 10min and supernatant was removed. One of the pellets was resuspended into 10ml of LB + 15% glycerol and stored at -80°C while the other one was used for plasmid isolation.

2.9.1.5 Plasmid isolation and analysis by sequencing

Plasmid was isolated using the GeneJET Plasmid Miniprep Kit (Thermo Scientific, UK) according to manufacturer instructions but eluted in 25µl of elution buffer in order to get a plasmid preparation with a higher concentration.

In order to confirm that the gene of interest was inserted into the vector and no unwanted mutations were present, the plasmid was submitted to the Functional

Genomics Laboratory for determination of the sequence by Sanger sequencing.

The samples were prepared as previously mentioned.

| Primer name | Sequence |
|-----------------|--|
| Sgfl-NanHG63-F | AGGAGCGATCGCCGGTGAAGCTGCAGGTACTGCGCCATTATATT |
| Sgfl-NanHG23-F | GACGGCGATCGCCAACCTCTGATTTTTGGAAAAGC |
| PmeI-NanH23-R | ACGTGTTTAAACCCAGTTATAACTTACATTTAGACC |
| PmeI-NanHL435-R | ACGTGTTTAAACAAGTTCATCTGGTAATCCCCA |
| 7F | TAATACGACTCACTATAGGG |
| 7G | GCTAGTTATTGCTCAGCGGTG |
| pFN18K-seq-F | GTCTGAATCTGCTGCAAGA |

Table 11. Primers used for cloning procedure.

2.9.2 Protein expression

Expression was controlled with the addition of glucose and rhamnose. The *E. coli* strain KRX contains the rhamnose inducible promoter *rhaP_{BAD}* that controls the expression of T7 RNA polymerase. Additionally, transcription is controlled by a cAMP receptor protein (CRP) which is not activated when glucose is being used as a carbon source due to low levels of cAMP (Hartnett et al., 2006).

KRX strain is unable to metabolise rhamnose due to the deletion of *rhaBAD* (replaced by T7 RNA polymerase gene) however, it cannot induce expression until glucose has been completely catabolised and cAMP levels have risen.

Bacteria were grown by transferring one colony into 10ml of LB + 0.5% glucose + 50µg/ml kanamycin and incubating at 37°C with shaking for 8-12 hours. A sample of 500µl was taken after incubation, centrifuged at 3000 x g for 15min and resuspended into 50ml of expression media (LB + 0.05% glucose + 0.05% rhamnose + 50µg/ml kanamycin). The 50ml culture was incubated at 28°C with shaking for 20 hours.

The culture was centrifuged at 3000 x g for 20 minutes, a sample of 1ml was taken, filter sterilised and labelled as “Culture supernatant” or “Sup”. The remaining supernatant was discarded, cell pellet was afterwards resuspended in 10ml of PBS, centrifuged at 3000 x g for 10min, supernatant was removed and pellet was washed two more times with PBS to complete a total of 3 washes with PBS. After the last wash, the cell pellet was resuspended in 10ml of PBS.

Washed cell pellet was supplemented with 50µl of 25x cOmplete EDTA-free Protease inhibitor cocktail (Life technologies, UK) + benzamidine + DNase I (Sigma, UK) and disrupted in a constant systems cell disrupter at 12 KPSI.

Disrupted cells were centrifuged at 20000 x g for 25 minutes, the supernatant was filter sterilised and labelled as “Soluble lysate” or “Sol”. The pellet was washed in PBS three times and resuspended in 10ml of PBS. A 1ml sample was taken and labeled as “Insoluble cell debris” or “Ins”.

2.9.3 Protein purification by HaloTag system

Protein expression was induced as mentioned before however, when cultures were made for protein purification, the volumes were increased 10 times. Therefore, one colony of *E. coli* containing the plasmid construct with the sequence of the protein of interest was transferred to 10ml of LB + 50µg/ml kanamycin + 0.5% glucose, incubated at 37°C with shaking for 8-12 hours. A sample of 5ml was centrifuged at 3000 x g for 15 minutes, the pellet was resuspended in 500ml of LB + 50µg/ml kanamycin + 0.05% glucose + 0.05% rhamnose and incubated for an additional 20 hours at 28°C with shaking.

The culture was centrifuged at 3000 x g for 20 minutes, 1ml of supernatant was filtered sterilised and stored for further analysis. Cell pellet was washed three times with PBS, supplemented with 1 tablet of EDTA-free Protease inhibitor

cocktail (Life technologies, UK) + 1mM benzamidine (Sigma, UK) + 1µg/ml DNase I (Sigma, UK) and disrupted in a constant systems cell disrupter at 12 KPSI.

Cell lysate was centrifuged at 20000 x g for 25 minutes, soluble fraction was filter sterilised while insoluble cell debris was washed with PBS three times and 1 ml was stored for analysis.

HaloLink Resin (Promega, UK) was centrifuged at 1000 x g for 5min and washed three times with HaloTag Protein Purification Buffer (50mM HEPES (pH7.5), 150mM NaCl) for equilibration using the same centrifuge parameters. After the final wash, the resin was resuspended in 5ml of soluble cell lysate and incubated at room temperature for 1 hour in a tube rotator. The suspension was centrifuged at 1000 x g for 5min, a 100ml sample of the supernatant was stored for further analysis labelled as “Flowthrough” or “FT” and the resin was washed three times with HaloTag Protein Purification Buffer. The protein of interest was removed from the resin by adding 1ml of 6% TEV Protease (Promega, UK) and incubating at room temperature in tube rotator for 1 hour. Simultaneously, 10µl of 6% TEV Protease were added to 50µl of soluble cell lysate, incubated at room temperature for 1 hour and stored for analysis as “S-TEV”.

The resin was centrifuged at 3000 x g for 5 minutes, the supernatant was taken, the resin was resuspended in 1ml of HaloTag Protein Purification Buffer, centrifuged again at 3 000 x g for 5 minutes and the second supernatant was mixed with the first supernatant. A sample of 100µl was labelled as “elute 1” or “E1” and stored for analysis.

TEV protease has a x6 His-Tag so the enzyme was removed from the first elute by adding 50µl of 50% HisLink Resin (Promega, UK) and incubating at room temperature for 20 minutes in a tube rotator. The suspension was centrifuged at

1000 x g for 5 minutes, supernatant was filter sterilised and a 100µl sample was stored as “elute 2” or “E2”.

2.9.4 Anion exchange chromatography (AEC)

The original protocol published in the HaloTag System manual indicates that the second elute should be the purified protein. However, an additional step was included in later protein preparations after detecting HaloTag associated chaperonins in the first purified protein. This is explained in more detail in the results section.

Elute 2 was dialysed in a 10K MWCO dialysis membrane against 2L of AEC start buffer (20mM Tris-HCl, pH8.0) at 4°C for 24 hours. Dialysed protein preparation was taken out of the dialysis membrane and transferred to a 1ml HiTrap Capto Q column (GE Healthcare, UK) using a peristaltic pump. The protein was then eluted in an ÄKTAPrime purifier (GE Healthcare, UK) by increasing concentrations of the elution buffer (150mM Tris-HCl, 1M NaCl, pH8.0) and retrieving in 1ml fractions.

Fractions were analysis by SDS-PAGE stained with Coomassie blue. The fraction containing the protein of interest (judged by molecular weight) was dialysed against PBS pH7.4 at 4°C for 24 hours, dialysis buffer was changed for fresh PBS and left at 4°C for an additional 24 hours.

Protein was taken out of dialysis, aliquoted and the concentration was measured with Quant-iT Protein Assay Kit (Thermo Scientific, UK).

2.0.5 SDS-PAGE and western blot

Purified protein samples, fractions obtained from protein purification and crude cell lysates were analysed by gel electrophoresis either stained with Coomassie blue or transferred to a PVDF membrane for western blot.

Gels were prepared and run according to instructions of Biorad Mini Protean kit (Biorad, UK). The reagents needed to prepare the gels were mixed and placed in a gel cassette assembly with spacers with a thickness of 1mm for polymerisation. The final gel contained a 10% resolving gel made by adding 5ml of resolving gel solution to the cassette assembly and 2ml of stacking gel solution in addition to a 15 wells comb.

| Ingredients | 10% Resolving gel (10ml) | Stacking gel (10ml) |
|---|--------------------------|---------------------|
| Acrylamide/Bis-acrylamide 30% (Sigma, UK) | 3.3ml | 1.33ml |
| 1.5M Tris-HCl (Sigma, UK), pH 8.8 | 2.5ml | ----- |
| 0.5M Tris-HCl (Sigma, UK), pH 6.8 | ----- | 2.5ml |
| 10% SDS (Fisher Scientific, UK) | 100µl | 100µl |
| dH ₂ O | 4.05ml | 6.05ml |
| 10% APS (Sigma, UK) | 100µl | 100µl |
| TEMED (Sigma, UK) | 10µl | 10µl |

Table 12. Volume of ingredients required for preparing a polyacrylamide gel.

Samples to be analysed were diluted in 2x sample buffer (62.5 mM Tris-HCl pH6.8, 40% glycerol, 0.01% bromophenol blue) and heated at 70°C for 10min on a dry block heater. Denatured samples were loaded in the gels at volumes of 10µl per well. Electrophoresis was performed in Tris-glycine running buffer (25mM Tris base, 192mM glycine, 0.1% SDS) at 200V for 50min.

Coomassie blue staining

Gels were removed from cassette assembly and dyed in Coomassie blue stain (0.1% Coomassie blue R250, 10% acetic acid, 50% methanol) for 1 hour. Dye was removed and gels were transferred to a destain solution (10% acetic acid, 50%

methanol) to remove excess of Coomassie blue R250. Coomassie blue destain solution was changed until protein bands became visible.

Western blot

After removing gels from cassette assembly, they were washed in transfer buffer (25mM Tris base, 190mM glycine, 20% methanol) and placed in a transfer sandwich assembled by 2 pads soaked in transfer buffer, 1 filter paper, 1 protein gel, 1 Amersham Hybond P 0.2 PVDF membrane (GE Healthcare Life Sciences, UK) (previously activated in methanol and washed in transfer buffer), 1 filter paper and 3 pads soaked in transfer buffer. Protein blotting was performed at 40V, for 90 min in a transfer tank containing ice cold water.

The membrane was soaked in 3% milk diluted in PBS and incubated either at 4°C for overnight or at 37°C for 1 hour. The membrane was transferred to a solution containing the primary antibody diluted in 3% milk according to optimised conditions and incubated at 37°C for 2 hours. The membrane was washed three times in PBS + 0.1% Tween and transferred to the secondary antibody solution diluted in 3% milk and incubated at 37°C for 1 hour. The membrane was washed three times in PBS + 0.1% Tween and developed by either ECL or 4-chloro-1-naphtol solution.

Horseradish peroxidase (HRP) detection with 4-chloro-1-naphtol solution

A developing solution was prepared by diluting 30mg of 4-chloro-1-naphtol (Sigma, UK) in 10ml of methanol, 40ml PBS and 30µl hydrogen peroxide. The membrane was soaked in the developing solution and placed in the dark for 15 minutes. Finally, the membrane was washed in dH₂O and photographed. Western blots

performed to detect the HaloTag portion of the fusion were developed by this procedure.

| Antibody | Origin | Clonality |
|---|--------|-----------|
| Anti-HaloTag (Promega, UK) | Mouse | mAb |
| Anti-NanHcat | Mouse | pAb |
| Anti-mouse IgG HRP conjugated (R&D Systems, UK) | Goat | pAb |

Table 13. Origin and clonality of antibodies used for western blot. mAb = monoclonal antibody, pAb = polyclonal antibody.

Detection by enhanced chemiluminescence (ECL)

Due to the low sensitivity of the antibody raised against NanHcat, a different developing method was employed in order to increase the signal detection. The developing solution was prepared by adding 1ml of each detection reagent of the ECL Western Blotting Analysis System (GE Healthcare, UK). The membrane was soaked in the developing solution and incubated at room temperature for 5min. The membrane was carefully shaken to remove excessive solution and placed in a plastic bag and in an X-ray film cassette. In a dark room, a sheet of autoradiography film (GE Healthcare, UK) was placed on top of the membrane and the cassette was closed for exposure. Time of exposure was optimised depending on the antibodies that were used.

2.9.6 Mass spectrometry

Orbitrap mass spectrometry service was provided by The Advanced Mass Spectrometry Facility in the School of Biosciences at the University of Birmingham. Samples were submitted for protein identification by excising protein bands from Coomassie blue stained polyacrylamide gels. The samples were trypsin digested

in the Mass Spectrometry facility and analysed by liquid chromatography tandem mass spectrometry (LC MS/MS) (<http://www.birmingham.ac.uk/facilities/advanced-mass-spectrometry/about/index.aspx>).

2.9.7 Neuraminidase activity assay

A neuraminidase purified from *Clostridium perfringens* (Sigma, UK) was used to make a standard curve to calculate specific activity, defined by manufacturer as: “One unit will hydrolyze 1.0 micromole of 2'-(4-Methylumbelliferyl)-a-D-N-acetylneuraminic acid (MUAN) per minute at pH 5.0 at 37°C”. The enzyme was reconstituted at a concentration of 0.1U/μl in 0.2% BSA and stored at -20°C. Afterwards, the fluorogenic substrate MUAN (Carbosynth, UK) was reconstituted at a concentration of 3.5mg/ml in dH₂O and stored at -20°C.

A 96 wells plate with flat bottom was used to run every assay in which columns 1 to 6 were used to make a standard curve while columns 7 to 12 were used for testing the activity of samples.

2.9.7.1 Standard curve

First, 120μl of citrate-phosphates buffer (CPB) (Citric acid 0.1M + Sodium phosphate 0.2M pH6.5) were added to rows B1-B3 to H1-H3 and A4-A6 to G4-G6. Then, 200μl of CPB were added to row A1-A3 in addition to 40μl of 0.005U/μl *C. perfringens* neuraminidase. Using a multichannel pipette, 120μl were transferred from row A1-A3 to row B1-B3, mixed by pipetting up and down and transferred to the next row to make double dilutions. Dilutions were made up to row H1-H3, then from this row, they were continued to row A4-A6 until row G4-G6. The last 120μl were discarded in order to have a volume of 120μl in each well. The layout for the assays is shown in table 14.

2.9.7.2 Sample dilutions

Depending on the number of samples, 100µl of CPB were added per sample by triplicate as shown in the layout. Afterwards, 20µl of the sample to be tested were added to each well.

2.9.7.3 Substrate

Substrate MUAN was diluted to 300µM by adding 4.2µl of 3.5mg/ml MUAN in 100µl of CPB per sample.

Using a multichannel pipette, 100µl of 300µM MUAN were added to each well and the plate was transferred to a Fluostar Omega microplate reader (BMG Labtech, UK) to read fluorescence at an excitation of 366 and an emission of 446 every minute for 2 hours.

| | 1 | 2 | 3 | 4 | 5 | 6 | 7 | 8 | 9 | 10 | 11 | 12 |
|---|--------------|--------------|--------------|---------|---------|---------|--------|--------|--------|-----|-----|-----|
| A | Neu 0.1 U | Neu 0.1 U | Neu 0.1 U | 1:256 | 1:256 | 1:256 | Ctrl + | Ctrl + | Ctrl + | X8 | X8 | X8 |
| B | 1:2 | 1:2 | 1:2 | 1:512 | 1:512 | 1:512 | X1 | X1 | X1 | X9 | X9 | X9 |
| C | 1:4 | 1:4 | 1:4 | 1:1024 | 1:1024 | 1:1024 | X2 | X2 | X2 | X10 | X10 | X10 |
| D | 1:8 | 1:8 | 1:8 | 1:2048 | 1:2048 | 1:2048 | X3 | X3 | X3 | X11 | X11 | X11 |
| E | 1:16 | 1:16 | 1:16 | 1:4096 | 1:4096 | 1:4096 | X4 | X4 | X4 | X12 | X12 | X12 |
| F | 1:32 | 1:32 | 1:32 | 1:8192 | 1:8192 | 1:8192 | X5 | X5 | X5 | X13 | X13 | X13 |
| G | 1:64 | 1:64 | 1:64 | 1:16384 | 1:16384 | 1:16384 | X6 | X6 | X6 | X14 | X14 | X14 |
| H | 1:128 | 1:128 | 1:128 | PBS | PBS | PBS | X7 | X7 | X7 | X15 | X15 | X15 |

Table 14. Sample layout of neuraminidase activity assay. Each sample was run by triplicate. Columns 1 to 6 contain neuraminidase of *C. perfringens* with a known specific activity serially diluted. Columns 7 to 12 contain test samples X = Any sample, Ctrl + = NanH23 purified.

2.9.7.4 Neuraminidase specific activity

As a standard time point, the 15 minute read was considered. The fluorescence intensity read of every sample was blank corrected by subtracting the average fluorescence of samples containing PBS and substrate.

Blank corrected data were normalised to percentage using the formula:

$$\%Neu = (A \times 100)/B$$

A = Blank corrected average fluorescence intensity of triplicates of each sample.

B = average fluorescence intensity of 0.1U of *C. perfringens* neuraminidase.

%Neu = Percentage of neuraminidase activity of each sample.

Using normalised values, a standard curve was made by plotting neuraminidase activity units in the X axis and percentage activity in the Y axis. Values were fitted into a non-linear regression curve. Unknown neuraminidase activity values of test samples were calculated by interpolating to the standard curve using a four parameter logistic equation:

$$Y = a + (d - a) / (1 + 10^{((\text{LogEC50} - X) * b)})$$

a = Minimum Y value determined by the plateau formed by values obtained with a low concentration of neuraminidase (a = 0% in normalised data).

d = Maximum Y value determined by the fluorescence detected with 0.1U of neuraminidase (d = 100% in normalised data).

b = Hill's slope, it describes the steepness of the curve.

Ec50 = Refers to the midpoint of the curve, also known as "Effective concentration".

X = Unknown log(Neuraminidase activity units) of test sample.

Y = Percentage activity of test sample.

Considering that data were distributed in a sigmoidal curve, samples with values of neuraminidase activity that do not fit in the slope of the curve and fit either in the bottom or top plateau cannot be used to calculate neuraminidase activity units. Therefore, two cut-off points were established by plotting the data of 5 standard curves run independently and selecting the neuraminidase activity values of 5% and 95% neuraminidase activity since all the data within this range avoid the bottom and top plateaus. Therefore, any sample with a neuraminidase activity value below 5% neuraminidase activity was considered as “below detection level”. If a sample value was calculated as higher than 95% neuraminidase activity, the result was considered as “above detection level” and the sample was analysed again at a higher dilution.

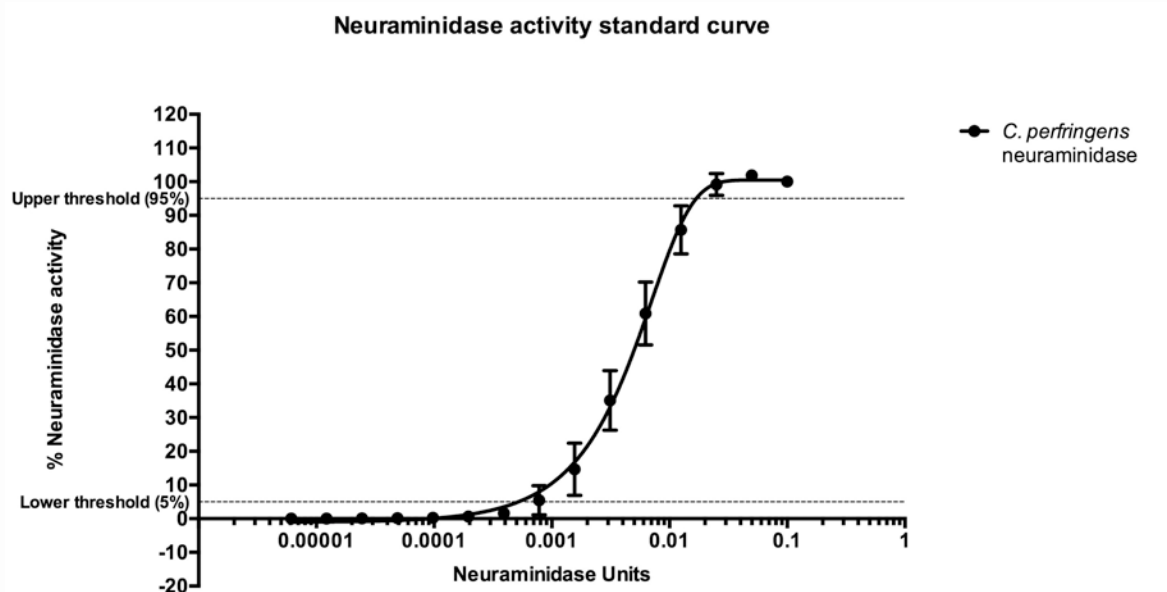


Figure 5. A standard curve was made by plotting the neuraminidase activity (%) ($n = 3, \pm SD$) of *C. perfringens* neuraminidase obtained *in vitro* when tested at different known concentrations (Neuraminidase units) in order to determine the threshold values (dashed lines) for interpolation of test samples into the curve. Neuraminidase units were defined by the manufacturer of *C. perfringens* neuraminidase (Sigma, UK) as: “One unit will hydrolyze 1.0 micromole of 2’-(4-Methylumbelliferyl)- α -D-N-actetylneuraminic acid (MUAN) per minute at pH 5.0 at 37°C”. Neuraminidase activity was normalised considering 0.1 U of *C. perfringens* neuraminidase as 100%. The concentration of test samples (Neuraminidase

Units) was calculated by interpolating the normalised value of neuraminidase activity into a standard curve that was plotted for each assay run. Only samples with a neuraminidase activity between 5% and 95% were interpolated.

Finally, data were standardised by calculating the total protein concentration of the samples using Quant-iT Protein Assay Kit (Thermo Scientific, UK) and calculating specific neuraminidase activity (U/mg) (Figure 5).

2.9.8 Production of an anti-NanH antibody

NanH catalytic domain was purified by HaloTag system and anion exchange chromatography (described in detail in results chapters). After dialysis, the protein was filter sterilised using a 0.2µm pore syringe filter and diluted in alhydrogel at a ratio of 1:4 (NanH:alhydrogel) to a final concentration of 0.1µg/µl.

Three MF1 mice (CharlesRiver, UK) were inoculated subcutaneously with 100µl of the protein supplemented with alhydrogel as an adjuvant. Therefore, each dose contained 10µg of purified NanH. The mice were boosted after 14 days and after 28 days with the same dose. Mice were humanely sacrificed by exanguination by cardiac puncture under general anaesthesia and death was confirmed by neck dislocation as specified in schedule 1 of Home Office regulations.

Blood was centrifuged at 2000 x g for 5 minutes to obtain sera which were aliquoted and stored at -20°C

2.10 *M. haemolytica* NanH catalytic domain

2.10.1 Site directed mutagenesis

Single amino acid substitutions were made with the QuikChange II XL Site-Directed Mutagenesis Kit (Agilent, UK) using as template the plasmid

pFN18KNanH23. Required primers were designed using the online tool made available by the supplier¹.

¹ (<http://www.genomics.agilent.com/primerDesignProgram.jsp>).

| Mutation | Primer name | Sequence |
|----------|--------------|---|
| W164A | NanH-W164A-F | TCTATGTCGGATCAACAAGCGTATGGTGGGCGTGTTC |
| | NanH-W164A-R | GGAACACGCCCACCATACGCTTGTTGATCCGACATAGA |
| Q239Y | NanH-Q239Y-F | TGCAAGATGGTACGTTGGTTTTCCCAATTTATACCGCACATCAAAT |
| | NanH-Q239Y-R | ATTTTGATGTGCGGTATAAATTGGGAAAACCAACGTACCATCTTGCA |
| E277A | NanH-E277A-F | CACCGAACCAAAGTTCTTTAGCAAATATGGTGTGTTGAACTCGA |
| | NanH-E277A-R | TCGAGTTCAAACACCATATTTGCTAAAGAACTTTGGTTCGGTG |
| D138A | NanH-D138A-F | AGCACGCCGTTCAATGGCTCCAACGCTATTACATA |
| | NanH-D138A-R | TATGTAATAGCGTTGGAGCCATTGAACGGCGTGCT |
| Y390D | NanH-Y390D-F | GCCGCTGGTGCTGGTGATTCTCTTTAGCCT |
| | NanH-Y390D-R | AGGCTAAAGAGGAATCACCAGCACCAGCGGC |
| S330A | NanH-S330A-F | ACAACCAACTCAAGGCTCTGCTATCTATGTAACACTACC |
| | NanH-S330A-R | GGTAGTGTTACATAGATAGCAGAGCCTTGAGTTGGTTGT |
| R356A | NanH-R356A-F | CAGATGGAAAGAATGATGGGTGGAAAGCGGGTGATATTACAC TT |
| | NanH-R356A-R | AAGTGTAATATCACCCGCTTTCCACCCATCATTCTTTCCATCTG |
| D100A | NanH-D100A-F | CTGGAATCGTGCGTATGCCCAAGATCGTATTGATC |
| | NanH-D100A-R | GATCAATACGATCTTGGGCATACGCACGATTCCAG |

Table 15. List of primers used for site directed mutagenesis.

First, a copy of the plasmid with the expected mutation was made by PCR amplification using the required primer pair as shown in table 15. Reaction mixes and PCR conditions were set as follows:

| Component | Concentration |
|-----------------------------|------------------------------|
| 10x Reaction buffer | 5µl |
| DNA Template (pFN18KNanH23) | 10ng |
| Primers | 125ng each |
| dNTP mix | 1µl |
| PfuUltra HF DNA polymerase | 1µl |
| QuikSolution reagent | 3µl |
| Water (Molecular grade) | Made up to 50µl per reaction |

Table 16. Concentration of components required for PCR using QuikChange II XL Site-Directed Mutagenesis Kit (Agilent, UK).

| Step | Temperature | Time | Cycles |
|------------------|-------------|--------------------|--------|
| Initial denature | 95°C | 1 min | 1 |
| Denature | 95°C | 50s | |
| Annealing | 60°C | 50s | 18 |
| Extension | 68°C | 6 min (1 min / kb) | |
| Final extension | 68°C | 7 min | 1 |
| Final hold | 4°C | Indefinite | |

Table 17. Temperature conditions required for PCR using QuikChange II XL Site-Directed Mutagenesis Kit (Agilent, UK), pFN18KNanH23 plasmid as template and primers required for amplification of the plasmid with the desired mutation.

Methylated DNA used as a template was digested by adding 10U of *Dpn* I to the PCR mix after amplification and incubating at 37°C for 1 hour.

Amplified plasmid was cloned into *E. coli* strain XL10-Gold ultracompetent cells by chemical transformation. Cells were defrosted on ice and transferred to pre-chilled 1.5 ml microfuge tubes in a volume of 45 µl per tube. One tube was set per PCR amplification along with one negative control and one positive control. Cells were supplemented with 2µl of β-mercaptoethanol to increase transformation efficiency

and incubated for 10 minutes. A sample of 5µl of mutated DNA was added to each tube, 5µl of molecular grade water were added to negative control tube and 1µl (~100ng) of parent pFN18KNanH23 was added to the positive control tube. The cells were incubated on ice for 30 minutes followed by a heat shock at 42°C for 30 seconds in a water bath and transferred immediately to an ice box for a 2 minute incubation. Finally, cells were supplemented with 500µl of NZY+ broth pre warmed at 42°C and incubated at 37°C with shaking for 1 hour.

After incubation, bacteria containing a mutated plasmid were transferred in volumes of 100µl to 1 plate of LB agar and 4 plates of LB + 50µg/ml kanamycin, they were distributed along the plate with a sterile bacterial cell spreader and incubated at 37° for overnight. The same procedure was repeated for control bacteria but only 1 LB agar and 1 LB agar + 50µg/ml kanamycin plates were prepared.

Around 10 colonies obtained from the mutated plasmid reactions were transferred to an LB + 50µg/ml kanamycin plate with a grid drawn on the outside to isolate and properly identify each colony. The plate was incubated at 37°C for overnight and stored at 4°C.

One colony per mutation reaction was grown in 10ml of LB broth + 50µg/ml kanamycin by duplicate at 37°C with shaking for overnight. Cells were centrifuged and one of the obtained pellets was resuspended in 10ml of LB + 15% glycerol for storage at -80°C while the other pellet was disrupted for plasmid isolation using the GeneJet Plasmid Miniprep Kit (Thermo Fisher Scientific, UK).

The isolated plasmids were submitted to the Functional Genomics Laboratory in the School of Biosciences at the University of Birmingham for Sanger sequencing using primers pFN18K-seq-F, 7G and NanH-int-R2. The data was trimmed

according to peak quality and aligned against the sequence of pFN18KNanH23 to confirm the expected mutations.

Plasmids with confirmed sequence were transferred to competent *E. coli* KRX cells by chemical transformation. Obtained colonies were analysed by colony PCR using primers 7F and 7G in order to confirm transformation. A colony of each mutant was grown in 10ml of LB + 50µg/ml kanamycin at 37°C for overnight, cells were concentrated by centrifugation and resuspended in 10ml of LB + 15% glycerol for storage at -80°C.

3 Sequence analysis

M. haemolytica has been reported to produce sialidase activity in cell lysates and culture supernatants but the protein responsible has not been studied. The locus of the neuraminidase NanH has been annotated in published genome sequences of *M. haemolytica* (Gioia et al., 2006).

The available sequences were retrieved from the NCBI database in order to compare the possible variation of *nanH* among isolates. The loci of other genes related to NanH were identified in order to formulate a hypothesis on the NanH export mechanism and its role in sialic acid metabolism.

The accession number and metadata of the sequences used in this study are shown in Table 18. The sequences were either retrieved as complete close genome sequences or as draft contigs. Accession numbers of single genes are mentioned as well.

Three unpublished strains were included. Strain ATCC 33396 is a type strain that was genome sequenced as part of this project.

| Accession No. | Strain name | ST | Host | Status | Reference |
|---------------|-----------------------|-------|-------------------|-----------|------------------------------------|
| CP011098 | 89010807 | A1 | Bovine | BRD | (Heaton et al., 2015) |
| CP006619 | USMARC_2286 | A1 | Bovine | Healthy | Smith, 2013 (Direct submission) |
| CP005383 | M42548 | A1 | Bovine | BRD | (Eidam et al., 2013) |
| CP005972 | D153 | A1 | Bovine | BRD | (Hauglund et al., 2013) |
| CP006574 | D174 | A6 | Bovine | BRD | (Hauglund et al., 2015b) |
| CP004753 | USDA-ARS-SAM-185 | A6 | Bovine | BRD | (Harhay et al., 2013) |
| CP004752 | USDA-ARS-SAM-183 | A1 | Bovine | BRD | (Harhay et al., 2013) |
| CP006957 | USDA-ARS-SAM-184 | A2 | Bovine | Healthy | Harhay, 2013 (Direct submission) |
| CP006573 | D171 | A2 | Bovine | BRD | (Hauglund et al., 2015a) |
| DQ680221 | M7/2 | A1 | Bovine | | (Roehrig et al., 2007) |
| AASA01000000 | PHL213 / ATCC BAA-410 | A1 | Bovine | BRD | (Gioia et al., 2006) |
| ACZX01000000 | “Ovine” | A2 | Ovine | BRD | (Lawrence et al., 2010) |
| ACZY01000000 | “Bovine” | A2 | Bovine | BRD | (Lawrence et al., 2010) |
| AOGP01000000 | H23 | A6 | Bovine | BRD | (Klima et al., 2013) |
| ATSY01000000 | D193 | A1 | Bovine | BRD | (Hauglund et al., 2013) |
| ATSZ01000000 | MhBrain2012 | A1 | Bovine cerebellum | | Hauglund, 2013 (Direct submission) |
| ATTA01000000 | MhSwine2000 | A1 | Porcine | Pneumonia | Hauglund, 2013 (Direct submission) |
| AUNK01000000 | D35 | A2 | Bovine | BRD | (Hauglund et al., 2015a) |
| AUNL01000000 | D38 | A6 | Bovine | BRD | (Hauglund et al., 2015b) |
| JANJ01000000 | PKL10 | A1/A6 | Deer spleen | BRD | (Lawrence et al., 2014) |

| Accession No. | Strain name | ST | Host | Status | Reference |
|---------------|--|----|--------|---------|--|
| JPIZ01000000 | Mh10517 | | Ovine | BRD | (Kidanimariam Gelaw et al., 2015) |
| LFXV01000000 | T14 | A6 | Bovine | BRD | (Klima et al., 2016) |
| LFXW01000000 | T2 | A2 | Bovine | BRD | (Klima et al., 2016) |
| LFXX01000000 | L024A | A1 | Bovine | BRD | (Klima et al., 2016) |
| LFXY01000000 | L044A | A1 | Bovine | BRD | (Klima et al., 2016) |
| LFXZ01000000 | L033A | A2 | Bovine | BRD | (Klima et al., 2016) |
| LFYA01000000 | L038A | A6 | Bovine | BRD | (Klima et al., 2016) |
| LFYB01000000 | 535A | A1 | Bovine | BRD | (Klima et al., 2016) |
| LFYC01000000 | 587A | A2 | Bovine | Healthy | (Klima et al., 2016) |
| LFYD01000000 | 157-4-1 | A1 | Bovine | Healthy | (Klima et al., 2016) |
| LFYE01000000 | 3927A | A6 | Bovine | Healthy | (Klima et al., 2016) |
| MEHR01000000 | NIVEDI/MH/1 | | Ovine | | Sahay, 2016 (Direct submission) |
| EF215852 | CECT924-Reglero-BHIB/A | | | | |
| | ATCC 33396 / NCTC 9380 / CCUG 12392 / J.A. Watt 1266&B | A2 | Ovine | | Type strain (Angen et al., 1999). Whole genome sequenced by our group. |
| | MexA1 | A1 | | | Unpublished DNA provided by Dr Morales |
| | MexA2 | A2 | | | Unpublished DNA provided by Dr Morales |

Table 18. Information about the sequences retrieved for comparison of genes of interest for this study.

3.1 Identification of sialic acid metabolism enzymes

The putative metabolic pathways and reactions in which *M. haemolytica* is predicted to degrade or synthesise Neu5Ac were retrieved from the metacyc database (Caspi et al., 2016). The genes codifying for the enzymes that were identified in the pathway were aligned against *M. haemolytica* whole genome sequences by BLAST. Out of 12 compared enzymes, 9 were identified in all strains with a sequence identity that oscillated from 98 to 100%. Since the sequence of all enzymes was conserved within each of the analysed serotypes (i.e. A1, A2 and A6), the sequence of one representative strain for each serotype was used to identify the locus of each enzyme (Table 19).

The enzyme sequences that showed variability were NmaA, absent in A2 and with a 93% sequence identity between A1 and A6 (Figure 6); NmaB in which the identity between A1 and A6 was 96% however, the sequence in A2 was only around 60% to both A1 and A6 (Figure 7). Finally, the α -2,8-polysialyltransferase gene was only present in A2.

| Enzyme | A1 (NC_021743) | | A2 (CP006957) | | A6 (CP004753) | |
|---|----------------|--------------|---------------|------------|---------------|---------------------------|
| | CDS | Locus tag | CDS | Locus tag | CDS | Locus tag |
| CMP-N-acetylneuraminate-β-galactosamine-α-2,3-sialyltransferase | WP_006247883 | F382_RS03950 | AJE08613 | B824_18180 | AGI35814 | D648_18090/ D648_18100 |
| UDP-N-acetylglucosamine 2-epimerase (NeuC-like) | WP_006247885 | F382_RS03960 | AJE08615 | B824_18200 | AGI35816 | D648_18120 |
| N-acylneuraminate cytidyltransferase | WP_006247886 | F382_RS03965 | AJE08616 | B824_18210 | AGI35817 | D648_18130 |
| NeuNAc condensing enzyme | WP_006247887 | F382_RS03970 | AJE08617 | B824_18220 | AGI35818 | D648_18140 |
| N-acetylmannosamine-6-phosphate 2-epimerase | WP_006253448 | F382_RS07685 | AJE06887 | B824_920 | AGI34077 | D648_720 |
| N-acetylmannosamine kinase | WP_006248965 | F382_RS07690 | AJE06888 | B824_930 | AGI34076 | D648_710 |
| N-acetylneuraminate lyase | WP_006248966 | F382_RS07695 | AJE06889 | B824_940 | AGI34075 | D648_700 |
| UDP-N-acetyl-D-mannosamine dehydrogenase (NmaB) | WP_006248280 | F382_RS08015 | AJE07152 | B824_3570 | AGI34007 | D648_20 |
| UDP-N-acetylglucosamine 2-epimerase (NmaA) | WP_006248279 | F382_RS08020 | N/A | N/A | AGI34006 | D648_10 |
| glucosamine-6-phosphate deaminase | WP_006250130 | F382_RS10250 | AJE08978 | B824_21830 | AGI34498 | D648_4930 |
| N-acetylglucosamine-6-phosphate deacetylase | WP_006250472 | F382_RS10255 | AJE08977 | B824_21820 | AGI34499 | D648_4940 |
| α-2,8-polysialyltransferase | N/A | N/A | AJE06943 | B824_1480 | N/A | N/A |

Table 19. Loci of genes that codify for enzymes involved in sialic acid metabolism identified in strains D153, USDA-ARS-SAM-184 and USDA-ARS-SAM-185 as representatives of serotypes A1, A2 and A6 respectively.

The nucleotide sequence of the enzymes that showed variability was translated according to the annotated CDS. A multiple sequence alignment of the amino acid sequence was performed using the CLUSTALO tool. Sequence variability was calculated using the EMBOSS needle protein alignment tool (Rice et al., 2000).

| | | | | |
|---------------|-----|-------------------|--|----------------------|
| A6 (CP004753) | 1 | MRYLVFVGRPEV | IKMAPLVEGFKKSGLNFKVCVTAQHRK | MLDQVLELFEITPDYDLDIM |
| A1 (CP005972) | 1 | MRYLVFVGRPEA | IKMAPLVEGFKKSGLNFKVCVTAQHRQ | MLDQVLELFEITPDYDLDIM |
| | | | | |
| A6 (CP004753) | 61 | SNKQTLSTVTS | SAILEKIQPVIAEYKPTTIFVHGDTATTLA | SLAAYNROIDIAHIEAGLR |
| A1 (CP005972) | 61 | SNKQTLSTVTS | SAILEKIQPVIAEYKPTTIFVHGDTATTLA | SLAAYNROIDIAHIEAGLR |
| | | | | |
| A6 (CP004753) | 121 | THNIYSPWPEEGNRKLT | GALAKYHFAPTQSTKKNLLNENI | TEDTIYVTGNTVIDALF |
| A1 (CP005972) | 121 | THNIYSPWPEEGNRKLT | AALAKYHFAPTQSTKKNLLNENI | ABGDIYVTGNTVIDALFLAC |
| | | | | |
| A6 (CP004753) | 181 | KKLDENV | DLSSLQEKFSYIKSKRTILITGHRRENFGNGFENICKAVSTLASDFPDVQFI | |
| A1 (CP005972) | 181 | KKLDENI | DLSSLQEKFSYIKSKRTILITGHRRENFGNGFENICKAVSTLASDFPDVQFI | |
| | | | | |
| A6 (CP004753) | 241 | YPVHLNPNVREPVNRL | LADKSNVHLIEPCDYLSFVYLMRESYLILTDSSGGIQEEAPSLGK | |
| A1 (CP005972) | 241 | YPVHLNPNVREPVNRL | LADKSNVHLIEPCDYLSFVYLMRESYLILTDSSGGIQEEAPSLGK | |
| | | | | |
| A6 (CP004753) | 301 | PVLVMRDTERPEAVEAG | TVKLVGTAQSEIIKQVTELLNDQAAYTKMSEAHNPYGDGTAV | |
| A1 (CP005972) | 301 | PVLVMRDTERPEAVEAG | TVKLVGTAQSEIIKQVTELLNDQAAYTKMSEAHNPYGDGTAV | |
| | | | | |
| A6 (CP004753) | 361 | KQILSVFQSK | . | |
| A1 (CP005972) | 361 | KQILSVFQSK | Q | |

Full conservation

Conserved properties

Figure 6. Alignment of the NmaA sequence shows high conservation between serotype A1 (strain D153) and A6 (strain USDA-ARS-SAM-185). The gene for NmaA was not found in serotype A2.

A6 (CP004753) 1 ...MSN**FNTI**SVV**GLGYIGLPT**ATVFAQHGLNVIGVDVNLAVD**TINQKIHIVEPDL**DV
 A1 (NC_021743) 1 ...MSN**FNTI**SVV**GLGYIGLPT**ATVFAQHGLNVIGVDVNLAVD**HINQKIHIVEPDL**DV
 A2 (CP006957) 1 MMSK**TEFNTI**C**LLGLGYIGLPT**SVV**FANAC**K**QVIGVDIN**PQ**VVAS**L**NQGN**I**HIVEPDL**QT

A6 (CP004753) 58 AVH**QCVSS**CKLK**ATLTPEP**AB**AF**L**IAVPTP**FK**GEDYE**P**DL**S**YIQ**AA**CKAIAP**V**LEK**D**NLV**
 A1 (NC_021743) 58 AVH**QCVSS**CKLK**ATLTPEP**AB**AF**L**IAVPTP**FK**GEDYE**P**DL**S**YIQ**AA**CKAIAP**V**LEK**G**NLV**
 A2 (CP006957) 61 A**FTQ**AV**KKCN**FF**ATA**K**PQ**PA**DAFI**L**IAVPTP**L**CGK**..**Q**P**DL**S**YIQ**NA**AA**M**IAPC**L**ER**G**NLV**

A6 (CP004753) 118 I**LE**STSPV**GA**T**EQMAE**W**LAEYR**PE**LSFP**Q**QAG**ED**S**D**IRI**A**H**CP**ER**VL**PGQ**VM**RE**L**I**T**EN**DR
 A1 (NC_021743) 118 I**LE**STSPV**GA**T**EQMAE**W**LAEYR**PE**LSFP**Q**QAG**ED**S**D**IRI**A**H**CP**ER**VL**PGQ**VM**RE**L**I**T**EN**DR
 A2 (CP006957) 119 V**LE**STSPV**GT**T**EN**L**AE**W**L**S**QAR**PE**DL**A**FP**A.....**D**V**S**I**A**Y**CP**ER**VL**PG**NI**M**TE**L**I**T**EN**DR

A6 (CP004753) 178 I**V**GG**MT**N**KCS**K**QAV**D**LY**K**T**F**V**K**G**D**C**I**V**T**N**AR**TA**E**M**CK**L**T**EN**S**FR**D**V**NI**A**F**AN**E**S**I**C**D**R**
 A1 (NC_021743) 178 I**V**GG**MT**N**KCS**V**QAV**N**LY**K**T**F**V**K**G**D**C**I**V**T**N**AR**TA**E**M**CK**L**T**EN**S**FR**D**V**NI**A**F**AN**E**S**I**C**D**R**
 A2 (CP006957) 173 I**I**GG**LS**E**Q**C**S**Q**QAV**D**LY**Q**I**F**A**K**R**C**V**T**T**I**AR**TA**E**M**CK**L**V**EN**S**FR**D**V**NI**A**F**AN**E**S**I**M**I**C**D**A

A6 (CP004753) 238 L**D**IN**V**W**E**L**I**A**L**AN**R**H**PR**V**N**I**L**Q**P**G**C**G**V**GG**H**C**L**AV**D**P**W**F**I**V**N**K**T**P**D**L**A**K**I**I**R**T**A**R**E**V**N**D**Y**K
 A1 (NC_021743) 238 L**D**IN**V**W**E**L**I**A**L**AN**R**H**PR**V**N**I**L**Q**P**G**C**G**V**GG**H**C**L**AV**D**P**W**F**I**V**N**K**T**P**D**L**A**K**I**I**R**T**A**R**E**V**N**D**H**K
 A2 (CP006957) 233 L**K**IN**V**W**E**L**I**B**L**AN**L**H**PR**V**N**I**L**Q**P**G**A**G**V**GG**H**C**L**AV**D**P**W**F**I**V**S**T**S**E**Q**Q**AR**L**I**R**T**A**R**E**V**N**D**S**K**

A6 (CP004753) 298 P**E**W**V**I**S**K**V**N**E**A**V**I**E**A**L**Q**K**T**G**K**S**I**D**Q**I**K**I**A**C**L**G**L**A**F**K**P**D**I**D**D**L**R**E**S**P**A**L**K**I**T**E**K**L**A**E**K**Y**V**G**
 A1 (NC_021743) 298 P**E**W**V**I**S**K**M**N**E**A**V**I**Y**A**L**Q**K**T**G**K**S**I**D**Q**I**K**I**A**C**L**G**L**A**F**K**P**D**I**D**D**L**R**E**S**P**A**L**K**I**T**E**K**L**A**E**K**Y**P**N**
 A2 (CP006957) 293 P**Q**W**V**I**E**Q**V**K**T**A**V**A**D**C**A**M**E**Q**D**C**K**P**S**E**L**T**I**A**C**L**G**L**A**F**K**P**N**I**D**D**L**R**E**S**P**A**L**A**I**T**R**Q**L**A**A**W**H**Q**G**

A6 (CP004753) 358 Q**I**L**A**V**E**P**N**V**E**E**L**P**K**K**L**A**K**K**N**I**S**L**I**V**T**V**D**E**A**L**K**L**A**D**V**V**V**V**L**V**D**H**R**E**F**R**E**L**A**A**I**.**P**S**H**I**T**V**I**D
 A1 (NC_021743) 358 Q**V**F**A**V**E**P**N**V**E**E**L**P**K**K**L**A**N**K**N**I**S**L**I**S**V**D**E**A**L**E**V**A**D**V**V**V**V**L**V**D**H**S**E**F**K**L**V**K**P**V**F**L**N**D**I**C**V**V**D**
 A2 (CP006957) 353 S**I**L**A**V**E**P**N**I**Q**Q**L**.....**A**G**E**K**I**L**I**V**D**L**N**T**A**L**S**Q**A**D**I**L**V**L**L**V**D**H**T**S**E**K**Q**I**S**R**E**Q**I**R**Q**R**H**I**D**

A6 (CP004753) 417 T**K**G**I**Y..
 A1 (NC_021743) 418 T**K**G**I**W**R**.
 A2 (CP006957) 409 C**R**G**V**W**V**R

Full conservation

Conserved properties

Figure 7. Alignment of the NmaB sequence shows high variability in A2 (~60%) compared to the identity between A1 and A6 (~93%).

3.2 Autotransporters

Published sequencing data of *M. haemolytica* suggests the possibility of NanH being exported via TVSS (Gioia et al., 2006) in addition to other hypothetical proteins being exported by the same mechanism. The nucleotide sequences codifying for putative autotransporters in *M. haemolytica* were aligned against publicly available sequences using the tool BLAST. The representative sequences for two YadA-like and two pertactin-like proteins were taken from Gioia et al annotations (Gioia et al., 2006) while the *ssa1* sequence was retrieved from CDS M62363 submitted by Lo et al (direct submission) and *nanH* from EF215852 submitted by Fernández et al (direct submission). Accession numbers of query sequences are shown in table 20.

| Accession no. | Locus | Description |
|---------------|------------------------|-------------------------------------|
| MHA_2701 | DS264703 (15307-21378) | YadA-like 1 |
| MHA_1367 | DS264622 (19593-23744) | YadA-like 2 |
| MHA_0563 | DS264612 (14484-18680) | Pertactin-like 1 |
| MHA_2800 | DS264709 (6100-10611) | Pertactin-like 2 |
| EF215852 | 1-2376 | Neuraminidase |
| M62363 | 1-3628 | Serotype 1 specific antigen (Ssa 1) |

Table 20. Accession number of putative autotransporters of *M. haemolytica*.

3.3 Autotransporter chaperones

The chaperones Skp, FkpA, SurA and DegP are known to aid the TVSS in *E. coli* however, they have not been described as functional proteins in Pasteurellaceae species. Homologues to these chaperones were found from the annotation of *P. multocida* strain PM70 genome sequence (AE004439) (May et al., 2001). No specific annotation was made for *M. haemolytica* so the sequences of *P. multocida*

putative chaperones were aligned to the available whole genome sequences of *M. haemolytica*. All sequences showed homology to at least one protein from *M. haemolytica* annotated in the genome sequence of strain M42548 (CP005383) (Table 21).

| Chaperone id | <i>P. multocida</i> | <i>M. haemolytica</i> | | % identity |
|--------------|---------------------|-----------------------|------------------|------------|
| | Accession no. | Accession no. | Locus | |
| Skp | AAK04077 | WP_006248430 | c1529879-1529088 | 33% |
| FkpA | AAK03651 | WP_006249898 | 939761-940354 | 84% |
| SurA | AAK03292 | WP_006250204 | c1392081-1391137 | 51% |
| DegP | AAK02818 | WP_006249698 | c1070963-1069569 | 72% |

Table 21. Accession number of identified chaperones in *P. multocida* PM70 and homologues in *M. haemolytica* (CP005383).

The nucleotide sequence that codifies for each gene was aligned against available sequences of *M. haemolytica* finding a high degree of conservation among strains that oscillated only between 98 to 100% of sequence identity. Only the strain PKL10 (Lawrence et al., 2014) had a lower identity, which was 80%. PKL10 however, has been proposed as a new *Mannheimia* sp.

3.4 NanH sequence conservation

The sequence of *nanH* was retrieved from the NCBI nucleotide database with the accession number EF215852, directly submitted to NCBI by Fernández et al (Fernández Martínez, 2007). The sequence was aligned against the available sequences of *M. haemolytica* and the sequence of the strain 33396 using BLAST. A total of 30 additional sequences that matched EF215852 sequence were retrieved from the database. A multiple sequence alignment was performed using all thirty sequences and 27/30 shared 100% identity (Figure 8).

The sequence AUNK01000051 showed the substitution G1535A which resulted in the amino acid substitution R512I (Figure 9). The sequence was obtained by the Roche (454) GS FLX titanium platform and was published as a draft therefore, additional sequencing needs to be performed to confirm the possible mutation.

LFYB01000017 is another draft genome obtained by Roche platform that shows a mutation in *nanH* (Figure 10). This sequence shows the deletion of A2281 that results in a frame shift that affects the translated sequence from residue 762 disrupting the putative autotransporter domain without affecting the catalytic domain. However, the mutation must be confirmed by additional sequencing as well.

The sequence of PHL213 published by Gioia et al shows an incomplete *nanH* gene due to being found at the beginning of contig18 (Gioia et al., 2006). The gene *nanH* was amplified by PCR from genomic DNA obtained from this strain and the sequence of the whole gene was obtained by Sanger sequencing. Additionally, *nanH* was amplified from the genomic DNA obtained from the two strains isolated in Mexico: MexA1 and MexA2. The sequence of strain ATCC 33396 was identified from the genome sequence obtained for this project.

A consensus of NanH sequence was obtained from the multiple sequence alignment made with publicly available sequences. Sequences of *nanH* obtained from PHL213, ATCC 33396, MexA1 and MexA2 were translated into protein sequence and aligned against NanH sequence consensus. The whole sequence obtained from ATCC 33396, MexA1 and MexA2 was identical. However, in PHL213, five aminoacid substitutions were found: Y77H, R107C, V156I, H158R, S162C (Numbering according to consensus sequence) (Figure 11).

It should be noted that automated annotation tools consider a different reading frame to EF215852 which contains the additional upstream sequence MEKM.

However, residues numbering of this project is based on the reading frame submitted by Fernandez et al (Fernández Martínez, 2007).

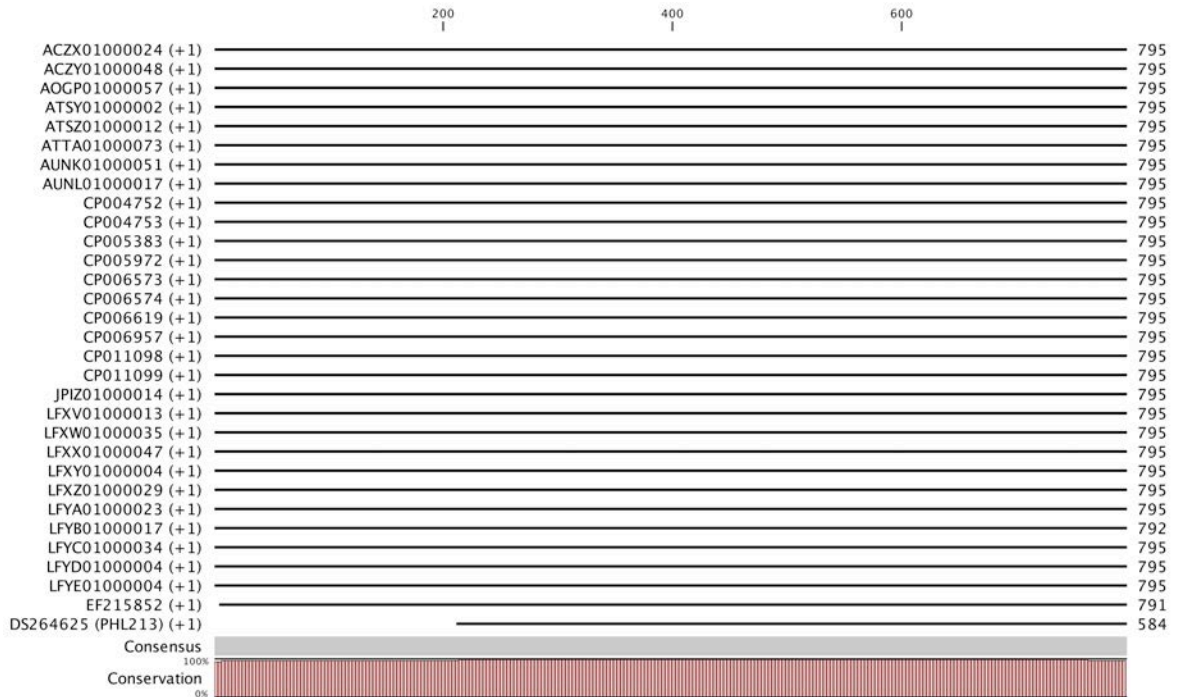


Figure 8. Multiple sequence alignment of publicly available sequences of *M. haemolytica* NanH shows a high sequence conservation.

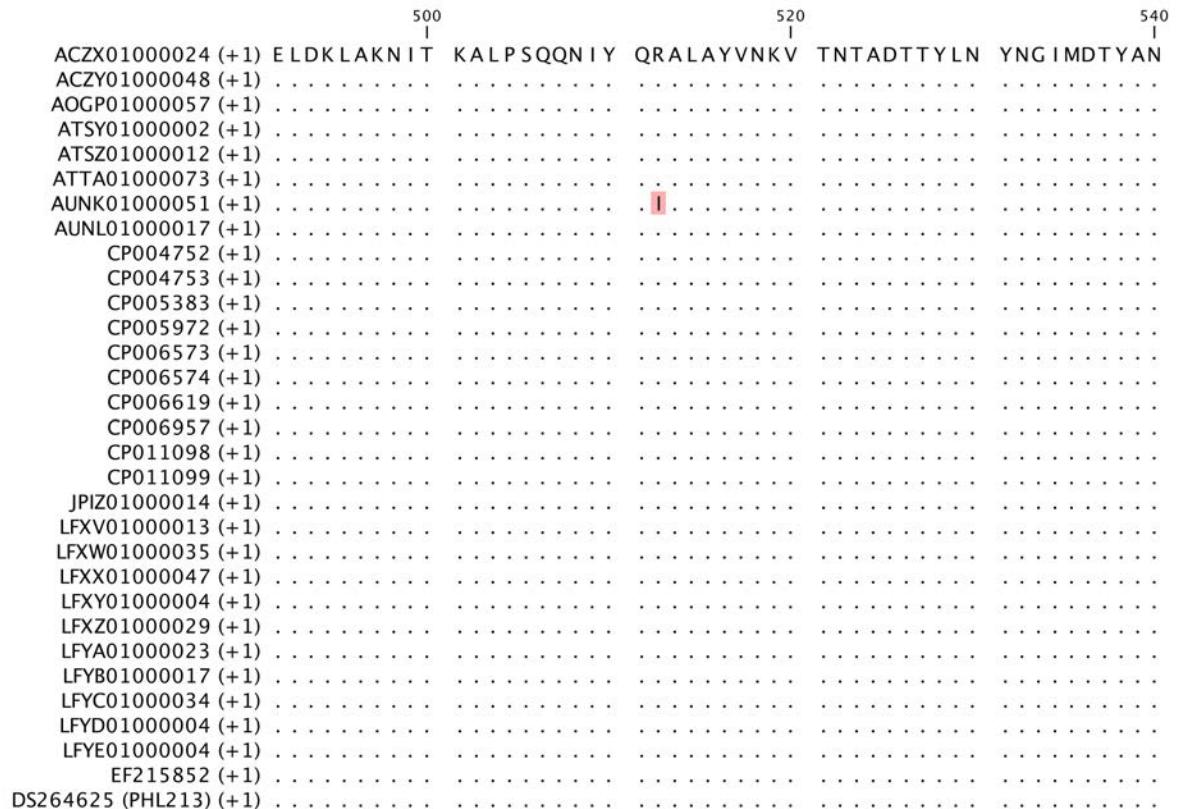


Figure 9. Multiple sequence alignment of translated *nanH* sequences. The amino acid substitution R512I was found in AUNK01000017 due to the G1535A substitution. Matching

residues are shown as dots, the mutation is shown by the aminoacid single letter code shaded in red.

| | | | | | | |
|------------------------|-------------|-----|------------|-----|------------|-----------------------|
| | | 760 | | 780 | | |
| | | | | | | |
| ACZX01000024 (+1) | NVYSVTTLGLK | | KRFANGVALG | | ADFKLHRYGS | QTTESNFGLN VSYNW- 795 |
| ACZY01000048 (+1) | | | | | | 795 |
| AOGP01000057 (+1) | | | | | | 795 |
| ATSY01000002 (+1) | | | | | | 795 |
| ATSZ01000012 (+1) | | | | | | 795 |
| ATTA01000073 (+1) | | | | | | 795 |
| AUNK01000051 (+1) | | | | | | 795 |
| AUNL01000017 (+1) | | | | | | 795 |
| CP004752 (+1) | | | | | | 795 |
| CP004753 (+1) | | | | | | 795 |
| CP005383 (+1) | | | | | | 795 |
| CP005972 (+1) | | | | | | 795 |
| CP006573 (+1) | | | | | | 795 |
| CP006574 (+1) | | | | | | 795 |
| CP006619 (+1) | | | | | | 795 |
| CP006957 (+1) | | | | | | 795 |
| CP011098 (+1) | | | | | | 795 |
| CP011099 (+1) | | | | | | 795 |
| JPIZ01000014 (+1) | | | | | | 795 |
| LFXV01000013 (+1) | | | | | | 795 |
| LFXW01000035 (+1) | | | | | | 795 |
| LFXX01000047 (+1) | | | | | | 795 |
| LFXY01000004 (+1) | | | | | | 795 |
| LFXZ01000029 (+1) | | | | | | 795 |
| LFYA01000023 (+1) | | | | | | 795 |
| LFYB01000017 (+1) | | | TLCKWCGIR | | G-*FQITSLW | FSN-Y-*K*F R.K-CK 792 |
| LFYC01000034 (+1) | | | | | | 795 |
| LFYD01000004 (+1) | | | | | | 795 |
| LFYE01000004 (+1) | | | | | | 795 |
| EF215852 (+1) | | | | | | 791 |
| DS264625 (PHL213) (+1) | | | | | | 584 |

Figure 10. Multiple sequence alignment of translated *nanH* sequence. A frame shift in LFYB01000017 was found due to the A2281 deletion. Matching residues are shown as dots, mutations are shown by the aminoacid single letter code shaded in red.

| | | | | | | |
|----------------|-------------|-----|-------------|-----|-------------|---|
| | | 20 | | 40 | | 60 |
| | | | | | | |
| NanH Consensus | MEKMMRKINQ | | LIISPYFFLS | | ILSASANSDF | WKSDDLNFNLT NITKRVGVDN FTTPVAGEPW 60 |
| PHL213 | | | | | | 60 |
| ATCC 33396 | | | | | | 60 |
| MexA1 | | | | | | 60 |
| MexA2 | | | | | | 60 |
| | | 80 | | 100 | | 120 |
| | | | | | | |
| NanH Consensus | AGIGPNGEAA | | GTAPLYYSRI | | PAMQVTEENK | LVVMFDLRWN RAYDQDRIDP GIAISSDGGH 120 |
| PHL213 | | | H..... | | | C..... 120 |
| ATCC 33396 | | | | | | 120 |
| MexA1 | | | | | | 120 |
| MexA2 | | | | | | 120 |
| | | 140 | | 160 | | 180 |
| | | | | | | |
| NanH Consensus | TWTKKTAWSF | | DRTNHPARRS | | MDPTLLHNP I | DNSLYVMHGT WSMSDQQWYG GRVPHFNSGS 180 |
| PHL213 | | | | | | I.R.C..... 180 |
| ATCC 33396 | | | | | | 180 |
| MexA1 | | | | | | 180 |
| MexA2 | | | | | | 180 |
| | | 200 | | 220 | | 240 |
| | | | | | | |
| NanH Consensus | WAAT IYKSTD | | GGLNWEKNT E | | FSKFSNLDVF | SKVTKNGKPT LGFLGGVGS G IVMQDGT L VF 240 |
| PHL213 | | | | | | 240 |
| ATCC 33396 | | | | | | 240 |
| MexA1 | | | | | | 240 |
| MexA2 | | | | | | 240 |

Figure 11. Sequence alignment of NanH sequences determined by Sanger sequencing from strains PHL213, ATCC 33396, MexA1 and MexA2. Five substitutions were found in PHL213 sequence. Matching residues are shown as dots, mutations are shown by the aminoacid single letter code shaded in red.

The sequence of NanH was also compared to the sequence of other members of the Pasteurellaceae family of veterinary importance which are NanH of *H.parasuis* and both neuraminidases of *P. multocida*: NanH and NanB.

First, conservation of the neuraminidase genes of *P. multocida* and *H.parasuis* was evaluated by performing multiple sequence alignments using the tool CLUSTALO in CLC Main workbench between the published sequences of the genes without considering incomplete gene sequences. The three neuraminidases showed a degree of variation (Appendices I and II) so a consensus sequence for each was extracted considering the most common sequences.

A multiple sequence alignment was performed between *M. haemolytica* NanH and the consensus sequences of *H.parasuis* NanH, *P. multocida* NanH and NanB (Figure 12). All the sequences show a conserved RIP motif, three similar aspartate boxes and a semi-conserved β -barrel signal motif. Most of the catalytic residues are identical except for the fifth residue of NanB in which an aspartate substitutes the glutamate of the three NanHs.

Mh_NanH 1MRKINQLIISFYFFLSILSASANSDFWKS¹DLNFNLTNTTKRVGV²DNFTTPVAGEP
 Hp_NanH 1 MKRRLSKNVKCSFVPSLIFLALASNLHATTFWKS¹DLNENLTHITKRVG²DNFTVVAEDGRL
 Pm_NanH 1MKKPVFLLSLLASTSMVAHGN¹FWKADLHENLTNTTKRVGV²DNFTVNKEGQP
 Pm_NanB 1MKKFNP¹SVLALSIS²SLLLTSTLTFGQIQQQ³.....DKALF⁴GVKEHQES

Mh_NanH 56 WAGIGPNGEAGTAPLIY¹SRIPAMQVTE²DNKLVVMFDLRW³NRAYDQDRIDPGIA⁴ISDGG
 Hp_NanH 60 WPGIGPNGEAGTAVLLY¹SRIPAMTIITDDNKMVVMYDLRW³NRAYDQDRIDPGVSI⁴SEDDG
 Pm_NanH 54 WPGIGPNGEAGTAVLLY¹SRIPAMTIITDDNKMVVMYDLRW³KTASDQNRIDPGAA⁴ISEDDG
 Pm_NanB 44 LLLFHQSLVKQGS¹DNVPIW²RIPSLLR³TKDGVLIAAADKRW⁴QHRGDWGDIDTAIR⁵SHDDG

RIP motif Asp box

Mh_NanH 116 FTWTKK¹TAW²SFDRTNHPARRS.....MDF³TLLHN⁴PTD⁵NS
 Hp_NanH 120 NTWLSK¹TAW²TFND³SKMPLRRA.....MDF⁴TILY⁵NSIDGS
 Pm_NanH 114 HSWKRI¹TAW²NFND³SKISL⁴RRA.....MDF⁵TLLY⁶NSIDGS
 Pm_NanB 103 KTWGNI¹TI²LLDL³PSK⁴NGEKSPSPADPVTFNAWGDRPNCTTYCNSAFL⁵IDAQMV⁶QDKRNGR

Mh_NanH 150 LYVMHGTW¹SM²S.....DQ³QWY⁴GG.....
 Hp_NanH 154 IYVAMHGTW¹AT²G.....NRN³WY⁴QD.....
 Pm_NanH 148 LYVMHGTW¹AG.....TQ²NWY³RD.....
 Pm_NanB 163 IFLAVDMF¹AD²GAGFFGVKDSGNGRINIDGKQYPI³LNEKQSG⁴R⁵WTLRENGEVFDHENKKT

Mh_NanH 168R¹.VPHFNSGS²WAA³TIYKST⁴DG⁵GLN⁶W
 Hp_NanH 172R¹.FNYPQNNI²WAT³TIYKSID⁴GCKT⁵W
 Pm_NanH 166R¹.LSYFNQNI²WAT³TIYKSID⁴GGLSW
 Pm_NanB 223 SYRVVVEGDPKLNFKDLGDIYNERNEKXGNIY¹LKDR²NTPL³LA⁴INTAYVWL⁵THSD⁶DN⁷GCKT⁸W

Mh_NanH 192 EKNTEFSKFS¹NLDVFS²KVTK³RN.GKPTLGF⁴LG⁵VGSG⁶IVM⁷QDCT⁸LVFPIQTAHQ⁹NCIA¹⁰.TT
 Hp_NanH 196 EKNAEFSKLSN¹PDVFS²KVSK³GPNNP⁴VVSE⁵LG⁶VGSG⁷IVMR⁸NC⁹TLVFPIQTAHN¹⁰XCIA¹¹.AT
 Pm_NanH 190 QKNTEFSNTV¹NRDVF²MKV³QKAGAGN⁴PTIG⁵LG⁶VGSG⁷IVMK⁸DCT⁹LVFPIQTAHRE¹⁰CIA¹¹.TT
 Pm_NanB 283 SNPIDL¹LSAQVKK²DWM³.....K⁴FP⁵GT⁶GP⁷GV⁸GI⁹QTK¹⁰GNLL¹¹FP¹²IY¹³TNQ¹⁴H¹⁵CK¹⁶QSSA

Mh_NanH 250 IMY¹SKDN²CKT³WEMPEIDNPV⁴AP⁵NQS⁶SLE.....NMV⁷FE⁸LEP⁹GKL¹⁰..VMT¹¹G
 Hp_NanH 255 IMY¹SKDN²CKT³WEMPEITDLP⁴AP⁵NQISLE.....NMV⁷FE⁸MGDKL⁹..IMV¹⁰G
 Pm_NanH 249 IMY¹SKDN²CKT³WDM⁴PAIN⁵NAL⁶AP⁷NQS⁸SLE.....NMV⁹FE¹⁰IDN¹¹KL¹²..VMT¹³G
 Pm_NanB 332 LVI¹SKDG²CKT³WDLGASP⁴NDSR⁵EDLYGQ⁶NSQTLRTNQRGHELTE⁷SQ⁸LV⁹E¹⁰LEN¹¹GDLKLF¹²MRN

Asp box

Mh_NanH 293RGNS¹RWAY²SSTDM³CKT⁴WELF⁵PTNGLLPTSS⁶QPT⁷QGS⁸SI⁹YV¹⁰TLPN¹¹CR¹²KV¹³LLI
 Hp_NanH 297 REARVRGTQADK¹RWAY²YTEDM³CKSW⁴HAYE⁵PAS.FGSSTA⁶QPT⁷QGS⁸SI⁹YV¹⁰TLPN¹¹CR¹²RV¹³LLV
 Pm_NanH 291 REDN...RRKT¹RWAY²YTEDM³CKT⁴WHVYE⁵EVNGFSATTAAP⁶QGS⁷SI⁸YV⁹TLPS¹⁰CKRV¹¹LLV
 Pm_NanB 392 TSGRV.....MMS¹TSK²DG³CY⁴TWLD⁵THQVSELKHGYS⁶QL..SVIK⁷Y⁸SKKIN⁹CKEY¹⁰IYF

Asp box

Mh_NanH 345 SKP...DCKNDG¹WK²RGD³ITLWMLDAKDP⁴.SHKHK...VH⁵IT⁶IRP⁷...GS⁸NA⁹AG¹⁰AG¹¹YSS¹²L
 Hp_NanH 356 SKP...NCGNDN¹WARCN²LALWMLDAKDP³.QH⁴VYE...VA⁵IT⁶IRP⁷...GS⁸NK⁹AG¹⁰AG¹¹YSS¹²L
 Pm_NanH 347 SKP...NCGNDY¹ARGN²LALWMLDAKDP³..HKHQ...VA⁴IT⁵IRP⁶...SG⁷..NA⁸AG⁹AG¹⁰YSS¹¹L
 Pm_NanB 442 SGQSV¹SGXGG²DLRR³NGK⁴LFLGEVQEDGSI⁵VWKTDKL⁶VRE⁷HSS⁸SGKAXR⁹GYPN¹⁰G¹¹YV¹²YSS¹³M

Mh_NanH 394 A.YKEGNLF¹VAFENDGDISVKNL²TEHIAEMEA³KAI⁴EWGL⁵LPD.....E⁶LTP
 Hp_NanH 405 A.YKEGNLF¹VAYEDDGNITVKNL²TEYMTDIQAKALE³WNLPD.....E⁴IEP
 Pm_NanH 393 A.YKEGNLF¹IAFEDDGDITVKNL²SEHMQAIEE³KAT⁴EWGL⁵TD.....E⁶IAT
 Pm_NanB 502 AELGDSIGL¹AYENTTDYTTIM...YLP²IEMQEF³WRD⁴GKIFSDIRQKTPLTVTY⁵NGAD

Mh_NanH 438 ALDKINALPYLNKAQKETLVEKMRRA.....NDTATAQ.....
 Hp_NanH 449 DVKINALMHNLQKQKDELIAKLRRA.....NDNAIAQ.....
 Pm_NanH 437 EVKINSLHNLKQKQKETSAAKMRRA.....NDNAVAE.....
 Pm_NanB 558 SLKIGDGIKQGVGESLGGVTVSEGLVLAQKSEQDKNKAFDVTLNKTGILQVESVQ

Mh_NanH 471 ...SFVINKEMY.....NLKNNSDE.....L.....DKLAKNITKALPSCQNIYQRATA
 Hp_NanH 482 ...SITLDQAMS.....ELKLSFA.....L.....SQQAVSFEKALPSNLKNFQDALA
 Pm_NanH 470 ...SNVLNREMH.....ELKDEATS.....L.....EQKSVAMRKALPSKMKQFKRDLG
 Pm_NanB 618 NIDTLTVNNEASGYIQFSVSDSETPMLNIAKGVSGKEVKLVNLQKKLKPNDKGYHAAQG

Mh_NanH 512YVNKVTNTA.....DTTYL.....
 Hp_NanH 523SINTISESK.....NTTNV.....
 Pm_NanH 511EVRDLTQLT.....NETYL.....
 Pm_NanB 678 EELIAFKDNGQVKWRLVNDELKDGMYVYTLASVAKPSVLRRTSQPHSLYLTNKLITADGK

Mh_NanH 526NYN.....GIMDTYANTYESYL.....ALNTKLDFF
 Hp_NanH 537NYL.....GVHDLYDSLTYTMFL.....ALNNPLDFF
 Pm_NanH 525NYL.....GIQGLMAMLNGSFL.....ALNTLDFF
 Pm_NanB 738 AVSTVAPLKAPLTVNARPQVNPVLAASYLTANLALNKMSEQLQQSFMHETRLLQEKDRSIF

Mh_NanH 551 TRYIQKARKFNEVNTDILYRSFDNFFAHYDTGVRH...NNLSLGLNLTKLSENLRGGLF
 Hp_NanH 562 TKYIEQAKHLNEYNDILYRSFDVDFAHYSGGSKY...NKLSLGGNKTVSEKVAAGLF
 Pm_NanH 550 SKYIKG.EKLNLSYDIDILYSTYKVF.VEYDSVIKNSQHRPTIALGLNTRLTDQTQAGVF
 Pm_NanB 798 VKYLNKGQKY...LGSNLSFIDYGYDENASV...L...SGVMLGKGVWQSERGNHALY

Mh_NanH 606 FEYSNFRNRNSVQIT.....GARAKYEMDN.....HQISGFLRYRGVKKHDMLAR
 Hp_NanH 617 FEYGNKHQKSYHV.....GMRAKYQLDN.....HQIAGFIRYRGVKKHDFIER
 Pm_NanH 608 YEHEKQKQVDAF.....GVRAQYTKGD.....NVLAAFLRYRTVKHDDVIDR
 Pm_NanB 845 TAL...NKTSYKYVTPKAVDGETKAKYQSWGGSSINWHSNLPHNLIVDLSAGYQKHKGDIH

Mh_NanH 649 NNSVDGYL.....NYAYRIQLDDKLSISPSVGCAYVSRSSRLID.....EDLAINSRITVY
 Hp_NanH 660 NNNVDLYL.....NYAYQLRLSEDLVSPSFGAYISRSNRTLLD.....QDVAVNKRITVY
 Pm_NanH 651 NNNVDLYI.....NYAKNVNID.HLTLSPFVGCAYTSLSSRTLLD.....EDVAVNKRILVM
 Pm_NanB 902 AGHVKGYTFNIGALGRYQWMKNAFTBMVGLHYLYASLSDVNDQANKALLKYNNEFAL

Mh_NanH 699 ASDVGLNIHYKLNIDAYIRFSITGFVNGDITLSOSNDMTNTYKIKDKSNVYSVITGLKR
 Hp_NanH 710 AGDVGNLMYKINDINVNIIRNIAFINDSLKLSOSNDKSNVYKISSHNTIYGLATSINKA
 Pm_NanH 700 AGDVGLDIRYRLADISVSIIRNIAFIKDGFTLSQANYQDNQYKIKSTNMVYALNVGVEKQ
 Pm_NanB 962 KTNLGVVNYRIGKFEVKGLLSYDMYQK...TRQLYVDDVAKQKGLADITLHLNTIQFVAH

Mh_NanH 759 FANGVALGADFKLHRYGSQTTFSNFGLNVSYNW
 Hp_NanH 770 FSNGLVGSTLELQKYGSTYSNVNLGVDISYTW
 Pm_NanH 760 FTPHL..AGSMKLGKYGSAASEVSLGVNLSYHW
 Pm_NanB 1020 LTPRFASFTEVGFQHA.RNKGQSSFAVGAHYQE

β-barrel motif



Figure 12. Multiple sequence alignment of *M. haemolytica* NanH (Mh_NanH), *H.parasuis* NanH (Hp_NanH), *P. multocida* NanH (Pm_NanH) and NanB (Pm_NanB). Catalytic residues are marked with an inverted triangle and conservative motifs are marked in a dashed square.

3.5 Conclusions

The loci of the enzymes required for sialic acid metabolism were identified and three of them were associated to a serotype. The loci of four putative autotransporter chaperones were identified by sequence homology to *P. multocida* Pm70 sequence. These data suggest that there is evidence in the genome sequence of *M. haemolytica* supporting the hypotheses of NanH role in the bacterium metabolism and its export mechanism. The next step is to evaluate gene expression and functionality of the predicted proteins.

Sequence conservation of NanH was confirmed, increasing the possibility of proposing it as a therapeutic prophylactic target.

4 Prediction of NanH tertiary structure

Even though the sequence of various neuraminidases of different origin can be highly variable, the catalytic mechanism remains conserved. For instance, the neuraminidase of influenza A and B only have 30% of sequence identity but their tertiary structure and catalytic mechanism is identical (Shtyrya et al., 2009). Therefore, by sequence homology to known sialidases, we can predict the tertiary structure, mechanism and catalytic residues of NanH before attempting to solve the coordinates by crystallography.

For this part of the project, a 3D model was proposed, the putative key residues were hypothesised and they represent the basis for the laboratory work.

4.1 NanH architecture (BLAST)

The sequence of NanH obtained from GenBank database accession number ABN42196.1 submitted by Fernandez-Martinez et al (Translation of EF215852) was compared to non-redundant protein sequences using the tool BLAST in order to predict the functional domains by sequence homology. Results showed a sialidase domain (cd15482) on the N-terminus, formed by residues A65 to T416 and an autotransporter domain (pfam03797) on the C-terminus formed by residues N586 to T778. In addition to the BLAST search, NanH sequence was submitted to the server SignalP 4.1 and a signal peptide was predicted from M1 to A22 (Figure 13).

The sequence shows a domain arrangement typical of the type V secretion system formed by a signal peptide that suggests export from the cytoplasm into the periplasmic space via Sec machinery, followed by an N-terminal passenger domain formed by the sialidase domain and a C-terminal β -barrel domain. An

additional molecular signature of the β -barrel domain was observed even though it was not aligned by BLAST to the pfam03797 consensus sequence. The motif (Y/V/I/F/W)-X-(F/W) is present at the end of the sequence of NanH as YXW (Henderson et al., 1998).

The catalytic domain was classified in the conserved domain family of non-viral sialidases (cd15482) (Figure 14). It contains a RIP motif in positions 75 to 77 followed by three aspartate boxes formed by residues S111-W118, S253-W260 and S302-W309. The catalytic site was predicted to be formed by amino acids R75, D100, E277, R293, R356, Y390 and E405. Finally, five blades that form the typical β -propeller structure of sialidases, were predicted to be formed by residues S74-F126, S136-V205, G218-I265, L275-F312 and S322-I378.

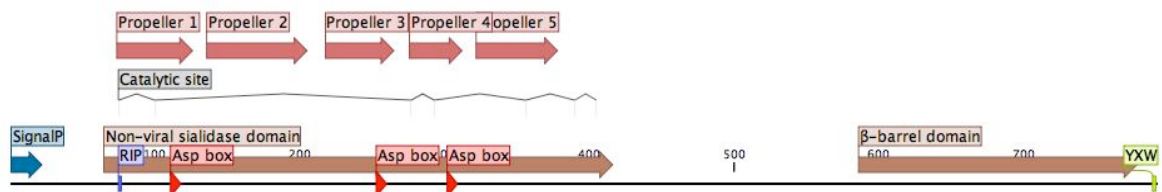


Figure 13. Diagram of NanH domains according to predictions made by sequence homology with BLAST, signal sequence prediction made with SignalP 4.1 and additional identification of YXW motif in the sequence. Continuous line illustrates the length of the aminoacid sequence (black), overlaying arrows show the location of three Asp box motifs (bright red), overlaying rectangles show the RIP and YXW motifs (purple and green respectively). Predicted signal peptide (blue arrow) and functional domains sialidase and β -barrel (brown) are shown above the sequence. Location of the putative catalytic aminoacids of the sialidase domain are marked with grey lines. Aminoacids that putatively form the propeller-like folds are shown at the top (pale red arrows).

| Domain | Accession no. | Interval | E-value |
|---------------------|---------------|----------|------------------------|
| Non-viral sialidase | Cd15482 | 65-416 | 2.26×10 ⁻⁵³ |

Pssm-ID: 271234 [Multi-domain] Cd Length: 339 Bit Score: 187.28 E-value: 2.26e-53

```

      10      20      30      40      50      60      70      80
Query_94607 65 AAGTAPLYYSRIPAMQVTEDNKLVVMFDLRWNRAYDQ-DRIDPGIAISSDGGHTWTKKTAWSFDRTNHPARRSMDPTLLH 143
Cdd:cd15482  5 VPGDEGSDSYRIPSLVTTPNGTLLAFADGRYEGAGDLgGDIDIVVRRSTGGKTWSEPVTV-VDGGGSGGASYGDPSLVV 83

      90     100     110     120     130     140     150     160
Query_94607 144 NPIDNSLYVMHGTWMSDQQWYGGRvphfnsGSWAATIYKSTDGGLNWEKNTefskfsnLDVFSKVTKNKPtlGFLGGV 223
Cdd:cd15482 84 DPDTGRIFLFYTSGPGGGEALTGD-----GTVRVRLSTSDDDGKTWSEPR-----DLTPQVKPSGWK--FFTGP 147

     170     180     190     200     210     220     230     240
Query_94607 224 GSGIVMQDGTLVFPIQT--AHQNGIATTIMYSKDNGKTWEMPEIDNPVAPNqsSLENMVFELEPKLVMTGR---GNSR 297
Cdd:cd15482 148 GRGIQLSDGRLVFPAYArnGGGGGDGAVVIYSDDGGKTWTRGGGVPSSGAG--GDEPSIVELSDGRLLMNARnsqgGGGR 225

     250     260     270     280     290     300     310     320
Query_94607 298 WAYSSTDMGKTWELFTPTNGLLPTSSqptQGSSIYVTLPNGRKVLLISKPDGKNDGwkRGDITLWMLDAkDPSHKHVHI 377
Cdd:cd15482 226 AVAESTDGGETWSEPVPTPSLPDPGC---QGSLIRLP-DGGRKVLLFSNPASPGK--RTNLTLRLSDD--GGKTWDPVRV 298

     330     340     350     360
Query_94607 378 IRPGSgnaaGAGYSSLAY-KEGNLFVAFENDGDISVKNLT 416
Cdd:cd15482 299 LEDGP---GSGYSSLTQlPDGTIGLLYEEGRGGYEGIK 334

```

| Domain | Accession no. | Interval | E-value |
|-----------------------------|---------------|----------|-----------------------|
| Autotransporter beta-domain | Pfam03797 | 586-774 | 3.86×10 ⁻⁵ |

Pssm-ID: 304612 Cd Length: 263 Bit Score: 44.75 E-value: 3.86e-05

```

      10      20      30      40      50      60      70      80
Query_94607 586 NNLSLGLNTKLSENLRGGLFFEYSNKNRNSVQIGARAKyeMDNHQLSGFLRYRGV-----KHKDMLA- 647
Cdd:pfam03797 31 GGLQVGADARLGGGWRLGLAAGYGRSSFDVDRGGSGK--VDSYQAGVYGGWFLQggglyldgvlgygrndndTRRDVDLg 108

      90     100     110     120     130     140     150     160
Query_94607 648 -----RNNSVDGYLNYAIRIQLDDKLSISPSVGAYVSRSSRSLIDE-----DLAINSRTVYA--SDVGLNIHYKLN 711
Cdd:pfam03797 109 tsetakgdyDGHGLGASLEAGYRFKLSGGLSLTPFAGLAYQLRQDGFTEsggsfGLSVDSQSYDSltGRLGLRLDYRFA 188

     170     180     190     200     210     220     230
Query_94607 712 DIDAYIRPSIGF-----VNGDITLSQSNDMTNTYKIKDKSNVYSVTTGLKKRFANGVALGADFKLHRY 774
Cdd:pfam03797 189 LGGGKLQPYARLgwahefgdsravPTAGTTGLGTAGSFVVAGTPLARNSAELGAGASLKLGNLSLYLNYNGYDL 263

```

Figure 14. Alignment of NanH to consensus sequence of non-viral sialidases (Cd15482) and consensus sequence of the autotransporter domain family (Pfam03797). Residues marked in red are identical to the consensus sequence of the family, residues with a low conservation are marked in blue and unaligned residues are marked in grey.

4.2 Prediction of tertiary structure

The tertiary structure of NanH was predicted by sequence homology using the server Phyre² (Kelley and Sternberg, 2009, Kelley et al., 2015). A multi-domain

model was constructed by multi-template modelling of the whole NanH sequence as shown in figure 15.

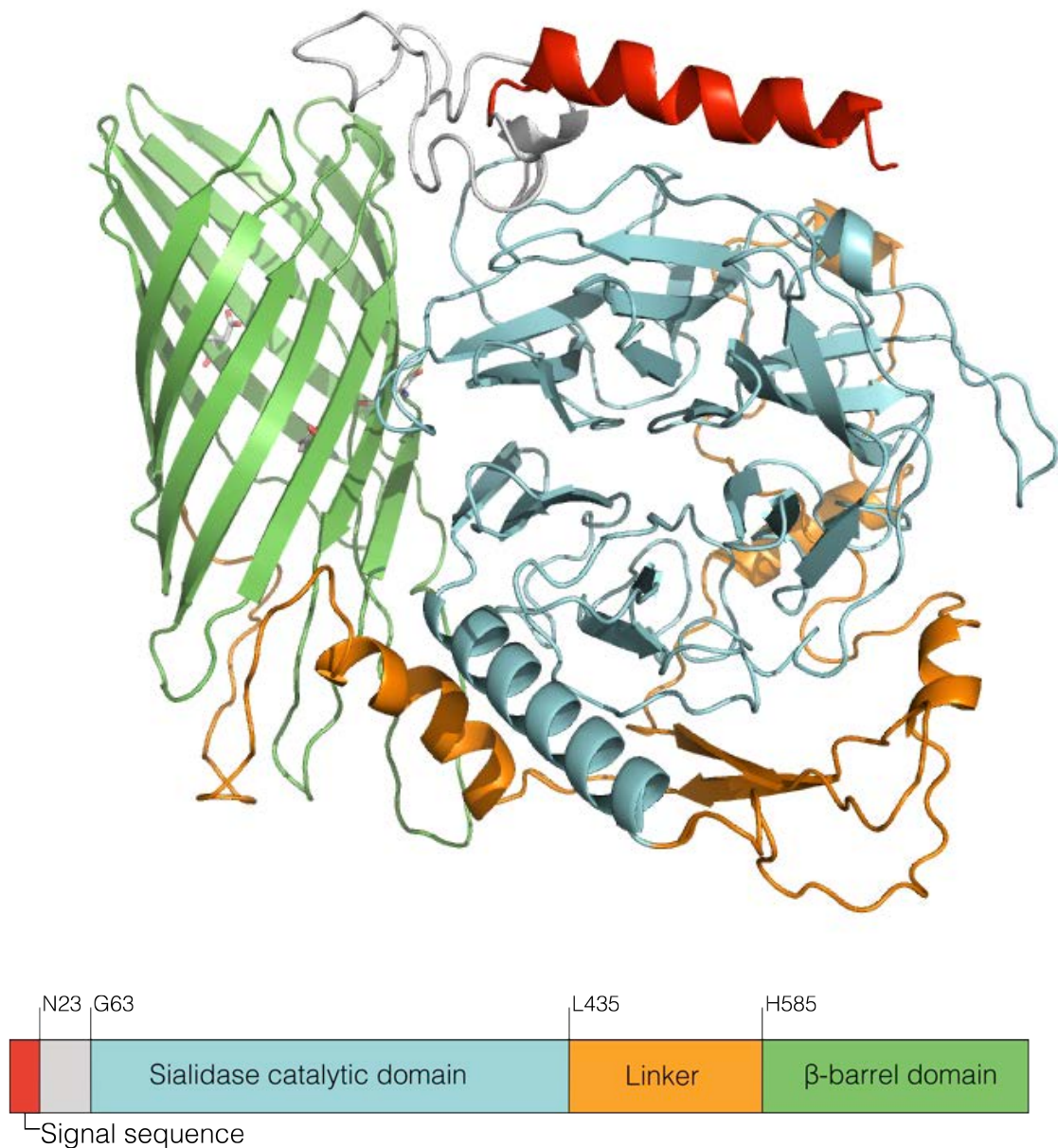


Figure 15. A multidomain model was made with Phyre² to illustrate the putative folding of NanH domains. However, folding into a single molecule is unlikely to exist because the signal peptide is thought to be cleaved after Sec translocation into the periplasmic space followed by cleavage of the β -barrel domain after translocation into the extracellular space. The predicted signal sequence is coloured in red (Residues 1 to 22) followed by residues 23 to 62 coloured in grey which were modelled by *ab initio*. Predicted sialidase domain structure is coloured in cyan (residues 63 to 435) followed by a second region modelled by

ab initio in orange (residues 436 to 585). Finally, the C-terminus β -barrel in colour green (residues 586 to 791). A linear map illustrates the length in aminoacid residues of the predicted domains.

In order to obtain a final multi-domain model, the sialidase and the β -barrel domains were modelled by sequence homology at a confidence higher than 90%, which means that 74% of the tertiary structure was predicted by homology to models solved by crystallography (Table 22). The rest of the model was made by the method *ab initio* which predicts the secondary and tertiary structure by amino acid physical properties and by their interaction according to their arrangement. However, the latter method is less accurate therefore, confidence in the prediction of those areas of the model is lower.

| Template (PDB accession) | Template description | Alignment coverage | % Model confidence | % Identity |
|--------------------------------|--|-----------------------|-----------------------|------------|
| c1n1vA | <i>Trypanosoma rangeli</i> sialidase in complex with DANA | 62-435 | 100 | 31 |
| d1n1ta2 | <i>Trypanosoma rangeli</i> sialidase in complex with DANA at 1.6 Å | 61-435 | 100 | 33 |
| d2ah2a2 | <i>Trypanosoma cruzi</i> trans-sialidase in complex with 2,3-difluorosialic acid (covalent intermediate) | 61-435 | 100 | 30 |
| c4bbwA | The crystal structure of Sialidase VPI 5482 (BTSA) from <i>Bacteroides thetaiotaomicron</i> | 61-415 | 100 | 29 |
| c4fj6C | Crystal structure of a glycoside hydrolase family 33, candidate sialidase (BDI_2946) from <i>Parabacteroides distasonis</i> ATCC 8503 at 1.90 Å resolution | 59-415 | 100 | 29 |
| c3aehB | Integral membrane domain of autotransporter Hbp | 583-791 | 97.9 | 21 |
| c3sljA | Pre-cleavage Structure of the Autotransporter EspP - N1023A mutant | 583-791 | 97.8 | 15 |
| c2qomB | The crystal structure of the <i>E. coli</i> EspP autotransporter Beta-domain | 583-791 | 97.5 | 13 |
| c3kvnA | Crystal structure of the full-length autotransporter EstA from <i>Pseudomonas aeruginosa</i> | 581-791 | 97.5 | 21 |

Table 22. Summary of data used by Phyre² to predict a 3D model of NanH. The first five rows show the top 5 coordinates used to model the sialidase domain of NanH, the remaining four rows show the coordinates used to model the autotransporter domain.

4.3 Homology to TrSA

As shown in Table 22, the sequences with the highest identity that were used to make a model of the sialidase domain of NanH were those of the *T. rangeli* sialidase TrSA (Figure 16). The 3D model was constructed from residues G62 to L435 which showed 31% of sequence identity to the catalytic domain of TrSA (PDB: 1n1v).

Despite the low sequence identity, the six blades that form the β -propeller structure could be modelled from the predicted secondary structure of NanH. The three aspartate boxes and six catalytic amino acids predicted by BLAST were aligned to those of TrSA (Figure 17).

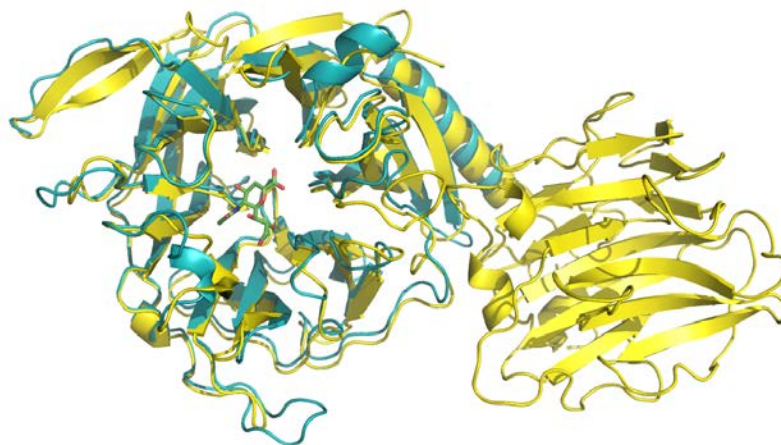


Figure 16. The predicted 3D model of the NanH catalytic domain was superimposed to the catalytic domain of TrSA to illustrate the potential conserved architecture of NanH. The cartoon of the catalytic domain of NanH is shown in cyan, the cartoon of TrSA (PDB: 1n1v) is shown in yellow and a DANA molecule cartoon located in the catalytic site is shown coloured by element (carbon atoms are coloured in green and oxygen atoms are coloured in red).

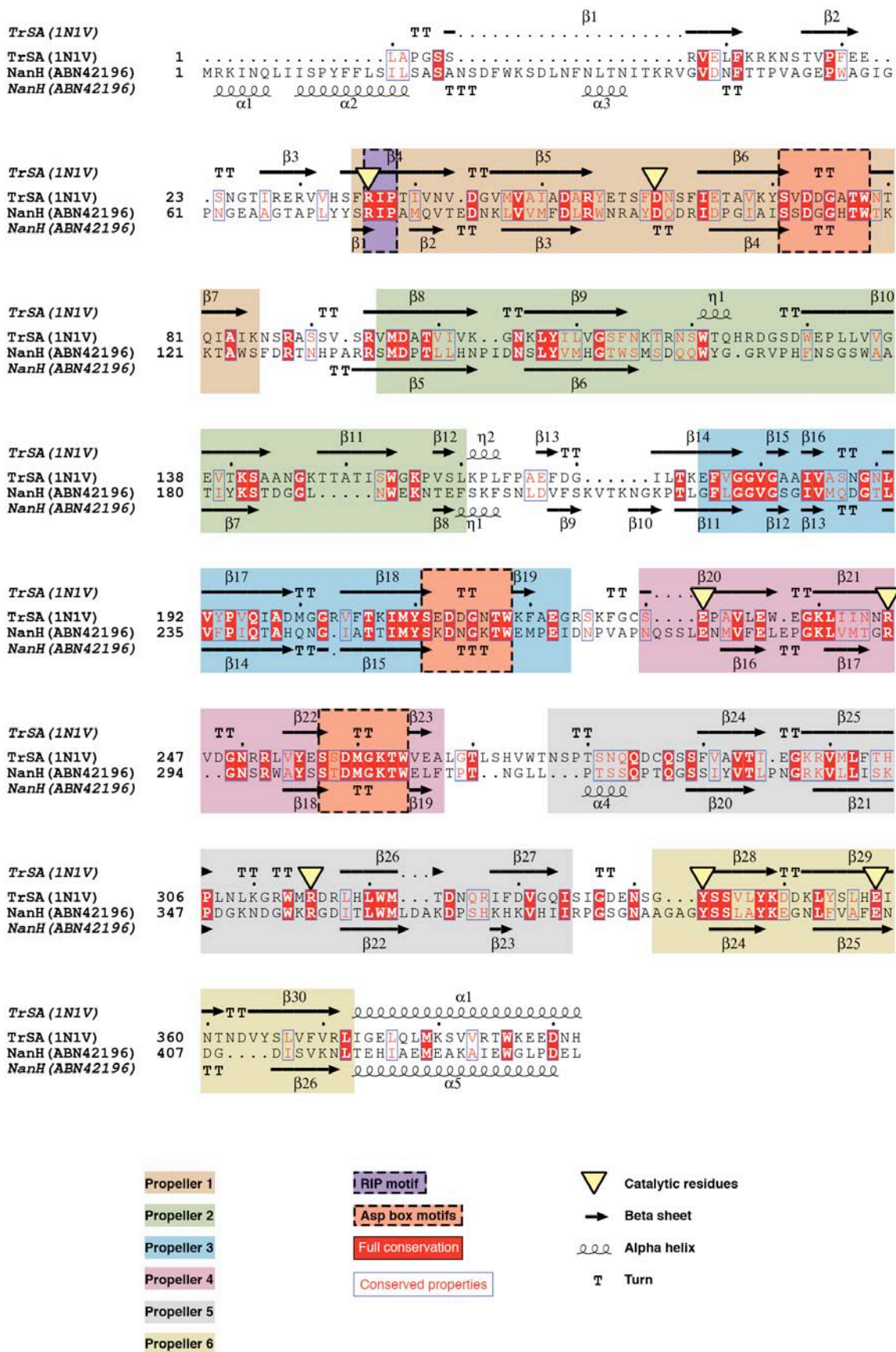


Figure 17. Pairwise alignment of the catalytic domain of TrSA (PDB: 1N1V) and NanH (conserved aminoacids are shown in white font and red background, aminoacids with conserved properties are shown in red font and marked with a blue rectangle and residues

with no conservation are shown in black font). The secondary structure of NanH (depicted below the sequence) was predicted by sequence homology to the known secondary structure of TrSA (depicted above the sequence) and represents the basis for the construction of a 3D model of NanH. The residues that were predicted to form the propeller-like folds of NanH were highlighted in different colours according to homology to known propellers of TrSA. Location of the sialidase motifs RIP and Asp boxes was highlighted in purple and orange rectangles with dashed edges. The putative catalytic residues of NanH were predicted to be identical to TrSA (inverted triangles above the sequence). Pairwise alignment and secondary structure prediction were performed by Phyre². Secondary structure and pairwise alignment shading were drawn automatically by server ESPript 3.0 (Robert and Gouet, 2014). Propellers, motifs and catalytic residues were manually illustrated.

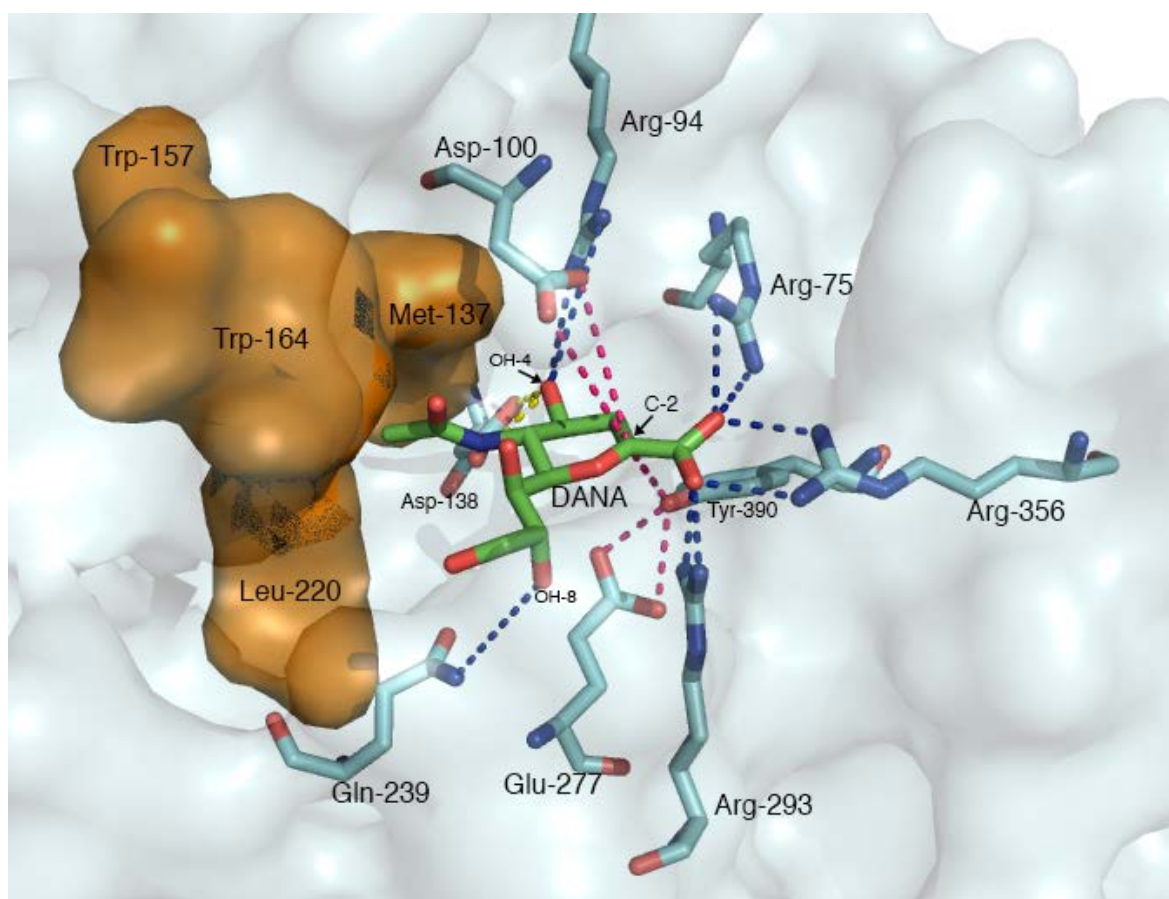


Figure 18. Predicted interaction of NanH with DANA by superimposing the 3D model to the solved structure of TrSA in complex with DANA at a 1.6Å resolution (1N1T). Blue dashed lines show residue coordination of the arginine triad to the carboxylic group and the possible interactions of Asp100 and Gln239 with OH-4 and Gln239 respectively. Yellow dashed line shows an additional interaction of Asp138 with OH-4. Pink dashed lines depict the amino acids involved in the acid/base reactions with C-2 that are required for cleavage of the O-linked glycan. Hydrophobic pocket formed by Trp157, Trp164, Met137 and Leu220 is shown in orange.

4.4 Predicted catalytic mechanism

The 3D model of NanH was aligned against the coordinates of TrSA in complex with the inhibitor DANA (1N1T). Following the proposed mechanism published for TrSA (Amaya et al., 2003) and sequence homology to NanH, we predicted the function of the residues that might interact with the inhibitor according to the alignment to the model (Figure 18) and how they might interact with the substrate (Figure 19).

The arginine triad formed was predicted to be formed by Arg75, Arg293 and Arg356 in NanH. Even though Arg293 of NanH was aligned against Val247 of TrSA, Arg293 was hypothesised to be part of the triad due to the predicted position in the catalytic site and its proximity to the carboxylate of Neu5Ac in the model.

In the TrSA model, Asp60 was designated as the proton donor necessary for the release of the O-linked glycan (Buschiazzo et al., 2000). In the NanH structure prediction, Asp100 was homologous to Asp60 of TrSA therefore, it is possible that Asp100 acts as a proton donor. Additionally, Arg94 and Asp138 in NanH are in proximity to OH-4 therefore, it is possible that they interact with that hydroxyl group.

Amino Acids that stabilise the intermediate state by interacting with the oxocarbonium formed by C-2 were predicted to be formed by Glu277 and Tyr390. Therefore, Tyr390 might form a covalent bond with C-2 in the intermediate state and Glu277 participates in the acid/base reaction that results in the release of Neu5Ac.

A hydrophobic pocket that might accommodate the N-acetyl chain of the Neu5Ac derivatives was predicted to be formed by Met137, Trp157, Trp164 and Leu220.

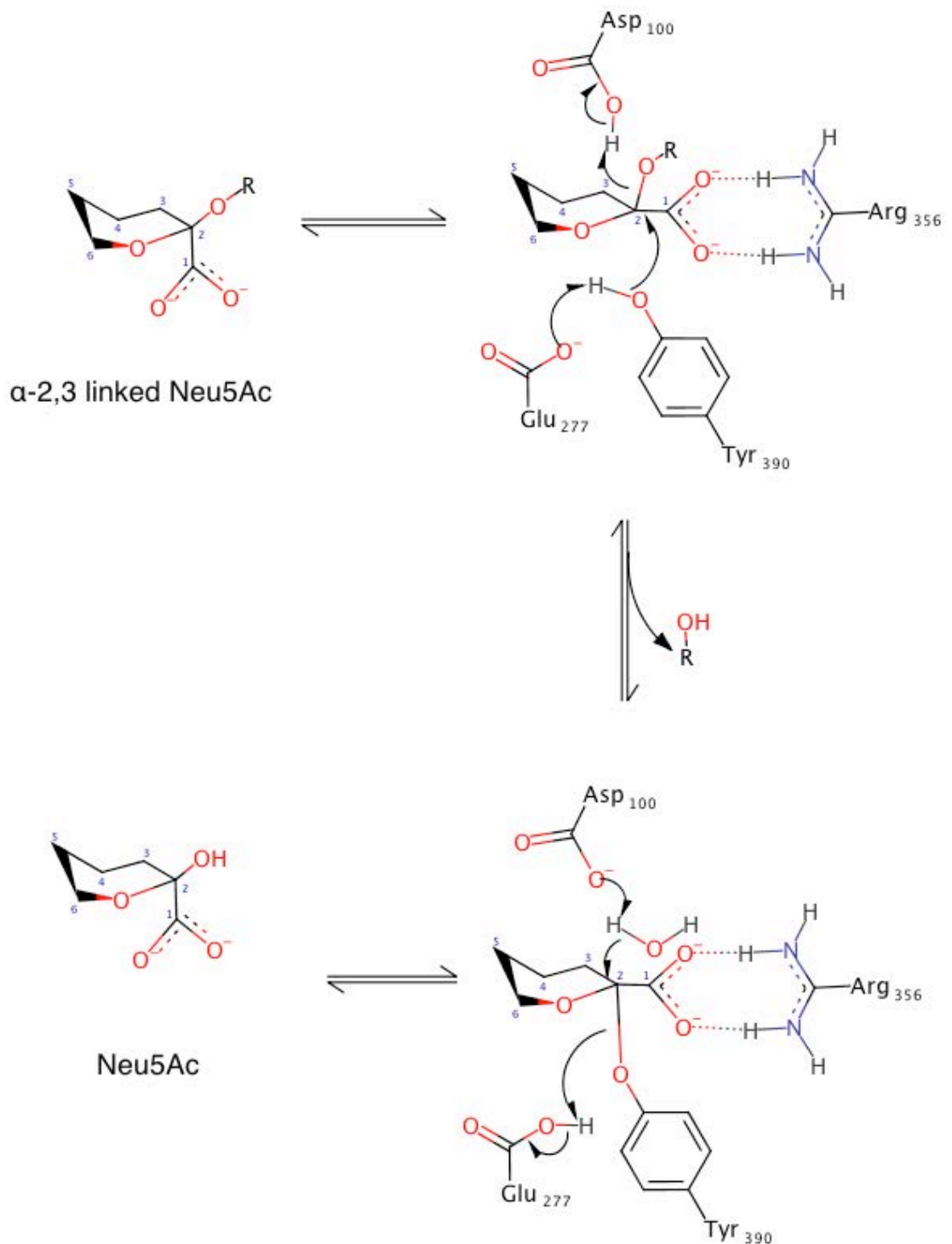


Figure 19. Diagram showing the proposed hydrolytic mechanism of NanH in which a terminal Neu5Ac is cleaved off of an α -2,3 linked sialylated glycan (R = any glycan). The reaction begins when the arginine triad formed by Arg75, Arg356 and Arg293 bind to a carboxylate in the substrate formed by C-1. The interaction induces a change in conformation followed by the hydroxylation of O-2 by Asp100. The glycan is now hydroxylated and released (ROH). The Neu5Ac molecule is stabilised as a carbocation by the interaction of Tyr390 and Glu277. Finally, a water molecule is used to hydroxylate the oxocarbenium (C-2) and the free Neu5Ac molecule is released. Nitrogen atoms are coloured

in blue, while oxygen atoms and carboxylic groups are coloured in red to illustrate positive and negative charges respectively. The Diagram was made with MarvinSketch (ChemAxon).

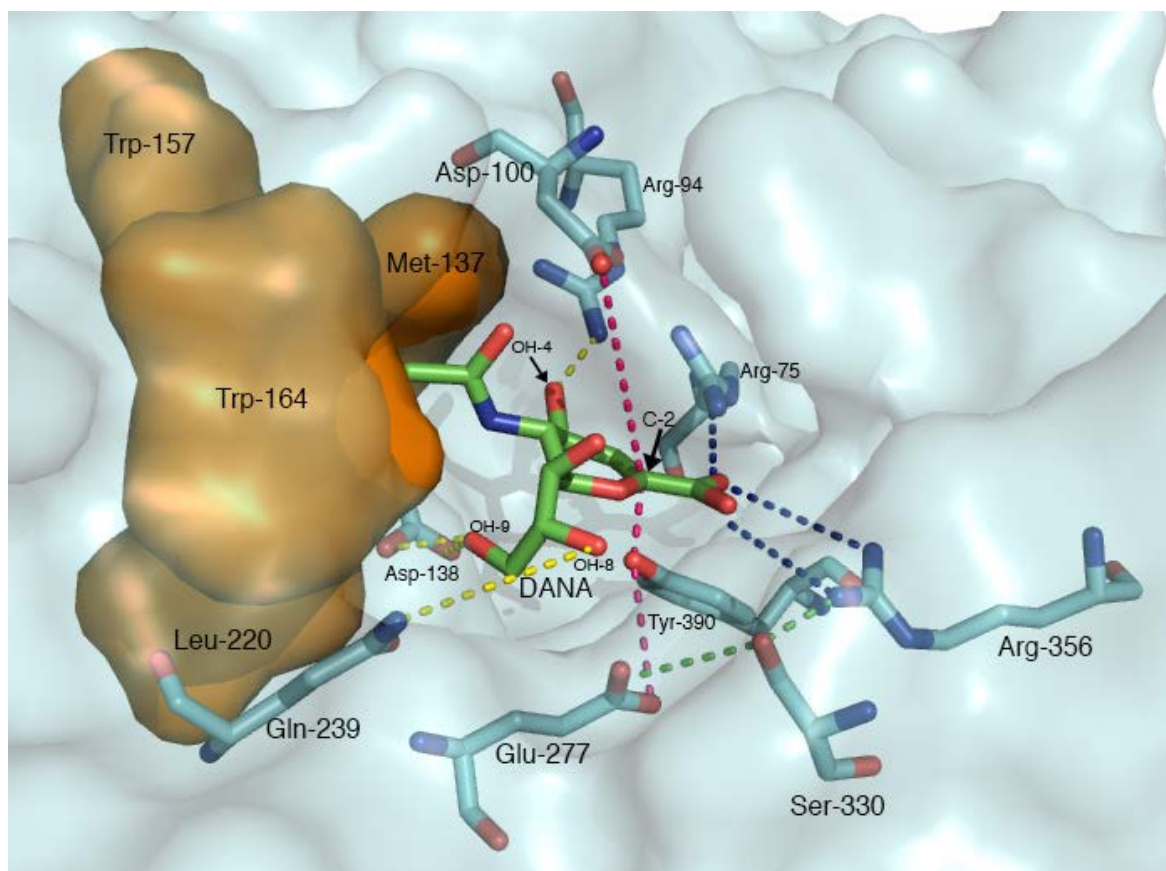


Figure 20. Prediction of the catalytic domain of NanH by sequence homology to NanB of *S.pneumoniae*. Arginine coordination is marked by a blue dashed line, proton transfer is marked by a pink dashed line, side interactions are marked by a yellow dashed line and the aminoacids that form the hydrophobic pocket are shown in orange.

An additional 3D model of NanH was made by Dr V. Bavro using the tools I-Tasser and MAFFT structural alignment for making a model similar to NanB of *S.pneumoniae* by aligning against coordinates 4XOG (Figure 20). The predicted catalytic domain in this model shared the same residues predicted by phyre². However, Ser330 was positioned in proximity to the binding pocket, suggesting a coordination of the side chains of Glu277 and Arg356. In this model, only Arg94 is interacting with OH-4 and Asp138 is interacting with OH-9.

4.5 Homology to Hbp and completion of β -barrel model

A model of the 3D structure of the autotransporter domain of NanH was built by homology to the Hbp autotransporter of *E. coli*. The secondary structure suggests the formation of a β -barrel from residues 585 to 791 however, the pore model is incomplete so it is possible that the residues that are immediately next to the N-terminus of the predicted autotransporter domain, are also part of the β -barrel (Figure 21). The YNW sequence at the C-terminus suggests the presence of a β -barrel signal. The EVNNLN motif, conserved among members of the SPATE family was not observed in NanH (Figure 22).

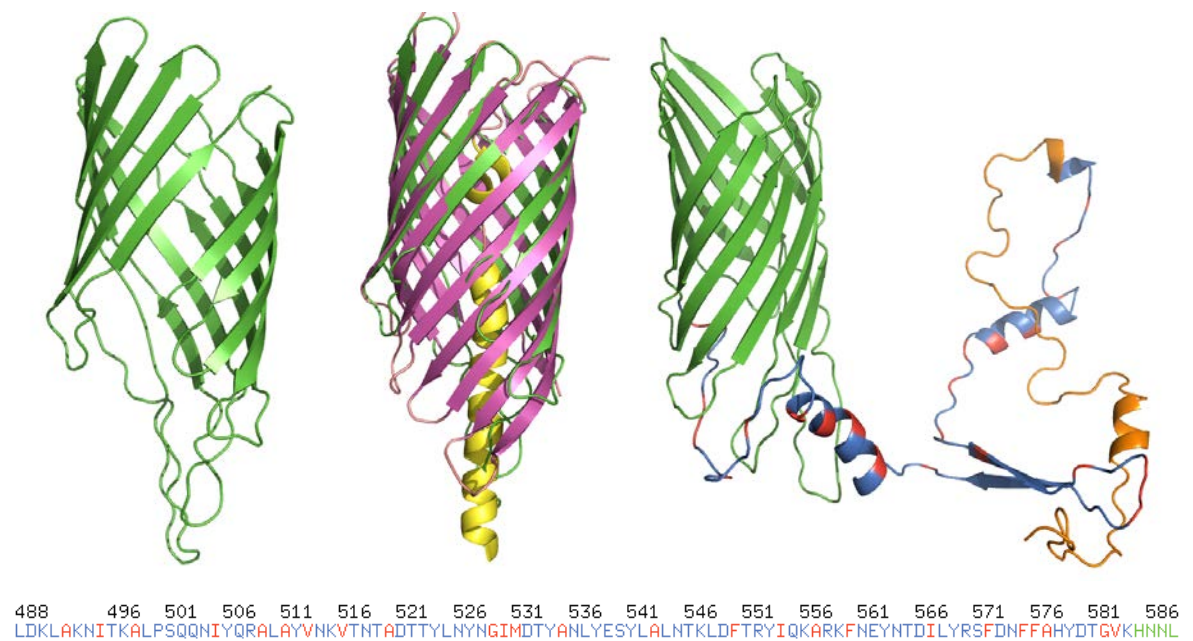


Figure 21. The predicted 3D model of the autotransporter domain of NanH (Green) shows incomplete homology to Hbp (Pink and yellow). The secondary structure of residues 488 to 584 shows an amphipatic nature (Blue: hydrophilic residues. Red: hydrophobic residues) typical of β -barrel domains however, it is difficult to suggest the completion of the pore due to the prediction of an α -helix before the β -sheets formed from 519 to 541 that could complete the model.

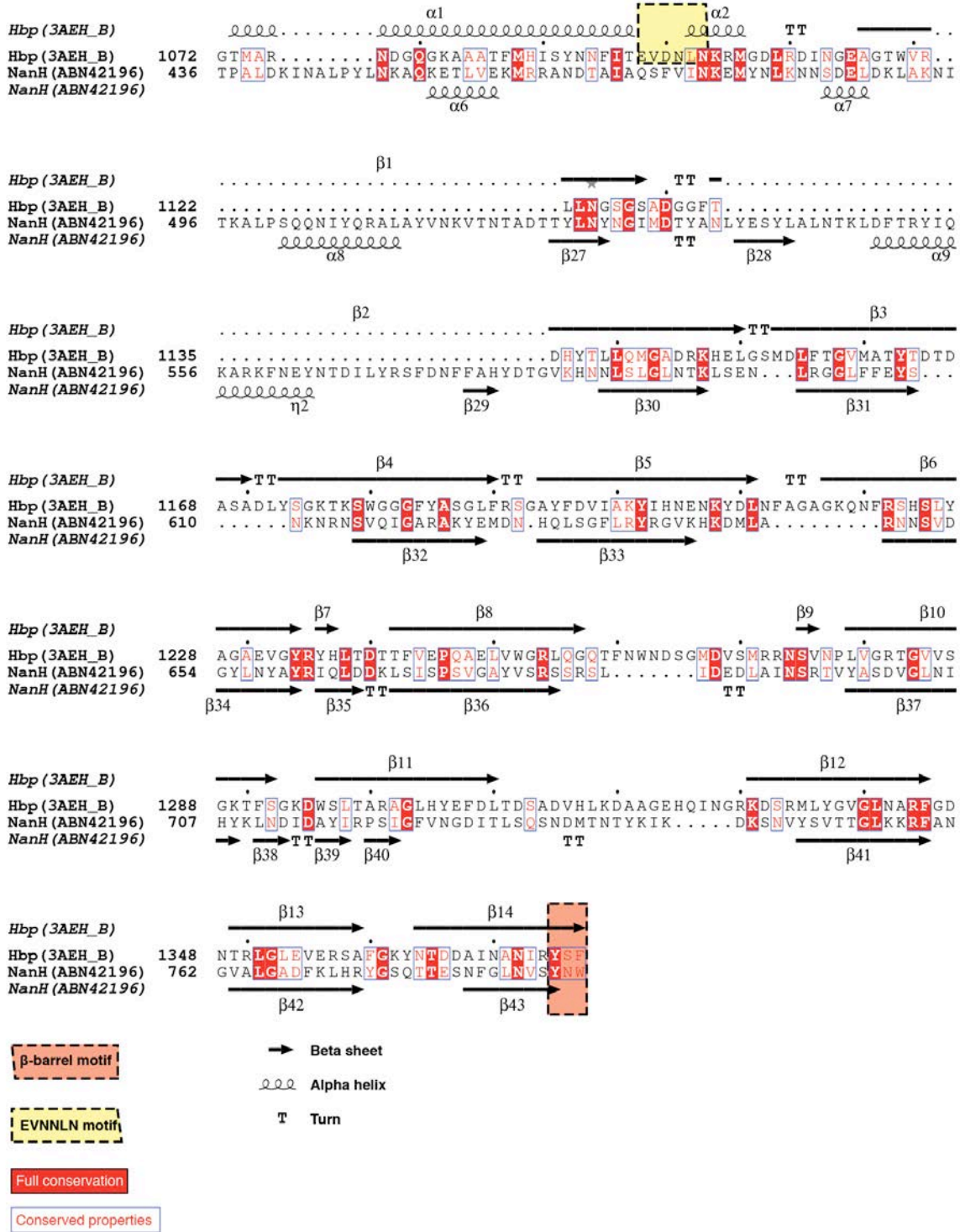


Figure 22. Sequence alignment of Hbp and NanH residues 436 to 791 shows a semi-conserved β -barrel signal motif and a similar secondary structure. The motif EVNNLN, typical of the SPATE family, is missing in NanH.

4.6 Conclusions

Using bioinformatic tools for sequence analysis and protein structure modelling, the putative functional domains of NanH were predicted. By following the known hydrolytic mechanism of neuraminidases, we hypothesised the structure of the catalytic site of NanH and its key amino acids. These data are the basis for the laboratory experiments performed for this project.

5 Delineation of the catalytic domain of NanH

Sequence homology predictions of NanH showed the putative arrangement of the functional domains. Those results show a putative delimitation of the catalytic domain of NanH and suggest an extracellular export mechanism.

It is known that other neuraminidases have a delimited catalytic domain in addition to other domains of variable functions among species however, only sialidases produced by members of the *Pasteurellaceae* family have been predicted to have an autotransporter domain and therefore be exported via TVSS.

The objective in this section was to isolate an active catalytic domain in NanH in order to support that particular bioinformatic prediction and in the future study the functionality of the additional domains.

5.1 Identification of neuraminidase activity in *M. haemolytica*

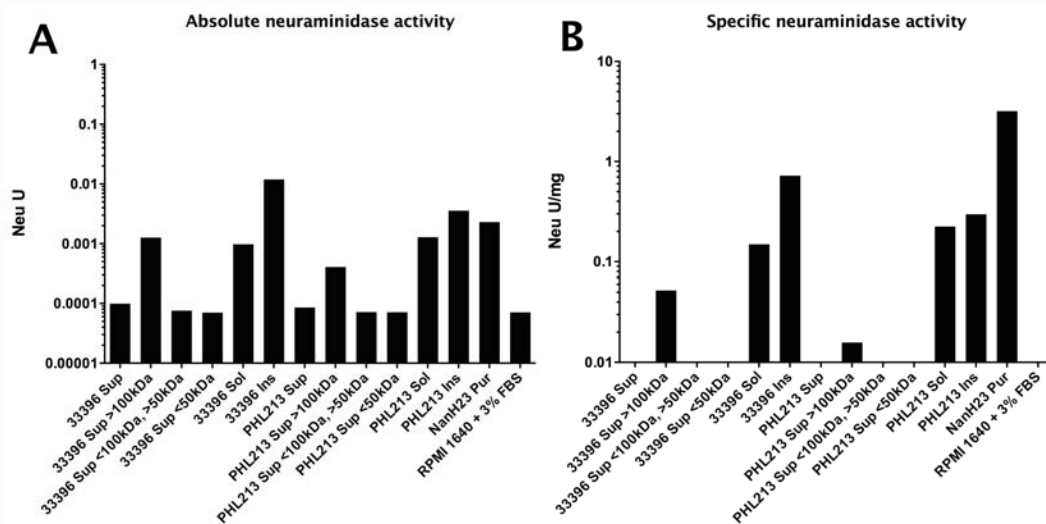


Figure 23. Absolute (A) and specific (B) neuraminidase activity of *M. haemolytica* serotypes A1 (strain PHL213) and A2 (strain 33396) lysate fractions. The supernatant of *M. haemolytica* cultures was fractionated by molecular size using two filter devices. The cell pellets were lysed in a cell disrupter. Activity was detected in the >100kDa supernatant fraction and in both cell fractions for both strains. Graph A shows the absolute neuraminidase activity of the samples used for the experiment. Graph B shows the relative neuraminidase activity per milligram of sample.

The strains ATCC33396 and PHL213 of *M. haemolytica* were grown in 200ml RPMI-1640 + 3% FBS (section 2.8). The cells were disrupted and the supernatants were concentrated using two centrifuge filter devices in order to obtain two solute fractions (section 2.8.1). A neuraminidase activity assay was performed to detect the presence or absence of neuraminidase in the supernatant fractions and in the soluble and insoluble cell fractions. Neuraminidase activity was detected in the supernatant only in the fraction of solutes higher than 100kDa. In the cellular fraction, activity was detected in both the soluble lysate and the insoluble debris (Figure 23).

5.2 Expression and purification of NanH

5.2.1 Cloning and expression of NanH23 (Signal peptide absent)

The construct pFN18KNanH23 was made by PCR amplification of *nanH* from genomic DNA of *M. haemolytica* strain 33396 using primers Sgfl-NanH23-F and PmeI-NanH23-R. The obtained PCR product does not contain the signal peptide predicted to be formed by residues 1 to 22 in order to prevent the export of the protein to the periplasmic space and maximise cytoplasmic concentrations of the protein. The resulting plasmid was cloned into *E. coli* strain KRX for both plasmid replication and protein expression (Figure 24).

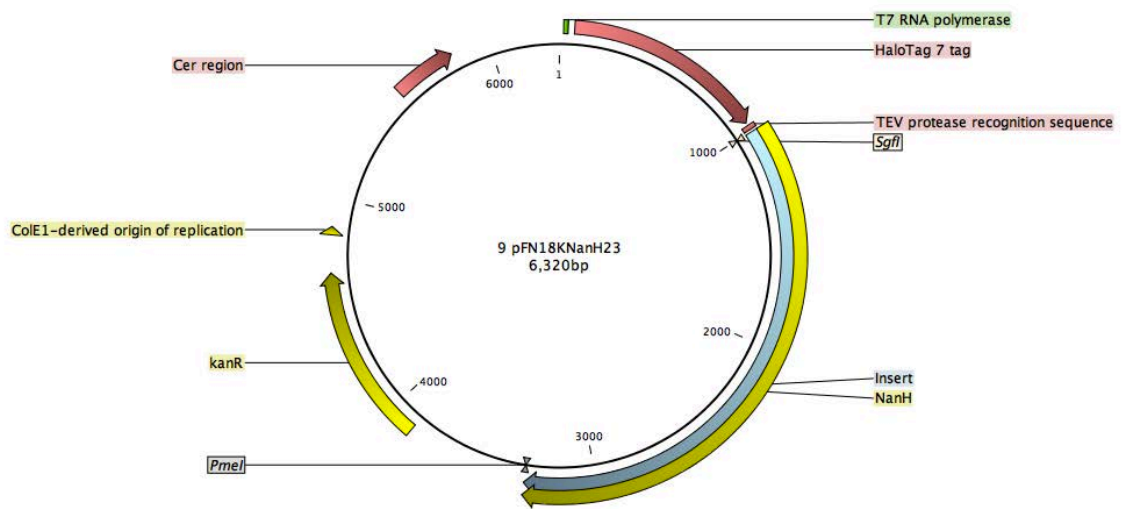


Figure 24. Map of NanH23 in pFN18KNanH23. The backbone plasmid pFN18K contains a T7 promoter region followed by a *haloTag* gene, a TEV protease recognition sequence, a cloning site that is delimited by the restriction sites *SgfI* and *PmeI* and a kanamycin resistance gene. The gene *nanH23* was cloned into pFN18K with the restriction enzymes *SgfI* and *PmeI* and tagged with a HaloTag.

E. coli KRX containing pFN18KNanH23 was grown for protein expression in 50ml of expression media. Filter sterilised culture supernatant, cleared cell lysate and insoluble debris were analysed by SDS-PAGE as shown in figure 25. The size of the fusion between the HaloTag and NanH23 was predicted to be 121.716 kDa. However, the expected protein can only be detected clearly in the insoluble cell debris.

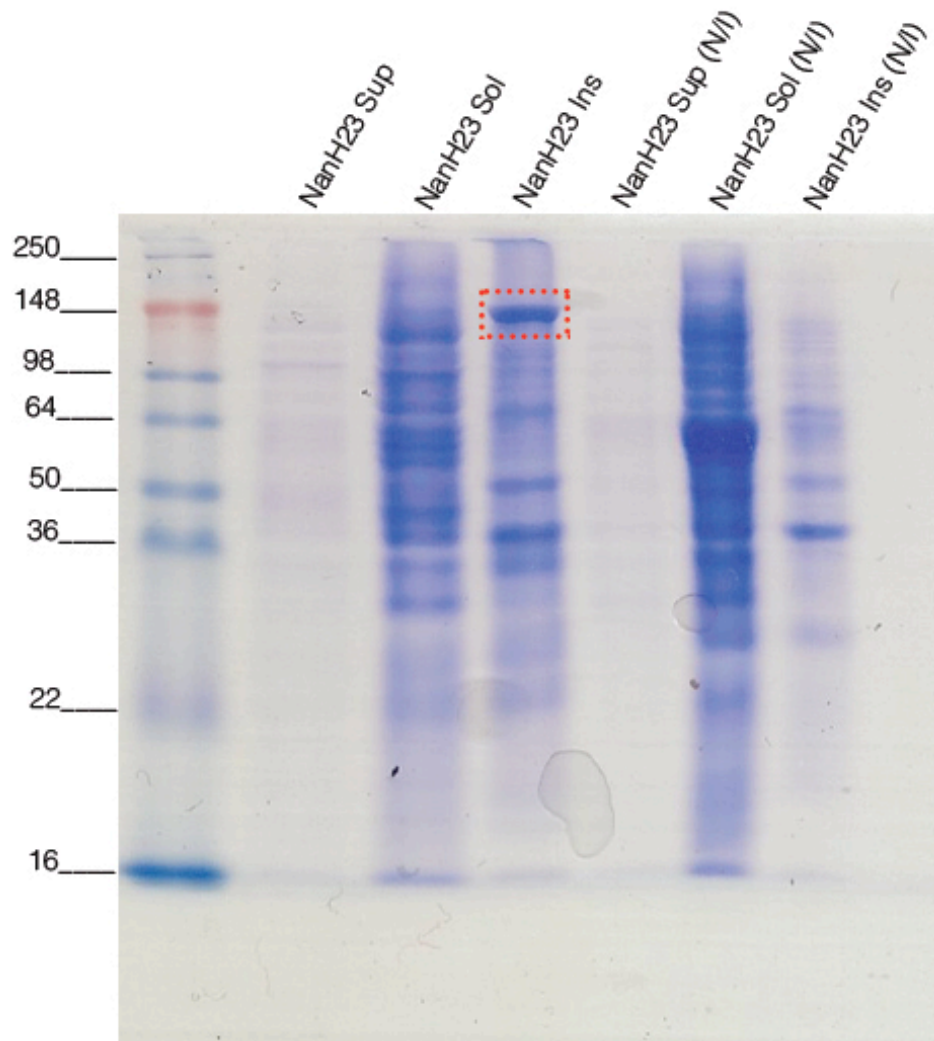


Figure 25. Coomassie blue stained gel of NanH23 expression in *E. coli* KRX. Lanes on the left side show samples from the culture containing 0.05% glucose (Promoter repressor) and 0.05% Rhamnose (Promoter inducer) while lanes on the right show samples from a culture containing only 0.05% Glucose (Promoter repressor) (N/I = Not induced). Expected size of HaloTagged NanH23 = 122kDa (Band marked in red dashed rectangle).

Despite the low expression in the soluble lysate, a 500ml culture was grown in induction media for protein purification. The cell pellet was disrupted and HaloTag protein purification was performed. When the protein purification fractions were analysed by SDS-PAGE, a strong signal was again only observed in the insoluble debris fraction (Figure 26). A band can be observed in the first elute but it does not have the expected size of cleaved NanH23 (i.e. 87kDa) and it is not observed in the second elute. In order to determine if there was active protein in any of the

fractions, a neuraminidase assay was performed. The results suggested that the protein was present although at very low concentrations that could not be detected by a Coomassie blue stained gel.

The second elute of protein purification (E2) that should contain a purified protein without HaloTag and free of TEV protease, was filter sterilised and concentrated using a 50KDa filter device in order to increase the signal detected by a Coomassie blue stained gel. The concentrated protein was analysed by SDS-PAGE and three bands were detected as shown in figure 27.

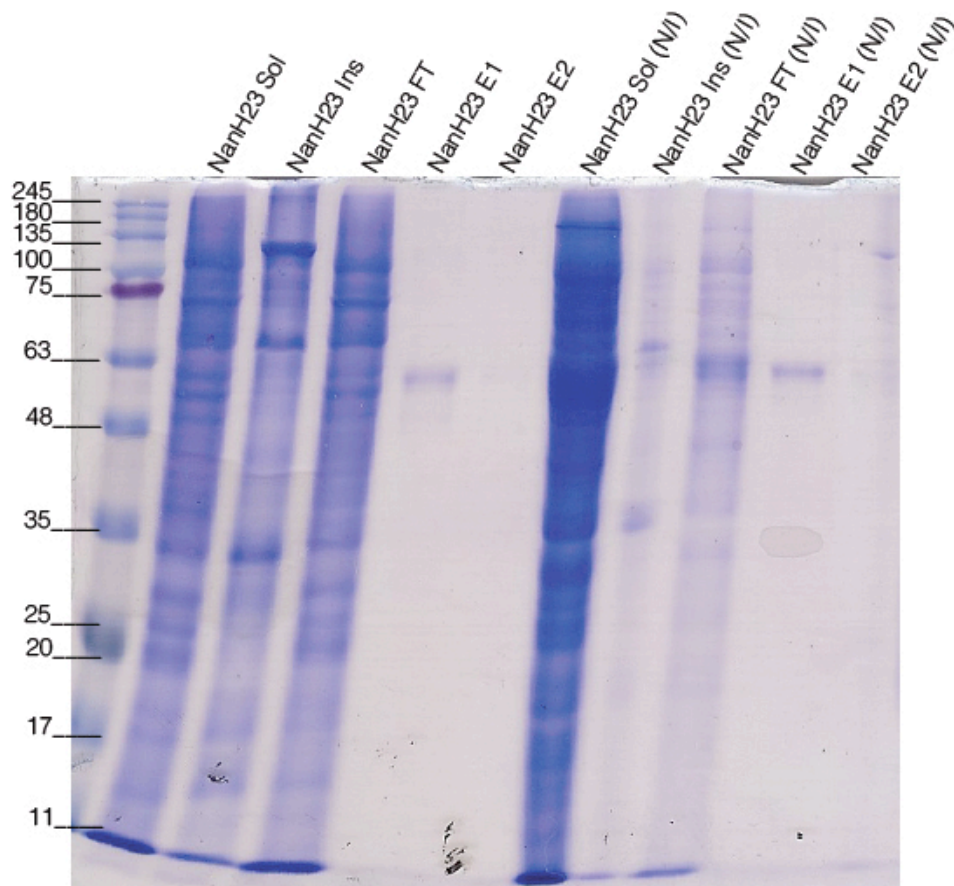


Figure 26. Coomassie blue stained gel containing samples obtained from the different steps of NanH23 purification by HaloTag system. Lanes on the left side show samples from the culture containing 0.05% glucose and 0.05% Rhamnose while lanes on the right show samples from a culture containing only 0.05% Glucose (N/I = Not induced). Expected size of HaloTagged NanH23 = 122kDa. Expected size of TEV cleaved NanH23 = 87kDa.

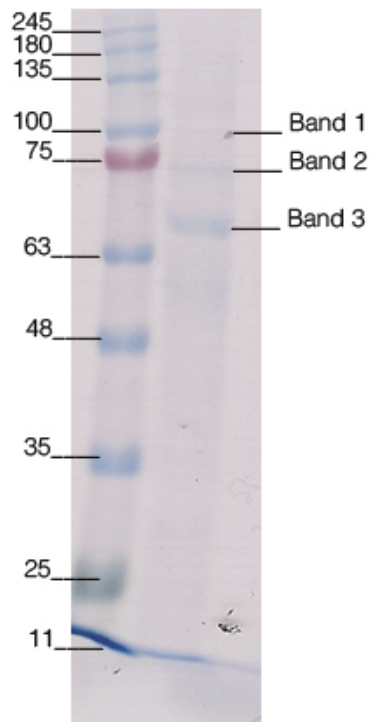


Figure 27. Coomassie blue stained gel containing NanH23 E2 after protein concentration.

The three bands were analysed by mass spectrometry. The results were compared to the protein database of both *E. coli* and *M. haemolytica* to determine if the protein preparation contained NanH and whether the bands were formed by degradation of the protein or an *E. coli* contaminant protein was present.

When the sequence of peptides obtained from band 3 were compared to *M. haemolytica*, 34 peptides were identified as NanH (Accession A3F737) unique peptides. However, the comparison against *E. coli* also showed that 29 amino acids matched the sequence of chaperonin GroL (Accession A0A080GAD6). These data suggests that even though NanH was adequately expressed, chaperonines from the expression host were not completely removed and NanH concentration in protein preparation might be too low even after concentration in filter device.

5.3 Cloning and expression of different *nanH* truncations

Following predictions of NanH tertiary structure by sequence homology to TrSA, we sought to identify the catalytic domain of NanH. Hence, four constructs with different truncations in the sequence were made as shown in Table 23.

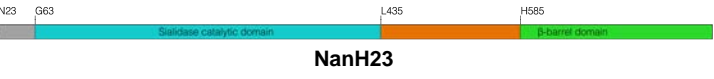
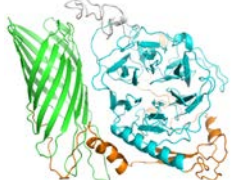




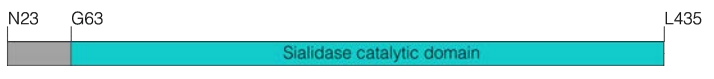

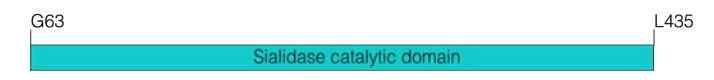
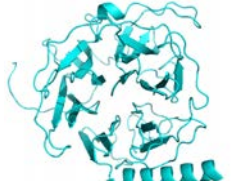
| Sequence diagram | Putative tertiary structure | Cloning primers |
|---|---|--|
|  <p>NanH23</p> |  | Sgfl- NanH23-F PmeI- NanH23-R |
|  <p>NanH23 ΔAT</p> |  | Sgfl- NanH23-F PmeI- NanHH585- R |
|  <p>NanH63 ΔAT</p> |  | Sgfl- NanH63-F PmeI- NanHH585- R |
|  <p>NanH23 cat (NanHcat)</p> |  | Sgfl- NanH23-F PmeI- NanHL435- R |
|  <p>NanH63 cat</p> |  | Sgfl- NanH63-F PmeI- NanHL435- R |

Table 23. Diagrams depicting truncations made in NanH. Putative tertiary structures were added for clarity as the actual folding of each mutant protein was not predicted. Primer sequences are shown in table 11 of materials and methods section.

The constructs containing the mutations were made in plasmid backbone pFN18K, as previously described for NanH23, and cloned into *E. coli* KRX strain.

The bacteria containing the plasmids were grown in 50ml cultures for protein expression. The cellular fraction was lysed for analysis of neuraminidase activity in culture supernatants (Figure 28), soluble cells lysates and insoluble cell debris. Expression was confirmed by SDS-PAGE (Figure 29) and Western blot with an anti-HaloTag antibody (Figure 30).

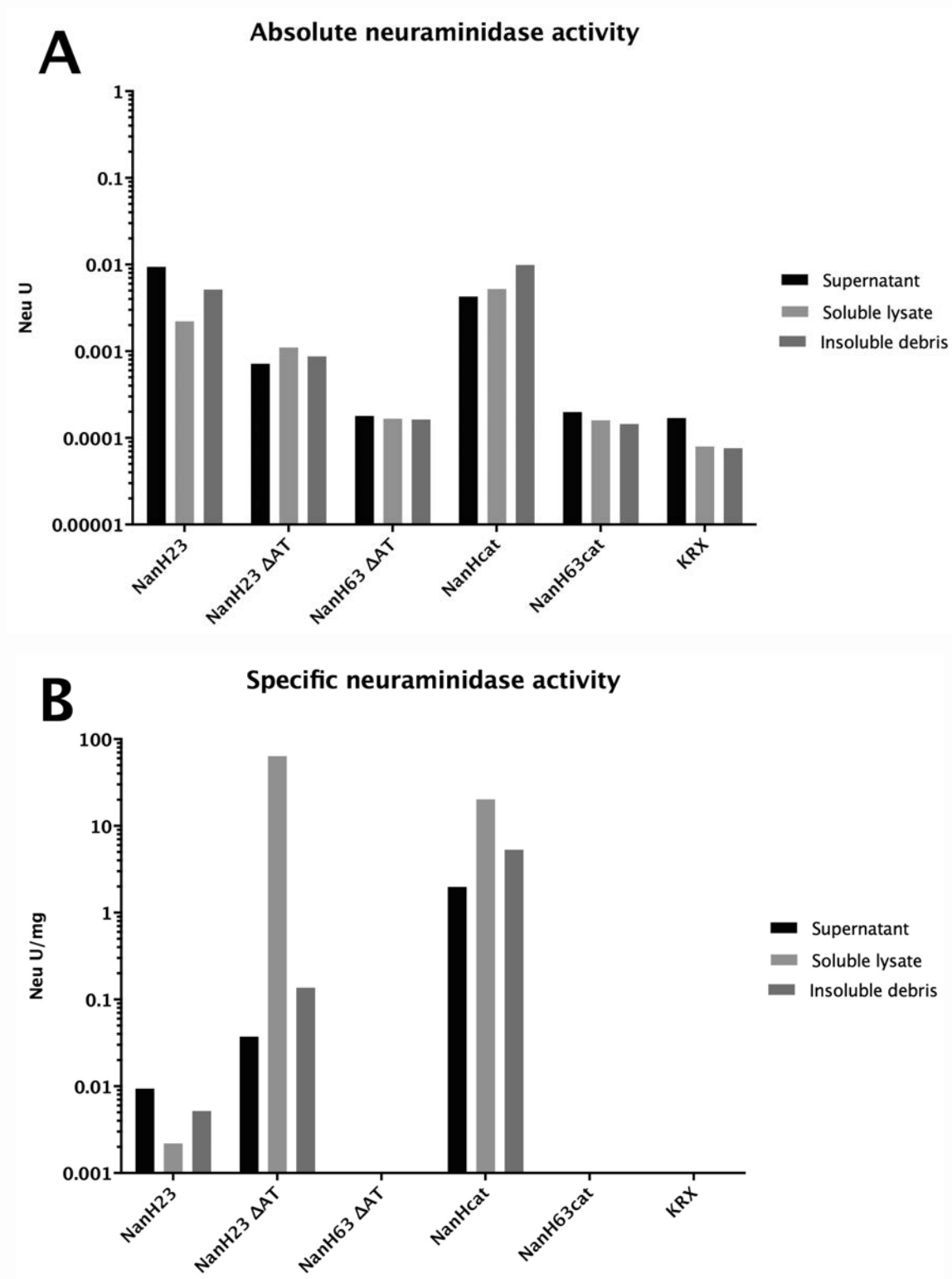


Figure 28. Absolute (A) and specific (B) neuraminidase activity of NanH truncations expressed in *E. coli*. Constructs containing residues 23 to 63 produced neuraminidase activity in the cellular and extracellular fractions while constructs NanH63 ΔAT and NanH63cat did not show any activity. Control cells *E. coli* KRX without a plasmid, did not show any activity either.

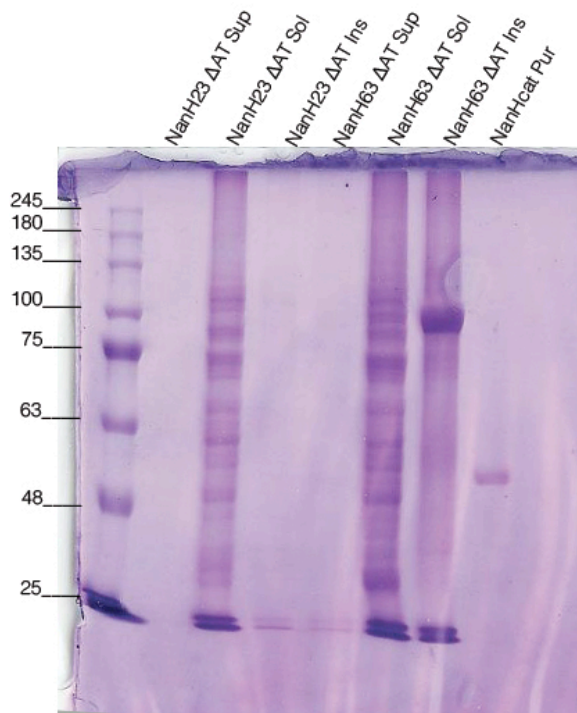
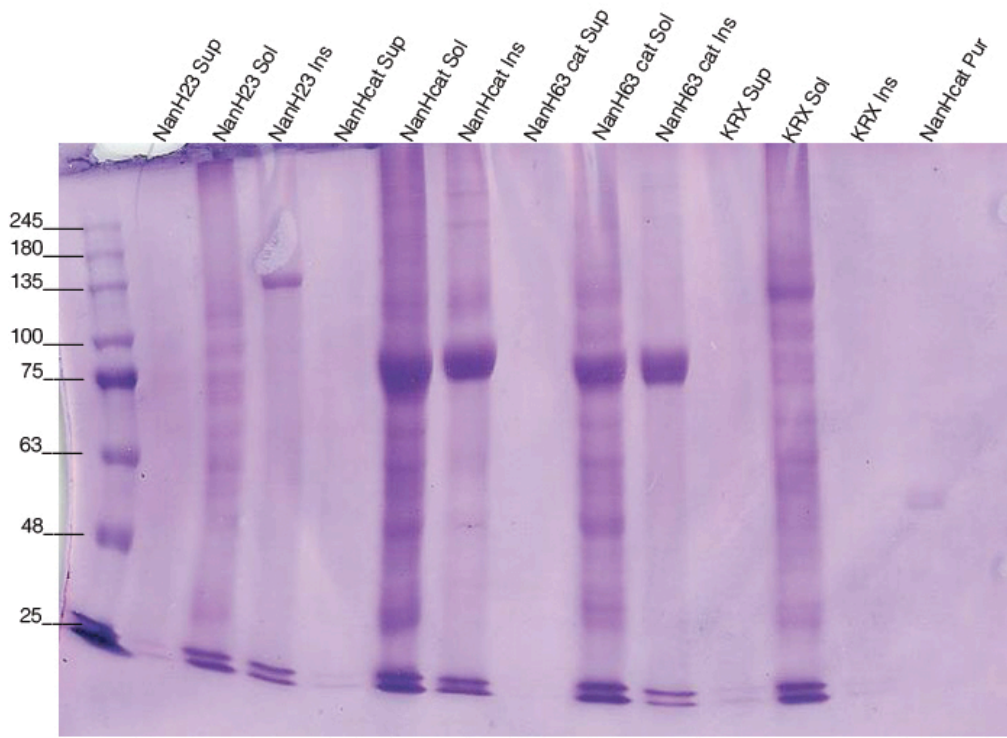


Figure 29. Coomassie blue stained gels showing expression of the different truncations of NanH. Expected size: HaloTagged NanH23 = 122kDa, HaloTagged NanHcat = 81kDa, HaloTagged NanH63 cat = 77kDa, HaloTagged NanH23 Δ AT = 99kDa, HaloTagged NanH63 Δ AT = 94kDa.

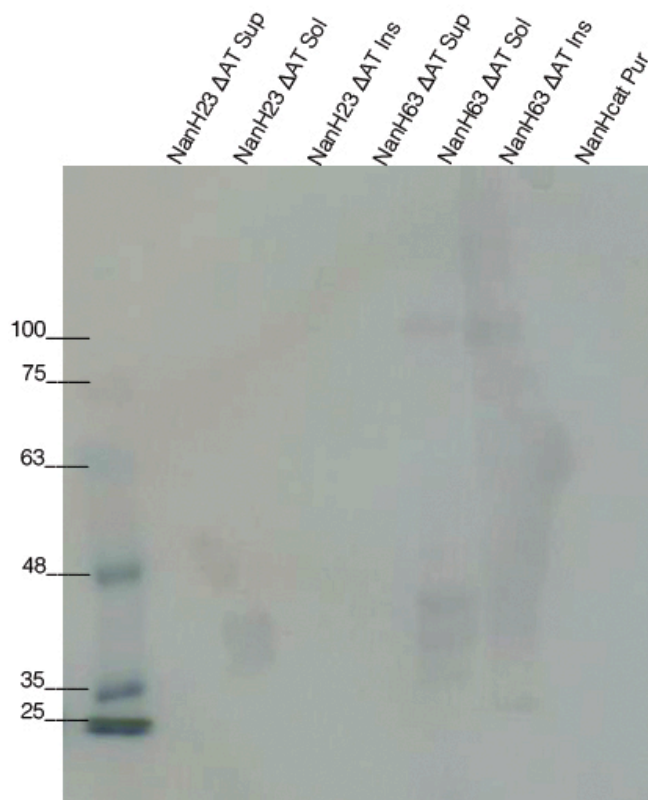
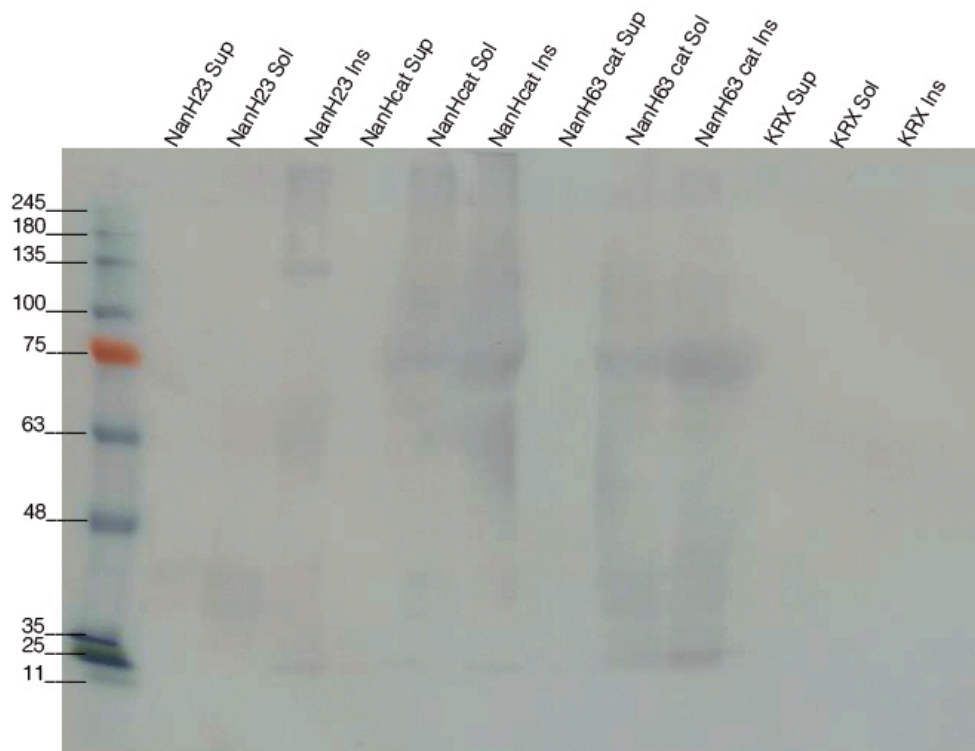


Figure 30. Western blots using anti-HaloTag antibody and developed by chloronaphthol method, showing expression of NanH truncations. Expected size: HaloTagged NanH23 = 122kDa, HaloTagged NanHcat = 81kDa, HaloTagged NanH63 cat = 77kDa, HaloTagged NanH23 Δ AT = 99kDa, HaloTagged NanH63 Δ AT = 94kDa.

The mutants NanH63 Δ AT and NanH63cat, which did not contain residues 23 to 62, lost activity completely. The bioinformatics predictions however, considered that the catalytic domain is formed by a six propeller blades contained within residues S74 to L415 in addition to two α -helices formed by N62 to Y73 and T416 to L435. Therefore, an additional structure contained within residues was not predicted by sequence homology and it seems to be essential for NanH to be active. Probably the additional sequence is required for proper protein folding.

Contrastingly, when the putative β -domain and linker regions were removed, the specific activity was not lost and is even increased. However, we must consider that these results were obtained by calculating the specific neuraminidase activity per milligramme of total protein mass contained in the different fractions of lysed bacterial cultures. Despite that fact, we can conclude that residues N23 to L435 are sufficient for neuraminidase activity. Therefore, the additional sequence might have an additional function.

5.4 Purification of the catalytic domain

Protein NanHcat was expressed in *E. coli* KRX containing plasmid pFN18KNanHcat in a 500ml culture in order to purify the catalytic domain of NanH from a soluble lysate by the HaloTag system procedure.

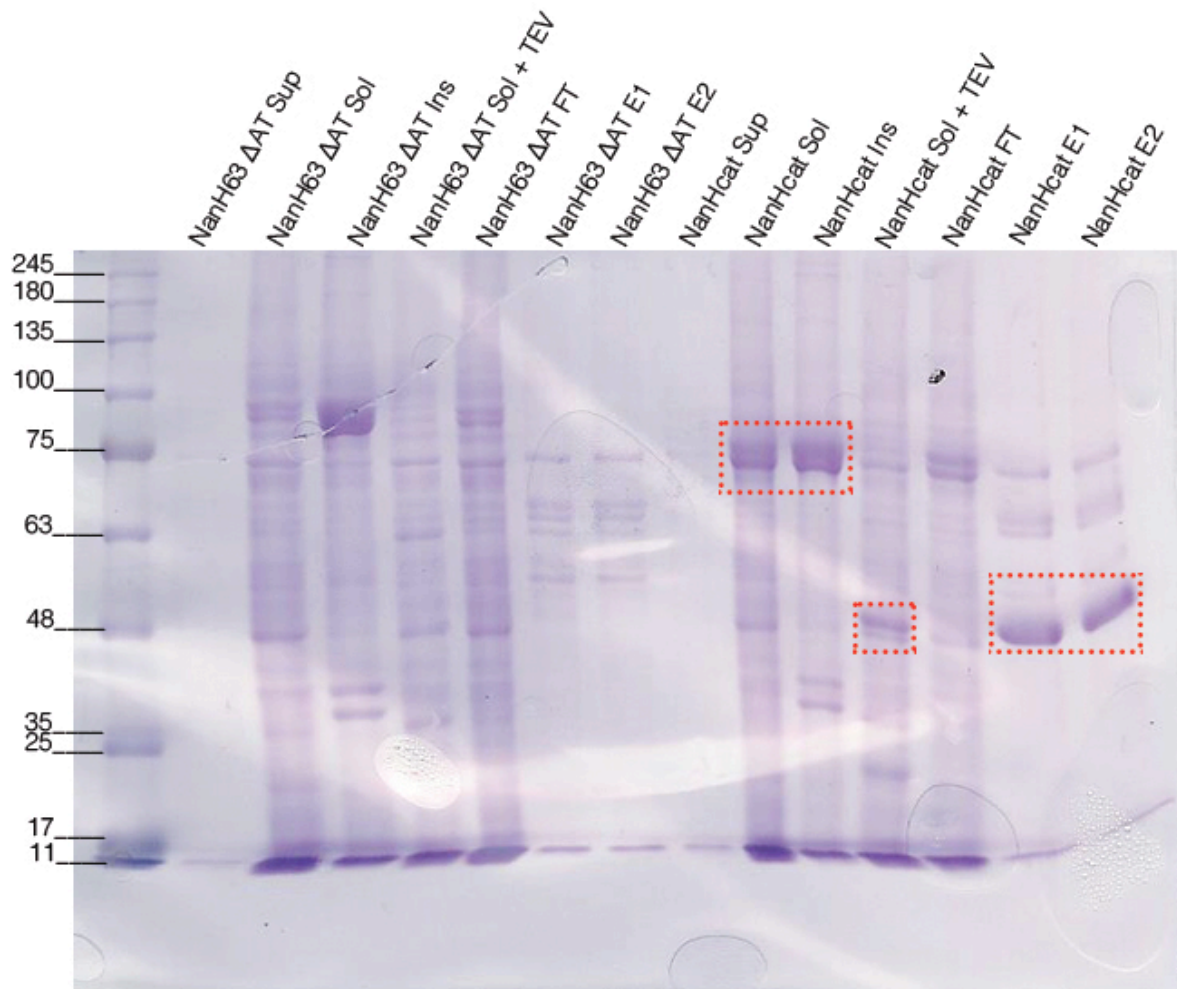


Figure 31. Coomassie blue stained gel showing samples taken at different steps of purification of NanH63 Δ AT and NanHcat. HaloTagged NanHcat expected size = 81kDa, TEV cleaved NanHcat expected size = 46kDa. The bands containing the expressed protein are marked in red dashed rectangles. For this study, we only worked with purified NanHcat but NanH63 Δ AT was purified in parallel.

A Coomassie blue stained gel of the samples taken during the protein purification steps show that the soluble fraction of NanHcat in figure 31 shows a thicker band than the soluble fraction of NanH23 shown in figure 26. Additionally, the final elutes showed a more evident band despite still being contaminated with other bands which presumably are *E. coli* chaperonines.

We then aimed to reduce contamination so the protein was transferred to a CaptoQ column for cleaning the protein by AEC. Figure 32 shows that two of the fractions obtained after elution contain an isolated band with a molecular weight of

~48KDa. According to the protein properties predicted from the sequence, NanHcat should have a molecular weight of 46.269 kDa when expressed fused to a HaloTag domain and cleaved with TEV protease.

Eluted fraction 9 was dialysed against PBS pH 7.4 and analysed for neuraminidase activity along with samples from previous purification steps (Figure 33).

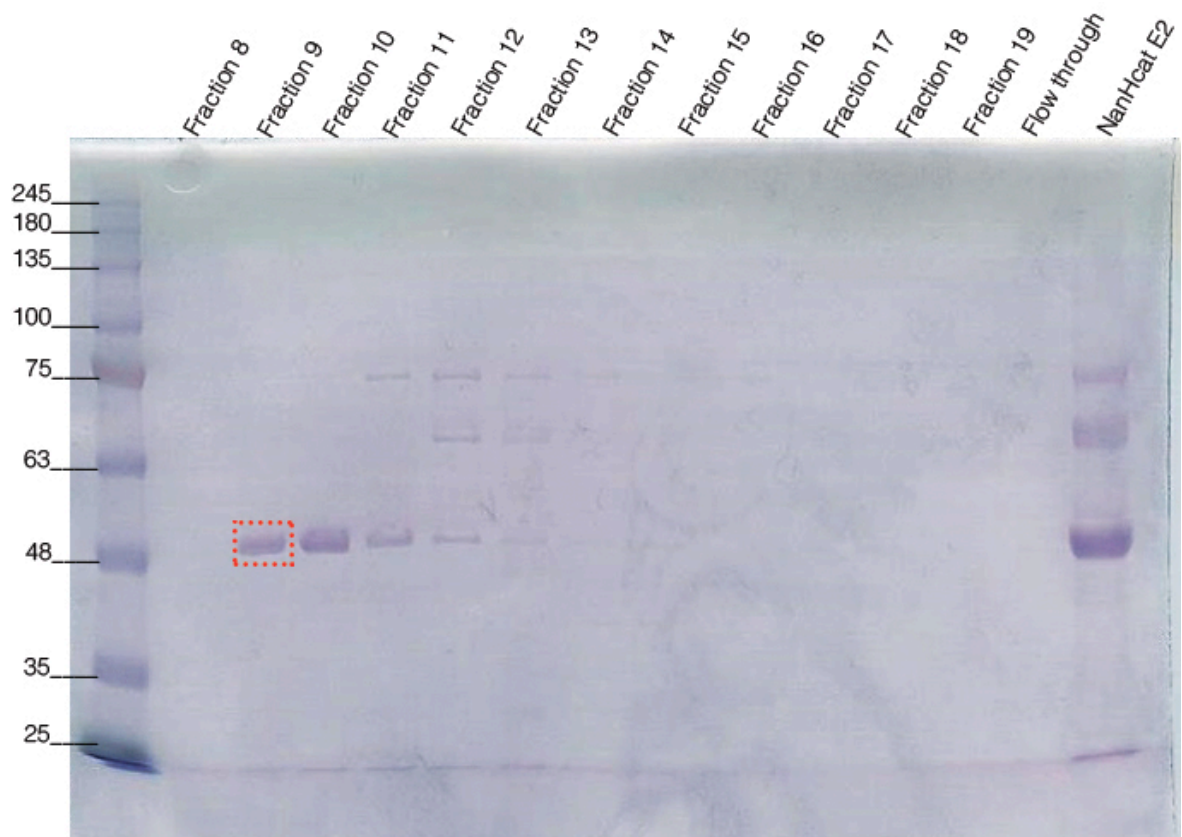


Figure 32. Coomassie blue stained gel of AEC purification fractions of NanHcat. The band from fraction 9 (marked in a red dashed rectangle) was excised for protein identification by mass spectrometry.

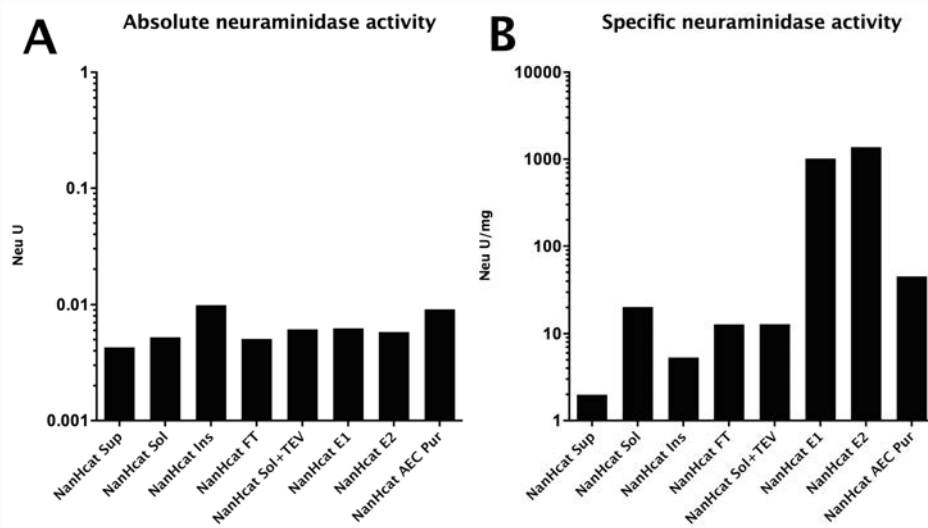


Figure 33. Absolute (A) and specific (B) neuraminidase activity of samples taken at each step of the HaloTag and AEC purification of NanHcat.

The band seen in the fraction 9 sample was excised from the Coomassie blue stained gel and submitted to the Proteomics facility for mass spectrometry.

The sequence of the peptides analysed by mass spectrometry were aligned to proteins of *E. coli* (Table 24) and *M. haemolytica* (Table 25). Protein identification was determined by considering three or more unique peptides as a cut off point. Results showed only 4 matches to *E. coli* K12 proteins and only one unique peptide of each was recognised. Contrastingly, when the data were compared to proteins of *M. haemolytica*, NanH was identified as the top hit with 26 unique peptides being recognised. Seven more proteins of *M. haemolytica* were matched but only 1 unique peptide in each was identified.

| Accession | Description | Score | Coverage | # Proteins | # Unique Peptides | # Peptides | # PSMs | # AAs | MW [kDa] | calc. pI |
|-----------|--|-------|----------|------------|-------------------|------------|--------|-------|----------|----------|
| P0AG55 | 50S ribosomal protein L6 OS=Escherichia coli (strain K12) GN=rpL6 PE=1 SV=2 - [RL6_ECOLI] | 2.55 | 6.78 | 1 | 1 | 1 | 1 | 177 | 18.9 | 9.70 |
| P37014 | Uncharacterized protein YfaD OS=Escherichia coli (strain K12) GN=yfaD PE=3 SV=3 - [YFAD_ECOLI] | 1.91 | 3.34 | 2 | 1 | 1 | 1 | 299 | 34.9 | 5.34 |
| P0AEA2 | CurlJ production assembly/transport component CsgG OS=Escherichia coli (strain K12) GN=csgG PE=1 SV=1 - [CSGG_ECOLI] | 0.00 | 16.25 | 1 | 1 | 1 | 1 | 277 | 30.5 | 7.28 |
| P0A733 | 50S ribosomal protein L10 OS=Escherichia coli (strain K12) GN=rpL10 PE=1 SV=2 - [RL10_ECOLI] | 0.00 | 6.67 | 1 | 1 | 1 | 1 | 165 | 17.7 | 8.98 |

Table 24. List of proteins matched to peptides identified by mass spectrometry. Peptide sequences aligned against *E. coli* database. No protein was identified with more than three unique peptides therefore, the sample was considered to be free of contamination by *E. coli* proteins.

| Accession | Description | Score | Coverage | # Proteins | # Unique Peptides | # Peptides | # PSMs | # AAs | MW [kDa] | calc. pI |
|------------|---|--------|----------|------------|-------------------|------------|--------|-------|----------|----------|
| A3F737 | Neuraminidase OS=Mannheimia haemolytica GN=nanH PE=4 SV=1 - [A3F737_MANHA] | 496.59 | 24.91 | 3 | 26 | 26 | 190 | 791 | 88.7 | 8.85 |
| A0A011NAR7 | Elongation factor Tu (Fragment) OS=Mannheimia haemolytica serotype A1/A6 str. PKL10 GN=AK33_10315 PE=4 SV=1 - [A0A011NAR7_MANHA] | 2.93 | 15.00 | 5 | 1 | 1 | 1 | 80 | 8.8 | 8.56 |
| E2P5W3 | Sheath protein gpL OS=Mannheimia haemolytica serotype A2 str. BOVINE GN=COK_0542 PE=4 SV=1 - [E2P5W3_MANHA] | 2.27 | 2.67 | 2 | 1 | 1 | 1 | 487 | 53.2 | 5.94 |
| E2P6M9 | Putative LexA family repressor/S24 family protease OS=Mannheimia haemolytica serotype A2 str. BOVINE GN=COK_0809 PE=4 SV=1 - [E2P6M9_MANHA] | 1.93 | 4.85 | 2 | 1 | 1 | 1 | 227 | 26.0 | 5.38 |
| A0A011NDP2 | 50S ribosomal protein L10 OS=Mannheimia haemolytica serotype A1/A6 str. PKL10 GN=rpL10 PE=3 SV=1 - [A0A011NDP2_MANHA] | 0.00 | 6.75 | 3 | 1 | 1 | 1 | 163 | 17.5 | 6.19 |
| A0A0B5B1Y9 | Xylose transport system permease protein xylH OS=Mannheimia haemolytica USDA-ARS-USMARC-184 GN=B824_320 PE=4 SV=1 - [A0A0B5B1Y9_MANHA] | 0.00 | 3.20 | 3 | 1 | 1 | 2 | 375 | 39.6 | 9.60 |
| M9X478 | Phage-related minor tail protein OS=Mannheimia haemolytica M42548 GN=MHH_c24770 PE=4 SV=1 - [M9X478_MANHA] | 0.00 | 2.77 | 1 | 1 | 1 | 1 | 759 | 81.5 | 9.23 |
| E2P7W7 | K+ uptake protein OS=Mannheimia haemolytica serotype A2 str. BOVINE GN=COK_1253 PE=3 SV=1 - [E2P7W7_MANHA] | 0.00 | 10.44 | 1 | 1 | 1 | 2 | 249 | 28.1 | 5.35 |

Table 25. List of proteins matched to peptides identified by mass spectrometry. Peptide sequences aligned against *M. haemolytica* database. Only neuraminidase (Accession no. A3F737) was identified with more than three peptides therefore, the sample was considered to only contain *M. haemolytica* neuraminidase.

Since mass spectrometry provided results that increase our confidence on the purity of the NanH catalytic domain, we sought to produce an antibody in mice that would recognise such region of the protein.

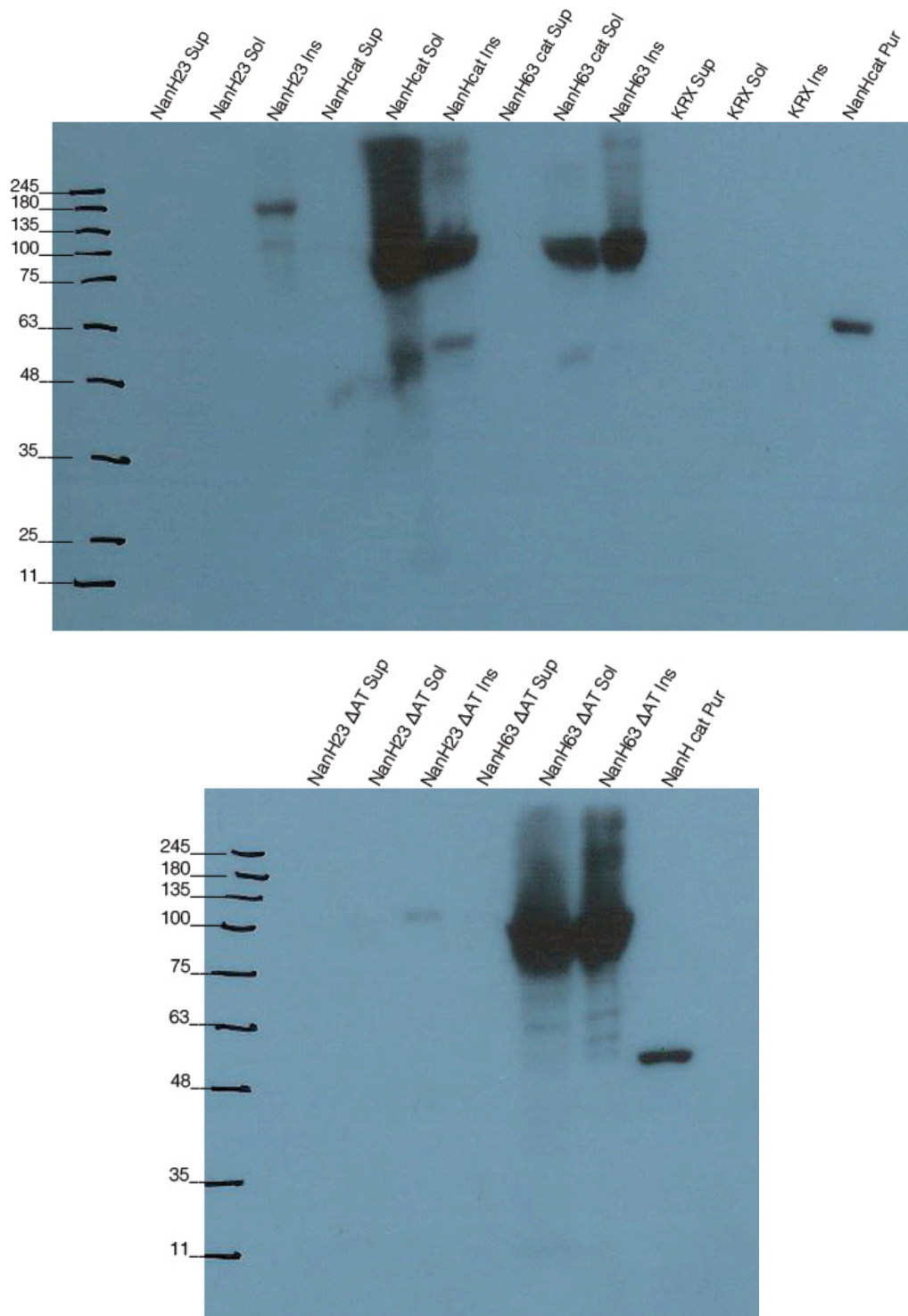


Figure 34. Western blot using anti-NanHcat antibody at 1:1000 and developed by ECL. Culture supernatants and lysates of *E. coli* expressing different NanH truncations. Expected size: HaloTagged NanH23 = 122kDa, HaloTagged NanHcat = 81kDa, HaloTagged NanH63 cat = 77kDa, HaloTagged NanH23 Δ AT = 99kDa, HaloTagged NanH63 Δ AT = 94kDa.

The antibody was used to analyse, by western blot, the cell lysates previously obtained in order to confirm that NanH was expressed in the cultures (Figure 34). Even though the samples were standardised by loading 10µg of the supernatant, 10µg of soluble lysate and 5µg of insoluble lysate (concentration was reduced due to the low solubility of the sample), cell fractions of *E. coli* expressing NanH23 and NanH23 ΔAT showed a weak signal that is only visible in the insoluble fraction. Considering that the neuraminidase activity assay showed a strong response compared to the negative control, NanH is presumably present but at very low concentrations.

5.5 Conclusions

Expression of three active versions of NanH (NanH23, NanHcat and NanH23 ΔAT) demonstrate that the catalytic domain of this sialidase is located within residues 23 and 435.

Expression of NanH63 ΔAT and NanH63 cat suggests that residues 23 to 62 are essential for neuraminidase activity. Probably they are required for adequate folding.

6 Evaluation of NanH catalytic residues by amino acid substitution

The hydrolysis mechanism is highly conserved among sialidases. However, the interaction between key residues might determine whether an inhibitor has an effect against specific neuraminidases.

According to the hydrolytic mechanism of known sialidases, the main components of a neuraminidase are an arginine triad that interacts with the hydroxyl group of Neu5Ac, an aspartic acid that acts as proton donor to the oxygen forming the α -ketosidical link, a tyrosine and a glutamic acid that stabilise the intermediate state and a hydrophobic pocket that interacts with the N-acetyl group linked to C-5.

The objective at this stage was to evaluate the predictions made by sequence homology on the putative catalytic residues by amino acid substitutions.

6.1 Cloning and expression of mutants in NanH23 and NanHcat.

The site-directed mutations described in this chapter were initially made using as template the plasmid pFN18KNanH23 and expressed in *E. coli* strain KRX under the same conditions as NanH23. As expected, the proteins were found in a higher proportion in the insoluble debris fraction than in the soluble lysate (Figure 35).

The neuraminidase activity was apparently abolished after making most of the mutations in NanH23 but the effect could have been caused by low protein concentrations. Therefore, the catalytic domain formed by residues N23-L435 was cloned from each mutant into pFN18K with the aim of increasing expression (Figure 36) of soluble protein similarly to wild type NanHcat described in section 5.4.

Neuraminidase activity results of mutants made in both NanH23 and NanHcat were divided into five sections according to the rationale of the amino acid substitutions. The graphs show the result of the described mutations compared to the result obtained from lysate fractions of NanH23, NanHcat and *E. coli* strain KRX containing no plasmid. Results obtained from NanH23 and NanHcat are reiterated in the graphs for clarity.

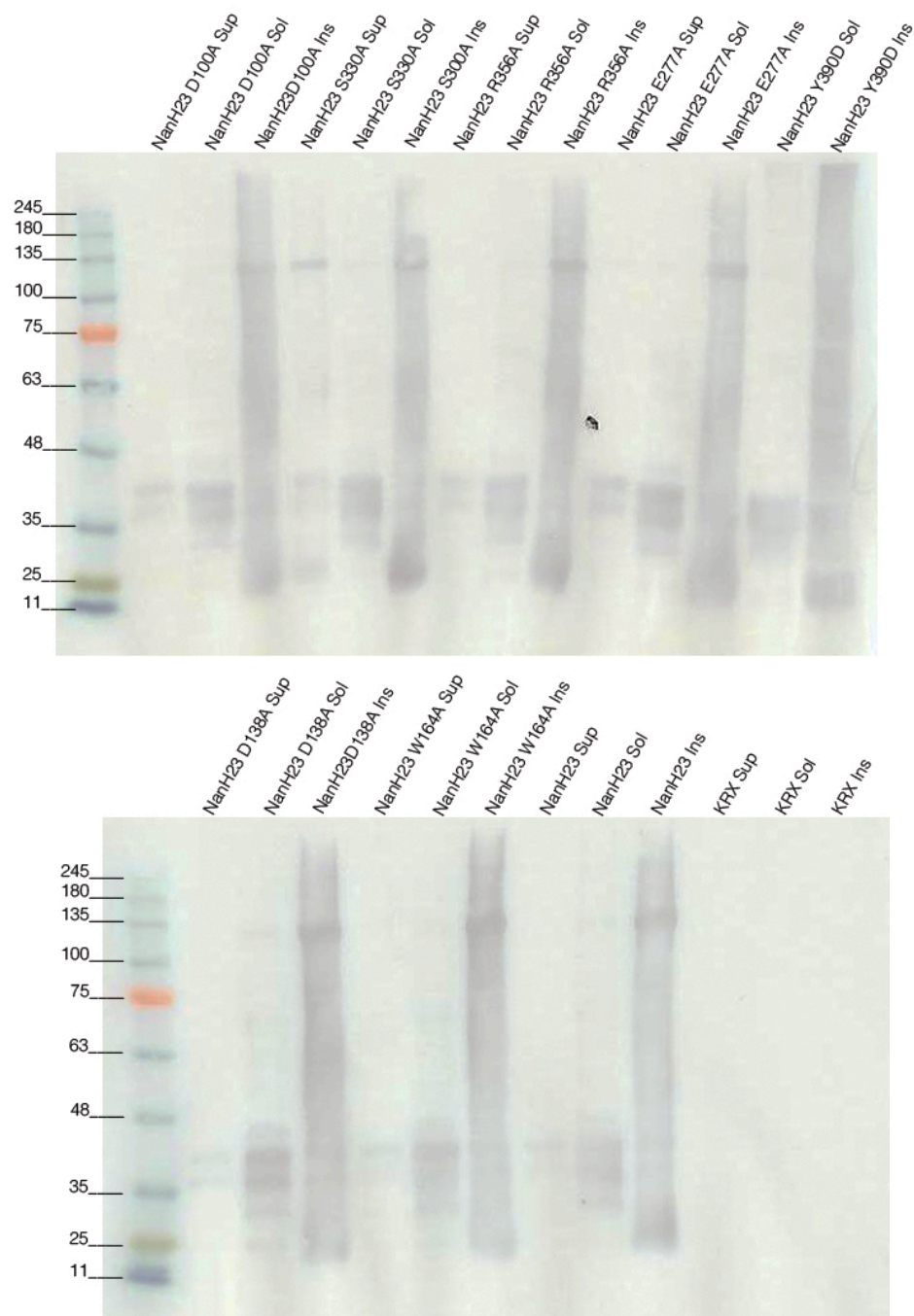


Figure 35. Western blot showing expression of mutants made in NanH23 using a monoclonal anti-HaloTag antibody. Expected size of all proteins is 122kDa.

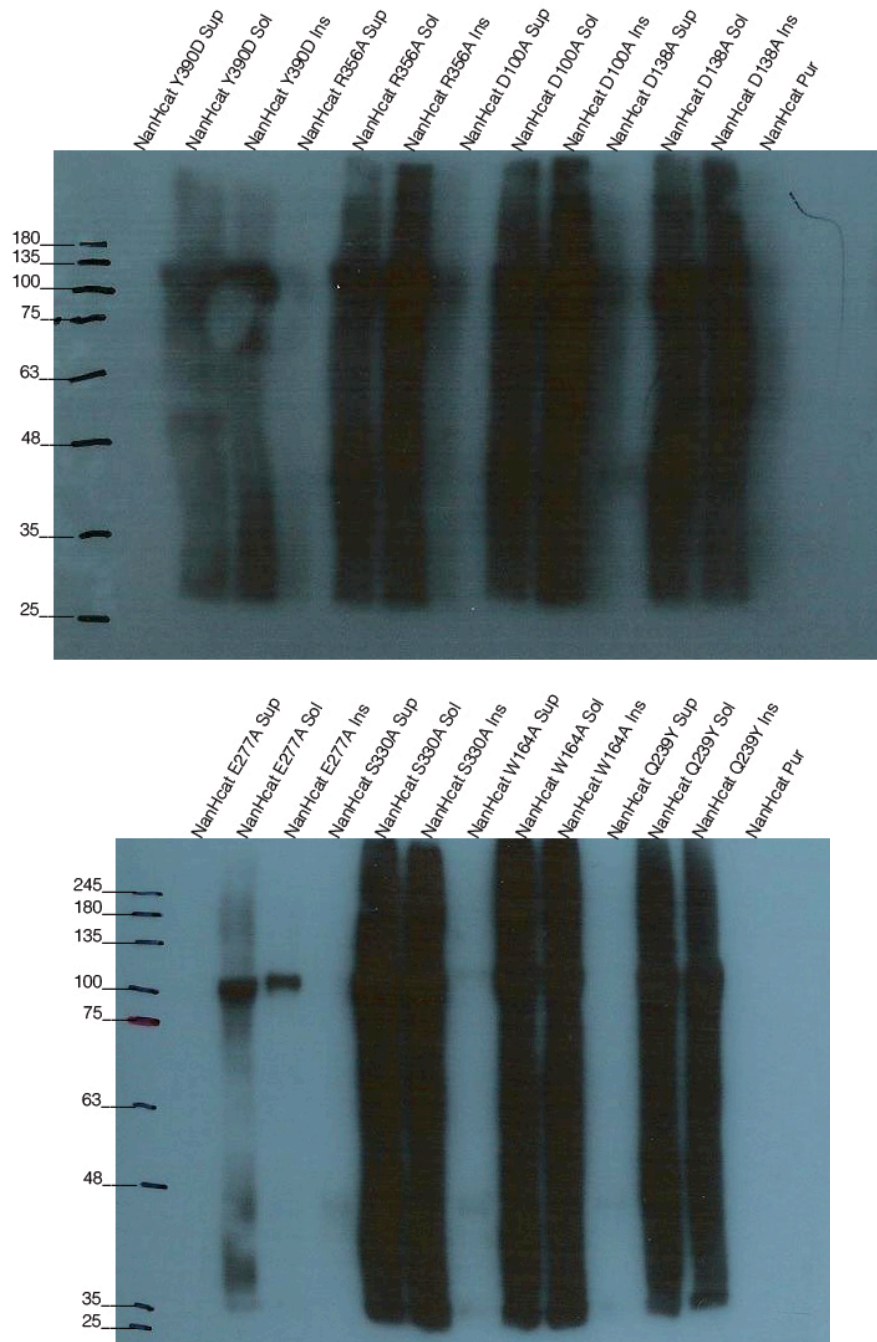


Figure 36. Western blot showing expression of mutants made in NanHcat using monoclonal anti-Halo Tag antibody at a 1:4000 concentration and developed with ECL. Strong signal makes visualisation difficult therefore, these results only confirm the expression of a HaloTagged protein in the soluble lysate and insoluble cell debris. Only in E277A mutant, the molecular size can be calculated. Expected size of all proteins is 81kDa.

6.2 Disruption of arginine triad

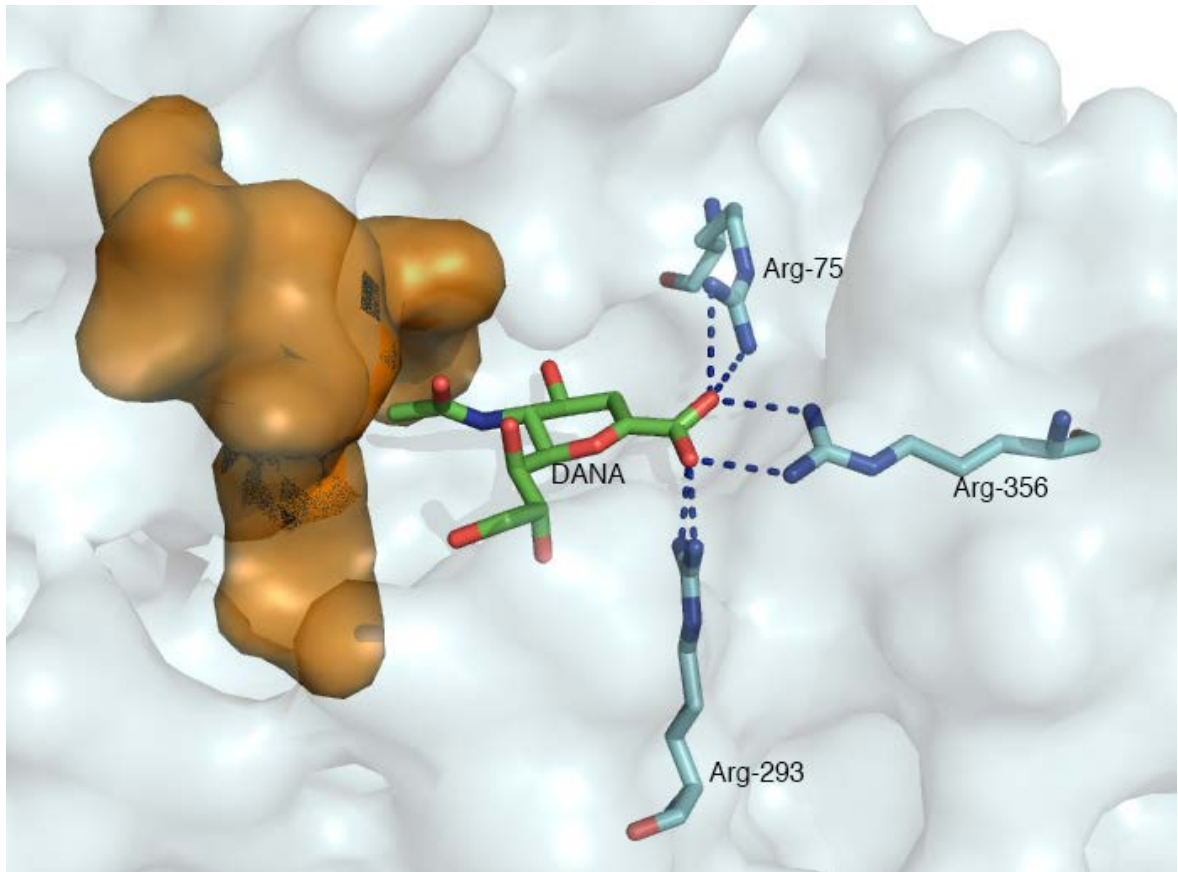


Figure 37. Diagram showing putative arginine triad in NanH.

The arginine triad putatively formed by Arg75, Arg293 and Arg356 was disrupted by substituting Arg356 (Figure 37) for an alanine in order to decrease the ionic charge without abolishing it completely by only removing one of the bonds to the carboxylic group formed by C-1 of the sialic residue. Therefore, enzymatic activity was expected to decrease but not to be completely lost due to the presence of Arg75 and Arg293.

The mutation was sufficient to abolish activity completely only in NanH23 lysates. Fractions obtained from NanHcat R356A cultures clearly had lower activity but did not lose it completely as the substrate was cleaved with the soluble lysate sample (Figure 38).

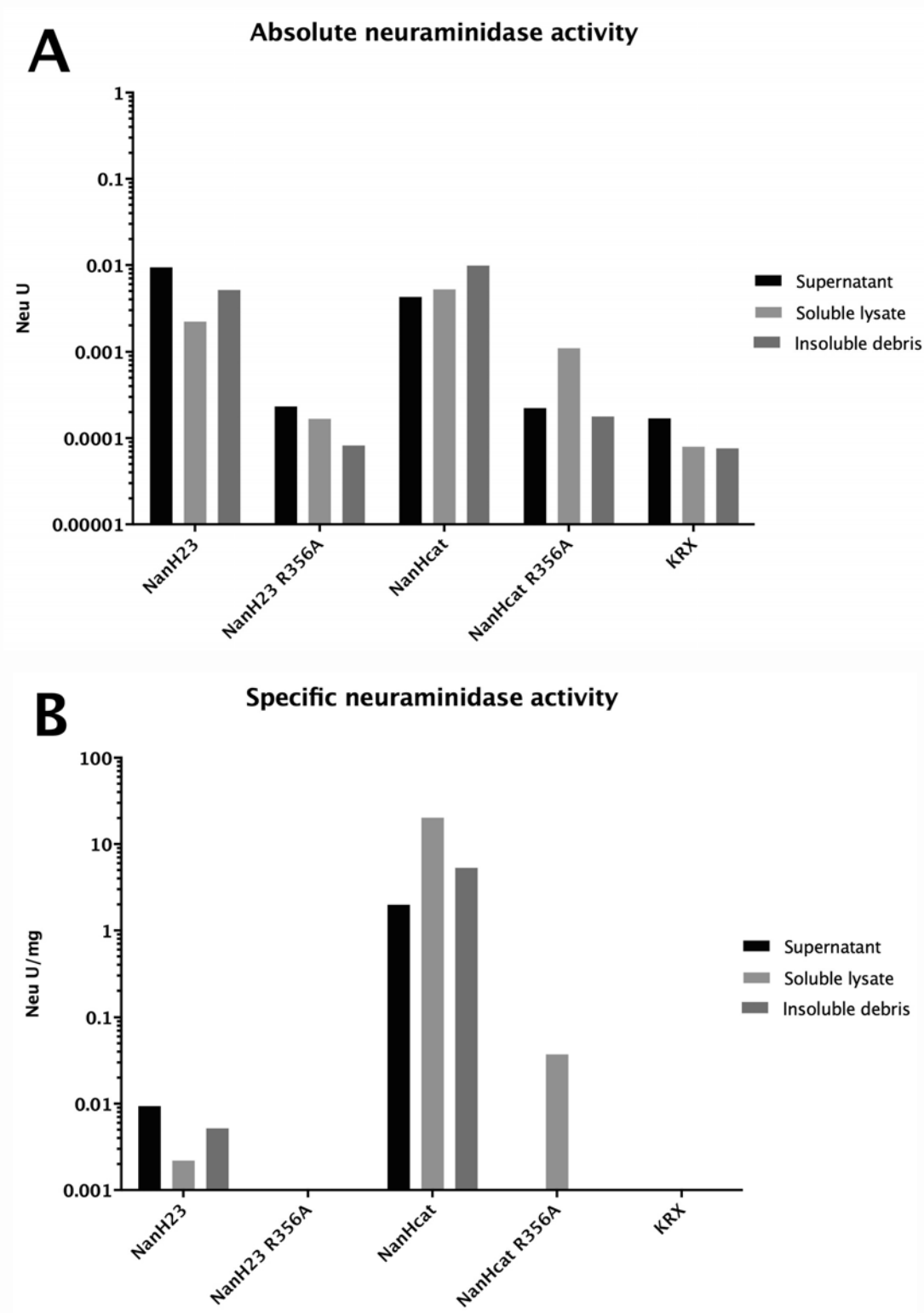


Figure 38. Absolute (A) and specific (B) neuraminidase activity of *E. Coli* culture fractions taken after expression of NanH23 and NanHcat with an R356A substitution to represent a disruption in the arginine triad.

6.3 Disruption on stabilisation of intermediate state

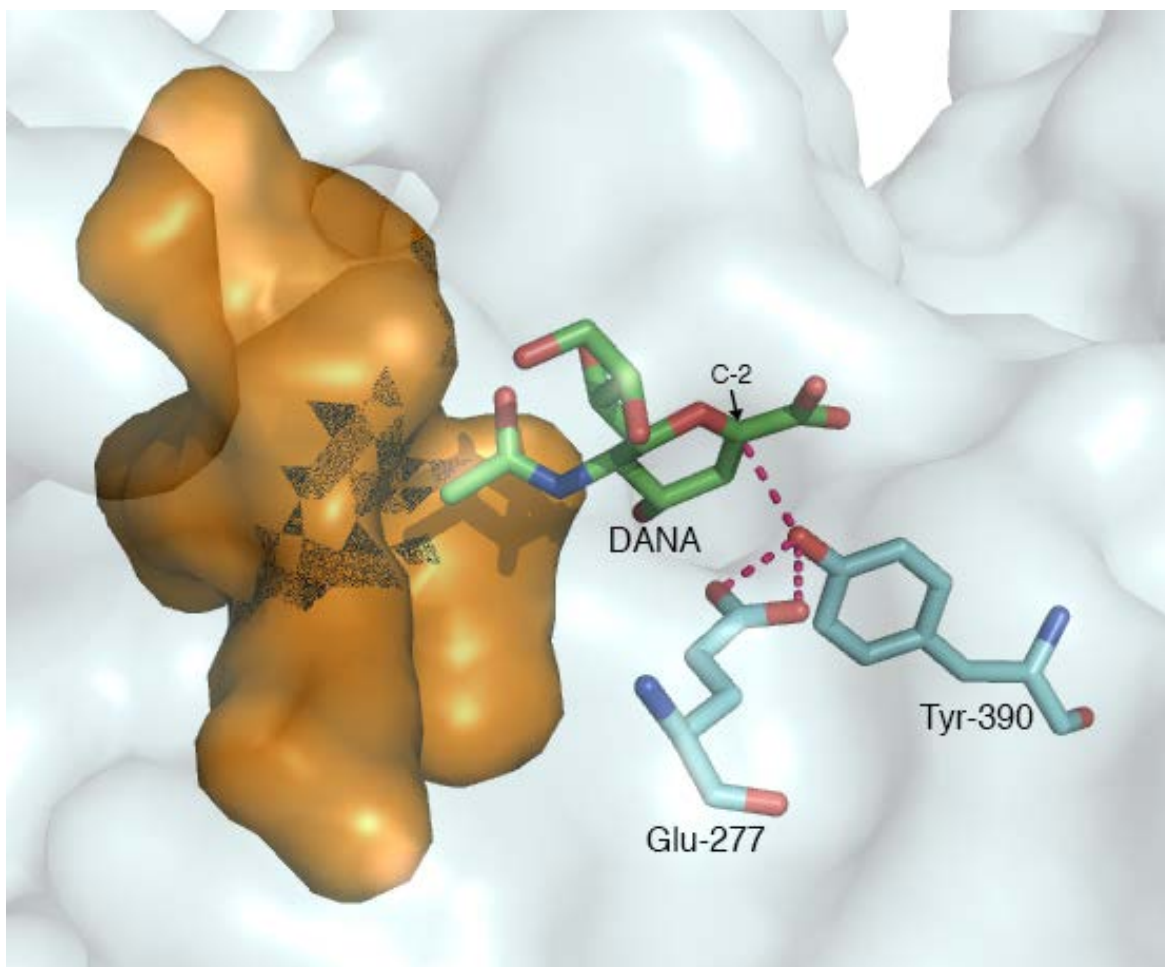


Figure 39. Diagram showing putative amino acids that stabilise intermediate state.

As mentioned in chapter 1, Tyr390 is thought to form a covalent bond that stabilises the intermediate state, aided by Glu277 which might be important for adequate positioning (Figure 39).

The first mutant had a substitution of Glu277 for an alanine in order to test if the Tyr390 bond could be disrupted indirectly. The mutation of both NanH23 and NanHcat abolished activity (Figure 40).

The second mutant contained a mutation of Tyr390 directly, which was substituted by an aspartate. Therefore, by removing the hydroxyl group provided by Tyr390 the oxocarbenium cannot be stabilised. Additionally, the proximity of the negatively charged side chain of Glu277 might repel the newly added aspartate with a negative charge too (Figure 39). The mutation also resulted in depletion of activity

of both NanH23 and NanHcat (Figure 40). However, protein expression of the NanHcat E277A mutant was lower than the others because samples loaded for western blot were standardised to 10µg of total protein per well (5µg of insoluble fraction) and the signal detected by the anti-HaloTag antibody was weaker than the other mutants (Figure 36).

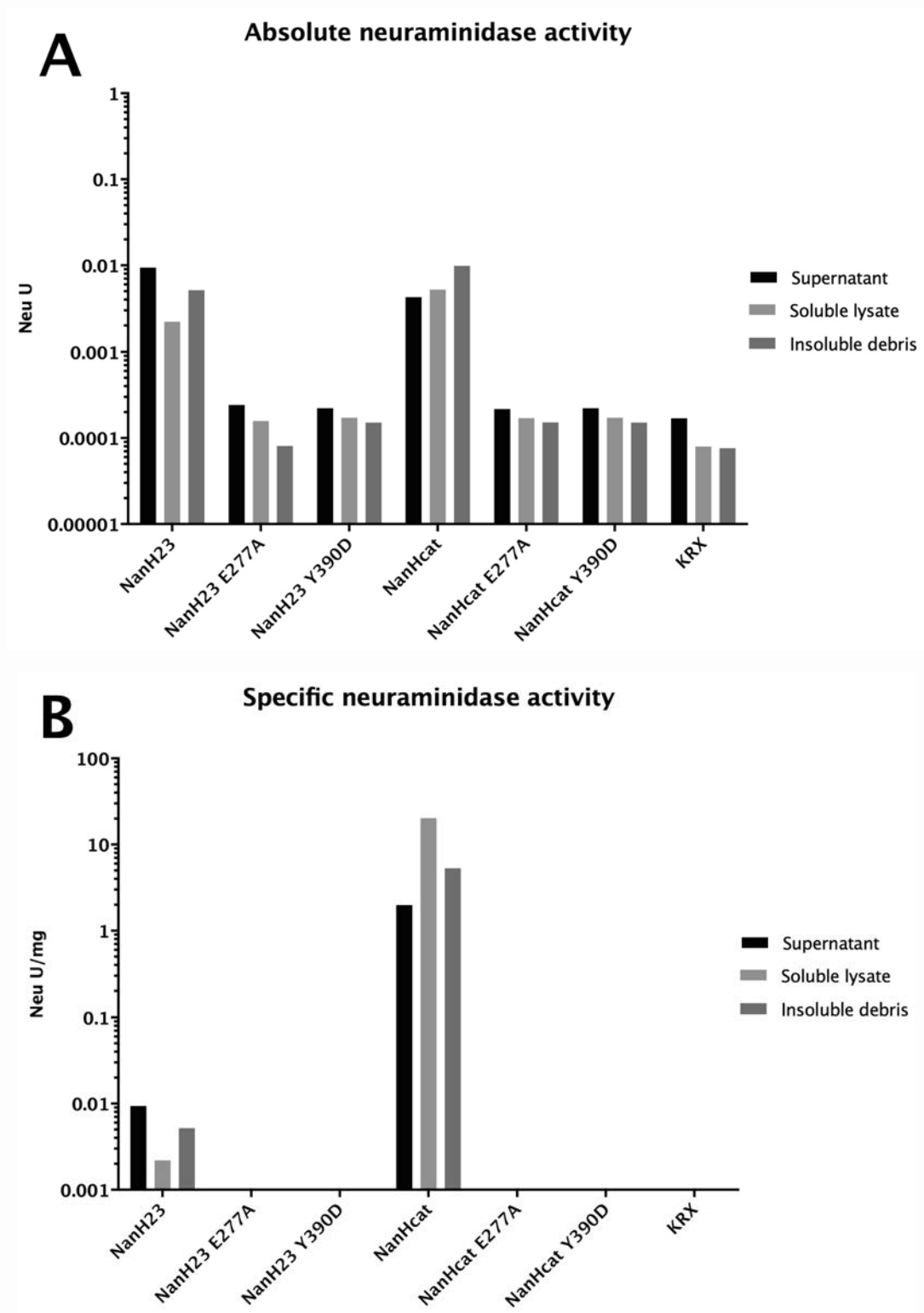


Figure 40. Absolute (A) and specific (B) neuraminidase activity of *E. Coli* culture fractions taken after expression of NanH23 and NanHcat with an E277A substitution or a Y390D substitution to test the disruption of the intermediate state stabilisation.

6.4 Proton donor residue

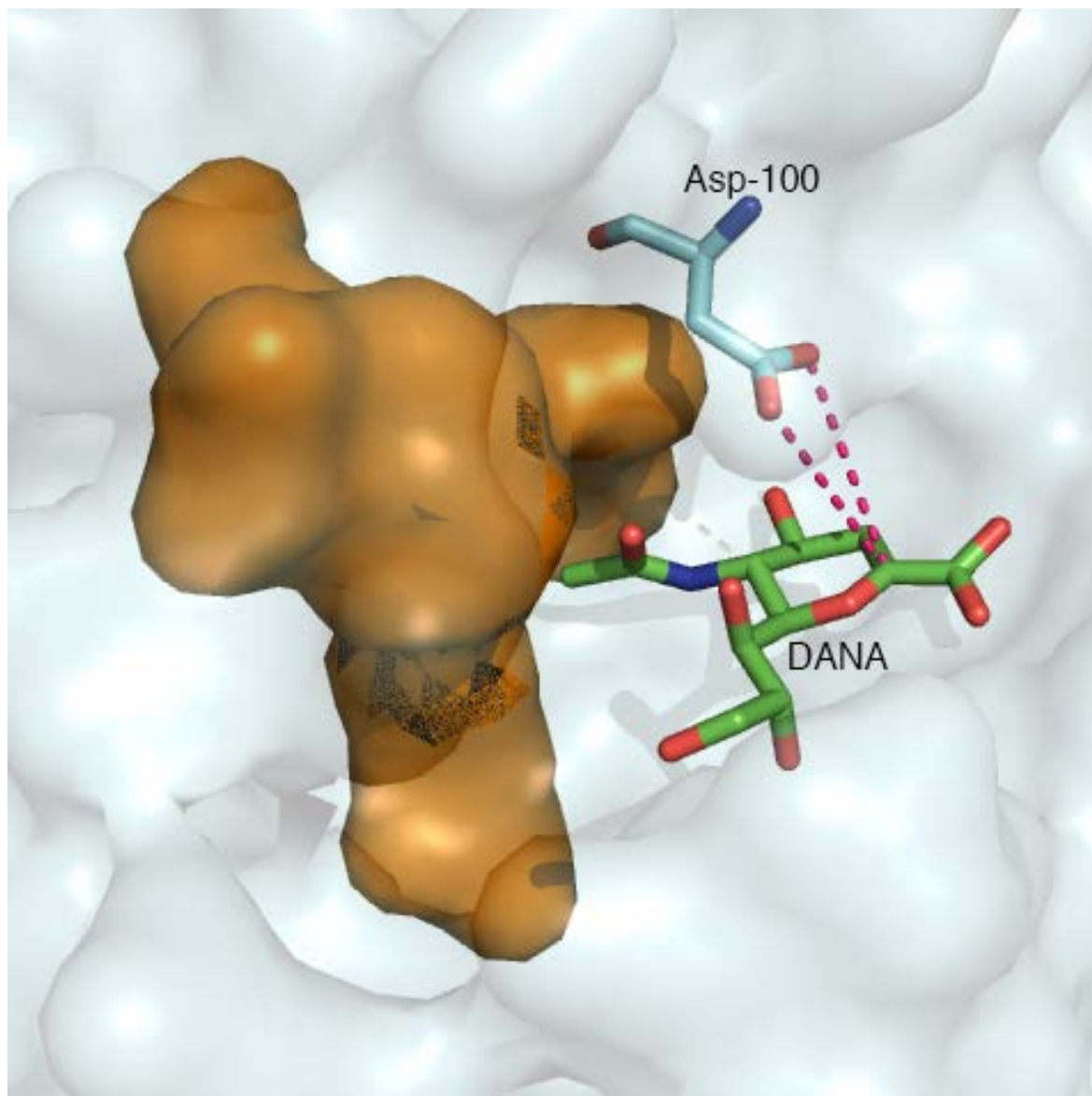


Figure 41. Diagram showing putative proton donor.

According to homology to TrSA, Asp100 is believed to hydrogenate the oxygen that forms the cleaved α -ketosidical linkage therefore, is thought to be essential in the catalytic mechanism (Figure 41). When the residue was substituted for an alanine, a total loss of activity was predicted. However, activity was preserved in the soluble lysate of the NanHcat mutant (Figure 42). Therefore, despite playing an important role in catalysis, Asp100 is not essential.

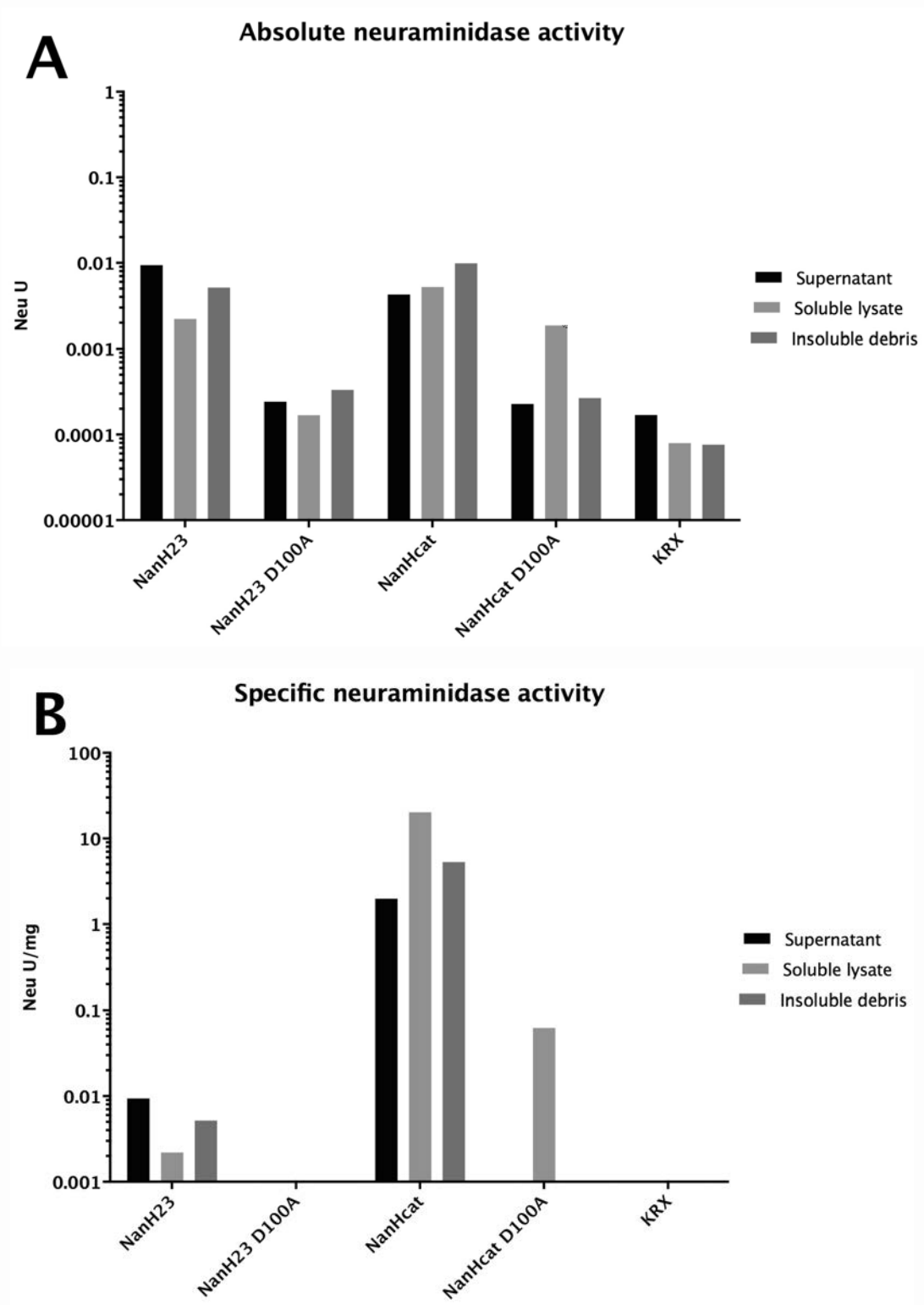


Figure 42. Absolute (A) and specific (B) neuraminidase activity of *E. Coli* culture fractions taken after expression of NanH23 and NanHcat with a D100A substitution to test whether it is the essential proton donor.

6.5 Hydrophobic pocket

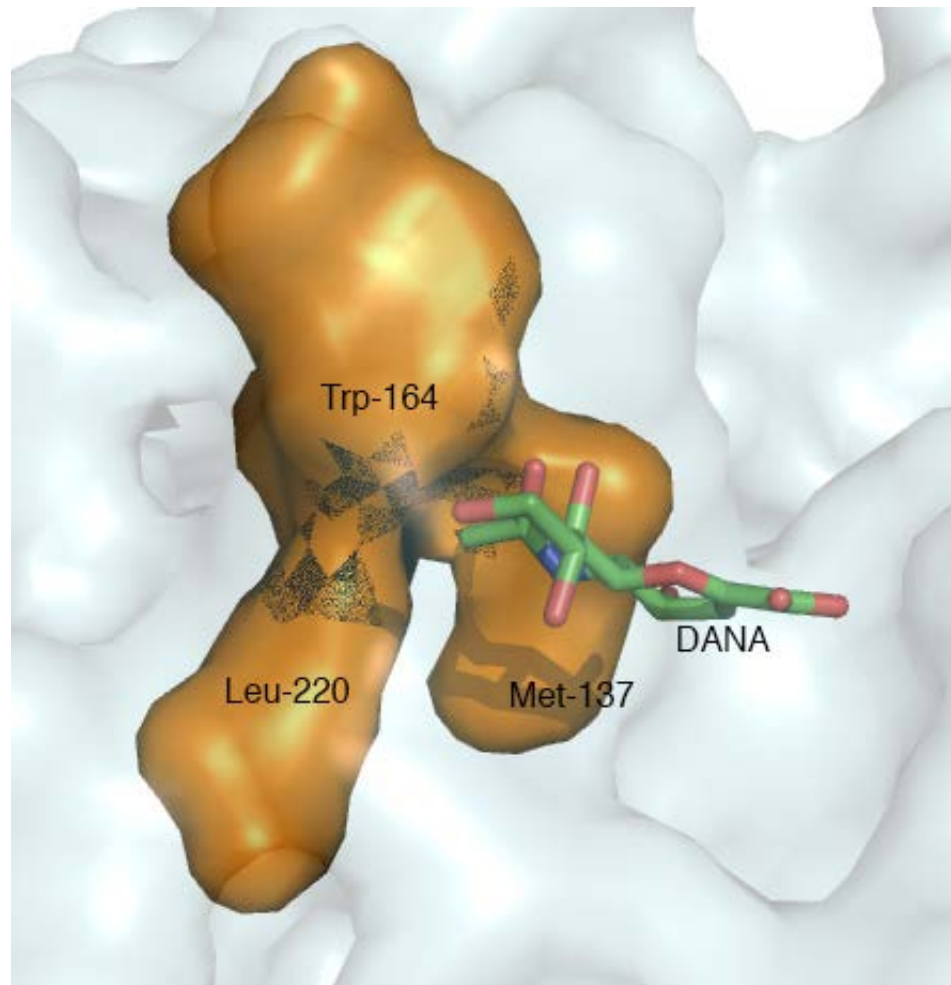


Figure 43. Diagram showing putative hydrophobic pocket.

A hydrophobic pocket was predicted to be formed around the N-acetyl chain of Nau5Ac by residues Met137, Trp157, Trp164 and Leu220. One of the Tryptophan residues was substituted for an alanine in order to test if the pocket stabilisation was compromised (Figure 43). Activity in NanH23 was only observed in the soluble lysate fraction while it was preserved in NanHcat but with an apparent decrease (Figure 44).

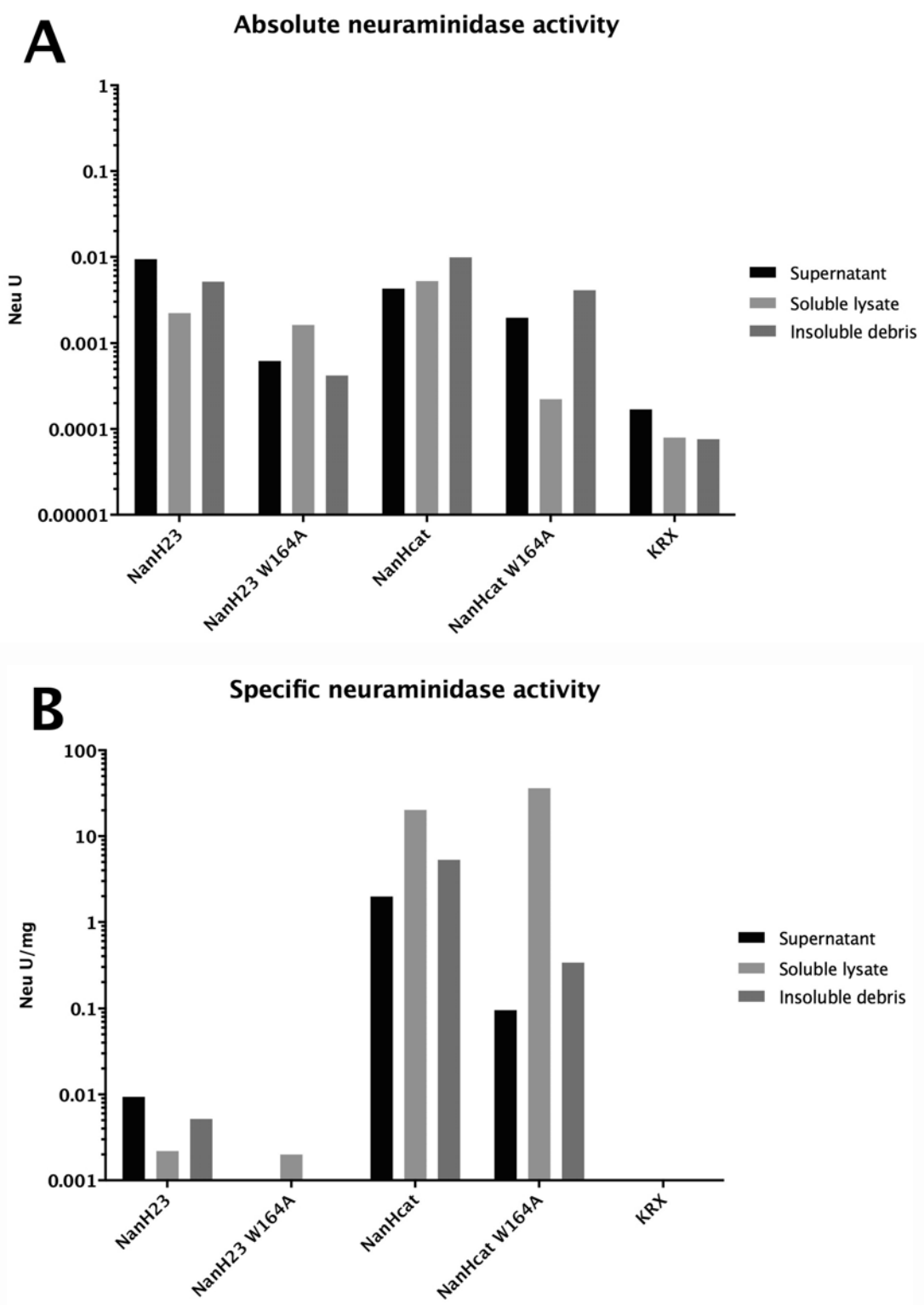


Figure 44. Absolute (A) and specific (B) neuraminidase activity of *E. Coli* culture fractions taken after expression of NanH23 and NanHcat with a W164A substitution to represent an alteration in the hydrophobic pocket.

6.6 Mutation of residues possibly involved indirectly

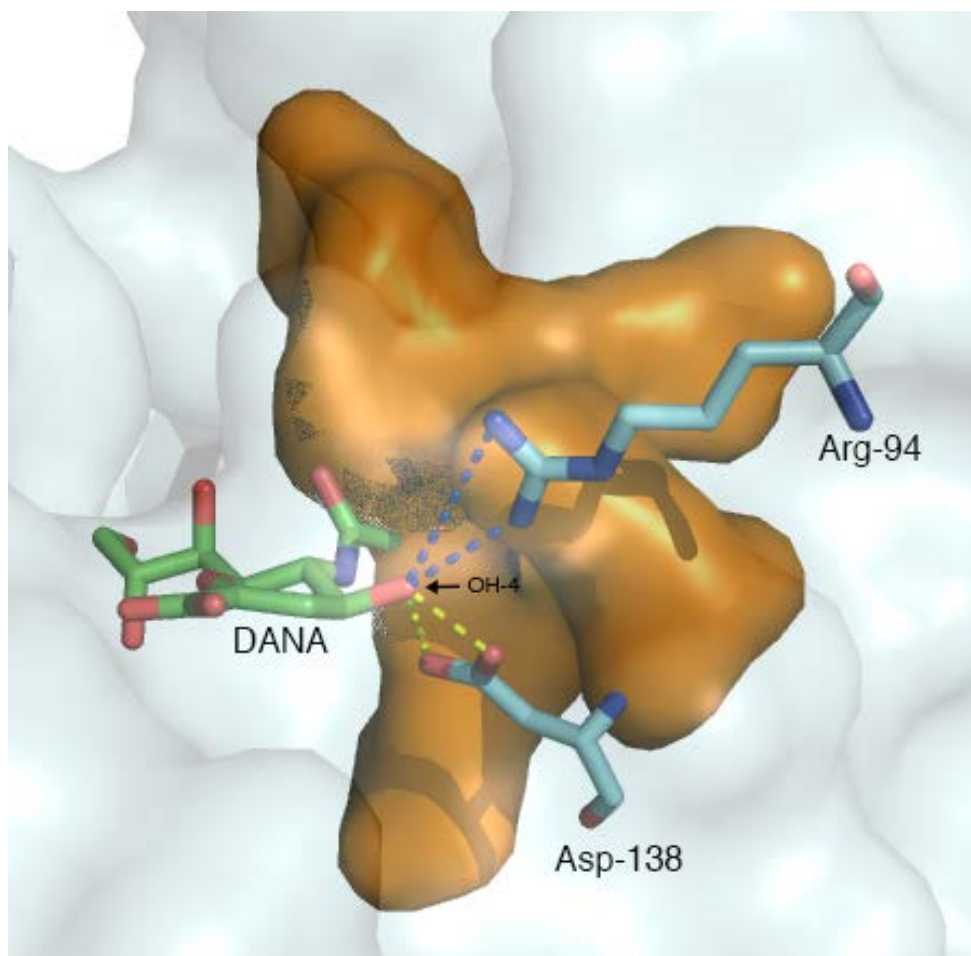


Figure 45. Diagram showing putative interactions with OH-4.

Two residues were predicted to interact with OH-4 which are Arg94 and Asp138 (Figure 45). By substituting only one of those residues, a decrease in activity was expected as the other one could be compensating the coordination. When Asp138 was disrupted, activity was abolished completely in both NanH constructs (Figure 47).

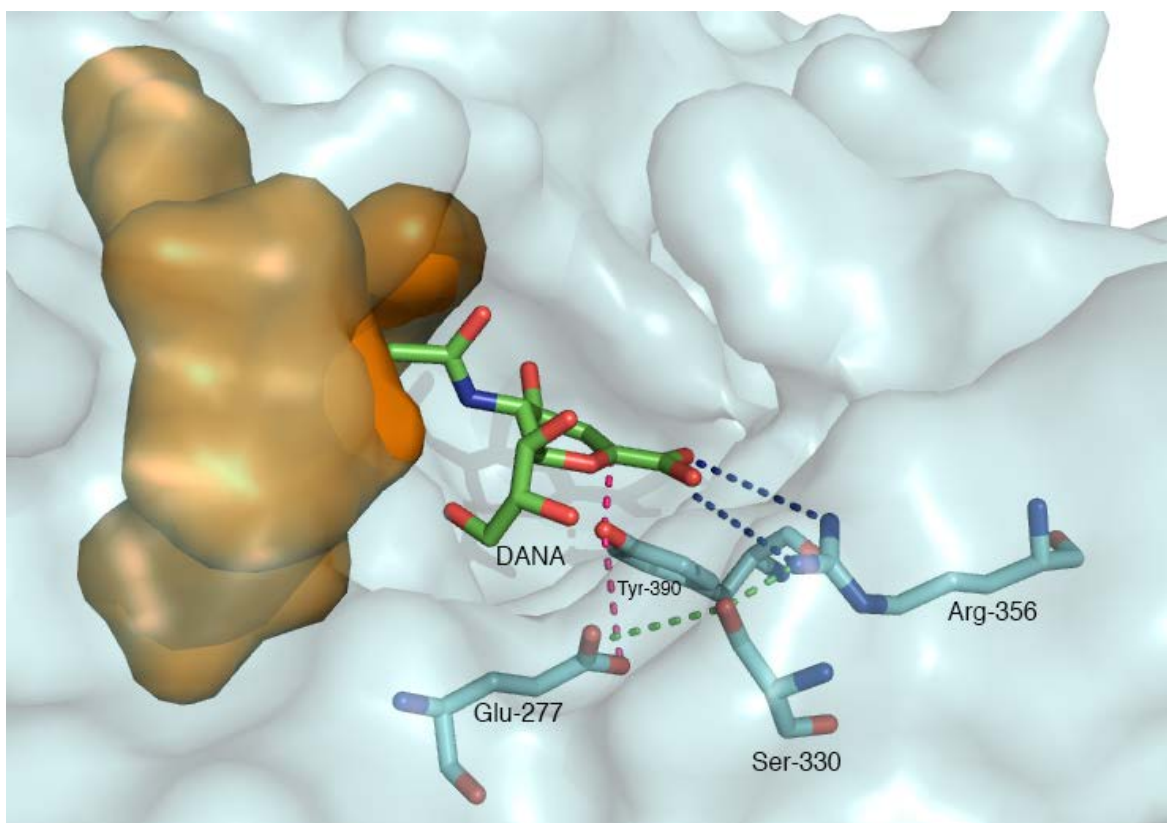


Figure 46. Diagram showing alternative docking model in which Ser330 coordinates Glu277 and Arg356.

According to the model obtained by homology to NanB, Ser330 was predicted to be in proximity to the catalytic residues Glu277 and R356 (Figure 46). However, in the model obtained with phyre², Ser330 appears to have little influence on the catalytic site structure. By making an S330A mutation, a hydroxyl group that could be stabilising the structure was removed. Even though no activity was detected in the insoluble debris of the mutant made in NanH23, the activity in the supernatant and soluble fraction of both NanH23 and NanHcat was still present.

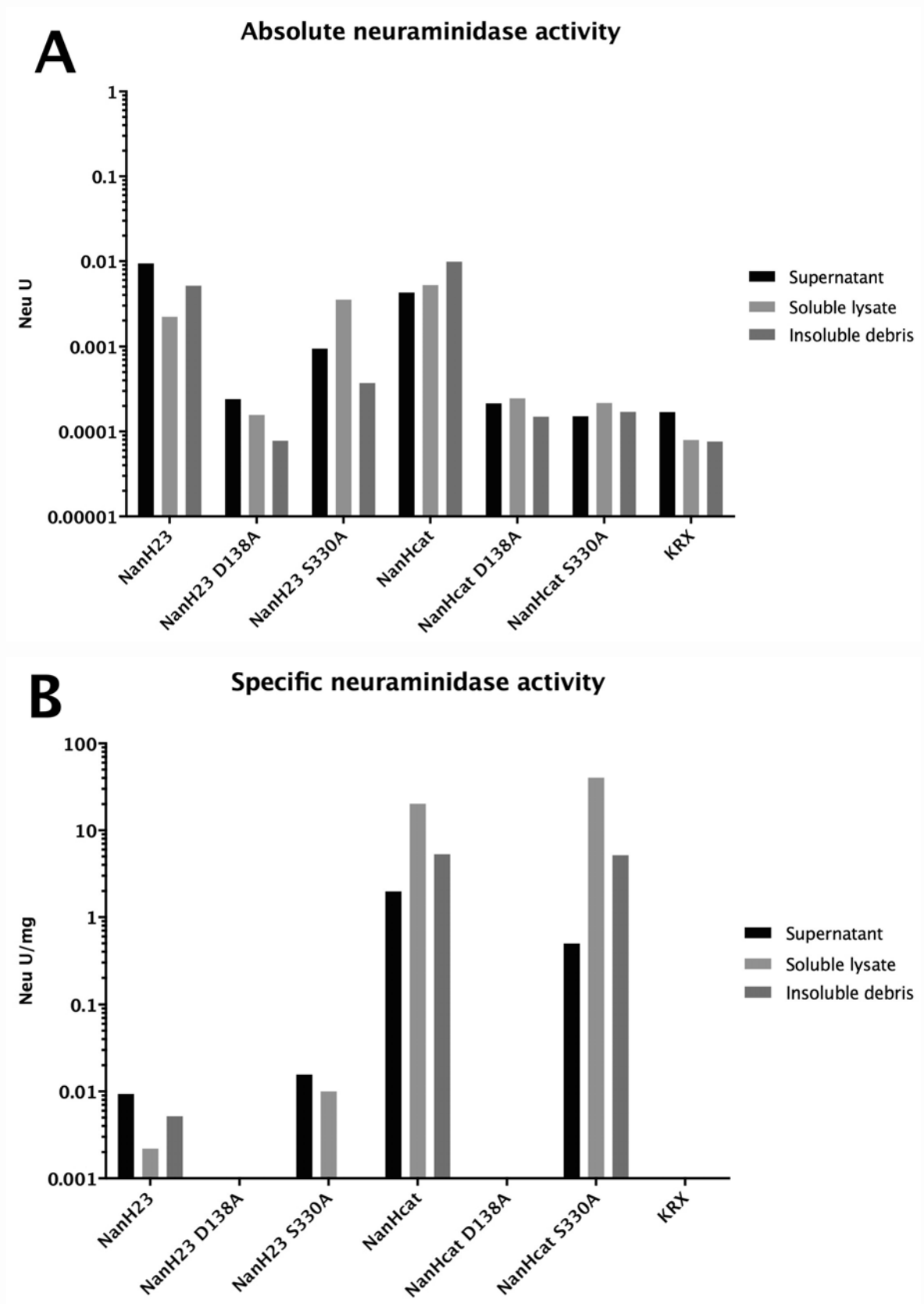


Figure 47. Absolute (A) and specific (B) neuraminidase activity of *E. Coli* culture fractions taken after expression of NanH23 and NanHcat with an D138A substitution to test the coordination of OH-4. Additionally, the S330A was performed to assess the docking method based on homology to *S. pneumoniae* NanB.

6.7 Comparison of enzyme activity after mutation.

Neuraminidase activity data described for cell culture fractions can only provide a general idea of the result after making amino acid substitutions or truncations in the NanH sequence. Therefore, active proteins were purified by the HaloTag system followed by anion exchange chromatography. Additionally, NanH23 was purified again but the AEC step was added after HaloTag purification.

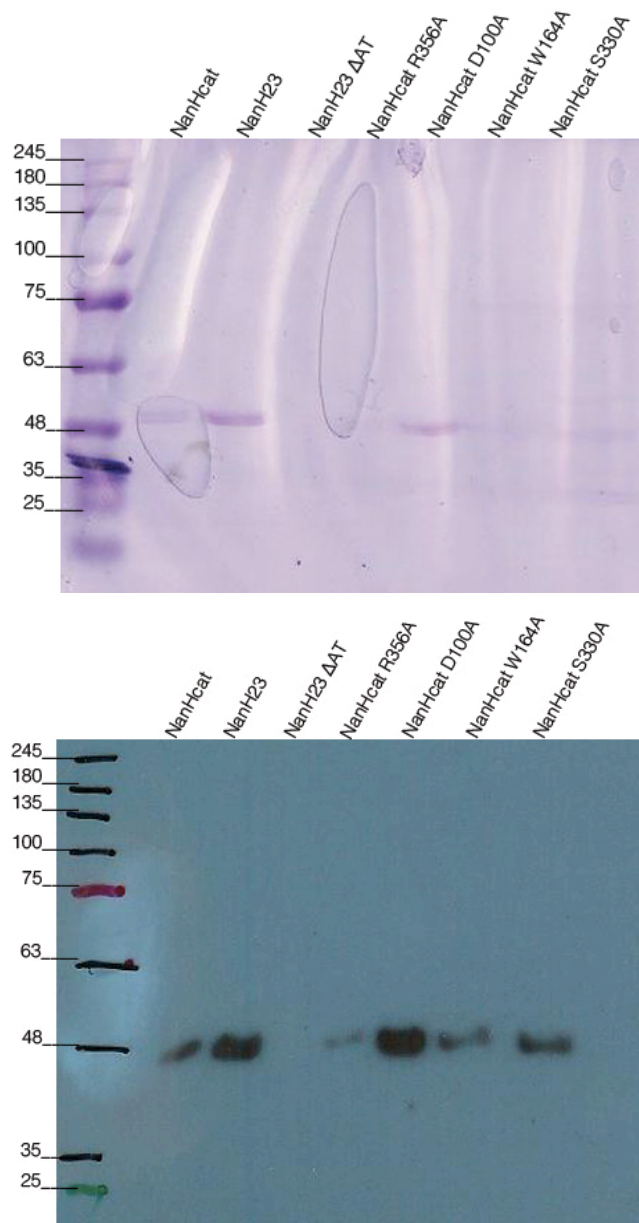


Figure 48. Purified proteins are shown in a Coomassie blue stained gel and western blot using anti-NanHcat antibody at 1:1000 and developed by ECL. Expected protein size: NanHcat and NanHcat mutants = 46kDa, NanH23 = 122kDa, NanH23 ΔAT = 64kDa.

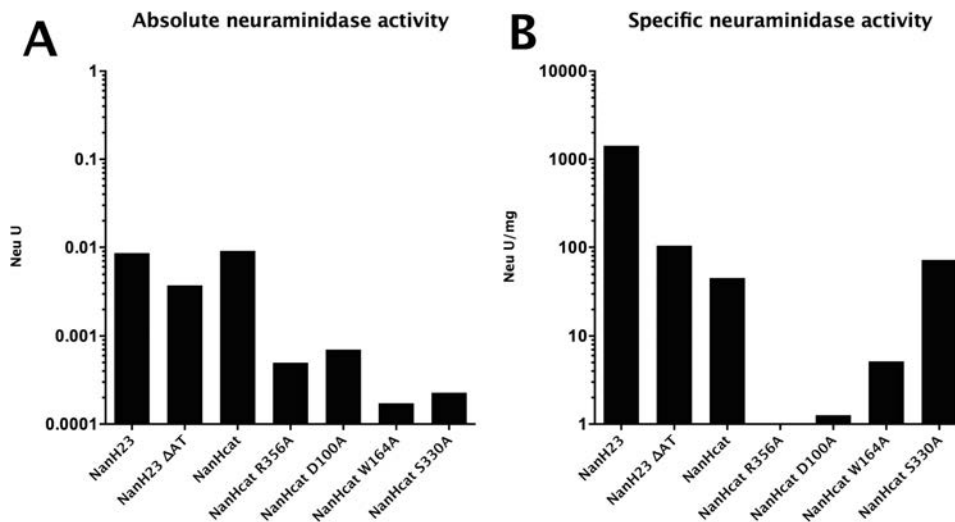


Figure 49. Absolute (A) and specific (B) neuraminidase activity of the purified proteins. Most of the purified proteins preserved the neuraminidase activity except for R356A which was only weakly detected by western blot therefore, the concentration might be too low for this mutant to show any activity.

The band observed in the Coomassie blue stained gel and western blot of both constructs appears to be of the same size (Figure 48). Specific neuraminidase activity of NanH23 was higher than NanHcat after AEC purification (Figure 49).

In order to identify if the putative autotransporter domain could be involved in cleavage of the catalytic domain, the purification of NanH23 ΔAT was attempted. Despite showing a specific activity comparable to NanHcat or NanH23, no band was detected in the Coomassie blue stained gel or western blot so confirmation could not be done.

The activity of purified D100A and W164 confirm a reduction in activity observed in the assays run with samples from bacterial culture supernatants and lysates. The activity of R356A could not be detected even though it was detected in the soluble cell lysate before.

6.8 Conclusions

The complete depletion of activity seen in mutants D138A and Y390D shows that these two amino acid substitutions were sufficient for disrupting the catalytic site. Despite not being able to detect neuraminidase activity from the E277A mutant, different expression of the protein hinders the possibility of reaching the same conclusion.

Substitutions in D100A, W164A, R356A and S330A had an effect to different degrees but none of them was sufficient for abolishing neuraminidase activity completely.

7 Discussion

Neuraminidase activity of respiratory pathogens has proven to be important for colonisation of the upper respiratory tract since mucin is a major component of mucosa (Caswell, 2014). In human respiratory disease, both viral and bacterial agents have neuraminidase activity (Air, 2012, Kadioglu et al., 2008). A viral neuraminidase that could be present in the ruminant disease is produced by BPIV-3 (Ellis, 2010). It is therefore, possible that viral neuraminidase contributes for debilitating the respiratory mucosa in addition to NanH.

Neuraminidase in influenza is a major antigen and virulence factor with a highly variable sequence but with conserved activity (Shtyrya et al., 2009). The pneumococcal neuraminidase NanA also has a variable sequence (King et al., 2005). In contrast, the sequences of NanH and the *P. multocida* neuraminidases are apparently highly conserved and can therefore, be proposed as therapeutic or prophylactic targets in BRD.

Even though we were unable to detect NanH by western blot in *M. haemolytica* culture supernatant, we detected neuraminidase activity in all the cell fractions. Mizan et al (Mizan et al., 2000), were unable to detect any of the *P. multocida* neuraminidases extracellularly. The neuraminidase activity data described in the work in this thesis, in addition to data published by Straus et al on *M. haemolytica* and *P. multocida* (Straus and Purdy, 1995), might not provide a definitive answer on whether *M. haemolytica* NanH and the *P. multocida* neuraminidases purified by Mizan et al are secreted but the possibility has not been disregarded. Future experiments should identify the optimal growth conditions for NanH expression. Upregulation of *nanA* and *nanB* in the presence of a sialic acid rich media was demonstrated in *S.pneumoniae* by Trappetti et al (Trappetti et al., 2009) therefore,

M. haemolytica could be supplemented with Neu5Ac as well in order to attempt to augment NanH production.

Other neuraminidases including *S.pneumoniae* NanA and NanB, *Vibrio cholerae* VCNA, *T.rangeli* TrSA, *T.cruzi* TcTS and *Trypanosoma congolense* TconTS contain additional lectin-like domains that increase binding to carbohydrates (Xu et al., 2008, Moustafa et al., 2004, Waespy et al., 2015, Buschiazzi et al., 2000). The tertiary structure of lectin-like domains is a β -barrel however, the arrangement of the predicted secondary structure of the C-terminus domain of NanH and the amphipathic nature of the amino acid sequence, suggests the presence of an autotransporter domain. So far, there is no confirmation of a neuraminidase being exported by the TVSS however, *P. multocida* NanH and NanB (Mizan et al., 2000) in addition to *Pseudomonas aeruginosa* NanA (Soong et al., 2006) were also predicted to contain an autotransporter β -barrel from their sequence.

Therefore, in the case that NanH is really exported, we hypothesise that it might be by TVSS as the sequence suggests. A 3D model of the β -barrel domain that was constructed by sequence homology to Hbp shows an incomplete barrel as only 10 strands were modelled compared to the 12 strands formed in the *E. coli* autotransporter (Tajima et al., 2010). The autotransporter model of NanH was built considering residues 583 to 791 and even though the residues immediate to the N-terminal of the predicted β -barrel domain did not show homology to the additional two strands of Hbp, the amphipathic nature of the residues 520 to 582 could complete the pore.

By removing the putative autotransporter components which are the signal sequence, the linker domain and the β -barrel domain (Henderson et al., 2004), the catalytic domain of NanH was isolated.

The genome sequences available for *M. haemolytica* strains, suggest the presence of the TVSS chaperones Skp, FkpA, SurA and DegP which prevent folding of the β -barrel before reaching BamA at the outer membrane (Leo et al., 2012). However, whether these genes are expressed or not, is unknown.

Proteins that are secreted via TVSS, require Sec translocation through the inner membrane. Sec translocation of NanH was predicted from the sequence of the N-terminus which has the typical structure of a Sec translocated protein. Signal peptides of Sec dependent proteins are formed by an n-region containing positively charged residues, an h-region containing non-polar hydrophobic residues and a polar c-region (Kudva et al., 2013). In NanH, the n region would be formed by MRK, the h-region by INQLIISPY and the c-region by FFLSILSASA. Constructs NanH23, NanHcat and NanH Δ AT were designed considering a predicted signal sequence cleavage site between A22 and N23 (Petersen et al., 2011) resulting in the expression of active proteins. Current results therefore, support the possibility of NanH being a passenger domain.

The neuraminidase activity data obtained from *M. haemolytica* cultures show higher sialidase hydrolytic activity in the cellular fractions of *M. haemolytica* than in the supernatant fractions. These results agree with the authors who initially reported neuraminidase activity of *M. haemolytica* (Frank and Tabatabai, 1981, Straus et al., 1993a). Current autotransporter models suggest that a passenger domain is secreted to the extracellular space by either translocation through the β -barrel domain or the pore formed by BamA. In both models, the pore is too narrow for a folded protein to be translocated and the passenger domain would have to remain unfolded therefore, premature folding can result in reduced secretion efficiency (Leyton et al., 2012, Skillman et al., 2005). Higher neuraminidase activity in *M. haemolytica* cellular fractions suggests that the passenger domain is folding

prematurely and not being exported efficiently, probably by a reduced expression of one or more chaperones associated to TVSS. Work on the *Shigella flexneri* showed that when *skp* is deleted, the efficiency of the autotransporter protein *IcsA* is reduced (Wagner et al., 2009). It is also possible that premature folding is taking place prior to inner membrane translocation hence, a cell fractionation can be performed in order to compare the neuraminidase activity levels between cytoplasm and periplasm.

A self-cleavage site in the linker domain could not be predicted from the sequence. Proteins of the SPATE family are believed to be self-cleaved by asparagine cyclisation in the conserved motif EVNNLN through the interaction of an aspartate present in the β -barrel (Barnard et al., 2007, Dautin et al., 2007, Dautin, 2010). The autotransporter exported proteins BrkA and pertactin produced by *Bordetella pertussis* do not have the same motif as SPATE proteins but they are thought to be cleaved by the same mechanism by the cyclisation of an asparagine present in the sequence AESNAL (Oliver et al., 2003). The NanH sequence does not contain any of those motifs however, the sequence SQQNIY formed by residues 501 to 506 contains an asparagine with adjacent residues that have similar properties to the ones present in EVNNLN within a short α -helix in which cleavage might occur. Alternatively, NanH might be cleaved from the β -barrel by a different mechanism, probably aided by a protease. NanH23 was purified again during the final stage of this project and a band with the same size as NanHcat (~48KDa) was detected by western blot using anti-NanH antibody. Cleavage of the protein by the β -barrel or an *E. coli* protease could not be confirmed however, these hypotheses could be evaluated by altering the putative self-cleavage sites in both the passenger and autotransporter domains.

The functionality of the autotransporter domain could be evaluated by the deletion of the signal sequence in the *M. haemolytica* chromosome and determine whether the extracellular neuraminidase activity is eliminated. Additionally, the β -signal motif thought to be formed by YNW at the C-terminus of the sequence, could be altered in order to study an expected interaction between NanH and the BamA machinery in a similar way to *E. coli* autotransporters (Robert et al., 2006). An additional piece of evidence that would support the TVSS of *M. haemolytica* would be the identification of the periplasmic chaperones identified in the genome sequence. The sequence of *M. haemolytica* suggests the production of two pertactin-like and two YadA-like autotransporter proteins that, if functional, would benefit from the chaperones activity.

In order to study the catalytic domain of NanH, two 3D models were constructed based on homology to TrSA and *S.pneumoniae* NanB. Based on the TrSA model, constructs NanH63 cat and NanH63 Δ AT were designed however, they were not active compared to the constructs designed according to the signal sequence cleavage site prediction (i.e. NanH23, NanHcat and NanH23 Δ AT). The role of residues 23 to 62 is uncertain, that region of the sequence does not seem to contain a catalytic amino acid and were not predicted to be part of the blades that form the β -propeller according to both models. These results allowed the delimitation of two NanHcat boundaries that resulted in the expression of a highly soluble protein that might be useful for crystal formation and determination of the tertiary structure by X-ray.

Both models of NanH showed conserved catalytic residues but in order to obtain a model similar to NanB, Ser330 would have to coordinate two essential amino acids: Arg356 and Glu277. Serine coordination is not present in the NanB model solved by crystallography (Gut et al., 2008). However, it was necessary for the

sequence of NanH to fit the coordinates of NanB and helped to discriminate between docking models since the TrSA based model did not consider Ser330 to play a role in the catalytic site. Therefore, the preservation of activity in S330A supported the TrSA based model.

Based on sequence homology to TrSA, Asp100 was proposed as a crucial amino acid that acts as a proton donor on the released O-linked glycan (Buschiazzo et al., 2000). However, the substitution of Asp100 with an alanine did not eliminate activity completely. The influenza neuraminidase model proposes that Asp151 (homologous to Asp100 in NanH) and the neighbouring Arg152 bind a water molecule that acts as proton donor (Taylor and von Itzstein, 1994). The adjacent residues to Asp100 (Tyr99 and Q101) could compensate as proton donors but it is also possible that Arg94 binds a water molecule required for the interaction despite not being completely adjacent to Asp100.

It is also possible that Asp100 plays a different role and even Asp138 could be the residue involved in cleavage of the α -ketosidical linkage since experimental data suggest that the latter is more crucial. The next immediate experiment would be to substitute Arg94 independently and in addition to the D100A mutation.

The arginine triad of sialidases is known to be responsible for the change of conformation in Neu5Ac that triggers catalysis (Kim et al., 2011). Experiments in which the neuraminidase of the Newcastle Disease Virus (NDV) has been mutated in a similar way by Iorio et al (Iorio et al., 2001) and Connaris et al (Connaris et al., 2002) but expressed in a mammalian vector, showed that the mutation of any arginine from the triad resulted in complete depletion of neuraminidase activity. Our initial results obtained after making the R356A mutation in NanH23 showed that activity was lost. However, when the mutation was performed in NanHcat, activity was observed in the soluble lysate. Despite high conservation in the

catalytic site of all neuraminidases, the difference in origin (viral and bacterial) and expression vector are variables that must be considered when results are compared. It is possible that a disruption in the central arginine of the triad does have a dramatic effect on the activity of the enzyme as observed with the NDV neuraminidase. However, we hypothesised that by mutating Arg356 for an alanine, folding of the binding pocket would remain stable and the other two arginines (i.e. Arg75 and Arg293) would be able to bind to the carboxylic group of Neu5Ac with the ability to change the substrate conformation to continue hydrolysis. Probably that effect was only detected because NanHcat was expressed as a small molecule, with a delimited catalytic domain and with higher solubility, compared to NanH23 that is even hard to detect in a western blot.

When the amino acids that putatively stabilise the intermediate state in the reaction were substituted, a complete depletion of activity was observed. By substituting Tyr390 for a negatively charged amino acid, we hypothesised that such mutation would cause a collapse of the catalytic site due to a repulsion between the newly introduced aspartate and Glu277. The mutation resulted in complete activity depletion, supporting our hypothesis. However, Vavricka et al (Vavricka et al., 2013) performed the same mutation in the influenza neuraminidase observing a 100-fold decrease of activity. The substitution of Glu277 also abolished neuraminidase activity, supporting the typical model of intermediate state stabilisation by a glutamate-tyrosine interaction.

The relevance of the work of Vavricka et al relies on the fact that they proposed Tyr406 as an antiviral target that could be inhibited through a covalent interaction with the inhibitor. Using the inhibitor 2 α ,3ax-difluoro-Neu5Ac, the activity of neuraminidases from influenza A and B viruses was abolished, including resistant mutants. If that conserved tyrosine can be targeted in bacterial neuraminidases as

well, the viral neuraminidase inhibitor could have an added value against sialidases of respiratory pathogens like the pneumococcal neuraminidases as previously proposed for zanamivir and oseltamivir (Gut et al., 2011). A drug targeting tyrosine could potentially be beneficial against BRD by inhibiting both viral and bacterial neuraminidases produced by BPI-3 virus and *Pasteurellaceae* bacteria respectively.

The hydrophobic pocket in which the N-acetyl group is placed has a more variable sequence compared to the residues directly involved in catalysis. The pneumococcal neuraminidase NanA has a hydrophobic pocket formed by Phe428 and Ile427 that are in proximity to the substrate and additional hydrophobic residues that include Leu551 and G552 located further away (Gut et al., 2011). In the TrSA model, Met96, Phe114, Trp121 and Val177 form a tighter pocket but perform the same function (Buschiazzi et al., 2000). We predicted NanH hydrophobic pocket to be formed by Met137, Trp157, Trp164 and Leu220 so by mutating W164 for a shorter hydrophobic amino acid, the W164A was expected to retain activity. We also hypothesised that a wider pocket, similar to NanA, would increase positioning of an inhibitor. So far we can confirm that the substrate is still positioned in the active site so the next step should be evaluating if neuraminidase inhibitors have higher binding.

Sialic acid is required for the synthesis of capsular polysaccharide of serotypes A1 and A2 of *M. haemolytica*. The synthesis of A2 capsule requires the production of CMP-Neu5Ac from Neu5Ac through a sialyltransferase (Solana et al., 2001), followed by the action of a polysialyl transferase in order to obtain α 2-8 linked polysialic acid (Lindhout et al., 2013). In contrast, the capsule of A1 requires the synthesis of ManNAc and ManNAcA from UDP-GlcNAc (Lo et al., 2001).

Neuraminidase plays the role of scavenging Neu5Ac from sialylated glycoproteins of the host although, the scavenging pathway is only essential for *P. multocida* since *M. haemolytica* can synthesise Neu5Ac *de novo* from UDP-GlcNAc (Vimr et al., 2004).

The relationship between NanH and capsule synthesis appears to be more direct in serotype A2 however, ManNAc can be produced by an aldolase from Neu5Ac (Vimr et al., 2004). If the amount of free sialic acid used for capsule synthesis is greater than the amount synthesised *de novo*, then inhibition of NanH could reduce the capsule quality and the outer membrane antigens of *M. haemolytica* would become easier to detect by the immune system.

8 Final conclusions

Despite the efforts to eradicate BRD caused by *M. Haemolytica*, the disease remains a problem to the ruminant industry. The understanding of respiratory disease in humans has highlighted the importance of viral and bacterial neuraminidases as a potential prophylactic and therapeutic target due to the role that it has in facilitating colonisation. The biological role of the neuraminidases produced by the primary and secondary agents of BRD has not been determined therefore we sought to characterise the neuraminidase produced by *M. haemolytica* NanH. By performing an analysis of the sequence, we hypothesised that NanH is an extracellular enzyme that is exported via the TVSS. Even though the secretion mechanism was not confirmed experimentally, the enzymatic domain of NanH was delimited by cloning truncated versions of the protein and identifying an active catalytic domain. Owing to the fact that the sialidase domain was identified at the N-terminus, the hypothetical presence of a C-terminal autotransporter domain is still supported. The tertiary structure of the catalytic domain of NanH was predicted by sequence homology to the neuraminidase produced by *T. rangeli*, TrSA. The 3D model was supported by substituting homologous residues of NanH that are essential for neuraminidase activity of TrSA resulting in the reduction or abolition of activity in NanH. These data represent the basis for the full molecular characterisation of *M. haemolytica* NanH and the initial steps for identifying the biological role of the enzyme in BRD. The following steps for the completion of the molecular characterisation should be the confirmation of the NanH secretion system, the confirmation of all the catalytic residues and the identification of the 3D model coordinates by crystallography. Finally, the complete and adequate characterisation of NanH will permit its

manipulation for experiments *in vivo* in which the enzyme can be chemically inhibited or genetically eliminated. Additionally, various conditions that might alter gene expression can be evaluated such as sialic acid or mannose availability in order to confirm their role in *M. haemolytica* metabolism.

9 References

- ADLAM, C., KNIGHTS, J. M., MUGRIDGE, A., LINDON, J. C., BAKER, P. R., BEESLEY, J. E., SPACEY, B., CRAIG, G. R. & NAGY, L. K. 1984. Purification, characterization and immunological properties of the serotype-specific capsular polysaccharide of *Pasteurella haemolytica* (serotype A1) organisms. *J Gen Microbiol*, 130, 2415-26.
- AIR, G. M. 2012. Influenza neuraminidase. *Influenza Other Respir Viruses*, 6, 245-56.
- AITKEN, I. D. 2007. Diseases of sheep. Fourth edition / ed. Oxford: Blackwell,.
- AMAYA, M. F., BUSCHIAZZO, A., NGUYEN, T. & ALZARI, P. M. 2003. The high resolution structures of free and inhibitor-bound *Trypanosoma rangeli* sialidase and its comparison with *T. cruzi* trans-sialidase. *J Mol Biol*, 325, 773-84.
- AMAYA, M. F., WATTS, A. G., DAMAGER, I., WEHENKEL, A., NGUYEN, T., BUSCHIAZZO, A., PARIS, G., FRASCH, A. C., WITHERS, S. G. & ALZARI, P. M. 2004. Structural insights into the catalytic mechanism of *Trypanosoma cruzi* trans-sialidase. *Structure*, 12, 775-84.
- ANGATA, T. & VARKI, A. 2002. Chemical diversity in the sialic acids and related alpha-keto acids: an evolutionary perspective. *Chem Rev*, 102, 439-69.
- ANGEN, O., MUTTERS, R., CAUGANT, D. A., OLSEN, J. E. & BISGAARD, M. 1999. Taxonomic relationships of the [*Pasteurella*] *haemolytica* complex as evaluated by DNA-DNA hybridizations and 16S rRNA sequencing with proposal of *Mannheimia haemolytica* gen. nov., comb. nov., *Mannheimia granulomatis* comb. nov., *Mannheimia glucosida* sp. nov., *Mannheimia ruminalis* sp. nov. and *Mannheimia varigena* sp. nov. *Int J Syst Bacteriol*, 49 Pt 1, 67-86.
- ARUMUGAM, N. D., AJAM, N., BLACKALL, P. J., ASIAH, N. M., RAMLAN, M., MARIA, J., YUSLAN, S. & THONG, K. L. 2011. Capsular serotyping of *Pasteurella multocida* from various animal hosts - a comparison of phenotypic and genotypic methods. *Trop Biomed*, 28, 55-63.
- AYALEW, S., BLACKWOOD, E. R. & CONFER, A. W. 2006. Sequence diversity of the immunogenic outer membrane lipoprotein PlpE from *Mannheimia haemolytica* serotypes 1, 2, and 6. *Vet Microbiol*, 114, 260-8.
- AYALEW, S., CONFER, A. W., PAYTON, M. E., GARRELS, K. D., SHRESTHA, B., INGRAM, K. R., MONTELONGO, M. A. & TAYLOR, J. D. 2008. *Mannheimia haemolytica* chimeric protein vaccine composed of the major surface-exposed epitope of outer membrane lipoprotein PlpE and the neutralizing epitope of leukotoxin. *Vaccine*, 26, 4955-61.
- AYALEW, S., SHRESTHA, B., MONTELONGO, M., WILSON, A. E. & CONFER, A. W. 2011. Immunogenicity of *Mannheimia haemolytica* recombinant outer membrane proteins serotype 1-specific antigen, OmpA, OmpP2, and OmpD15. *Clin Vaccine Immunol*, 18, 2067-74.
- AYALEW, S., STEP, D. L., MONTELONGO, M. & CONFER, A. W. 2009. Intranasal vaccination of calves with *Mannheimia haemolytica* chimeric protein containing the major surface epitope of outer membrane lipoprotein PlpE, the neutralizing epitope of leukotoxin, and cholera toxin subunit B. *Veterinary Immunology and Immunopathology*, 132, 295-302.
- BANERJEE, A., VAN SORGE, N. M., SHEEN, T. R., UCHIYAMA, S., MITCHELL, T. J. & DORAN, K. S. 2010. Activation of brain endothelium by pneumococcal neuraminidase NanA promotes bacterial internalization. *Cell Microbiol*, 12, 1576-88.

- BARNARD, T. J., DAUTIN, N., LUKACIK, P., BERNSTEIN, H. D. & BUCHANAN, S. K. 2007. Autotransporter structure reveals intra-barrel cleavage followed by conformational changes. *Nat Struct Mol Biol*, 14, 1214-20.
- BARNARD, T. J., GUMBART, J., PETERSON, J. H., NOINAJ, N., EASLEY, N. C., DAUTIN, N., KUSZAK, A. J., TAJKHORSHID, E., BERNSTEIN, H. D. & BUCHANAN, S. K. 2012. Molecular Basis for the Activation of a Catalytic Asparagine Residue in a Self-Cleaving Bacterial Autotransporter. *Journal of Molecular Biology*, 415, 128-142.
- BARRALLO, S., REGLERO, A., REVILLA-NUIN, B., MARTINEZ-BLANCO, H., RODRIGUEZ-APARICIO, L. B. & FERRERO, M. A. 1999. Regulation of capsular polysialic acid biosynthesis by temperature in *Pasteurella haemolytica* A2. *FEBS Lett*, 445, 325-8.
- BATRA, S. A., SHANTHALINGAM, S., DONOFRIO, G. & SRIKUMARAN, S. 2016. A chimeric protein comprising the immunogenic domains of *Mannheimia haemolytica* leukotoxin and outer membrane protein PlpE induces antibodies against leukotoxin and PlpE. *Vet Immunol Immunopathol*, 175, 36-41.
- BATRA, S. A., SHANTHALINGAM, S., MUNSKE, G. R., RAGHAVAN, B., KUGADAS, A., BAVANTHASIVAM, J., HIGHLANDER, S. K. & SRIKUMARAN, S. 2015. Acylation enhances, but is not required for, the cytotoxic activity of *Mannheimia haemolytica* leukotoxin in bighorn sheep. *Infect Immun*.
- BESSER, T. E., CASSIRER, E. F., POTTER, K. A., LAHMERS, K., OAKS, J. L., SHANTHALINGAM, S., SRIKUMARAN, S. & FOREYT, W. J. 2014. Epizootic pneumonia of bighorn sheep following experimental exposure to *Mycoplasma ovipneumoniae*. *PLoS One*, 9, e110039.
- BLACKALL, P. J., BOJESEN, A. M., CHRISTENSEN, H. & BISGAARD, M. 2007. Reclassification of [*Pasteurella*] *trehalosi* as *Bibersteinia trehalosi* gen. nov., comb. nov. *Int J Syst Evol Microbiol*, 57, 666-74.
- BRITTAN, J. L., BUCKERIDGE, T. J., FINN, A., KADIOGLU, A. & JENKINSON, H. F. 2012. Pneumococcal neuraminidase A: an essential upper airway colonization factor for *Streptococcus pneumoniae*. *Mol Oral Microbiol*, 27, 270-83.
- BURNAUGH, A. M., FRANTZ, L. J. & KING, S. J. 2008. Growth of *Streptococcus pneumoniae* on human glycoconjugates is dependent upon the sequential activity of bacterial exoglycosidases. *J Bacteriol*, 190, 221-30.
- BUSCHIAZZO, A., TAVARES, G. A., CAMPETELLA, O., SPINELLI, S., CREMONA, M. L., PARIS, G., AMAYA, M. F., FRASCH, A. C. & ALZARI, P. M. 2000. Structural basis of sialyltransferase activity in trypanosomal sialidases. *Embo j*, 19, 16-24.
- CAMARA, M., BOULNOIS, G. J., ANDREW, P. W. & MITCHELL, T. J. 1994. A neuraminidase from *Streptococcus pneumoniae* has the features of a surface protein. *Infect Immun*, 62, 3688-95.
- CASPI, R., BILLINGTON, R., FERRER, L., FOERSTER, H., FULCHER, C. A., KESELER, I. M., KOTHARI, A., KRUMMENACKER, M., LATENDRESSE, M., MUELLER, L. A., ONG, Q., PALEY, S., SUBHRAVETI, P., WEAVER, D. S. & KARP, P. D. 2016. The MetaCyc database of metabolic pathways and enzymes and the BioCyc collection of pathway/genome databases. *Nucleic Acids Res*, 44, D471-80.
- CASWELL, J. L. 2014. Failure of respiratory defenses in the pathogenesis of bacterial pneumonia of cattle. *Vet Pathol*, 51, 393-409.

- CASWELL, J. L., MIDDLETON, D. M. & GORDON, J. R. 1999. Production and functional characterization of recombinant bovine interleukin-8 as a specific neutrophil activator and chemoattractant. *Vet Immunol Immunopathol*, 67, 327-40.
- CHAE, C. H., GENTRY, M. J., CONFER, A. W. & ANDERSON, G. A. 1990. Resistance to host immune defense mechanisms afforded by capsular material of *Pasteurella haemolytica*, serotype 1. *Vet Microbiol*, 25, 241-51.
- CHENAL, A., GUIJARRO, J. I., RAYNAL, B., DELEPIERRE, M. & LADANT, D. 2009. RTX calcium binding motifs are intrinsically disordered in the absence of calcium: implication for protein secretion. *J Biol Chem*, 284, 1781-9.
- CHENAL, A., SOTOMAYOR-PEREZ, A. C. & LADANT, D. 2015. 23 - Structure and function of RTX toxins. *The Comprehensive Sourcebook of Bacterial Protein Toxins (Fourth Edition)*. Boston: Academic Press.
- CIOFFI, D. L., PANDEY, S., ALVAREZ, D. F. & CIOFFI, E. A. 2012. Terminal sialic acids are an important determinant of pulmonary endothelial barrier integrity. *Am J Physiol Lung Cell Mol Physiol*, 302, L1067-77.
- COATS, M. T., MURPHY, T., PATON, J. C., GRAY, B. & BRILES, D. E. 2011. Exposure of Thomsen-Friedenreich antigen in *Streptococcus pneumoniae* infection is dependent on pneumococcal neuraminidase A. *Microb Pathog*, 50, 343-9.
- CONFER, A. W. & AYALEW, S. 2013. The OmpA family of proteins: roles in bacterial pathogenesis and immunity. *Vet Microbiol*, 163, 207-22.
- CONFER, A. W., AYALEW, S., STEP, D. L., TROJAN, B. & MONTELONGO, M. 2009. Intranasal vaccination of young Holstein calves with Mannheimia haemolytica chimeric protein PlpE-LKT (SAC89) and cholera toxin. *Vet Immunol Immunopathol*, 132, 232-6.
- CONNARIS, H., TAKIMOTO, T., RUSSELL, R., CRENNELL, S., MOUSTAFA, I., PORTNER, A. & TAYLOR, G. 2002. Probing the sialic acid binding site of the hemagglutinin-neuraminidase of Newcastle disease virus: identification of key amino acids involved in cell binding, catalysis, and fusion. *J Virol*, 76, 1816-24.
- CORBEIL, L. B. 2007. *Histophilus somni* host-parasite relationships. *Anim Health Res Rev*, 8, 151-60.
- CORFIELD, T. 1992. Bacterial sialidases—roles in pathogenicity and nutrition. *Glycobiology*, 2, 509-521.
- CROUCH, C. F., LAFLEUR, R., RAMAGE, C., REDDICK, D., MURRAY, J., DONACHIE, W. & FRANCIS, M. J. 2012. Cross protection of a Mannheimia haemolytica A1 Lkt-/*Pasteurella multocida* DeltahyaE bovine respiratory disease vaccine against experimental challenge with Mannheimia haemolytica A6 in calves. *Vaccine*, 30, 2320-8.
- CZUPRYNSKI, C. J. 2009. Host response to bovine respiratory pathogens. *Anim Health Res Rev*, 10, 141-3.
- CZUPRYNSKI, C. J., NOEL, E. J. & ADLAM, C. 1991. Interaction of bovine alveolar macrophages with *Pasteurella haemolytica* A1 in vitro: modulation by purified capsular polysaccharide. *Vet Microbiol*, 26, 349-58.
- DABO, S. M., TAYLOR, J. D. & CONFER, A. W. 2007. *Pasteurella multocida* and bovine respiratory disease. *Anim Health Res Rev*, 8, 129-50.
- DAIGNEAULT, M. C. & LO, R. Y. 2009. Analysis of a collagen-binding trimeric autotransporter adhesin from Mannheimia haemolytica A1. *FEMS Microbiol Lett*, 300, 242-8.
- DASSANAYAKE, R. P., MAHESWARAN, S. K. & SRIKUMARAN, S. 2007a. Monomeric expression of bovine beta2-integrin subunits reveals their role in

- Mannheimia haemolytica leukotoxin-induced biological effects. *Infect Immun*, 75, 5004-10.
- DASSANAYAKE, R. P., SHANTHALINGAM, S., DAVIS, W. C. & SRIKUMARAN, S. 2007b. Mannheimia haemolytica leukotoxin-induced cytolysis of ovine (*Ovis aries*) leukocytes is mediated by CD18, the beta subunit of beta2-integrins. *Microb Pathog*, 42, 167-73.
- DASSANAYAKE, R. P., SHANTHALINGAM, S., HERNDON, C. N., SUBRAMANIAM, R., LAWRENCE, P. K., BAVANANTHASIVAM, J., CASSIRER, E. F., HALDORSON, G. J., FOREYT, W. J., RURANGIRWA, F. R., KNOWLES, D. P., BESSER, T. E. & SRIKUMARAN, S. 2010. Mycoplasma ovipneumoniae can predispose bighorn sheep to fatal Mannheimia haemolytica pneumonia. *Vet Microbiol*, 145, 354-9.
- DAUTIN, N. 2010. Serine protease autotransporters of enterobacteriaceae (SPATEs): biogenesis and function. *Toxins (Basel)*, 2, 1179-206.
- DAUTIN, N., BARNARD, T. J., ANDERSON, D. E. & BERNSTEIN, H. D. 2007. Cleavage of a bacterial autotransporter by an evolutionarily convergent autocatalytic mechanism. *Embo j*, 26, 1942-52.
- DAVIES, R. L., CAMPBELL, S. & WHITTAM, T. S. 2002. Mosaic structure and molecular evolution of the leukotoxin operon (lktCABD) in Mannheimia (*Pasteurella*) haemolytica, Mannheimia glucosida, and Pasteurella trehalosi. *J Bacteriol*, 184, 266-77.
- DAVIES, R. L. & DONACHIE, W. 1996. Intra-specific diversity and host specificity within Pasteurella haemolytica based on variation of capsular polysaccharide, lipopolysaccharide and outer-membrane proteins. *Microbiology*, 142 (Pt 7), 1895-907.
- DAVIES, R. L. & LEE, I. 2004. Sequence diversity and molecular evolution of the heat-modifiable outer membrane protein gene (ompA) of Mannheimia(*Pasteurella*) haemolytica, Mannheimia glucosida, and Pasteurella trehalosi. *J Bacteriol*, 186, 5741-52.
- DAVIES, R. L., WHITTAM, T. S. & SELANDER, R. K. 2001. Sequence diversity and molecular evolution of the leukotoxin (lktA) gene in bovine and ovine strains of Mannheimia (*Pasteurella*) haemolytica. *J Bacteriol*, 183, 1394-404.
- DE LA MORA, A., SUAREZ-GUEMES, F., TRIGO, F., GOROCICA, P., SOLORZANO, C., SLOMIANNY, M. C., AGUNDIS, C., PEREYRA, M. A. & ZENTENO, E. 2007. Purification of the receptor for the N-acetyl-D-glucosamine specific adhesin of Mannheimia haemolytica from bovine neutrophils. *Biochim Biophys Acta*, 1770, 1483-9.
- DE LA MORA, A., TRIGO, F., JARAMILLO, L., GARFIAS, Y., SOLORZANO, C., AGUNDIS, C., PEREYRA, A., LASCURAIN, R., ZENTENO, E. & SUAREZ-GUEMES, F. 2006. The N-acetyl-D-glucosamine specific adhesin from Mannheimia haemolytica activates bovine neutrophils oxidative burst. *Vet Immunol Immunopathol*, 113, 148-56.
- DELEPELAIRE, P. 2004. Type I secretion in gram-negative bacteria. *Biochim Biophys Acta*, 1694, 149-61.
- DILEEPAN, T., KANNAN, M. S., WALCHECK, B., THUMBIKAT, P. & MAHESWARAN, S. K. 2005a. Mapping of the binding site for Mannheimia haemolytica leukotoxin within bovine CD18. *Infect Immun*, 73, 5233-7.
- DILEEPAN, T., THUMBIKAT, P., WALCHECK, B., KANNAN, M. S. & MAHESWARAN, S. K. 2005b. Recombinant expression of bovine LFA-1 and characterization of its role as a receptor for Mannheimia haemolytica leukotoxin. *Microb Pathog*, 38, 249-57.

- DONACHIE, W. & GILMOUR, N. J. L. 1988. Sheep antibody response to cell wall antigens expressed in vivo by *Pasteurella haemolytica* serotype A2. *FEMS Microbiology Letters*, 56, 271-276.
- EDWARDS, T. A. 2010. Control methods for bovine respiratory disease for feedlot cattle. *Vet Clin North Am Food Anim Pract*, 26, 273-84.
- EIDAM, C., POEHLEIN, A., BRENNER MICHAEL, G., KADLEC, K., LIESEGANG, H., BRZUSZKIEWICZ, E., DANIEL, R., SWEENEY, M. T., MURRAY, R. W., WATTS, J. L. & SCHWARZ, S. 2013. Complete Genome Sequence of *Mannheimia haemolytica* Strain 42548 from a Case of Bovine Respiratory Disease. *Genome Announc*, 1.
- ELLIS, J. A. 2010. Bovine parainfluenza-3 virus. *Vet Clin North Am Food Anim Pract*, 26, 575-93.
- EWERS, C., LUBKE-BECKER, A., BETHE, A., KIEBLING, S., FILTER, M. & WIELER, L. H. 2006. Virulence genotype of *Pasteurella multocida* strains isolated from different hosts with various disease status. *Vet Microbiol*, 114, 304-17.
- FEDOROVA, N. D. & HIGHLANDER, S. K. 1997. Plasmids for heterologous expression in *Pasteurella haemolytica*. *Gene*, 186, 207-11.
- FENG, C., STAMATOS, N. M., DRAGAN, A. I., MEDVEDEV, A., WHITFORD, M., ZHANG, L., SONG, C., RALLABHANDI, P., COLE, L., NHU, Q. M., VOGEL, S. N., GEDDES, C. D. & CROSS, A. S. 2012. Sialyl residues modulate LPS-mediated signaling through the Toll-like receptor 4 complex. *PLoS One*, 7, e32359.
- FENG, C., ZHANG, L., NGUYEN, C., VOGEL, S. N., GOLDBLUM, S. E., BLACKWELDER, W. C. & CROSS, A. S. 2013. Neuraminidase reprograms lung tissue and potentiates lipopolysaccharide-induced acute lung injury in mice. *J Immunol*, 191, 4828-37.
- FERNÁNDEZ MARTÍNEZ, V. 2007. *Estudios moleculares sobre la neuraminidasa de "Mannheimia haemolytica 2"*. Tesis-Universidad de León Facultad de Veterinaria Departamento de Biología Molecular, 2007, Universidad de León, Secretariado de Publicaciones,.
- FERRERO, M. A. & APARICIO, L. R. 2010. Biosynthesis and production of polysialic acids in bacteria. *Appl Microbiol Biotechnol*, 86, 1621-35.
- FRANK, G. H. & TABATABAI, L. B. 1981. Neuraminidase activity of *Pasteurella haemolytica* isolates. *Infect Immun*, 32, 1119-22.
- FULTON, R. W., PURDY, C. W., CONFER, A. W., SALIKI, J. T., LOAN, R. W., BRIGGS, R. E. & BURGE, L. J. 2000. Bovine viral diarrhea viral infections in feeder calves with respiratory disease: interactions with *Pasteurella* spp., parainfluenza-3 virus, and bovine respiratory syncytial virus. *Can J Vet Res*, 64, 151-9.
- GASKELL, A., CRENNELL, S. & TAYLOR, G. 1995. The three domains of a bacterial sialidase: a beta-propeller, an immunoglobulin module and a galactose-binding jelly-roll. *Structure*, 3, 1197-205.
- GILMOUR, N. J., DONACHIE, W., SUTHERLAND, A. D., GILMOUR, J. S., JONES, G. E. & QUIRIE, M. 1991. Vaccine containing iron-regulated proteins of *Pasteurella haemolytica* A2 enhances protection against experimental pasteurellosis in lambs. *Vaccine*, 9, 137-40.
- GIOIA, J., QIN, X., JIANG, H., CLINKENBEARD, K., LO, R., LIU, Y., FOX, G. E., YERRAPRAGADA, S., MCLEOD, M. P., MCNEILL, T. Z., HEMPHILL, L., SODERGREN, E., WANG, Q., MUZNY, D. M., HOMSI, F. J., WEINSTOCK, G. M. & HIGHLANDER, S. K. 2006. The genome sequence of *Mannheimia*

- haemolytica A1: insights into virulence, natural competence, and Pasteurellaceae phylogeny. *J Bacteriol*, 188, 7257-66.
- GREWAL, P. K., AZIZ, P. V., UCHIYAMA, S., RUBIO, G. R., LARDONE, R. D., LE, D., VARKI, N. M., NIZET, V. & MARTH, J. D. 2013. Inducing host protection in pneumococcal sepsis by preactivation of the Ashwell-Morell receptor. *Proc Natl Acad Sci U S A*, 110, 20218-23.
- GREWAL, P. K., UCHIYAMA, S., DITTO, D., VARKI, N., LE, D. T., NIZET, V. & MARTH, J. D. 2008. The Ashwell receptor mitigates the lethal coagulopathy of sepsis. *Nat Med*, 14, 648-55.
- GUT, H., KING, S. J. & WALSH, M. A. 2008. Structural and functional studies of Streptococcus pneumoniae neuraminidase B: An intramolecular trans-sialidase. *FEBS Lett*, 582, 3348-52.
- GUT, H., XU, G., TAYLOR, G. L. & WALSH, M. A. 2011. Structural basis for Streptococcus pneumoniae NanA inhibition by influenza antivirals zanamivir and oseltamivir carboxylate. *J Mol Biol*, 409, 496-503.
- GYLES, C. L. 2004. *Pathogenesis of bacterial infections in animals*, Ames, Iowa, Oxford, Blackwell.
- HARHAY, G. P., KOREN, S., PHILLIPPY, A. M., MCVEY, D. S., KUSZAK, J., CLAWSON, M. L., HARHAY, D. M., HEATON, M. P., CHITKO-MCKOWN, C. G. & SMITH, T. P. 2013. Complete Closed Genome Sequences of Mannheimia haemolytica Serotypes A1 and A6, Isolated from Cattle. *Genome Announc*, 1.
- HARTNETT, J., GRACYALNY, J. & SLATER, M. R. 2006. The Single Step (KRX) Competent Cells: Efficient Cloning and High Protein Yields. Promega.
- HAUGLUND, M. J., TATUM, F. M., BAYLES, D. O., MAHESWARAN, S. K. & BRIGGS, R. E. 2013. Genome Sequences of Mannheimia haemolytica Serotype A1 Strains D153 and D193 from Bovine Pneumonia. *Genome Announc*, 1.
- HAUGLUND, M. J., TATUM, F. M., BAYLES, D. O., MAHESWARAN, S. K. & BRIGGS, R. E. 2015a. Genome Sequences of Mannheimia haemolytica Serotype A2 Isolates D171 and D35, Recovered from Bovine Pneumonia. *Genome Announc*, 3.
- HAUGLUND, M. J., TATUM, F. M., BAYLES, D. O., MAHESWARAN, S. K. & BRIGGS, R. E. 2015b. Genome Sequences of Serotype A6 Mannheimia haemolytica Isolates D174 and D38 Recovered from Bovine Pneumonia. *Genome Announc*, 3.
- HAYRE, J. K., XU, G., BORGIANNI, L., TAYLOR, G. L., ANDREW, P. W., DOCQUIER, J. D. & OGGIONI, M. R. 2012. Optimization of a direct spectrophotometric method to investigate the kinetics and inhibition of sialidases. *BMC Biochem*, 13, 19.
- HEATON, M. P., HARHAY, G. P., SMITH, T. P., BONO, J. L. & CHITKO-MCKOWN, C. G. 2015. Complete Closed Genome Sequences of a Mannheimia haemolytica Serotype A1 Leukotoxin Deletion Mutant and Its Wild-Type Parent Strain. *Genome Announc*, 3.
- HENDERSON, I. R., NAVARRO-GARCIA, F., DESVAUX, M., FERNANDEZ, R. C. & ALA'ALDEEN, D. 2004. Type V protein secretion pathway: the autotransporter story. *Microbiol Mol Biol Rev*, 68, 692-744.
- HENDERSON, I. R., NAVARRO-GARCIA, F. & NATARO, J. P. 1998. The great escape: structure and function of the autotransporter proteins. *Trends Microbiol*, 6, 370-8.
- HIGHLANDER, S. K., FEDOROVA, N. D., DUSEK, D. M., PANCIERA, R., ALVAREZ, L. E. & RINEHART, C. 2000. Inactivation of Pasteurella

- (Mannheimia) haemolytica leukotoxin causes partial attenuation of virulence in a calf challenge model. *Infect Immun*, 68, 3916-22.
- HINZ, K. H. & MULLER, H. E. 1977. [The occurrence of neuraminidase and N-acetylneuraminidate pyruvate lyase in Haemophilus paragallinarum and Haemophilus paravium n.sp (author's transl)]. *Zentralbl Bakteriol Orig A*, 237, 72-9.
- HODGSON, P. D., AICH, P., STOOKEY, J., POPOWYCH, Y., POTTER, A., BABIUK, L. & GRIEBEL, P. J. 2012. Stress significantly increases mortality following a secondary bacterial respiratory infection. *Vet Res*, 43, 21.
- HOUNSOME, J. D., BAILLIE, S., NOOFELI, M., RIBOLDI-TUNNICLIFFE, A., BURCHMORE, R. J., ISAACS, N. W. & DAVIES, R. L. 2011. Outer membrane protein A of bovine and ovine isolates of Mannheimia haemolytica is surface exposed and contains host species-specific epitopes. *Infect Immun*, 79, 4332-41.
- HSIAO, Y. S., PARKER, D., RATNER, A. J., PRINCE, A. & TONG, L. 2009. Crystal structures of respiratory pathogen neuraminidases. *Biochem Biophys Res Commun*, 380, 467-71.
- IORIO, R. M., FIELD, G. M., SAUVRON, J. M., MIRZA, A. M., DENG, R., MAHON, P. J. & LANGEDIJK, J. P. 2001. Structural and functional relationship between the receptor recognition and neuraminidase activities of the Newcastle disease virus hemagglutinin-neuraminidase protein: receptor recognition is dependent on neuraminidase activity. *J Virol*, 75, 1918-27.
- JARAMILLO, L., DIAZ, F., HERNANDEZ, P., DEBRAY, H., TRIGO, F., MENDOZA, G. & ZENTENO, E. 2000. Purification and characterization of an adhesin from Pasteurella haemolytica. *Glycobiology*, 10, 31-7.
- JARAMILLO-MEZA, L., AGUILAR-ROMERO, F., SUÁREZ-GÜEMES, F. & TRIGO-TAVERA, F. 2007. Challenge exposure of sheep immunized with live vaccine and culture supernatant of Mannheimia haemolytica A1: Effects of revaccination. *Small Ruminant Research*, 70, 209-217.
- JERICO, K. W., DARCEL, C. L. & LANGFORD, E. V. 1982. Respiratory disease in calves produced with aerosols of parainfluenza-3 virus and Pasteurella haemolytica. *Can J Comp Med*, 46, 293-301.
- JERS, C., MICHALAK, M., LARSEN, D. M., KEPP, K. P., LI, H., GUO, Y., KIRPEKAR, F., MEYER, A. S. & MIKKELSEN, J. D. 2014. Rational design of a new Trypanosoma rangeli trans-sialidase for efficient sialylation of glycans. *PLoS One*, 9, e83902.
- JONES, C. & CHOWDHURY, S. 2007. A review of the biology of bovine herpesvirus type 1 (BHV-1), its role as a cofactor in the bovine respiratory disease complex and development of improved vaccines. *Anim Health Res Rev*, 8, 187-205.
- KADIOGLU, A., WEISER, J. N., PATON, J. C. & ANDREW, P. W. 2008. The role of Streptococcus pneumoniae virulence factors in host respiratory colonization and disease. *Nat Rev Microbiol*, 6, 288-301.
- KELLEY, L. A., MEZULIS, S., YATES, C. M., WASS, M. N. & STERNBERG, M. J. E. 2015. The Phyre2 web portal for protein modeling, prediction and analysis. *Nat. Protocols*, 10, 845-858.
- KELLEY, L. A. & STERNBERG, M. J. 2009. Protein structure prediction on the Web: a case study using the Phyre server. *Nat Protoc*, 4, 363-71.
- KIDANEMARIAM GELAW, A., BIHON, W., FARANANI, R., MAFOFO, J., REES, J. & MADOROBA, E. 2015. Complete Genome Sequence of Mannheimia haemolytica Strain Mh10517, Isolated from Sheep in South Africa. *Genome Announc*, 3.

- KIM, S., OH, D. B., KANG, H. A. & KWON, O. 2011. Features and applications of bacterial sialidases. *Appl Microbiol Biotechnol*, 91, 1-15.
- KING, S. J., HIPPE, K. R. & WEISER, J. N. 2006. Deglycosylation of human glycoconjugates by the sequential activities of exoglycosidases expressed by *Streptococcus pneumoniae*. *Mol Microbiol*, 59, 961-74.
- KING, S. J., WHATMORE, A. M. & DOWSON, C. G. 2005. NanA, a neuraminidase from *Streptococcus pneumoniae*, shows high levels of sequence diversity, at least in part through recombination with *Streptococcus oralis*. *J Bacteriol*, 187, 5376-86.
- KIRBY, S. D., LAINSON, F. A., DONACHIE, W., OKABE, A., TOKUDA, M., HATASE, O. & SCHRYVERS, A. B. 1998. The *Pasteurella haemolytica* 35 kDa iron-regulated protein is an FbpA homologue. *Microbiology*, 144 (Pt 12), 3425-36.
- KISIELA, D. I. & CZUPRYNSKI, C. J. 2009. Identification of Mannheimia haemolytica adhesins involved in binding to bovine bronchial epithelial cells. *Infect Immun*, 77, 446-55.
- KLIMA, C. L., COOK, S. R., HAHN, K. R., AMOAKO, K. K., ALEXANDER, T. W., HENDRICK, S. & MCALLISTER, T. A. 2013. Draft Genome Sequence of a Mannheimia haemolytica Serotype 6 Isolate Collected from the Nasopharynx of a Beef Calf with Bovine Respiratory Disease. *Genome Announc*, 1, e0005113.
- KLIMA, C. L., COOK, S. R., ZAHEER, R., LAING, C., GANNON, V. P., XU, Y., RASMUSSEN, J., POTTER, A., HENDRICK, S., ALEXANDER, T. W. & MCALLISTER, T. A. 2016. Comparative Genomic Analysis of Mannheimia haemolytica from Bovine Sources. *PLoS One*, 11, e0149520.
- KLIMA, C. L., ZAHEER, R., COOK, S. R., BOOKER, C. W., HENDRICK, S., ALEXANDER, T. W. & MCALLISTER, T. A. 2014. Pathogens of bovine respiratory disease in North American feedlots conferring multidrug resistance via integrative conjugative elements. *J Clin Microbiol*, 52, 438-48.
- KUDVA, R., DENKS, K., KUHN, P., VOGT, A., MULLER, M. & KOCH, H. G. 2013. Protein translocation across the inner membrane of Gram-negative bacteria: the Sec and Tat dependent protein transport pathways. *Res Microbiol*, 164, 505-34.
- LACASTA, D., FERRER, L. M., RAMOS, J. J., GONZALEZ, J. M., ORTIN, A. & FTHENAKIS, G. C. 2015. Vaccination schedules in small ruminant farms. *Vet Microbiol*, 181, 34-46.
- LAINSON, F. A., HARKINS, D. C., WILSON, C. F., SUTHERLAND, A. D., MURRAY, J. E., DONACHIE, W. & BAIRD, G. D. 1991. Identification and localization of an iron-regulated 35 kDa protein of *Pasteurella haemolytica* serotype A2. *J Gen Microbiol*, 137, 219-26.
- LAWRENCE, P. K., BEY, R. F., WIENER, B., KITTICHOTIRAT, W. & BUMGARNER, R. E. 2014. Genome Sequence of a Presumptive Mannheimia haemolytica Strain with an A1/A6-Cross-Reactive Serotype from a White-Tailed Deer (*Odocoileus virginianus*). *Genome Announc*, 2.
- LAWRENCE, P. K., KITTICHOTIRAT, W., BUMGARNER, R. E., MCDERMOTT, J. E., HERNDON, D. R., KNOWLES, D. P. & SRIKUMARAN, S. 2010. Genome sequences of Mannheimia haemolytica serotype A2: ovine and bovine isolates. *J Bacteriol*, 192, 1167-8.
- LEITE, F., ATAPATTU, D., KUCKLEBURG, C., SCHULTZ, R. & CZUPRYNSKI, C. J. 2005. Incubation of bovine PMNs with conditioned medium from BHV-1 infected peripheral blood mononuclear cells increases their susceptibility to

- Mannheimia haemolytica leukotoxin. *Vet Immunol Immunopathol*, 103, 187-93.
- LEITE, F., SYLTE, M. J., O'BRIEN, S., SCHULTZ, R., PEEK, S., VAN REETH, K. & CZUPRYNSKI, C. J. 2002. Effect of experimental infection of cattle with bovine herpesvirus-1 (BHV-1) on the ex vivo interaction of bovine leukocytes with Mannheimia (Pasteurella) haemolytica leukotoxin. *Vet Immunol Immunopathol*, 84, 97-110.
- LEO, J. C., GRIN, I. & LINKE, D. 2012. Type V secretion: mechanism(s) of autotransport through the bacterial outer membrane. *Philos Trans R Soc Lond B Biol Sci*, 367, 1088-101.
- LEWIS, A. L. & LEWIS, W. G. 2012. Host sialoglycans and bacterial sialidases: a mucosal perspective. *Cell Microbiol*, 14, 1174-82.
- LEYTON, D. L., ROSSITER, A. E. & HENDERSON, I. R. 2012. From self sufficiency to dependence: mechanisms and factors important for autotransporter biogenesis. *Nat Rev Microbiol*, 10, 213-25.
- LI, Y. & CHEN, X. 2012. Sialic acid metabolism and sialyltransferases: natural functions and applications. *Appl Microbiol Biotechnol*, 94, 887-905.
- LICHTENSTEIGER, C. A. & VIMR, E. R. 1997. Neuraminidase (sialidase) activity of Haemophilus parasuis. *FEMS Microbiol Lett*, 152, 269-74.
- LINDHOUT, T., BAINBRIDGE, C. R., COSTAIN, W. J., GILBERT, M. & WAKARCHUK, W. W. 2013. Biochemical characterization of a polysialyltransferase from Mannheimia haemolytica A2 and comparison to other bacterial polysialyltransferases. *PLoS One*, 8, e69888.
- LINHARTOVA, I., BUMBA, L., MASIN, J., BASLER, M., OSICKA, R., KAMANOVA, J., PROCHAZKOVA, K., ADKINS, I., HEJNOVA-HOLUBOVA, J., SADILKOVA, L., MOROVA, J. & SEBO, P. 2010. RTX proteins: a highly diverse family secreted by a common mechanism. *FEMS Microbiol Rev*, 34, 1076-112.
- LO, R. Y., MCKERRAL, L. J., HILLS, T. L. & KOSTRZYNSKA, M. 2001. Analysis of the capsule biosynthetic locus of Mannheimia (Pasteurella) haemolytica A1 and proposal of a nomenclature system. *Infect Immun*, 69, 4458-64.
- LO, R. Y., STRATHDEE, C. A., SHEWEN, P. E. & COONEY, B. J. 1991. Molecular studies of Ssa1, a serotype-specific antigen of Pasteurella haemolytica A1. *Infect Immun*, 59, 3398-406.
- LOIRAT, C., SALAND, J. & BITZAN, M. 2012. Management of hemolytic uremic syndrome. *Presse Med*, 41, e115-35.
- LONG, J. P., TONG, H. H. & DEMARIA, T. F. 2004. Immunization with native or recombinant Streptococcus pneumoniae neuraminidase affords protection in the chinchilla otitis media model. *Infect Immun*, 72, 4309-13.
- MAHASRESHTI, P. J., MURPHY, G. L., WYCKOFF, J. H., 3RD, FARMER, S., HANCOCK, R. E. & CONFER, A. W. 1997. Purification and partial characterization of the OmpA family of proteins of Pasteurella haemolytica. *Infect Immun*, 65, 211-8.
- MANCO, S., HERNON, F., YESILKAYA, H., PATON, J. C., ANDREW, P. W. & KADIOGLU, A. 2006. Pneumococcal neuraminidases A and B both have essential roles during infection of the respiratory tract and sepsis. *Infect Immun*, 74, 4014-20.
- MARCHLER-BAUER, A., ANDERSON, J. B., CHITSAZ, F., DERBYSHIRE, M. K., DEWEESE-SCOTT, C., FONG, J. H., GEER, L. Y., GEER, R. C., GONZALES, N. R., GWADZ, M., HE, S., HURWITZ, D. I., JACKSON, J. D., KE, Z., LANCZYCKI, C. J., LIEBERT, C. A., LIU, C., LU, F., LU, S., MARCHLER, G. H., MULLOKANDOV, M., SONG, J. S., TASNEEM, A.,

- THANKI, N., YAMASHITA, R. A., ZHANG, D., ZHANG, N. & BRYANT, S. H. 2009. CDD: specific functional annotation with the Conserved Domain Database. *Nucleic Acids Res*, 37, D205-10.
- MARCHLER-BAUER, A. & BRYANT, S. H. 2004. CD-Search: protein domain annotations on the fly. *Nucleic Acids Res*, 32, W327-31.
- MARCHLER-BAUER, A., DERBYSHIRE, M. K., GONZALES, N. R., LU, S., CHITSAZ, F., GEER, L. Y., GEER, R. C., HE, J., GWADZ, M., HURWITZ, D. I., LANCZYCKI, C. J., LU, F., MARCHLER, G. H., SONG, J. S., THANKI, N., WANG, Z., YAMASHITA, R. A., ZHANG, D., ZHENG, C. & BRYANT, S. H. 2015. CDD: NCBI's conserved domain database. *Nucleic Acids Res*, 43, D222-6.
- MARCHLER-BAUER, A., LU, S., ANDERSON, J. B., CHITSAZ, F., DERBYSHIRE, M. K., DEWEESE-SCOTT, C., FONG, J. H., GEER, L. Y., GEER, R. C., GONZALES, N. R., GWADZ, M., HURWITZ, D. I., JACKSON, J. D., KE, Z., LANCZYCKI, C. J., LU, F., MARCHLER, G. H., MULLOKANDOV, M., OMELCHENKO, M. V., ROBERTSON, C. L., SONG, J. S., THANKI, N., YAMASHITA, R. A., ZHANG, D., ZHANG, N., ZHENG, C. & BRYANT, S. H. 2011. CDD: a Conserved Domain Database for the functional annotation of proteins. *Nucleic Acids Res*, 39, D225-9.
- MARION, C., BURNAUGH, A. M., WOODIGA, S. A. & KING, S. J. 2011. Sialic acid transport contributes to pneumococcal colonization. *Infect Immun*, 79, 1262-9.
- MAXIE, M. G. & JUBB, K. V. F. 2007. *Jubb, Kennedy & Palmer's pathology of domestic animals*, Edinburgh, New York, Elsevier Saunders.
- MAY, B. J., ZHANG, Q., LI, L. L., PAUSTIAN, M. L., WHITTAM, T. S. & KAPUR, V. 2001. Complete genomic sequence of *Pasteurella multocida*, Pm70. *Proc Natl Acad Sci U S A*, 98, 3460-5.
- MCCULLERS, J. A. 2004. Effect of antiviral treatment on the outcome of secondary bacterial pneumonia after influenza. *J Infect Dis*, 190, 519-26.
- MCGILL, J. L., RUSK, R. A., GUERRA-MAUPOME, M., BRIGGS, R. E. & SACCO, R. E. 2016. Bovine Gamma Delta T Cells Contribute to Exacerbated IL-17 Production in Response to Co-Infection with Bovine RSV and Mannheimia haemolytica. *PLoS One*, 11, e0151083.
- MCKERRAL, L. J. & LO, R. Y. 2002. Construction and characterization of an acapsular mutant of Mannheimia haemolytica A1. *Infect Immun*, 70, 2622-9.
- MEADE, K. G., O'GORMAN, G. M., NARCIANDI, F., MACHUGH, D. E. & O'FARRELLY, C. 2012. Functional characterisation of bovine interleukin 8 promoter haplotypes in vitro. *Mol Immunol*, 50, 108-16.
- MELE, C., REMUZZI, G. & NORIS, M. 2014. Hemolytic uremic syndrome. *Semin Immunopathol*.
- MILES, D. G. 2009. Overview of the North American beef cattle industry and the incidence of bovine respiratory disease (BRD). *Anim Health Res Rev*, 10, 101-3.
- MIZAN, S., HENK, A., STALLINGS, A., MAIER, M. & LEE, M. D. 2000. Cloning and characterization of sialidases with 2-6' and 2-3' sialyl lactose specificity from *Pasteurella multocida*. *J Bacteriol*, 182, 6874-83.
- MOUSTAFA, I., CONNARIS, H., TAYLOR, M., ZAITSEV, V., WILSON, J. C., KIEFEL, M. J., VON ITZSTEIN, M. & TAYLOR, G. 2004. Sialic acid recognition by *Vibrio cholerae* neuraminidase. *J Biol Chem*, 279, 40819-26.
- MULLER, H. E. & MANNHEIM, W. 1995. Occurrence of sialidase and N-acetylneuraminase lyase in *Pasteurella* species. *Zentralbl Bakteriol*, 283, 105-14.

- MUYLKENS, B., THIRY, J., KIRTEN, P., SCHYNTS, F. & THIRY, E. 2007. Bovine herpesvirus 1 infection and infectious bovine rhinotracheitis. *Vet Res*, 38, 181-209.
- OGGIONI, M. R., TRAPPETTI, C., KADIOGLU, A., CASSONE, M., IANNELLI, F., RICCI, S., ANDREW, P. W. & POZZI, G. 2006. Switch from planktonic to sessile life: a major event in pneumococcal pathogenesis. *Mol Microbiol*, 61, 1196-210.
- OLIVER, D. C., HUANG, G. & FERNANDEZ, R. C. 2003. Identification of secretion determinants of the Bordetella pertussis BrkA autotransporter. *J Bacteriol*, 185, 489-95.
- OVERBEEK, R., OLSON, R., PUSCH, G. D., OLSEN, G. J., DAVIS, J. J., DISZ, T., EDWARDS, R. A., GERDES, S., PARRELLO, B., SHUKLA, M., VONSTEIN, V., WATTAM, A. R., XIA, F. & STEVENS, R. 2014. The SEED and the Rapid Annotation of microbial genomes using Subsystems Technology (RAST). *Nucleic Acids Res*, 42, D206-14.
- PANCIERA, R. J. & CONFER, A. W. 2010. Pathogenesis and pathology of bovine pneumonia. *Vet Clin North Am Food Anim Pract*, 26, 191-214.
- PANDHER, K., CONFER, A. W. & MURPHY, G. L. 1998. Genetic and immunologic analyses of PlpE, a lipoprotein important in complement-mediated killing of Pasteurella haemolytica serotype 1. *Infect Immun*, 66, 5613-9.
- PANDHER, K., MURPHY, G. L. & CONFER, A. W. 1999. Identification of immunogenic, surface-exposed outer membrane proteins of Pasteurella haemolytica serotype 1. *Vet Microbiol*, 65, 215-26.
- PARIS, G., RATIER, L., AMAYA, M. F., NGUYEN, T., ALZARI, P. M. & FRASCH, A. C. 2005. A sialidase mutant displaying trans-sialidase activity. *J Mol Biol*, 345, 923-34.
- PARKER, D., SOONG, G., PLANET, P., BROWER, J., RATNER, A. J. & PRINCE, A. 2009. The NanA neuraminidase of Streptococcus pneumoniae is involved in biofilm formation. *Infect Immun*, 77, 3722-30.
- PETERSEN, T. N., BRUNAK, S., VON HEIJNE, G. & NIELSEN, H. 2011. SignalP 4.0: discriminating signal peptides from transmembrane regions. *Nat Methods*, 8, 785-6.
- PETTIGREW, M. M., FENNIE, K. P., YORK, M. P., DANIELS, J. & GHAFAR, F. 2006. Variation in the presence of neuraminidase genes among Streptococcus pneumoniae isolates with identical sequence types. *Infect Immun*, 74, 3360-5.
- QUINN, P. J. 2011. *Veterinary microbiology and microbial disease*, Chichester, Wiley-Blackwell.
- RAINBOLT, S., PILLAI, D. K., LUBBERS, B. V., MOORE, M., DAVIS, R., AMRINE, D. & MOSIER, D. 2016. Comparison of Mannheimia haemolytica isolates from an outbreak of bovine respiratory disease. *Vet Microbiol*, 182, 82-6.
- REHMTULLA, A. J. & THOMSON, R. G. 1981. A review of the lesions in shipping fever of cattle. *Can Vet J*, 22, 1-8.
- RICE, P., LONGDEN, I. & BLEASBY, A. 2000. EMBOS: the European Molecular Biology Open Software Suite. *Trends Genet*, 16, 276-7.
- ROBERT, V., VOLOKHINA, E. B., SENF, F., BOS, M. P., VAN GELDER, P. & TOMMASSEN, J. 2006. Assembly factor Omp85 recognizes its outer membrane protein substrates by a species-specific C-terminal motif. *PLoS Biol*, 4, e377.
- ROBERT, X. & GOUET, P. 2014. Deciphering key features in protein structures with the new ENDscript server. *Nucleic Acids Res*, 42, W320-4.

- ROEHRIG, S. C., TRAN, H. Q., SPEHR, V., GUNKEL, N., SELZER, P. M. & ULLRICH, H. J. 2007. The response of *Mannheimia haemolytica* to iron limitation: implications for the acquisition of iron in the bovine lung. *Vet Microbiol*, 121, 316-29.
- ROGGENTIN, P., ROTHE, B., KAPER, J. B., GALEN, J., LAWKRISUK, L., VIMR, E. R. & SCHAUER, R. 1989. Conserved sequences in bacterial and viral sialidases. *Glycoconj J*, 6, 349-53.
- SAADATI, M., GIBBS, H. A., PARTON, R. & COOTE, J. G. 1997. Characterisation of the leukotoxin produced by different strains of *Pasteurella haemolytica*. *J Med Microbiol*, 46, 276-84.
- SACCO, R. E., MCGILL, J. L., PILLATZKI, A. E., PALMER, M. V. & ACKERMANN, M. R. 2014. Respiratory syncytial virus infection in cattle. *Vet Pathol*, 51, 427-36.
- SAMANIEGO-BARRON, L., LUNA-CASTRO, S., PINA-VAZQUEZ, C., SUAREZ-GUEMES, F. & DE LA GARZA, M. 2016. Two outer membrane proteins are bovine lactoferrin-binding proteins in *Mannheimia haemolytica* A1. *Vet Res*, 47, 93.
- SARANGI, L. N., THOMAS, P., GUPTA, S. K., PRIYADARSHINI, A., KUMAR, S., NAGALEEKAR, V. K., KUMAR, A. & SINGH, V. P. 2015. Virulence gene profiling and antibiotic resistance pattern of Indian isolates of *Pasteurella multocida* of small ruminant origin. *Comp Immunol Microbiol Infect Dis*, 38, 33-9.
- SCHARMANN, W., DRZENIEK, R. & BLOBEL, H. 1970. Neuraminidase of *Pasteurella multocida*. *Infect Immun*, 1, 319-20.
- SCHNEIDER, M. J., TAIT, R. G., JR., BUSBY, W. D. & REECY, J. M. 2009. An evaluation of bovine respiratory disease complex in feedlot cattle: Impact on performance and carcass traits using treatment records and lung lesion scores. *J Anim Sci*, 87, 1821-7.
- SEVERI, E., HOOD, D. W. & THOMAS, G. H. 2007. Sialic acid utilization by bacterial pathogens. *Microbiology*, 153, 2817-22.
- SHARMA, R. & WOLDEHIWET, Z. 1990. Increased susceptibility to *Pasteurella haemolytica* in lambs infected with bovine respiratory syncytial virus. *J Comp Pathol*, 103, 411-20.
- SHTYRYA, Y. A., MOCHALOVA, L. V. & BOVIN, N. V. 2009. Influenza virus neuraminidase: structure and function. *Acta Naturae*, 1, 26-32.
- SIEVERS, F., WILM, A., DINEEN, D., GIBSON, T. J., KARPLUS, K., LI, W., LOPEZ, R., MCWILLIAM, H., REMMERT, M., SODING, J., THOMPSON, J. D. & HIGGINS, D. G. 2011. Fast, scalable generation of high-quality protein multiple sequence alignments using Clustal Omega. *Mol Syst Biol*, 7, 539.
- SINGH, K., RITCHEY, J. W. & CONFER, A. W. 2011. *Mannheimia haemolytica*: bacterial-host interactions in bovine pneumonia. *Vet Pathol*, 48, 338-48.
- SKILLMAN, K. M., BARNARD, T. J., PETERSON, J. H., GHIRLANDO, R. & BERNSTEIN, H. D. 2005. Efficient secretion of a folded protein domain by a monomeric bacterial autotransporter. *Mol Microbiol*, 58, 945-58.
- SMITH, A., JOHNSTON, C., INVERARITY, D., SLACK, M., DIGGLE, M. & MITCHELL, T. 2013. Investigating the role of pneumococcal neuraminidase A activity in isolates from pneumococcal haemolytic uraemic syndrome. *J Med Microbiol*, 62, 1735-42.
- SNOWDER, G. D., VAN VLECK, L. D., CUNDIFF, L. V., BENNETT, G. L., KOOHMARAIE, M. & DIKEMAN, M. E. 2007. Bovine respiratory disease in feedlot cattle: phenotypic, environmental, and genetic correlations with

- growth, carcass, and longissimus muscle palatability traits. *J Anim Sci*, 85, 1885-92.
- SOLANA, S., REGLERO, A. A., MARTINEZ-BLANCO, H., REVILLA-NUIN, B., BRAVO, I. G., RODRIGUEZ-APARICIO, L. B. & FERRERO, M. A. 2001. N-Acetylneuraminic acid uptake in *Pasteurella* (*Mannheimia*) *haemolytica* A2 occurs by an inducible and specific transport system. *FEBS Lett*, 509, 41-6.
- SONGER, J. G. & POST, K. W. 2005. *Veterinary microbiology : bacterial and fungal agents of animal disease*, St. Louis, Mo., Elsevier Saunders.
- SOONG, G., MUIR, A., GOMEZ, M. I., WAKS, J., REDDY, B., PLANET, P., SINGH, P. K., KANEKO, Y., WOLFGANG, M. C., HSIAO, Y. S., TONG, L. & PRINCE, A. 2006. Bacterial neuraminidase facilitates mucosal infection by participating in biofilm production. *J Clin Invest*, 116, 2297-2305.
- STEENBERGEN, S. M., LICHTENSTEIGER, C. A., CAUGHLAN, R., GARFINKLE, J., FULLER, T. E. & VIMR, E. R. 2005. Sialic Acid metabolism and systemic pasteurellosis. *Infect Immun*, 73, 1284-94.
- STRAUS, D. C., JOLLEY, W. L. & PURDY, C. W. 1993a. Characterization of neuraminidases produced by various serotypes of *Pasteurella haemolytica*. *Infect Immun*, 61, 4669-74.
- STRAUS, D. C. & PURDY, C. W. 1994. In vivo production of neuraminidase by *Pasteurella haemolytica* A1 in goats after transthoracic challenge. *Infect Immun*, 62, 4675-8.
- STRAUS, D. C. & PURDY, C. W. 1995. Extracellular neuraminidase production by *Pasteurella* species isolated from infected animals. *Curr Microbiol*, 31, 312-5.
- STRAUS, D. C., PURDY, C. W., LOAN, R. W., BRIGGS, R. F. & FRANK, G. H. 1998. In vivo production of neuraminidase by *Pasteurella haemolytica* in market stressed cattle after natural infection. *Curr Microbiol*, 37, 240-4.
- STRAUS, D. C., UNBEHAGEN, P. J. & PURDY, C. W. 1993b. Neuraminidase production by a *Pasteurella haemolytica* A1 strain associated with bovine pneumonia. *Infect Immun*, 61, 253-9.
- TAJIMA, N., KAWAI, F., PARK, S. Y. & TAME, J. R. 2010. A novel intein-like autoproteolytic mechanism in autotransporter proteins. *J Mol Biol*, 402, 645-56.
- TAYLOR, G. 1996. Sialidases: structures, biological significance and therapeutic potential. *Curr Opin Struct Biol*, 6, 830-7.
- TAYLOR, N. R. & VON ITZSTEIN, M. 1994. Molecular modeling studies on ligand binding to sialidase from influenza virus and the mechanism of catalysis. *J Med Chem*, 37, 616-24.
- THON, V., LI, Y., YU, H., LAU, K. & CHEN, X. 2012. PmST3 from *Pasteurella multocida* encoded by Pm1174 gene is a monofunctional alpha2-3-sialyltransferase. *Appl Microbiol Biotechnol*, 94, 977-85.
- TONG, H. H., LI, D., CHEN, S., LONG, J. P. & DEMARIA, T. F. 2005. Immunization with recombinant *Streptococcus pneumoniae* neuraminidase NanA protects chinchillas against nasopharyngeal colonization. *Infect Immun*, 73, 7775-8.
- TRAPPETTI, C., KADIOGLU, A., CARTER, M., HAYRE, J., IANNELLI, F., POZZI, G., ANDREW, P. W. & OGGIONI, M. R. 2009. Sialic acid: a preventable signal for pneumococcal biofilm formation, colonization, and invasion of the host. *J Infect Dis*, 199, 1497-505.
- TRIGO, F. J., BREEZE, R. G., LIGGITT, H. D., EVERMANN, J. F. & TRIGO, E. 1984. Interaction of bovine respiratory syncytial virus and *Pasteurella haemolytica* in the ovine lung. *Am J Vet Res*, 45, 1671-8.

- TSENG, T. T., TYLER, B. M. & SETUBAL, J. C. 2009. Protein secretion systems in bacterial-host associations, and their description in the Gene Ontology. *BMC Microbiol*, 9 Suppl 1, S2.
- UCHIYAMA, S., CARLIN, A. F., KHOSRAVI, A., WEIMAN, S., BANERJEE, A., QUACH, D., HIGHTOWER, G., MITCHELL, T. J., DORAN, K. S. & NIZET, V. 2009. The surface-anchored NanA protein promotes pneumococcal brain endothelial cell invasion. *J Exp Med*, 206, 1845-52.
- VALARCHER, J. F. & TAYLOR, G. 2007. Bovine respiratory syncytial virus infection. *Vet Res*, 38, 153-80.
- VARGHESE, J. N. & COLMAN, P. M. 1991. Three-dimensional structure of the neuraminidase of influenza virus A/Tokyo/3/67 at 2.2 Å resolution. *J Mol Biol*, 221, 473-86.
- VARKI, A. 1992. Diversity in the sialic acids. *Glycobiology*, 2, 25-40.
- VARKI, A. & SCHAUER, R. 2009. Sialic Acids. In: VARKI, A., CUMMINGS, R. D., ESKO, J. D., FREEZE, H. H., STANLEY, P., BERTOZZI, C. R., HART, G. W. & ETZLER, M. E. (eds.) *Essentials of Glycobiology*. Cold Spring Harbor (NY): Cold Spring Harbor Laboratory Press
- The Consortium of Glycobiology Editors, La Jolla, California.
- VAVRICKA, C. J., LIU, Y., KIYOTA, H., SRIWILAIJAROEN, N., QI, J., TANAKA, K., WU, Y., LI, Q., LI, Y., YAN, J., SUZUKI, Y. & GAO, G. F. 2013. Influenza neuraminidase operates via a nucleophilic mechanism and can be targeted by covalent inhibitors. *Nat Commun*, 4, 1491.
- VIMR, E. R., KALIVODA, K. A., DESZO, E. L. & STEENBERGEN, S. M. 2004. Diversity of microbial sialic acid metabolism. *Microbiol Mol Biol Rev*, 68, 132-53.
- WAESPY, M., GBEM, T. T., ELENSCHNEIDER, L., JECK, A. P., DAY, C. J., HARTLEY-TASSELL, L., BOVIN, N., TIRALONGO, J., HASELHORST, T. & KELM, S. 2015. Carbohydrate Recognition Specificity of Trans-sialidase Lectin Domain from Trypanosoma congolense. *PLoS Negl Trop Dis*, 9, e0004120.
- WAGNER, J. K., HEINDL, J. E., GRAY, A. N., JAIN, S. & GOLDBERG, M. B. 2009. Contribution of the periplasmic chaperone Skp to efficient presentation of the autotransporter IcsA on the surface of Shigella flexneri. *J Bacteriol*, 191, 815-21.
- WHITE, D. J., JOLLEY, W. L., PURDY, C. W. & STRAUS, D. C. 1995. Extracellular neuraminidase production by a Pasteurella multocida A:3 strain associated with bovine pneumonia. *Infect Immun*, 63, 1703-9.
- WITTUM, T. E., WOOLLEN, N. E., PERINO, L. J. & LITLEDIKE, E. T. 1996. Relationships among treatment for respiratory tract disease, pulmonary lesions evident at slaughter, and rate of weight gain in feedlot cattle. *J Am Vet Med Assoc*, 209, 814-8.
- XU, G., KIEFEL, M. J., WILSON, J. C., ANDREW, P. W., OGGIONI, M. R. & TAYLOR, G. L. 2011. Three Streptococcus pneumoniae sialidases: three different products. *J Am Chem Soc*, 133, 1718-21.
- XU, G., POTTER, J. A., RUSSELL, R. J., OGGIONI, M. R., ANDREW, P. W. & TAYLOR, G. L. 2008. Crystal structure of the NanB sialidase from Streptococcus pneumoniae. *J Mol Biol*, 384, 436-49.
- XU, Z., VON GRAFENSTEIN, S., WALTHER, E., FUCHS, J. E., LIEDL, K. R., SAUERBREI, A. & SCHMIDTKE, M. 2016. Sequence diversity of NanA manifests in distinct enzyme kinetics and inhibitor susceptibility. *Sci Rep*, 6, 25169.

- YATES, W. D., BABIUK, L. A. & JERICHO, K. W. 1983. Viral-bacterial pneumonia in calves: duration of the interaction between bovine herpesvirus 1 and *Pasteurella haemolytica*. *Can J Comp Med*, 47, 257-64.
- YEN, H. L. 2016. Current and novel antiviral strategies for influenza infection. *Curr Opin Virol*, 18, 126-34.
- YOO, H. S., MAHESWARAN, S. K., SRINAND, S., AMES, T. R. & SURESH, M. 1995a. Increased tumor necrosis factor-alpha and interleukin-1 beta expression in the lungs of calves with experimental pneumonic pasteurellosis. *Vet Immunol Immunopathol*, 49, 15-28.
- YOO, H. S., RAJAGOPAL, B. S., MAHESWARAN, S. K. & AMES, T. R. 1995b. Purified *Pasteurella haemolytica* leukotoxin induces expression of inflammatory cytokines from bovine alveolar macrophages. *Microb Pathog*, 18, 237-52.
- ZECCHINON, L., FETT, T. & DESMECHT, D. 2005. How *Mannheimia haemolytica* defeats host defence through a kiss of death mechanism. *Vet Res*, 36, 133-56.

YI SRNRT LLDQDVAVNKR... YI SRNRT LLDQDVAVNKR...

gll49848687/1-803 732 NIAFINDS LKLSQ... gll397319022/1-803 732 NIAFINDS LKLSQ...

NIAFINDS LKLSQ... NIAFINDS LKLSQ...

gll49848687/1-803 775 LKVGSTLELQ... gll397319022/1-803 775 LKVGSTLELQ...

LKVGSTLELQ... LKVGSTLELQ...

YI SRNRT LLDQDVAVNKR... YI SRNRT LLDQDVAVNKR...

gll49848687/1-803 646 FRYGVKQDF... gll397319022/1-803 646 FRYGVKQDF...

FRYGVKQDF... FRYGVKQDF...

gll49848687/1-803 689 YI SRNRT LLDQ... gll397319022/1-803 689 YI SRNRT LLDQ...

LKVGSTLELQ... LKVGSTLELQ...

gil12720940/1-832
 gil557249342/1-832
 gil504204011/1-802
 gil1039802229/1-802
 gil1039812199/1-802
 gil810359761/1-802
 gil492129126/1-798
 gil514187266/1-798
 gil504092044/1-798
 gil504480912/1-798
 gil974661134/1-798
 gil844687611/1-798
 gil1063921996/1-791
 gil514187847/1-778
 gil11464738/1-747

771 LSQANYQDNQYKIKSTNMVYALNVGVEKQFTPHALGSRMKLQ813
 771 LSQANYQDNQYKIKSTNMVYALNVGVEKQFTPHALGSRMKLQ813
 741 LSQANYQDNQYKIKSTNMVYALNVGVEKQFTPHALGSRMKLQ783
 741 LSQANYQDNQYKIKSTNMVYALNVGVEKQFTPHALGSRMKLQ783
 741 LSQANYQDNQYKIKSTNMVYALNVGVEKQFTPHALGSRMKLQ783
 741 LSQANYQDNQYKIKSTNMVYALNVGVEKQFTPHALGSRMKLQ783
 741 LSQANYQDNQYKIKSTNMVYALNVGVEKQFTPHALGSRMKLQ783
 737 LSQANYQDNQYKIKSTNMVYALNVGVEKQFTPHALGSRMKLQ779
 737 LSQANYQDNQYKIKSTNMVYALNVGVEKQFTPHALGSRMKLQ779
 737 LSQANYQDNQYKIKSTNMVYALNVGVEKQFTPHALGSRMKLQ779
 737 LSQANYQDNQYKIKSTNMVYALNVGVEKQFTPHALGSRMKLQ779
 737 LSQANYQDNQYKIKSTNMVYALNVGVEKQFTPHALGSRMKLQ779
 737 LSQANYQDNQYKIKSTNMVYALNVGVEKQFTPHALGSRMKLQ779
 737 LSQANYQDNQYKIKSTNMVYALNVGVEKQFTPHALGSRMKLQ779
 737 LSQANYQDNQYKIKSTNMVYALNVGVEKQFTPHALGSRMKLQ779
 730 LSQANYQDNQYKIKSTNMVYALNVGVEKQFTPHALGSRMKLQ772
 717 LSQANYQDNQYKIKSTNMVYALNVGVEKQFTPHALGSRMKLQ759
 737 FSOA IYRDNP F-----747

LSQANYQDNQYKIKSTNMVYALNVGVEKQFTPHALGSRMKLQ
LSQANYQDNQYKIKSTNMVYALNVGVEKQFTPHALGSRMKLQ

Consensus

LSQANYQDNQYKIKSTNMVYALNVGVEKQFTPHALGSRMKLQ

gil12720940/1-832
 gil557249342/1-832
 gil504204011/1-802
 gil1039802229/1-802
 gil1039812199/1-802
 gil810359761/1-802
 gil492129126/1-798
 gil514187266/1-798
 gil504092044/1-798
 gil504480912/1-798
 gil974661134/1-798
 gil844687611/1-798
 gil1063921996/1-791
 gil514187847/1-778
 gil11464738/1-747

814 KYGSQASEVSLGVNLSYHW
 814 KYGSQASEVSLGVNLSYHW
 784 KYGSQASEVSLGVNLSYHW
 784 KYGSQASEVSLGVNLSYHW
 784 KYGSQASEVSLGVNLSYHW
 784 KYGSQASEVSLGVNLSYHW
 780 KYGSQASEVSLGVNLSYHW
 780 KYGSQASEVSLGVNLSYHW
 780 KYGSQASEVSLGVNLSYHW
 780 KYGSQASEVSLGVNLSYHW
 780 KYGSQASEVSLGVNLSYHW
 780 KYGSQASEVSLGVNLSYHW
 780 KYGSQASEVSLGVNLSYHW
 780 KYGSQASEVSLGVNLSYHW
 780 KYGSQASEVSLGVNLSYHW
 773 KYGSQASEVSLGVNLSYHW
 760 KYGSQASEVSLGVNLSYHW
 -----747

Consensus

KYGSQASEVSLGVNLSYHW
KYGSQASEVSLGVNLSYHW

KYGSQASEVSLGVNLSYHW

WVHJWVWV

GHGHLETSQVLELENGDLKLFMRNTSGRVMWMTSKDGGYT

g/1499209421/1-1080
g/1492130021/1-1069
g/1039812328/1-1067
g/1514204233/1-1065
g/1504480758/1-1065
g/1974661197/1-1063
g/1810365999/1-1062
g/1504203721/1-1060
g/1492121591/1-1055
g/1545609639/1-1055
g/11002924980/1-1055
g/102924980/1-1055
g/1504091777/1-1051
g/1482661992/1-855
g/1482661974/1-848
g/1482661990/1-848
g/1523498503/1-819

Consensus

g/1499209421/1-1080
g/1492130021/1-1069
g/1039812328/1-1067
g/1514204233/1-1065
g/1504480758/1-1065
g/1974661197/1-1063
g/1810365999/1-1062
g/1504203721/1-1060
g/1492121591/1-1055
g/1545609639/1-1055
g/11002924980/1-1055
g/102924980/1-1055
g/1504091777/1-1051
g/1482661992/1-855
g/1482661974/1-848
g/1482661990/1-848
g/1523498503/1-819

Consensus

g/1499209421/1-1080
g/1492130021/1-1069
g/1039812328/1-1067
g/1514204233/1-1065
g/1504480758/1-1065
g/1974661197/1-1063
g/1810365999/1-1062
g/1504203721/1-1060
g/1492121591/1-1055
g/1545609639/1-1055
g/11002924980/1-1055
g/102924980/1-1055
g/1504091777/1-1051

436 WVNT EK INELDHGYSQLSVYKYSKRNGKXKXIVFSGQRSG476
421 W IETKQVPELNHGYSQLSVYKYSKKNKXKXIVFSGQSV5G461
419 W IETKQVPELNHGYSQLSVYKYSKKNKXKXIVFSGQSV5G459
421 W IETKQVPELNHGYSQLSVYKYSKKNKXKXIVFSGQSV5G461
418 WVST EK INELNHGYSQLSVYKYSKKNKXKXIVFSGQSV5G458
416 W IETKQVPELNHGYSQLSVYKYSKKNKXKXIVFSGQSV5G457
417 W IETKQVPELNHGYSQLSVYKYSKKNKXKXIVFSGQSV5G457
408 WLDTHQVSELKHGYSQLSVYKYSKKNKXKXIVFSGQSV5G448
408 WLDTHQVSELKHGYSQLSVYKYSKKNKXKXIVFSGQSV5G448
408 WLDTHQVSELKHGYSQLSVYKYSKKNKXKXIVFSGQSV5G448
319 W IETKQVPELNHGYSQLSVYKYSKKNKXKXIVFSGQSV5G439
311 WLDTHQVSELKHGYSQLSVYKYSKKNKXKXIVFSGQSV5G351
311 WVNT ERVNELNHGYSQLSVYKYSKKNKXKXIVFSGQSV5G351
176 WLDTHQVSELKHGYSQLSVYKYSKKNKXKXIVFSGQSV5G216

Consensus

477 QGDBNLRDQKFLFGEVQEDGSIKWDITNLVREIVSQKA-516
462 NSGDKLRRDQKFLFGEVQEDGSIKWDITNLVREIVSQKA-501
460 QSGDALLRRDQKFLFGEVQEDGSIKWDITNLVREIVSQKA-499
462 NSGDKLRRDQKFLFGEVQEDGSIKWDITNLVREIVSQKA-501
462 NSGDKLRRDQKFLFGEVQEDGSIKWDITNLVREIVSQKA-501
459 QSGDALLRRDQKFLFGEVQEDGSIKWDITNLVREIVSQKA-498
457 SGGDQLRRDQKFLFGEVQEDGSIKWDITNLVREIVSQKA-497
458 SGGDQLRRDQKFLFGEVQEDGSIKWDITNLVREIVSQKA-497
449 NGDQKRRDQKFLFGEVQEDGSIKWDITNLVREIVSQKA-488
449 QSGDALLRRDQKFLFGEVQEDGSIKWDITNLVREIVSQKA-488
449 NGDQKRRDQKFLFGEVQEDGSIKWDITNLVREIVSQKA-488
449 NGDQKRRDQKFLFGEVQEDGSIKWDITNLVREIVSQKA-488
449 QSGDALLRRDQKFLFGEVQEDGSIKWDITNLVREIVSQKA-488
360 SGGDQLRRDQKFLFGEVQEDGSIKWDITNLVREIVSQKA-400
352 NGDQKRRDQKFLFGEVQEDGSIKWDITNLVREIVSQKA-391
352 QGDBNLRDQKFLFGEVQEDGSIKWDITNLVREIVSQKA-391
217 QSGDALLRRDQKFLFGEVQEDGSIKWDITNLVREIVSQKA-236

Consensus

517 - - A - - - - G - - - - QPNGYVYSMAELGDGSIKWDITNLVREIVSQKA-516
502 - - K - - - - QSEVPNGYVYSMAELGDGSIKWDITNLVREIVSQKA-516
500 - - KONG - RS - - - - YPNGYVYSMAELGDGSIKWDITNLVREIVSQKA-516
502 - - A - - - - G - - - - QPNGYVYSMAELGDGSIKWDITNLVREIVSQKA-516
502 - - A - - - - G - - - - QPNGYVYSMAELGDGSIKWDITNLVREIVSQKA-516
499 - - N - - - - RT - - - - HPNGYVYSMAELGDGSIKWDITNLVREIVSQKA-516
498 TQN - - - - S - - - - YPNGYVYSMAELGDGSIKWDITNLVREIVSQKA-516
498 - - N - - - - RT - - - - HPNGYVYSMAELGDGSIKWDITNLVREIVSQKA-516
489 - - RQSNLRG - - - - YSNGYVYSMAELGDGSIKWDITNLVREIVSQKA-516
489 - - RQSNLRG - - - - YSNGYVYSMAELGDGSIKWDITNLVREIVSQKA-516
489 - - RQSNLRG - - - - YSNGYVYSMAELGDGSIKWDITNLVREIVSQKA-516
489 - - RQSNLRG - - - - YSNGYVYSMAELGDGSIKWDITNLVREIVSQKA-516
489 - - N - - - - RT - - - - HPNGYVYSMAELGDGSIKWDITNLVREIVSQKA-516

g/1482661992/1-855
g/1482661974/1-848
g/1482661990/1-848
g/1523498503/1-819

Consensus

g/1499209421/1-1080
g/1492130021/1-1069
g/1039812328/1-1067
g/1514204233/1-1065
g/1504480758/1-1065
g/1974661197/1-1063
g/1810365999/1-1062
g/1504203721/1-1060
g/1492121591/1-1055
g/1545609639/1-1055
g/11002924980/1-1055
g/102924980/1-1055
g/1504091777/1-1051
g/1482661992/1-855
g/1482661974/1-848
g/1482661990/1-848
g/1523498503/1-819

Consensus

g/1499209421/1-1080
g/1492130021/1-1069
g/1039812328/1-1067
g/1514204233/1-1065
g/1504480758/1-1065
g/1974661197/1-1063
g/1810365999/1-1062
g/1504203721/1-1060
g/1492121591/1-1055
g/1545609639/1-1055
g/11002924980/1-1055
g/102924980/1-1055
g/1504091777/1-1051
g/1482661992/1-855
g/1482661974/1-848
g/1482661990/1-848
g/1523498503/1-819

Consensus

g/1499209421/1-1080
g/1492130021/1-1069
g/1039812328/1-1067
g/1514204233/1-1065
g/1504480758/1-1065
g/1974661197/1-1063
g/1810365999/1-1062

401 TQN - - - - S - - - - YTPNGYVYSMAELGDGSIKWDITNLVREIVSQKA-516
392 - - - - RQSNLRG - - - - YSNGYVYSMAELGDGSIKWDITNLVREIVSQKA-516
392 - - - - RQSNLRG - - - - YSNGYVYSMAELGDGSIKWDITNLVREIVSQKA-516
257 - - - - N - - - - RT - - - - HPNGYVYSMAELGDGSIKWDITNLVREIVSQKA-516

Consensus

TQ+QSNLRGGSEVPNGYVYSMAELGDGSIKWDITNLVREIVSQKA-516
547 TT IMYLP IEMOEF FFWKAGK I FSDVRKQEP I FVDTGTE LLE587
536 TT IMYLP IEMOEF FFWKAGK I FSDVRKQEP I FVDTGTE LLE578
534 TT IMYLP IEMOEF FFWKAGK I FSDVRKQEP I FVDTGTE LLE574
532 TT IMYLP IEMOEF FFWKAGK I FSDVRKQEP I FVDTGTE LLE572
532 TT IMYLP IEMOEF FFWKAGK I FSDVRKQEP I FVDTGTE LLE572
532 TT IMYLP IEMOEF FFWKAGK I FSDVRKQEP I FVDTGTE LLE572
531 TT IMYLP IEMOEF FFWKAGK I FSDVRKQEP I FVDTGTE LLE570
530 TT IMYLP IEMOEF FFWKAGK I FSDVRKQEP I FVDTGTE LLE570
529 TT IMYLP IEMOEF FFWKAGK I FSDVRKQEP I FVDTGTE LLE569
524 TT IMYLP IEMOEF FFWKAGK I FSDVRKQEP I FVDTGTE LLE564
524 TT IMYLP IEMOEF FFWKAGK I FSDVRKQEP I FVDTGTE LLE564
524 TT IMYLP IEMOEF FFWKAGK I FSDVRKQEP I FVDTGTE LLE564
524 TT IMYLP IEMOEF FFWKAGK I FSDVRKQEP I FVDTGTE LLE564
520 TT IMYLP IEMOEF FFWKAGK I FSDVRKQEP I FVDTGTE LLE560
520 TT IMYLP IEMOEF FFWKAGK I FSDVRKQEP I FVDTGTE LLE560
434 TT IMYLP IEMOEF FFWKAGK I FSDVRKQEP I FVDTGTE LLE474
427 TT IMYLP IEMOEF FFWKAGK I FSDVRKQEP I FVDTGTE LLE467
427 TT IMYLP IEMOEF FFWKAGK I FSDVRKQEP I FVDTGTE LLE467
288 TT IMYLP IEMOEF FFWKAGK I FSDVRKQEP I FVDTGTE LLE328

Consensus

TT IMYLP IEMOEF FFWKAGK I FSDVRKQEP I FVDTGTE LLE328
588 KIGDGI AI KRGESESQSGI NVSEGL LVLDQTKDQKKAFT628
577 KIGDGI AI KRGESESQSGI NVSEGL LVLDQTKDQKKAFT617
575 KIGDVAI KRGESESQSGI NVSEGL LVLDQTKDQKKAFT615
573 KIGDVAI KRGESESQSGI NVSEGL LVLDQTKDQKKAFT613
573 KIGDVAI KRGESESQSGI NVSEGL LVLDQTKDQKKAFT613
571 KIGDVAI KRGESESQSGI NVSEGL LVLDQTKDQKKAFT611
572 KIGDVAI KRGESESQSGI NVSEGL LVLDQTKDQKKAFT611
570 KIGDVAI KRGESESQSGI NVSEGL LVLDQTKDQKKAFT610
565 KIGDVAI KRGESESQSGI NVSEGL LVLDQTKDQKKAFT605
565 KIGDVAI KRGESESQSGI NVSEGL LVLDQTKDQKKAFT605
563 KIGDVAI KRGESESQSGI NVSEGL LVLDQTKDQKKAFT605
563 KIGDVAI KRGESESQSGI NVSEGL LVLDQTKDQKKAFT605
561 KIGDVAI KRGESESQSGI NVSEGL LVLDQTKDQKKAFT601
475 KIGDVAI KRGESESQSGI NVSEGL LVLDQTKDQKKAFT515
468 KIGDVAI KRGESESQSGI NVSEGL LVLDQTKDQKKAFT508
468 KIGDVAI KRGESESQSGI NVSEGL LVLDQTKDQKKAFT508
329 KIGDVAI KRGESESQSGI NVSEGL LVLDQTKDQKKAFT369

Consensus

KIGDVAI KRGESESQSGI NVSEGL LVLDQTKDQKKAFT
629 QLT LNNSSGVAQVNSTQNDRLVFNNGATGYLQFTVDTHTS669
618 QLT LNNSSGVAQVNSTQNDRLVFNNGATGYLQFTVDTHTS656
616 QLT LNNSSGVAQVNSTQNDRLVFNNGATGYLQFTVDTHTS654
614 QLT LNNSSGVAQVNSTQNDRLVFNNGATGYLQFTVDTHTS654
614 QLT LNNSSGVAQVNSTQNDRLVFNNGATGYLQFTVDTHTS654
612 QLT LNNSSGVAQVNSTQNDRLVFNNGATGYLQFTVDTHTS652
612 QLT LNNSSGVAQVNSTQNDRLVFNNGATGYLQFTVDTHTS652
613 DVT LNKTC I LQVSEYQNI DTLTVNNEASGHIQLSVSDST653

KQKSGNLSHFDYGVDFVNASYSGVMLGCKVWQSERGNHALYT
KQKSGNLSHFDYGVDFVNASYSGVMLGCKVWQSERGNHALYT

Consensus

g/1499209421/1-1080
g/1492130021/1-1069
g/11039812328/1-1067
g/1514204233/1-1065
g/1504480758/1-1065
g/1974661197/1-1063
g/1810365999/1-1062
g/1504203721/1-1060
g/1492121591/1-1055
g/1545609639/1-1055
g/11039802409/1-1055
g/1504091777/1-1051
g/1482661992/1-855
g/1482661974/1-848
g/1482661990/1-848
g/1523498503/1-819

Consensus

g/1499209421/1-1080
g/1492130021/1-1069
g/11039812328/1-1067
g/1514204233/1-1065
g/1504480758/1-1065
g/1974661197/1-1063
g/1810365999/1-1062
g/1504203721/1-1060
g/1492121591/1-1055
g/1545609639/1-1055
g/11039802409/1-1055
g/1504091777/1-1051
g/1482661992/1-855
g/1482661974/1-848
g/1482661990/1-848
g/1523498503/1-819

Consensus

g/1499209421/1-1080
g/1492130021/1-1069
g/11039812328/1-1067
g/1514204233/1-1065
g/1504480758/1-1065
g/1974661197/1-1063
g/1810365999/1-1062
g/1504203721/1-1060
g/1492121591/1-1055
g/1545609639/1-1055
g/11039802409/1-1055
g/1504091777/1-1051
g/1482661992/1-855
g/1482661974/1-848
g/1482661990/1-848
g/1523498503/1-819

ALNKT SYKVT P K A V D G E T K A K Y S W G G S I N W H S N L P H N L I V 915
864 ALNKT SYKVT P K A V D G E T K A K Y S W G G S I N W H S N L P H N L I V 904
862 ALNKT SYKVT P K A V D G E T K A K Y S W G G S I N W H S N L P H N L I V 902
860 ALNKT SYKVT P K A V D G E T K A K Y S W G G S I N W H S N L P H N L I V 900
858 ALNKT SYKVT P K A V D G E T K A K Y S W G G S I N W H S N L P H N L I V 898
857 ALNKT SYKVT P K A V D G E T K A K Y S W G G S I N W H S N L P H N L I V 897
855 ALNKT SYKVT P K A V D G E T K A K Y S W G G S I N W H S N L P H N L I V 895
850 ALNKT SYKVT P K A V D G E T K A K Y S W G G S I N W H S N L P H N L I V 890
850 ALNKT SYKVT P K A V D G E T K A K Y S W G G S I N W H S N L P H N L I V 890
850 ALNKT SYKVT P K A V D G E T K A K Y S W G G S I N W H S N L P H N L I V 890
846 ALNKT SYKVT P K A V D G E T K A K Y S W G G S I N W H S N L P H N L I V 886
760 ALNKT SYKVT P K A V D G E T K A K Y S W G G S I N W H S N L P H N L I V 800
753 ALNKT SYKVT P K A V D G E T K A K Y S W G G S I N W H S N L P H N L I V 793
753 ALNKT SYKVT P K A V D G E T K A K Y S W G G S I N W H S N L P H N L I V 793
614 ALNKT SYKVT P K A V D G E T K A K Y S W G G S I N W H S N L P H N L I V 654

ALNKT SYKVT P K A V D G E T K A K Y S W G G S I N W H S N L P H N L I V
ALNKT SYKVT P K A V D G E T K A K Y S W G G S I N W H S N L P H N L I V

916 DLSAGYQKHKGD I E H A G H V K G Y T F N I G A D L G R Y Q W W M K N A F 956
905 DLSAGYQKHKGD I E H A G H V K G Y T F N I G A D L G R Y Q W W M K N A F 943
903 DLSAGYQKHKGD I E H A G H V K G Y T F N I G A D L G R Y Q W W M K N A F 941
901 DLSAGYQKHKGD I E H A G H V K G Y T F N I G A D L G R Y Q W W M K N A F 941
899 DLSAGYQKHKGD I E H A G H V K G Y T F N I G A D L G R Y Q W W M K N A F 939
898 DLSAGYQKHKGD I E H A G H V K G Y T F N I G A D L G R Y Q W W M K N A F 938
896 DLSAGYQKHKGD I E H A G H V K G Y T F N I G A D L G R Y Q W W M K N A F 936
891 DLSAGYQKHKGD I E H A G H V K G Y T F N I G A D L G R Y Q W W M K N A F 931
891 DLSAGYQKHKGD I E H A G H V K G Y T F N I G A D L G R Y Q W W M K N A F 931
887 DLSAGYQKHKGD I E H A G H V K G Y T F N I G A D L G R Y Q W W M K N A F 927
801 DLSAGYQKHKGD I E H A G H V K G Y T F N I G A D L G R Y Q W W M K N A F 841
794 DLSAGYQKHKGD I E H A G H V K G Y T F N I G A D L G R Y Q W W M K N A F 834
794 DLSAGYQKHKGD I E H A G H V K G Y T F N I G A D L G R Y Q W W M K N A F 834
655 DLSAGYQKHKGD I E H A G H V K G Y T F N I G A D L G R Y Q W W M K N A F 695

Consensus

g/1499209421/1-1080
g/1492130021/1-1069
g/11039812328/1-1067
g/1514204233/1-1065
g/1504480758/1-1065
g/1974661197/1-1063
g/1810365999/1-1062
g/1504203721/1-1060
g/1492121591/1-1055
g/1545609639/1-1055
g/11039802409/1-1055
g/1504091777/1-1051
g/1482661992/1-855
g/1482661974/1-848
g/1482661990/1-848
g/1523498503/1-819

Consensus

g/1499209421/1-1080
g/1492130021/1-1069
g/11039812328/1-1067
g/1514204233/1-1065
g/1504480758/1-1065
g/1974661197/1-1063
g/1810365999/1-1062
g/1504203721/1-1060
g/1492121591/1-1055
g/1545609639/1-1055
g/11039802409/1-1055
g/1504091777/1-1051
g/1482661992/1-855
g/1482661974/1-848
g/1482661990/1-848
g/1523498503/1-819

IPMVGLHYLYASLSDVNQDANKALLKYNFNALKTNLGVD972
928 ITPMVGLHYLYASLSDVNQDANKALLKYNFNALKTNLGVD966
842 ITPMVGLHYLYASLSDVNQDANKALLKYNFNALKTNLGVD966
835 ITPMVGLHYLYASLSDVNQDANKALLKYNFNALKTNLGVD966
835 ITPMVGLHYLYASLSDVNQDANKALLKYNFNALKTNLGVD966
835 ITPMVGLHYLYASLSDVNQDANKALLKYNFNALKTNLGVD966
696 ITPMVGLHYLYASLSDVNQDANKALLKYNFNALKTNLGVD976

IPMVGLHYLYASLSDVNQDANKALLKYNFNALKTNLGVD
IPMVGLHYLYASLSDVNQDANKALLKYNFNALKTNLGVD

998 VNYR I G K F E V K G L L S Y D M Y Q Q K T R Q L V Y D V A Y K Q G K L A D T 1038
987 VNYR I G K F E V K G L L S Y D M Y Q Q K T R Q L V Y D V A Y K Q G K L A D T 1027
985 VNYR I G K F E V K G L L S Y D M Y Q Q K T R Q L V Y D V A Y K Q G K L A D T 1025
983 VNYR I G K F E V K G L L S Y D M Y Q Q K T R Q L V Y D V A Y K Q G K L A D T 1023
981 VNYR I G K F E V K G L L S Y D M Y Q Q K T R Q L V Y D V A Y K Q G K L A D T 1021
980 VNYR I G K F E V K G L L S Y D M Y Q Q K T R Q L V Y D V A Y K Q G K L A D T 1020
978 VNYR I G K F E V K G L L S Y D M Y Q Q K T R Q L V Y D V A Y K Q G K L A D T 1018
973 VNYR I G K F E V K G L L S Y D M Y Q Q K T R Q L V Y D V A Y K Q G K L A D T 1013
973 VNYR I G K F E V K G L L S Y D M Y Q Q K T R Q L V Y D V A Y K Q G K L A D T 1013
973 VNYR I G K F E V K G L L S Y D M Y Q Q K T R Q L V Y D V A Y K Q G K L A D T 1013
969 VNYR I G K F E V K G L L S Y D M Y Q Q K T R Q L V Y D V A Y K Q G K L A D T 1009

Consensus

IPMVGLHYLYASLSDVNQDANKALLKYNFNALKTNLGVD
IPMVGLHYLYASLSDVNQDANKALLKYNFNALKTNLGVD

1039 LHLNTQFVAHLTPRFASFSTEVGFQFHARNKQQSSFAVGAHYQ1079
1028 LHLNTQFVAHLTPRFASFSTEVGFQFHARNKQQSSFAVGAHYQ1068
1026 LHLNTQFVAHLTPRFASFSTEVGFQFHARNKQQSSFAVGAHYQ1066
1024 LHLNTQFVAHLTPRFASFSTEVGFQFHARNKQQSSFAVGAHYQ1064
1022 LHLNTQFVAHLTPRFASFSTEVGFQFHARNKQQSSFAVGAHYQ1062
1020 LHLNTQFVAHLTPRFASFSTEVGFQFHARNKQQSSFAVGAHYQ1060
1019 LHLNTQFVAHLTPRFASFSTEVGFQFHARNKQQSSFAVGAHYQ1059
1014 LHLNTQFVAHLTPRFASFSTEVGFQFHARNKQQSSFAVGAHYQ1054
1014 LHLNTQFVAHLTPRFASFSTEVGFQFHARNKQQSSFAVGAHYQ1054
1010 LHLNTQFVAHLTPRFASFSTEVGFQFHARNKQQSSFAVGAHYQ1050

Consensus

LHLNTQFVAHLTPRFASFSTEVGFQFHARNKQQSSFAVGAHYQ
LHLNTQFVAHLTPRFASFSTEVGFQFHARNKQQSSFAVGAHYQ

g/1499209421/1-1080
g/1492130021/1-1069
g/11039812328/1-1067
g/1514204233/1-1065
g/1504480758/1-1065
g/1974661197/1-1063
g/1810365999/1-1062
g/1504203721/1-1060
g/1492121591/1-1055
g/1545609639/1-1055
g/11039802409/1-1055
g/1504091777/1-1051
g/1482661992/1-855
g/1482661974/1-848
g/1482661990/1-848
g/1523498503/1-819